

**ERROR ESTIMATION AND CONTROLLABILITY  
ANALYSIS OF CONTEMPORARY FUZZY LOGIC  
CONTROL MODELS**

**A Thesis  
submitted to**

**Thapar University  
Patiala, Punjab, India**

**For the award of the degree of**

**DOCTOR OF PHILOSOPHY**



**by  
Gagandeep Kaur  
(Registration No. 9041152)**

**Under the supervision of**

**Dr. Yaduvir Singh  
Associate Professor  
Department of Electrical & Instrumentation Engineering**

**THAPAR UNIVERSITY  
PATIALA-147004  
PUNJAB-INDIA**

**2012**

**DEDICATED**

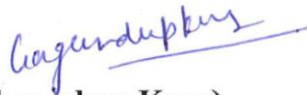
**TO**

**MY FAMILY**

## CERTIFICATE

I hereby certify that the work which is being presented in this thesis entitled “**Error Estimation and Controllability Analyses of Contemporary Fuzzy Logic Models**” in fulfillment of the requirements for award of degree of **Doctor of Philosophy** submitted in the Electrical and Instrumentation Engineering Department(EIED), Thapar University Patiala, Punjab, India.

It is an authentic record of my own work carried out under the supervision of Dr. Yaduvir Singh.



**(Gagandeep Kaur)**

Registration no. 9041152

It is an original research work carried out by her, under my supervision and guidance, and no part of this thesis has been submitted to any other university or institute for award of any degree.



**(Dr. Yaduvir Singh)**

*Associate Professor*

Electrical & Instrumentation Engineering Department

Thapar University, Patiala-147004

Punjab, INDIA

**Supervisor**

## ACKNOWLEDGEMENT

I express my profound and grateful veneration to my guide **Dr. Yaduvir Singh**, Associate Professor, Department of Electrical and Instrumentation Engineering, Thapar University Patiala. I am thankful to him for his supervision, valuable guidance, inspiration and intuition in the research area which enabled me in successful completion of Ph.D. thesis work.

I am grateful to **Dr. Abhijit Mukherjee**, Director Thapar University Patiala for providing me opportunity in Thapar University to carry out this research work. I express my gratitude to the Doctoral Committee for monitoring the progress and providing valuable suggestions time to time to carry out Ph. D research work.

I convey my sincere thanks to **Dr. Smarajit Ghosh**, Head of Electrical & Instrumentation Engineering, Thapar University, Patiala for his encouragement and co-operation and also for facilitating all the facilities for the execution of this work.

I wish to express my deep gratitude to **Dr. P. S. Bimbhra** for his counseling on certain electrical issues as taken in this work. I am immensely thankful to **Mrs. Prachi w/o Dr. Yaduvir Singh**, my supervisor, for motivating me during ups and downs in the Ph.D work.

Finally I would like to dedicate this thesis to my family. I wish to express deepest gratitude to my mother **Smt. Darshan Kaur** & my father **S. Gurjit Singh** whose support and motivation always proved to be the cause of all my achievements in the life. I am thankful to my loving sisters **Dr. Amandeep Kaur** & **Mehakdeep Kaur** for their support and care.

I owe the credit of this work to my husband **Mr. Parminder Pal Singh** and my charming daughter **Aman Assees Kaur** for enduring the pains on the account of their neglect.

I am obliged to **Mr. Vivek Sawhney** for helping me in the final editing of this document.

I am extremely thankful to all the **faculty & staff members** of EIED, Thapar University, Patiala.

Above all, I pay my reverence to Almighty God and to Veer ji.

**Date:**

**(Gagandeep Kaur)**

**Place:** Thapar University, Patiala

## ABSTRACT

This research work is outgrowth of many contemporary intelligent control techniques and their implementation. But logically intelligent actions cannot control the conventional models without certain techniques of control, control algorithms, knowledge base models, mathematical models and also the predominant contemporary fuzzy techniques which give us best results under all the factors like complexity, non linearity, parameters varying with time as well as dynamics interactions among all the parameters.

This thesis work highlights the need for managing intensive computations through modern upcoming technologies of artificial intelligence in the industry oriented problems. This work presents their association with new contemporary models. The purpose is to understand and explicate the interaction between advance fuzzy logic technologies and their impact on different uncertainties existing in industrial control systems/models.

The concept of Fuzzy Logic (FL) was conceived by Lofti Zadeh, is a problem solving industrial control system methodology that lends itself to implementation. Fuzzy set theory provides a mathematical setting for the integration of subjective categories represented by membership functions of all the parameters concerning that control activity. Fuzzy set theory and its contemporary theories are an extension of classical set theory where elements of a set have grades of membership ranging from zero for non-membership to one for full membership. Exactly as for classical sets, there exist operators, relations, and mappings appropriate for these fuzzy sets. Fuzzy set theory is established as a theoretical basis for ordination. The notion central to fuzzy systems is that truth-values in fuzzy logic type -1 or membership values in fuzzy sets are indicated by a value on the range  $[0.0, 1.0]$  with 0.0 representing absolute falseness and 1.0 representing absolute truth.

Type-2 fuzzy sets let us model and minimize the effects of uncertainties in rule-base fuzzy logic systems. However, they are difficult to understand for a variety of reasons, which we enunciate. Unfortunately, type-2 fuzzy sets are more difficult to use and understand than type-1 fuzzy sets; hence, their use is not yet widespread. In this thesis work we make type-2 fuzzy sets easy to use and understand in the hope that they will be widely used. There are (at least) four sources of uncertainties in type-1 FLCs: (1) The meanings of the words that are used in the antecedents and consequents of rules can be uncertain. (2) Consequents may have a histogram of

values associated with them, especially when knowledge is extracted from a group of experts who do not all agree. (3) Measurements that activate a type-1 FLCs may be noisy therefore uncertain. (4) The data that are used to tune the parameters of a type-1 FLCs may also be noisy. All of these uncertainties translate into uncertainties about fuzzy set membership functions. Type-1 fuzzy sets are not able to directly model such uncertainties because their membership functions are totally crisp. On the other hand, type-2 fuzzy sets are able to model such uncertainties because their membership functions are themselves fuzzy. Membership functions of type-1 fuzzy sets are two-dimensional, whereas membership functions of type-2 fuzzy sets are three-dimensional. It is the new third-dimension of type-2 fuzzy sets that provides additional degrees of freedom that make it possible to directly model uncertainties. The derivations of the formulas of type-2 fuzzy sets all rely on using Zadeh's extension principle, which in itself is a difficult concept and is somewhat adhoc, so that deriving things using it may be considered problematic; using type-2 fuzzy sets is computationally more complicated than using type-1 fuzzy sets. In this work, we focus on overcoming difficulties as stated above, because doing so makes type-2 fuzzy sets easy to use and understand. The price one must pay for achieving better performance in the face of uncertainties and is analogous to using probability rather than determinism.

A multilayer fuzzy logic model is used for the stability enhancement of the electric power system using dynamic strategies applicable to all the industrial systems. The proposed model can have multi-layers for controlling various parameters in the specified domain. The comparison with all the aforementioned models in the hierarchy shows the effectiveness of the proposed method for error estimation and controllability analysis. In multilayer structure the supervisory layer determines the region of operation of the controller based on the rate of change of the control signal of the machines. In effect, it determines membership values within the execution layer. With zero or negligible membership, values are not evaluated within the execution layer as they increase the execution time. The implementation of the supervisory layer is done by a set of fuzzy decision rules. In the execution layer, the control problem is divided into smaller sub problems, which are easier to solve. Fuzzy sets are then designed to handle each of the sub problems within the execution layer. All the sets are fuzzy in this work with a constant output but a non-fuzzy set can also be used if it is more suitable for a particular task or region of operation.

Neural network performance is dependent on the quality and quantity of training samples presented to the network for specific industrial case studies that are undertaken. Sometimes, when the training data set is small, or perhaps not fully representative of the possibility space, utilization of fuzzy techniques improves performance. One way to carry out this improvement is to represent precise data with fuzzy numbers. The neuro-fuzzy system considered in this work is a neural network that processes fuzzy numbers as well. Processing fuzzy numbers can be accomplished in a variety of ways.

Uncertainty may come from two aspects: the approximation space and the set being approximated. Using the function of fuzzy belongingness, we can define the fuzziness in the generalized fuzzy set as following; Fuzzy set theory has important mathematical tools to deal with inexact, vague and uncertain information. Every fuzzy set can be approximated by two approximation sets. Every conventional set can introduce a fuzzy set for functionality automatically. Thus conventional systems have some fuzziness too. In the present work, we have studied the uncertainty in generalized fuzzy sets based on a triangular norm. A measure of fuzziness in a conventional industrial control model has been introduced and some properties have been examined. This measure can be used to understand the essence of fuzzy set data analysis.

Incomplete data can be commonly seen in the real world applications. If all the values of uncertainties are not clearly defined then to deal with this incomplete quantitative data, Neuro Fuzzy theory can be efficiently applied. Fuzzy logic and Neuro fuzzy set modeling provide a rich and meaningful addition to standard logic. The fusion of neural network and fuzzy set can be done for the disposal of intelligent information. Fuzzy sets and fuzzy relations, which are isomorphic, could be defined uniquely. The approximation operators can be viewed by standard membership function as the core and support of fuzzy set. The neuro fuzzy theory built on training, although easy to analyze, may not provide a realistic view of relationships between elements of the universe, however a granulated view covers the universe by extending training. With the help of this hybrid theory, we can look forward for further research.

A general approach of forming effective model for implementation in the industry requires there efficient control over working models. When machine acting alone on load, has different representation. Major part of electrical power in the industry is utilized in driving these machines because they are the heart of the industrial control system.

In this Ph.D. work the industrial control system having two kinds of machines for different control operations are put forward and their problems i.e. errors in the control action are determined. They are controlled for compensation at that point so that the system could get normal operation output under any condition. Different methodologies of fuzzy logic, neuro fuzzy and multilayering are adopted for the same and best results are compared. The efficiency and the control of the system require the machine and driven machinery load has to have careful consideration for the uncertain parameter and also of the cause which directly or indirectly affects the system. The analytical approach to all the nonlinear problems through fuzzy logic and its contemporary models makes it easy. The function of fuzzy logic, neuro fuzzy and multilayer fuzzy set focuses on finding new frameworks for better performance results by abstracting the already existing systems.

# INTRODUCTION TO THESIS TEXT

This thesis focuses on error calculation and controllability analysis of contemporary fuzzy logic models with following objectives.

1. Study and analysis of an industrial control system
2. Study of various fuzzy logic models as stated earlier
3. Development of various fuzzy logic models for above industrial control system
4. Error estimation and controllability analysis of contemporary fuzzy logic models using IAE and ITAE
5. Recommendations for design and application of various fuzzy logic models

**Chapter 1** provides brief literature survey.

**Chapter 2** focuses on various design aspects of fuzzy logic model and its contemporaries. It includes description about type-1 fuzzy logic models, type-2 fuzzy logic models, neuro fuzzy models and multilayer models and the most recent fuzzy logic offshoots fuzzy set modeling. Type-1 fuzzy logic models are the most conventional non-linear compensators/controllers. Presently there are several fuzzy logic modules manufactured by various vendors. Type-1 fuzzy logic models have established their superiority and robustness as reported in the literature survey also and also verified in this research work. Type-2 fuzzy logic models have also been analyzed for several case studies in this work. Type-2 fuzzy logic models have shown better control efficiency as compared with type-1 fuzzy logic models in few cases. It is so because type-2 fuzzy logic model topography matches with the system models of few cases. Types-2 fuzzy logic models basically represent a case where there is conspicuous fuzziness in the designed fuzzy sets. The data analysis, pattern recognition, and data mining and knowledge discovery are certain latest aspects which can be optimally done with these existing methodologies of artificial intelligence. These methodologies, however, suffer from intensive computations, although some computation efficiency improvement has been made in some new developments. In this work, fuzzy neuro theory features control functions which further enhance the system performance. The representation is intended to describe the world with different universe of other contemporary model sets as a simple point set where one can put greater emphasis on analyzing

the hierarchical problem solving behavior expediently. In this work different models have been developed which have shown best results for different case studies.

In many industrial problems the task is the control of nonlinear systems, under parameter uncertainty, by an intelligent controller of known scheme structure that uses the values of the variables as per their effects on system performance which is already estimated for probable errors. In this work uncertainty of problem arises from the control requirements of an industrial system and is tackled by fuzzy logic and its contemporary methodologies help in estimating the variations of the unknown parameters, their control and compensation without external provisions. Extensive simulations have shown that these schemes work well in the case of industrial control systems.

**Chapter 3** undertakes case study of industrial control system application of engineering intelligently because intelligent techniques of fuzzy logic and its contemporaries help in estimating and controlling the errors to the extent that they can be controlled by goal driven path leading to solution from the current error state to controllable error free state. These methodologies are inevitably incorporated in real world build in uncertainties. Synchronous Generator with load as the case study is undertaken. The industrial control system requires controller models i.e type-1 fuzzy logic model, type-2 fuzzy logic model and neuro fuzzy model have been designed, developed simulated and tested for performance improvement of synchronous generator. Results have been obtained using IAE and ITAE for each of the above four models in this case. Comparisons have been made and relevant conclusions have been drawn.

The average error paper compares the performance results of conventional fuzzy logic (type-1) with advanced fuzzy logic (type-2), on a similar case study. A methodology has been presented using the linguistic knowledge for type-2 membership functions, rules, lookup tables and defuzzification along with various hard and soft decision boundaries.

It is concluded that fuzzy logic type-2 model efficiently minimizes the effect of uncertainty in the non-linear dynamical systems. It releases the burden of uncertainties, non-linearities and errors leading to efficient development of control strategy.

Type-1 membership functions are precise in the sense that once they have been chosen all the uncertainties disappear. Type-2 fuzzy sets are an extension of type-1 fuzzy sets with an additional dimension that represent the uncertainty about the degrees of membership. Type-2

fuzzy sets are difficult to use and understand than type-1 fuzzy logic controller. It is concluded that type-2 is a better control alternative over type-1. It is so, because type-2 fuzzy logic controller compensates for the fuzziness within the fuzzy sets, which is in the form of band instead of line on the boundaries of fuzzy sets. The modeling of type-2 fuzzy logic controller is comparatively complex as compare with type-1 and also the execution time of this controller is large.

The industrial applications, which are not very much speed specific, but complex, and aim at achieving highest possible accuracy at their outputs, for them type-2 fuzzy logic controller is a better control alternative. Type-1 controller is not capable of linguistic uncertainties. Type-2 fuzzy logic controller efficiently handles the linguistic uncertainties and also leads to the creation of mechanism by which the fuzzy sets can be made more flexible and adaptive. It also demonstrates the ease and flexible switching from conventional to revolutionized technologies.

**Chapter 4** undertakes case study of industrial application of DC Motor under loaded condition as the case study. The industrial control system requires controller models i.e type-1 fuzzy logic model, type-1 fuzzy logic model and neuro fuzzy model have been designed, developed simulated and tested for uncertainty compensation and speed control of DC Motor. Results have been obtained for best fuzzy entropy using IAE and ITAE for each of the above four models in this case. Comparisons have been made and relevant conclusions have been drawn.

**Chapter 5** compares all control models in an integrated manner for all the above two case studies as given in chapter 3 & 4. Various performance curves have been drawn. Complete controllability analyses have been done. Errors have been obtained in the various cases. Discussions have been made for compatibility of every control model and individual case study. It also deals with the conclusions and future scope. We have shown that models having best controllability and lowest error levels. Contemporary models, which are definitely superior over existing Fuzzy set models, follow it but somehow little inferior than contemporary ones especially in the cases of very high order non linear systems. It is concluded that hybrid neuro fuzzy contemporary models best follow conventional models. There are fluctuating performance results shown by type-1 and type-2 fuzzy logic models. In two case studies type-2 is better with regard to controllability and error over type-1. In one of the case study type-2 has shown inferior results and type-1 is better. It is concluded that reliability of the data is the key for selection of either type-1 fuzzy logic model or type-2 fuzzy logic model. It is further concluded that type-1

fuzzy logic model is definitely better than type-2 fuzzy logic model even for very higher order non linear systems if the data reproducibility and repeatability is not high. Type-2 fuzzy logic model is a definitely better control preposition.

During the course of this research work and based on comments of various reviewers several avenues for continuation of this study became evident. Like a practical system model, observability, state estimation and parameter identification have been ignored. All these can also be added to study comparative performance of contemporary fuzzy logic control models. This development in knowledge based control incorporating the overall effectiveness of the implemented intelligent algorithm proves their ability in improving the entire system response. It explores the possibilities of reducing the all kind of uncertain unknown errors in the real time processes running with these intelligent contemporary fuzzy based controllers. Fuzzy logic and its contemporary control techniques have been utilized in several typical conventionally used controllers. The upcoming systems which are integrated using all commercially & technically available models give ultimate results.

# LIST OF PUBLICATIONS

## International Journals

1. Kaur G., Singh Y, “Design and Development of Efficient Fuzzy Logic Based Selective Controller for Performance Improvement of Synchronous Generator” Journal on Advances-B Signal Processing and Pattern Recognition, Vol. 49, NO. 1, pp 1-14, 2006
2. Kaur G., Singh Y, “Uncertainty Compensation and Efficient Speed Control of DC Shunt Motor using Advanced Fuzzy Logic: a Case Study” Journal on Advances-C Automatic Control (Theory and Application), Vol. 62, NO. 2, pp 72-83, 2007
3. Kaur G., Singh Y, “An efficient neuro-fuzzy control of synchronous generator: a case study”, International Journal of Physical sciences, Vol. 6 (13), pp 3031-3040, 2011.

## National Journals

1. Kaur G., Singh Y, “Fuzzy sets, Rough sets and Quotient space: Issues and Comparison” Invertis Journal of Science and Technology, Vol. 2, No. 2, pp 133-144, April – June 2009

## International Conferences / National Conferences

1. Kaur G., Singh Y, “Speed Control of DC Motor using Advanced Fuzzy Logic Models” National Conference on Intelligent Systems and Networks, February 25-26, 2005, Jagadhari
2. Kaur G., Singh Y, “Efficient Speed Control of DC Motor using Advanced Fuzzy Logic” International Conference on Modelling and Simulation (MS-2006), April 3-5, 2006, Kuala Lumpur, Malaysia
3. Kaur G., Singh Y, “Fuzzy set theory, Rough set theory and Quotient space theory: A Study” in ICCIIS 2007 World Congress on Engineering 2007, July 2-4, 2007, London
4. Kaur G., Singh Y, “An Adaptive Algorithm for Speed Control of DC Motor” in ICCIIS 2007 World Congress on Engineering 2007, July 2-4, 2007, London

# TABLE OF CONTENTS

Certificate	iii	
Acknowledgement	iv	
Abstract	v –viii	
Introduction to Thesis Text	ix-xii	
List of Publications	xiii	
Table of Contents	xiv -xvi	
List of Figures	xvii -xxv	
List of Tables	xxvi	
List of Abbreviation	xxvii	
<b>Chapter- 1</b>	<b>Literature Review</b>	<b>1-19</b>
<b>Chapter-2</b>	<b>Fuzzy Logic and Its Contemporary Models</b>	<b>20-58</b>
Introduction		20
2.1 Fuzzy Logic		20
2.1.1 Type-1 Fuzzy Sets		24
2.1.2 Type-2 Fuzzy Sets		33
2.1.3 Artificial Neural Network		37
2.1.4 Neuro-Fuzzy System		42
2.1.4.1 Neuro-fuzzy Modeling		43
2.2 Robustness and Fuzzy Logic		49
2.3 Fuzzy Control		49
2.4 Hierarchical Modeling		56
2.5 Control Evaluation		57
2.6 Conclusions		58
<b>Chapter- 3</b>	<b>Synchronous Generator: Case Study</b>	<b>59-119</b>
Introduction		59
3.1 Synchronous Generator		59

3.2	Per phase equivalent diagram of synchronous generator	68
3.3	Steady state power angle characteristics	70
3.4	Power and torque in synchronous generators	73
3.5	Stability analysis	74
3.6	Mathematical modeling of synchronous generator	77
3.6.1	Reference Frame Theory	77
3.6.2	Model of a Basic 2 $\phi$ Salient Pole Synchronous Machine	79
3.6.3	Relative Angular Position between Rotor and Stator	79
3.6.4	Generator Model	80
3.6.4.1	Phase Variable Model	80
3.6.4.2	Torque Equation in Machine Variables	81
3.6.4.3	The d-q Variable Model	81
3.7	Coupling of synchronous generator with exciter system	87
3.8	Speed control of synchronous generator system: proposed system	92
3.8.1	Type-1 membership function for fuzzy control	96
3.8.2	Type-2 membership function for fuzzy control	98
3.8.3	Fuzzy speed control of synchronous generator with load	102
3.8.4	No load condition	104
3.8.5	On load condition	106
3.9	Neuro-fuzzy control of synchronous generator	113
3.10	Control Parameter Evaluation	119
3.11	Conclusion	119
<b>Chapter- 4</b>	<b>DC Motor: Case Study</b>	<b>120-160</b>
	Introduction	120
4.1	Features of DC motor	121
4.2	DC motor modeling	123
4.3	Separately excited shunt DC motor	128
4.4	Speed control of DC motor	135
4.5	Starting of 5 Hp, 240V, DC motor with a 3 step resistance starter	136
4.6	Speed control of separately excited DC motor	140
4.7	Type-1 membership function for fuzzy control	143

4.8	Type-2 membership function for fuzzy control	146
4.9	Fuzzy controller for DC motor (Type-1)	150
4.10	Neuro-fuzzy control of DC motor	154
4.11	Speed control of DC motor at different load conditions	156
4.12	Conclusion	160
<b>Chapter- 5</b>	<b>Results and Discussions</b>	<b>161-176</b>
5.1	Control evaluation	161
5.1.1	Control evaluation: Synchronous generator	162
5.1.2	Control evaluation: DC motor	170
5.2	Control parameters	174
5.2.1	Synchronous generator	175
5.2.2	DC motor	175
5.3	Conclusion	176
	<b>Conclusion and Future Scopes</b>	<b>177-178</b>
	<b>References</b>	<b>179-201</b>

## LIST OF FIGURES

Figure 2.1	Fuzzy logic membership function	24
Figure 2.2	Various types of fuzzy logic membership function	27
Figure 2.2 (a)	Triangular membership	27
Figure 2.2 (b)	Trapezoidal membership	27
Figure 2.2 (c)	Gauss membership	27
Figure 2.2 (d)	Generalized bell membership	27
Figure 2.3	Block diagram of fuzzy logic system	28
Figure 2.4	MAMDANI based fuzzy inference system	29
Figure 2.5	Sugeno type fuzzy inference system	29
Figure 2.6	Fuzzy rule bases in the case of a Mamdani fuzzy inference system	31
Figure 2.7	Surface view in the case of a MAMDANI fuzzy inference system	32
Figure 2.8	Membership function interval type 2 fuzzy logic set	33
Figure 2.9	Operation on interval type 2 membership function	34
Figure 2.10	Mamdani fuzzy inference system on interval type 2 fuzzy logic	35
Figure 2.11	Karnik-mendel algorithms to locate centroid on interval type 2 fuzzy logic	36
Figure 2.12	Type 2 fuzzy logic system	37
Figure 2.13	Structure of single neuron	38
Figure 2.14	Different types of nonlinear activation function	39
Figure 2.14 (a)	Signum function or hard limiter	39
Figure 2.14(b)	Threshold function	39

Figure 2.14 (c)	Sigmoid function	39
Figure 2.14 (d)	Piecewise linear	39
Figure 2.15(a)	MLP block diagram	40
Figure 2.15(b)	MLP structure	40
Figure 2.15(c)	Flow chart for solving ANN	41
Figure 2.16	Schematic of neuro-fuzzy system	43
Figure 2.17	General architecture of ANFIS	44
Figure 2.18	Schematic of ANFIS in MATLAB	44
Figure 2.19	Design process for system with fuzzy hardware	45
Figure 2.20	Structural description of fuzzy hardware	46
Figure 2.21	Layout generation for fuzzy hardware	46
Figure 2.22	FuzzyTech software screenshot	47
Figure 2.23	Fuzzy tank controller using fuzzytech	48
Figure 2.24	Classical feedback control structure	49
Figure 2.25	Fuzzy logic control structure	50
Figure 2.26	Membership functions for inputs and output	52
Figure 2.27	MAMDANI based fuzzy control system	52
Figure 2.28	Surface plot of inputs and output	53
Figure 2.29	Self organizing fuzzy logic control system	54
Figure 3.1	Basic prime-mover generator system	60
Figure 3.2	Classification of synchronous generator system	61
Figure 3.3	The synchronous generator on load	62
Figure 3.4	EMF and current phasors	62

Figure 3.5	Synchronous generator connected with load	63
Figure 3.6 (a)	Schematic illustration of synchronous machine salient pole	64
Figure 3.6 (b)	Round or cylindrical rotor	64
Figure 3.7	Flux density distribution in air gap and induced EMF in the phase winding	65
Figure 3.7 (a)	Two pole	65
Figure 3.7 (b)	Four pole synchronous machine	65
Figure 3.8 (a)	Rotating magnetic field	67
Figure 3.8 (b)	The air gap performance per pole v/s rotor position	67
Figure 3.9 (a)	Equivalent circuit diagram of synchronous generator along d and q axis	69
Figure 3.9 (b)	Circuit for cross coupling saturation	69
Figure 3.10	Power flow diagram of synchronous generator	70
Figure 3.11	Synchronous machine connected to an external system	71
Figure 3.12	Graph between $E_{af}$ v/s power and $V_t$ v/s power angle of the synchronous generator	72
Figure 3.13	Phasor models	73
Figure 3.13 (a)	Lagging power factor (Over excited)	73
Figure 3.13 (b)	Leading power factor (Under excited)	73
Figure 3.14	Frequency response and stability analysis of synchronous generator	76
Figure 3.15	Synchronous generator frequency response gain and phase margin	76
Figure 3.16	d-q model of synchronous generator	77
Figure 3.17 (a)	d-q axis representation in the case of synchronous generator	78
Figure 3.17 (b)	d-q model of synchronous generator	78
Figure 3.18	Equivalent circuit of generator in reference frame	83
Figure 3.19	Round rotor machine phasor equation	83
Figure 3.20	Phasor diagram of power flow of synchronous generator	84

Figure 3.21	d-q mathematical model of synchronous generator	84
Figure 3.22	Simulink model of synchronous generator	85
Figure 3.23 (a)	Simulation of synchronous generator with Simulink	85
Figure 3.23 (b)	Rotor speed of synchronous generator	86
Figure 3.23 (c )	Field voltage of synchronous generator	86
Figure 3.23 (d)	Stator current of synchronous generator	86
Figure 3.23 (e)	Ia and Va of synchronous generator	86
Figure 3.24	Different transient and steady state parameters of synchronous generator at step increase in torque	86
Figure 3.25	Simulink representation of synchronous generator with exciter system	87
Figure 3.26	Voltage of diode D1 and current of diode D1 and D3	88
Figure 3.27	3 phase voltage and current	89
Figure 3.28	3 phase voltage and current	89
Figure 3.29	Speed regulation of synchronous generator connected with exciter system	90
Figure 3.30	Synchronous machine without load	91
Figure 3.31	Graphs for stator current, rotor speed, torque, field voltage when the synchronous machine is started	92
Figure 3.32	Control block diagram of proposed system	92
Figure 3.33	Flow chart of control system design and evaluation	94
Figure 3.34	Schematic diagram of synchronous generator	95
Figure 3.35	Membership function for type I fuzzy inputs $e(t)$ and $de(t)$	97
Figure 3.36	Membership function for fuzzy type I output	97
Figure 3.37	Membership function for type II fuzzy inputs $e(t)$ and $de(t)$	98
Figure 3.38	Membership function for fuzzy type II output	99
Figure 3.39	Fuzzy type I control of synchronous generator	100
Figure 3.40	Graphs for stator current, rotor speed, torque, voltage for type I	100

	fuzzy membership function	
Figure 3.41 (a,f)	Electromagnetic torque	101
Figure 3.41 (b,e)	Speed	101
Figure 3.41 (c,d)	Stator current and voltage	101
Figure 3.42	Fuzzy speed control of synchronous generator with load	102
Figure 3.43	Graphs for rotor speed, torque, power and electrical torque	103
Figure 3.44	Graphs for armature voltage	103
Figure 3.45	Graphs for rotor speed, mechanical torque, electrical power and torque	104
Figure 3.46	Variation in voltage and current when no load is added	105
Figure 3.47	Variation in power and torque when no load is added	105
Figure 3.48	Variation in torque, $V_f$ , power at no load condition	106
Figure 3.49	Variation in $V_f$ and $I_s$ at reactive load condition	106
Figure 3.50	Variation in torque, $V_f$ , power at reactive load condition	107
Figure 3.51	Variation in $V_f$ in pure reactive load condition	107
Figure 3.52	Variation in voltage and $I_s$ at load condition added after 50 VAR	108
Figure 3.53	Variation of $V_f$ added after 50 VAR	109
Figure 3.54	Variation in torque power at no load added after 50 VAR	109
Figure 3.55	Variation in $V_f$ at load condition added after 200Hz	110
Figure 3.56	Variation in voltage and current load condition added after 200Hz	110
Figure 3.57	Variation in torque, $V_f$ , power at 200Hz load	111
Figure 3.58	Variation in voltage and current at active load	111
Figure 3.59	Variation in torque, $V_f$ and power at 200W	112
Figure 3.60	Neuro-Fuzzy controller for synchronous generator	113
Figure 3.61	Detailed schematic diagram for adaptive controller for synchronous generator	114
Figure 3.62	Graph between error and epoch of neural network	116
Figure 3.63	Fuzzy-neuro architecture implemented in synchronous generator	116

Figure 3.64	Simulink representation of neuro-fuzzy control of synchronous generator	117
Figure 3.65	Response curve of stator current, rotor speed, torque in fuzzy-neuro control of synchronous generator	118
Figure 4.1	DC motor operation (current and magnetic field direction)	122
Figure 4.1 (a)	DC motor operation	122
Figure 4.1 (b)	Change in current direction when conductor passes through neutral zone	122
Figure 4.1 (c)	Change in direction of magnetic field when conductor passes through neutral zone	122
Figure 4.2	Case study DC motor	123
Figure 4.3	Armature controlled DC motor circuit	123
Figure 4.4	Block diagram representation of armature controlled DC motor	124
Figure 4.5	Functional block diagram of armature controlled DC motor	125
Figure 4.6	Simulink model of armature controlled DC motor for step input	126
Figure 4.7	Graph of velocity for step input for an armature controlled DC motor	126
Figure 4.8	Graph of angle for step input for an armature controlled DC motor	127
Figure 4.9	Simulink model of armature controlled DC motor for ramp input	127
Figure 4.10	Graph of velocity for ramp input for an armature controlled DC motor	128
Figure 4.11	Graph of angle for ramp input for an armature controlled DC motor	128
Figure 4.12	Equivalent circuit diagram for separately excited DC motor	129
Figure 4.13	Equivalent circuit diagram for shunt DC motor	129
Figure 4.14	Graph of speed and armature voltage at different torques	131
Figure 4.15 (a)	Torque	132
Figure 4.15 (b)	Power limitations of combined armature-voltage and field-current methods of speed control	132
Figure 4.16	Torque v/s speed characteristics of a shunt DC motor	133

Figure 4.17	Speed v/s field resistance of a shunt DC motor	133
Figure 4.18	Speed v/s torque for a series DC motor	134
Figure 4.19	Simulink model of field resistance speed control method	135
Figure 4.20	Simulink model of armature voltage speed control method	136
Figure 4.21	Simulink model of starting of a DC motor	136
Figure 4.22	X-Y graph between speed and armature current of DC motor	137
Figure 4.23	Speed of DC motor	137
Figure 4.24	Armature current of DC motor	138
Figure 4.25	Torque of DC motor	138
Figure 4.26	Armature voltage of DC motor	139
Figure 4.27	Switching scheme for PWM	140
Figure 4.28	Speed control scheme of DC motor	140
Figure 4.29	Simulink model of speed control of a DC motor using speed controller and current controller	142
Figure 4.30	Graphs for armature voltage, armature current and speed of speed control of a DC motor using speed controller and current controller	142
Figure 4.31	Graphs for armature voltage, armature current and speed of speed control of a DC motor using speed controller and current controller	143
Figure 4.32	Fuzzy membership function for type I fuzzy inputs, $e(t)$ and $de(t)$	144
Figure 4.33	Fuzzy membership function for type I fuzzy output	145
Figure 4.34	Surface view of fuzzy inference system	146
Figure 4.35	Fuzzy membership function for type II fuzzy inputs $e(t)$ and $de(t)$	146
Figure 4.36	Fuzzy membership function for type-II fuzzy output $u(t)$	147
Figure 4.37	Artificial neural network used for training neuro fuzzy controller	147
Figure 4.38	Neuro-fuzzy speed control block diagram for DC motor	148
Figure 4.39	Simulink model of DC motor speed control	148

Figure 4.40	Graph for armature current and torque of DC motor	149
Figure 4.41	Graph for $w$ (rad/sec) of DC motor	149
Figure 4.42	Simulink model of fuzzy type I based speed control of DC motor	150
Figure 4.43	Speed response of DC motor using type I fuzzy controller	150
Figure 4.44	Speed response of DC motor using type II fuzzy controller	151
Figure 4.45	Bode magnitude and phase response of DC motor	151
Figure 4.46	Simulink model of DC motor with PI controllers in current and velocity loop	152
Figure 4.47	Simulink model of DC motor with PI controllers in current and velocity loops	152
Figure 4.48	Simulink model of DC motor with fuzzy controller in current loop	159
Figure 4.49 (a)	Armature current plot	159
Figure 4.49 (b)	Rotor Speed plot	159
Figure 4.50	Architecture of artificial neural network	154
Figure 4.51	Simulink model of DC motor speed control using artificial neural network controller	154
Figure 4.52	Angular speed controlled by neuro-fuzzy control	155
Figure 4.53	Current of DC motor controlled by neuro-fuzzy control	155
Figure 4.54	Torque of DC motor controlled by neuro-fuzzy control	155
Figure 4.55	Armature voltage, armature current and rotor speed of DC motor with no load condition	156
Figure 4.56	Armature voltage, armature current and rotor speed of DC motor with pure resistive load condition	157
Figure 4.57	Armature voltage, armature current and rotor speed of DC motor with reactive load condition at 50 VAR	158
Figure 4.58	Armature voltage, armature current and rotor speed of DC motor with frequency load condition added 200Hz	159
Figure 4.59	Armature voltage, armature current and rotor speed of DC motor with frequency load condition	160
Figure 5.1	Variation in voltage and current of synchronous generator at no load condition	162
Figure 5.2	Variation in torque, $V_f$ and power of synchronous generator at no load condition	163
Figure 5.3	Variation in voltage and current of synchronous generator at resistive load	164

Figure 5.4	Variation in torque, $V_f$ and power of synchronous generator at resistive load	165
Figure 5.5	Variation in voltage and current of synchronous generator at inductance load	166
Figure 5.6	Variation in torque, $V_f$ and power of synchronous generator at load added at 50VAR	167
Figure 5.7	Variation in voltage, current of synchronous generator at frequency load added at 200Hz	167
Figure 5.8	Variation in torque, $V_f$ and power at 200Hz load	168
Figure 5.9	Variation in voltage and current when active power load added at 200W	169
Figure 5.10	Variation in torque, $V_f$ and power at 200W load condition	170
Figure 5.11	$V_a$ , $I_a$ and $w_m$ of DC motor with no load condition	171
Figure 5.12	$V_a$ , $I_a$ and $w_m$ of DC motor with pure resistive load condition	172
Figure 5.13	$V_a$ , $I_a$ and $w_m$ of DC motor with reactive load condition at 50 VAR	173
Figure 5.14	$V_a$ , $I_a$ and $w_m$ of DC motor with frequency load condition added 200Hz	174

## LIST OF TABLES

Table 2.1	Linguistic variables for fuzzy control	51
Table 2.2	Rule matrix for MAMDANI fuzzy inference system	53
Table 2.3	Different performance indices in classical control system	57
Table 3.1	Linguistic variable for type –I fuzzy control	97
Table 3.2	If-then rule base for fuzzy control	98
Table 3.3	Fuzzy rule base for inputs and output	115
Table 3.4	IAE and ITAE calculations	119
Table 4.1	Fuzzy Rule Base and fuzzy inference system	145
Table 4.2	If-then rule base	145
Table 5.1	Different control parameters for controllers in synchronous generator	175
Table 5.2	Different control criterion for controllers in synchronous generator	175
Table 5.3	Different control parameters for controllers in DC motor	175
Table 5.4	Different control parameters for controllers in synchronous generator	175

## **LIST OF ABBREVIATIONS**

ANN	Artificial Neural Network
ANFIS	Adaptive Neuro-Fuzzy Inference System
DC	Direct Current
EMF	Electro Magnetic Force
FIS	Fuzzy Inference System
FMRLC	Fuzzy Model Reference Learning Controller
IAE	Integral Absolute Error
ITAE	Integral Time Absolute Error
MMF	Magneto Motive Force
MLP	Multi Layer Perceptron
SG	Synchronous Generator

---

# CHAPTER-1

## LITERATURE SURVEY

---

**Hussein F. Soliman** et.al developed a novel fuzzy logic control scheme to regulate the speed of a permanent magnet dc motor drive via armature voltage control. The pm dc motor drive is fed from a 3 phase thyristor controlled rectifier. The proposed FL rule based controller scheme utilizes both motor current and speed errors. The firing delay angle of the 3-phase converter is determined as the output of a modified weighted centre of area defuzzifier stage, with an assigned rule base. The controller utilizes novel on-line adjustable defuzzification weighting criteria to ensure minimum speed overshoot/undershoot as well as reduced motor transient inrush current conditions. The on-line tuning criterion is based on the speed error excursion level [1].

**Yiming Yu** et.al presents a new method of rule based fuzzy logic inferencing solely based on a many-valued logic. Fuzzy logic can be considered as an extended set many-valued logic. Many-valued logic is extended from two-valued logic but differs from it in that each has different sets of primitives. The authors believe that fuzzy logic should be solely based on many-valued logic. There are many fuzzy logic inferencing methods. Most of them are not solely based on many-valued logic and their inferencing equations can not be derived from many valued logic. Thus, their compositions are not necessarily dependent on their conditional propositions. In this paper, an implication connective of Lukasiewicz many-valued logic is proposed to be a basis of the conditional proposition in a new fuzzy logic inferencing method. Corresponding to this implication connective, a  $\max-\partial$  composition is derived from Lukasiewicz many-valued logic and it is shown to fit human intuition. The advantage of the new fuzzy logic inferencing, over other fuzzy logic inferencing, is that it provides a solid theoretical basis for further study of its inferencing behavior when used in a certain application, such as in a fuzzy controller [2].

**Pierre Guillemin** et.al has implemented the fuzzy logic in a standard microcontroller to regulate the speed of a universal motor by a real time adjustment of the motor current. This microcontroller directly tunes the motor current by means of a chopper converter. Starting from a basic food process or application, the paper practically shows how a fuzzy logic approach can be applied to build a closed speed regulation loop from a very low cost tachogenerator. Practical guidelines are successively given from the initial concept analysis phase, up to the final generation of the executable code to be loaded in the microcontroller. It also gives the practical procedure to define the input parameters and to build fuzzy logic rules using the fuzzy logic development tool. Finally, the major benefits of this paper lie in an original approach where fuzzy logic is applied to fast “real-time” regulation loop without requiring any specific expertise in conventional methods of regulation. Benefits are discussed and concrete results are given in the paper [7].

**F. Ashrafzadeh** et.al proposes an optimal synthesis of a sliding mode controller using fuzzy logic which outperforms the traditional sliding mode controller. A description of a variable structure control with sliding mode is presented. The problems associated with this control technique are then addressed. Fuzzy logic as one solution to these problems is explained. The concept of a fuzzy switching surface is introduced to solve the chattering problem in the switching mode. The optimal membership function for this fuzzy surface is then found using a genetic algorithm. In the reaching mode, another variable structure is introduced by fuzzy partitioning the state space which is different from the variable structure at the switching surface in the sense of having a control action with variable amplitude but constant sign. The optimal structure of each side of the fuzzy switching surface is found by optimal input membership functions and output singletons using the proposed approach. This approach is applied to the indirect field oriented control of an induction motor. The simulation results verify the efficiency of the proposed approach [16].

**Juan Moreno** et.al advantages of using fuzzy logic in steady-state efficiency optimization for induction motor drives are described. Experimental results of a fuzzy logic based optimum flux search controller are presented. For transient states, a new original idea is introduced which has a fuzzy logic based controller and actuator as a supervisor. It is proposed to work with reduced flux levels during transients to optimize

efficiency also in dynamic mode. Two different rule tables are designed, for torque transitions and for reference speed changes. With this controller, efficiency can be improved in transients, and also search controller convergence speed is increased. Experimental results with a 1.5 kW induction motor drive demonstrate the validity of the proposed methods [31].

**Mao-Fu Lai** et.al presents a novel design using fuzzy logic control and phase-locked loop to obtain a DC motor speed control system with excellent regulation and high robustness. The fuzzy logic controller is incorporated in order to achieve quick control of motor speed smoothly. The fuzzy logic controller enhances the robustness of the motor control system, which can handle abrupt load variation and exhibit good disturbance behavior. The PLL becomes effective at steady state conditions when the speed error is small. A control scheme using fuzzy control of DC motor speed with extremely accuracy provided by PLL is implemented. Simulation demonstrates the effectiveness of the proposed scheme. Test results show that a system which consists of both fuzzy control and PLL can yield a high performance DC motor speed control system [49].

**F.S. Smith** et.al aimed to form the basis of a methodology to guide the selection of an appropriate fuzzy logic controller for a given task. Different fuzzy inference techniques used in fuzzy logic controllers are compared initially and then the effects of using different defuzzification techniques on the same fuzzy logic controller are examined. The results of these experiments could then be used as the basis for a selection methodology for choosing an appropriate fuzzy logic controller. An initial examination of the performance of the various fuzzy logic controllers revealed those fuzzy logic controllers that failed to perform satisfactorily. A more detailed comparison, between those different controllers that performed satisfactorily, was made using a wide range of criteria, including the average force applied to the system and the range of initial states of the system that the controller can control [64].

**J. K. Chatterjee** et.al presents a hybrid i.e a combination of fuzzy and PI closed loop speed controller and its design for vector controlled induction motor drive (VCIMD). This controller has been implemented on a three phase, 415V, 0.75kW squirrel cage induction motor. Results are presented for the response of a vector controlled induction motor drive with a hybrid controller, combining the fuzzy logic and PI controller. The drive response

obtained using hybrid controller are compared to the corresponding drive performance obtained using PI and fuzzy logic controller. Test responses of the developed variable speed drive along with simulated response are calculated and discussed in detail [71].

**E Cheong** et.al has concluded that in conventional fuzzy logic controllers, the computational complexity increases with the dimensions of the system variables. The number of rules increases exponentially as the number of system variables increases. Hierarchical fuzzy logic controllers have been introduced to reduce the number of rules to a linear function of system variables. However, the use of hierarchical fuzzy logic controllers raises new issues in the automatic design of controllers, namely the coordination of outputs of sub-controllers at lower levels of the hierarchy. In this paper, a method for automating the design of hierarchical fuzzy logic controllers using an evolutionary algorithm called differential evolution has been implemented. The applicability of this method lies in developing a two-stage hierarchical fuzzy logic controller for controlling a cart-pole with four state variables [87].

**S. Palani.** et.al has obtained the tracking of maximum efficiency point of a lightly loaded induction motor using search technique which is time consuming and the machine is subjected to many step changes of voltage which is undesirable. This paper presents a novel technique for energy efficient operation of voltage controlled induction motor drive using fuzzy logic principles. In the proposed method, the time required to converge to the best efficiency point of the drive is minimum and the machine is subjected only to one step change of voltage, irrespective of load change. The fuzzy logic variables and the fuzzy rules are formulated based on experimental investigations. The rule base for the optimum voltage identification is generated in the entire operating range of the motor with a no priori knowledge of the machine parameters. The fuzzy logic estimator is then used for performance optimization of induction motor and the simulation results are presented. The simulation results demonstrate the efficiency of the fuzzy logic estimator based voltage controller [88].

**Jong-Bae Lee** et.al focuses on a low cost speed control system using a fuzzy logic controller for a brushless DC motor. In a digital controller of brushless DC motor, the control accuracy is of a high level and it has a fast response time. They used a hall IC signal for the permanent magnet rotor position and for the speed feedback signals, and

also for a micro controller of 8-bit type (80C86). They also designed the fuzzy logic controller and implemented it for the speed control system of brushless DC motor. To acquire an accurate fuzzy logic control algorithm, a simulation with the MATLAB program had been made, while the performance of the system, done with an experiment for a unit step response was also verified [95].

**Sumana Chowdhuri** et.al has given the fact that the conventional controllers used for DC machines are static and their parameters are fixed through proper design. The classical approach is to use a PID controller with constant parameters after analyzing the stability criterion. Modern approach is to use controllers based on fuzzy logic or other AI techniques. The authors have chosen a speed-tracking problem where a dc machine has to follow a time varying speed demand. The controller coefficients are fixed through an evolutionary algorithm. Representative values of steady state error, maximum overshoot and transient rise time are computed through feature extraction algorithms. Then the fitness of each member is computed as a fuzzy value based on some predefined fuzzy functions involving the feature values. This fuzzy fitness value governs the selection of coefficients through a genetic algorithm until convergence is obtained. The performance has been studied with various fitness functions and the results are found to be satisfactory [116].

**Ahmed Rubaai** et.al presents an online identification and control method for DC motor using learning adaptation of neural networks. This paper tackles the problem of the speed control of a DC motor in a very general sense. Use is made of the power of feed forward artificial neural networks to capture and emulate detailed nonlinear mappings, in order to implement a full nonlinear control law. The random training for the neural networks is accomplished online, which enables better absorption of system uncertainties into the neural controller. An adaptive learning algorithm attempts to keep the learning rate as large as possible while maintaining the stability of the learning process is proposed. This simplifies the learning algorithm in terms of computation time which is of special importance in real-time implementation. The effectiveness of the control topologies with the proposed adaptive learning algorithm is demonstrated. It is found that the proposed adaptive learning mechanism accelerates training speed. Promising results have also been

observed when the neural controller is trained in an environment contaminated with noise [121].

**M. N. Uddin** et.al presents a novel speed control scheme of an induction motor (IM) using fuzzy logic control. The fuzzy logic controller (FLC) is based on the indirect vector control. The fuzzy logic speed controller is employed in the outer loop. The complete vector control scheme of the IM drive incorporating the FLC is experimentally implemented using a digital signal processor board DS-1102 for the laboratory 1 hp cage induction motor. The performances of the proposed FLC based IM drive are investigated and compared to those obtained from the proportional integral (PI) controller based drive both theoretically and experimentally at different dynamic operating conditions such as sudden change in command speed, step change in load, etc. The comparative experimental results show that the FLC is more robust and hence found to be a suitable replacement of the conventional PI controller for the high performance industrial drive applications [125].

**Jun Oh Jang** et.al has designed a deadzone compensator is designed for a dc motor system using a fuzzy logic controller. The classification property of fuzzy logic systems makes them a natural candidate for the rejection of errors induced by the deadzone, which has regions in which it behaves differently. A tuning algorithm is given for the fuzzy logic parameters, so that the deadzone compensation scheme becomes adaptive, guaranteeing small tracking errors and bounded parameter estimates. Formal nonlinear stability proofs are given to show that the tracking error is small. The fuzzy logic deadzone compensator is implemented on a dc motor system to show its efficacy [134].

**R. Sankaran** et.al presented a paper on adaptive neuro-fuzzy controller for improved performance of a permanent magnet brushless DC motor. This paper deals with the mathematical modeling of a permanent magnet brushless DC (PMBLDC) motor, considering the non-linearities in the torque-balance equation under closed loop operation with a set reference speed. A controller based on adaptive neuro-fuzzy inference system (ANFIS) is developed to minimize overshoot and settling time following sudden changes in load torque. The entire system is modeled and simulated using the Simulink toolbox. The advantages of fuzzy logic and neural network are fused together to form a connectionist adaptive network based fuzzy logic controller. Required data for training

the ANFIS controller is generated by simulation of the closed loop system with Conventional PID controller. The overshoot present in the transient response with conventional controller is eliminated using the ANFIS controller. The transient deviation of the response from the set reference following variation in load torque is found to be negligibly small along with 8 desirable reduction in settling time for the ANFIS controller [139].

**Daniel Ramot** et.al has proposed a novel framework for logical reasoning, termed complex fuzzy logic. Complex fuzzy logic is a generalization of traditional fuzzy logic, based on complex fuzzy sets. In complex fuzzy logic, inference rules are constructed and fired in a manner that closely parallels traditional fuzzy logic. The novelty of complex fuzzy logic is that the sets used in the reasoning process are complex fuzzy sets, characterized by complex-valued membership functions. The range of these membership functions is extended from the traditional fuzzy range of  $[0,1]$  to the unit circle in the complex plane, thus providing a method for describing membership in a set in terms of a complex number. Several mathematical properties of complex fuzzy sets, which serve as a basis for the derivation of complex fuzzy logic, are reviewed in this paper. These properties include basic set theoretic operations on complex fuzzy sets namely complex fuzzy union and intersection, complex fuzzy relations and their composition, and a novel form of set aggregation i.e vector aggregation. Complex fuzzy logic is designed to maintain the advantages of traditional fuzzy logic, while benefiting from the properties of complex numbers and complex fuzzy sets. The introduction of complex-valued grades of membership to the realm of fuzzy logic generates a framework with unique mathematical properties, and considerable potential for further research and application [165].

**Colin Grantham** et.al presents a new method of on-line estimation for the stator and rotor resistances of the induction motor in the indirect vector controlled drive, using fuzzy logic and artificial neural networks. The back propagation algorithm is used for the training of the neural networks for rotor resistance identification. The error between the desired state variable of an induction motor and the actual state variable of a neural model is back propagated to adjust the weights of the neural model, so that the actual state variable tracks the desired value. A fuzzy logic real time estimator is used as the stator resistance observer, to eliminate the error in rotor resistance estimation. The

performance of the induction motor drive with the above rotor and stator resistance estimators, is investigated for torque and flux responses, to analyze the effects of stator resistance observer on rotor resistance identification, for variations in the stator and rotor resistances from their nominal values. Both these resistances are estimated experimentally, in a vector controlled induction motor drive and found to give accurate estimates. The rotor resistance estimation was found to be insensitive to the stator resistance variations both in simulation and experiment [169].

**Yen-Shin Lai** et.al has presented a new hybrid fuzzy controller for direct torque control (DTC) induction motor drives. The newly developed hybrid fuzzy control law consists of proportional-integral (PI) control at steady state, PI-type fuzzy logic control at transient state, and a simple switching mechanism between steady and transient states, to achieve satisfied performance under steady and transient conditions. The features of the presented new hybrid fuzzy controller will be highlighted by comparing the performance of various control approaches, including PI control, PI-type fuzzy logic control (FLC), proportional-derivative (PD) type FLC, and combination of PD-type FLC and I control, for DTC-based induction motor drives. The pros and cons of these controllers will be demonstrated by intensive experimental results. It will be shown that the presented induction motor drive is with fast tracking capability, less steady state error, and robust to load disturbance while not resorting to complicated control method or adaptive tuning mechanism. Experimental results derived from a test system will be presented confirming the above-mentioned claims [170].

**Khwaja M. Rahman** et.al presents a method for estimating the machine parameters of a synchronous motor. The presented method is equally applicable for wound filled synchronous motor, synchronous reluctance motor, or permanent magnet (PM) synchronous motor, both interior and surface mount type. The method works particularly well for machines having a significant amount of space harmonics, such as synchronous reluctance and interior PM (IPM) machines, where the harmonics are predominantly the slot harmonics. It is also well suited for surface PM machines operating under saturation, where the harmonics are saturation induced. The presence of these harmonics makes the parameter identification difficult. Most of the methods presented so far in the literature failed to properly identify machine parameters in the presence of space harmonics. In this

paper, the machine parameters, identified by using a proposed algorithm, are compared with the Finite element and the experimental results to demonstrate the effectiveness of the presented method. Both interior PM and surface PM machines are considered [171].

**Ozer Ciftciogh** et.al has given interpretation about fuzzy logic systems which finds application especially in engineering systems due to their suitability for applications dealing with the concept of Takagi-Sugeno fuzzy model. However, the fuzzy concept is particularly valid also in the areas where information is qualitative. Exact science applications deal with the information by modeling and thereafter identifying the relationships in the model by suitable computation. In contrast, the fuzzy logic employment in soft sciences is not as straightforward as it is in exact sciences and special care should be taken in the former case. Analogous to exact sciences, the majority of soft information sources belongs to soft sciences where the quantities dealt with are usually not measurable in the engineering sense. Therefore, for soft sciences fuzzy logic is an important means for dealing with associated imprecise information processing. In spite of this, the employment of fuzzy logic in soft sciences is not common. In this work, aspects of fuzzy logic implementation in the areas of soft sciences are pointed out. This is exemplified by a design application in building technology using a soft design data set from a real life environment [176].

**Shinji Ichikawa** et.al propose an on-line parameter identification method for all types of synchronous motors especially, three main types, surface permanent magnet synchronous motors, interior permanent magnet synchronous motors, and synchronous reluctance motors. And sensorless control of synchronous motors using these identified parameters is realized. The proposed estimation method is based on an extended EMF model, so the sensorless control method can be applied for all types of synchronous motors. And this identification method is based on the motor model that takes into account magnetic saturation, motor parameters can be identified in spite of generating magnetic saturation. The proposed method is verified by experiments of three kinds of synchronous motors [182].

**Victor H. Elenita** et.al has proposed a neural block control for a synchronous electric generator. In this paper we present a novel identification and control scheme which is able to identify and to control a synchronous generator using a neural identifier. The

generator is modeled as a full eight order one. A third order neural network such as the one presented in is used to identify the dynamics of the synchronous generator. Moreover, a discontinuous control law based on the neural identifier is designed using the block control technique in order to track reference signals and rejects external disturbances caused by generator terminal short circuits. Simulation results are presented in order to test the applicability of the proposed approach [183].

**Yujie Song** et.al presents a paper on brushless DC motor speed estimator based on space-frequency localized Wavelet Neural Networks (WNNs). A novel highly-accurate speed estimator using a recurrent wavelet neural network (WNN) is proposed and validated for BEDC motor drives. The experimental results show that the WNN speed estimator yields promising results over a wide operating range including low-speed bands and transient operating conditions [186].

**Scott Dick** et.al suggests that complex fuzzy logic is a postulated logic system that is isomorphic to the complex fuzzy sets. This concept is analogous to the many-valued logics that are isomorphic to type-1 fuzzy sets, commonly known as fuzzy logic. As with fuzzy logics, a complex fuzzy logic would be defined by particular choices of the conjunction, disjunction and complement operators. In this paper, an important assertion that only the modulus of a complex fuzzy membership should be considered in set theoretic or logical operations. A more general mathematical formulation i.e the property of rotational invariance is proposed for this assertion, and the impact of this property on the form of complex fuzzy logic operations is examined. All complex fuzzy logics based on the modulus of a vector are shown to be rotationally invariant. The case of complex fuzzy logics that are not rotationally invariant is examined using the framework of vector logic. Conjunction operator was identified, and the existence of a dual disjunction was proven. Finally, a discussion on the possible applications of complex fuzzy logic focuses on the phenomenon of regularity as a possible fuzzification of stationarity [188].

**Jung-Wook Park** et.al has presented a paper on MLP/RBF neural-networks-based online global model identification of synchronous generator. This paper compares the performances of a multilayer perceptron neural network (MLPN) and a radial basis function neural network (RBFN) for online identification of the nonlinear dynamics of a synchronous generator in a power system. The computational requirement to process the

data during the online training, local convergence, and online global convergence properties are investigated by time-domain simulations. The performances of the identifiers as a global model, which are trained at different stable operating conditions, are compared using the actual signals as well as the deviation signals for the inputs of the identifiers. Such an online-trained identifier with fixed optimal weights after the global convergence test is needed to provide information about the plant to a neuro controller. The use of the fixed weights is to provide against a sensor failure in which case the training of the identifiers would be automatically stopped, and their weights frozen, but the control action, which uses the identifier, would be able to continue [189].

**Jia-Qiang Yang** et.al establishes a fuzzy speed PI regulator, which applies the principles and method of fuzzy logic to adjust the proportional coefficient  $k_p$  and integral coefficient  $k_i$  of the PI regulator on-line, and finally get the system to adapt to different speed variations. The proposed method is implemented with a single board microcomputer that uses TMS320LF2407A DSP. The experimental results show that the fuzzy speed regulator can ensure swift speed response, small overshooting, and high steady speed precision both in high and low speed. Additionally, the proposed regulator improves the observation precision of the stator flux and enhances the robustness of the whole system [190].

**Narayan C Kar** has designed a computer model for saturated synchronous motors using the synchronous machine voltage and flux linkage differential equations considering the saturation. The effect of the main flux saturation both in the direct and quadrature axes and of the cross-magnetizing phenomenon i.e the magnetic coupling between the direct and quadrature axes, on the determination of the transient performance of synchronous motors due to the voltage sag at the terminals is the main objective of this paper [193].

**Hans Brink Hansen** et.al presents a novel approach to modeling of a Brush-Less Direct Current Motor (BLDCM) driven by an inverter using hybrid systems theory. Hybrid systems combine continuous and discrete i.e event-based dynamics, which is exactly the case in an inverter-driven BLDCM. The model presented in this work consists of a general automaton with discrete states, combined with a set of continuous dynamic equations describing the electro-mechanical behavior of the motor. One of the significant benefits of this strategy is that the model describes the motor under all possible operating

conditions. The model is derived for the common case of a BLDCM in wye-connection with a three-leg inverter. The model is verified on a real BLDCM drive and shows good agreement with experiments [199].

**Yodyium Tipsuwan** et.al has proposed an experimental study of network-based dc motor speed control using SANFIS. Abstract-network-based control (NBC) systems can provide several advantages among traditional control systems. Nevertheless, the performances of NBC systems can be degraded due to undesired network behaviors such as network-induced delays. Several NBC algorithms usually neglect several network behaviors due to assumptions in problem formulations. The incompleteness and ambiguity of this network information implies ambiguities in NBC performances. In this paper, we applied a novel NBC gain scheduling scheme by applying a SANFIS (Self-Adaptive Neuro-Fuzzy Inference System) along with gain scheduling to handle ambiguities in network behaviors. The SANFIS is utilized to classify a current network condition in order to select an optimal gain for this condition. An experimental result shows that the PI controller with the proposed approach yields significantly better NBC performances [201].

**Yuan Kang** et.al has presented a method of self-tuning neural speed regulator applied to dc servo motor. This study utilizes the direct neural control (DNC) based on back propagation neural networks (BPN) with specialized learning architecture applied to regulate the speed of a DC servo motor. The proposed neural controller is treated as a speed regulator to keep the motor in constant speed without the specified reference model. A tangent hyperbolic function is used as the activation function, and the back propagation error is approximated by a linear combination of error and error's differential. The simulation and experiment results reveal that the proposed speed regulator keeps motor in constant speed with high convergent speed, and enhances the adaptability of the accurate speed control system [202].

**Shahram Najafi** et.al has proposed a voltage profile due to a short-circuit at the motor terminals where the motor terminal voltage requires a certain period of time to fall to zero value and, following the clearing of the fault, the terminal voltage also requires a certain period of time to recover to a post-short-circuit value. Three models of permanent magnet synchronous motors have been developed to demonstrate the effect of the main flux

saturation on the determination of the transient performance of permanent magnet synchronous motors employing the proposed short circuit voltage profile [203].

**L. Barazane** et.al proposed modeling approach is to provide a fuzzy set based representation of the cascade sliding mode control of an induction motor fed by PWM voltage source inverter, which operates in a fixed reference frame. For this purpose, a new decoupled and reduced model is first proposed. Then, a set of simple surfaces and associated control laws are synthesized. A piecewise smooth control function with a threshold is adopted. However, the magnitude of this function depends closely on the upper bound of uncertainties, which include parameter variations and external disturbances. This bound is difficult to obtain prior to motor operation. To solve this problem, a fuzzy modeling approach is presented to improve the design and tuning of a fuzzy logic controller using variable structure control theory. The fuzzy controller is designed in order to improve the control performances and to reduce the control energy and the chattering phenomenon. Simulation results reveal some very interesting features [206].

**J.A. Cortajarena** et.al has presented a new high performance induction motor drive. The induction motor is controlled with four proportional plus fuzzy PI controllers (P+FUZZY PI). This hybrid controller replaces the conventional PI controllers traditionally used for indirect vector control of induction motors. The hybrid indirect vector control using the fuzzy controllers offers enhanced performance both in mathematical simulations and during actual test utilizing a 7.5 kW induction motor. The results demonstrate the superior performance and robustness of the fuzzy logic controller over the conventional controller when there are mismatched motor parameters. Notably the performance of the fuzzy logic controller is retained when a new different motor replaces the test motor [208].

**Simon Coupland** et.al presents a novel approach to the representation of type-1 and type-2 fuzzy sets utilizing computational geometry. To achieve this basic approach borrows ideas from the field of computational geometry and applies these techniques in the novel setting of fuzzy logic. It provides new algorithms for various operations on type-1 and type-2 fuzzy sets and for defuzzification. Results of experiments indicate that this approach reduces the execution speed of these operations [209].

**Damir Sumina** et.al has given a simulation model of neural network based synchronous generator excitation control. Usage of neural network based excitation control on single machine infinite bus and its simulation studies are reported in this paper. The proposed feed forward neural network integrates a voltage regulator and a power system stabilizer. It is trained on-line from input and output signals of a synchronous generator. A modified error function used for training the neural network by the back propagation algorithm uses the reference and terminal voltage as controlling voltage and active power deviation to provide stabilization. The complete algorithm is simulated in Matlab Simulink. Synchronous generator (83 kVA, 50 Hz, 400V) is connected over transmission lines to AC power system. The proposed algorithm shows advantages of this method and satisfactory results [212].

**Hong Guo** et.al presents an electrical/mechanical hybrid four-redundancy brushless DC motor (BLDCM) and the corresponding driving control system. High reliability can be achieved by adopting the electrical/mechanical hybrid structure. An engineering prototype is designed and developed whereas the reliability of the BLDCM is analyzed theoretically. Moreover the control and driving system is designed to compose a position servo. Experimental results are presented to demonstrate the feasibility and performance of the electrical/mechanical hybrid four-redundancy BLDCM [213].

**Shady M. Gadoue** et.al presents a neural network based stator current MRAS observer for speed sensorless induction motor drives. This paper presents a novel Model Reference Adaptive System (MRAS) speed observer for induction motor drives based on stator currents. The measured currents are used as reference model for the MRAS observer to avoid the use of a pure integrator. A two layer Neural Network (NN) stator current observer is used as the adaptive model which requires the rotor flux information. This can be obtained from the voltage or current model but instability and dc drift can downgrade the overall observer performance. To overcome these problems another off-line trained multilayer feedforward NN is proposed here as a rotor flux observer. Speed estimation performance of the MRAS scheme using the three different rotor flux observers is studied and compared when applied to an indirect vector control induction motor drive. Promising results have been obtained when using the NN flux observer with less

sensitivity to parameter variation and stability in the regenerating mode of operation [214].

**Christian Wagner** et.al introduces an alternative approach termed zSlices for representing general type-2 sets based on interval type-2 sets. Thus, this will lead to a smooth transition from interval to general type-2 fuzzy systems. The proposed approach will lead to a significant reduction in both the complexity and the computational requirements for general type-2 fuzzy logic systems. Hence, this will lead to facilitating the application of general type-2 fuzzy logic to many real world applications [215].

**Changliang Xia** et.al present a current threshold on-line identification control based on intelligent controller for four-switch three phase brushless dc motor. The brushless DC motor has such advantages as simple structure, convenient to control, high reliability, and has been applied in many industrial fields. In order to simplify the converter topology and lower the system cost, four-switch three phase BLDCM recently becomes research highlight of scholars. Conventional hysteresis controllers suffer from big phase current ripple and inaccuracy current threshold adjusting of the four switch three-phase BLDCM. To overcome the shortcomings of the hysteresis controller, this paper presents a novel direct current control strategy based on current threshold on-line identification using intelligent controller for four-switch three phase BLDCM. A radial basis function neural network is built to identify the relationship of load, current threshold and expected speed on-line. When the given speed and load is setting, current threshold identifier give the suitable threshold output to the current controller. Also the system use two PID controller based on RBF neural network on-line regulation to control phase current  $I_a$  and  $I_b$  separately. Current controller constructs the on-line reference model, implements self-learning of PID controller parameters by RBF neural network. The intelligent controller individually regulates duty cycle of PWM signals working on the inverter bridge to make phase current fall in the specified threshold quickly and smoothly. Simulated and experimental systems are building to fully prove the performance of the control scheme. Excellent flexibility and adaptability as well as high precision and good robustness are obtained by the proposed strategy [216].

**Sukumar Kamalasan** et.al has proposed an intelligent hybrid controller for speed control and stabilization of synchronous generator. In this paper, an intelligent approach

to synchronous generator control is described. This method combines two controllers, one a neural network based controller with explicit neuro-identifier, and the other an intelligent adaptive controller implemented as a Model Reference Adaptive Controller (MRAC) to perform a hybrid control operation. The neuro-control identifier combination is used to approximate the nonlinear function and the MRAC control adapts when plant parametric set changes. Additionally, a Feed Forward Neural Network (FFNN) identifier is used to predict system response to control values and those values adjusted to obtain improved system response. The FFNN is trained offline with extensive test data, and is also adjusted online. Main advantage and uniqueness of the proposed scheme is the controller's ability to complement each other in case of parametric and functional uncertainty. Moreover, the online neural network produces a plant functional approximation. The theoretical results are validated by conducting simulation studies on a single machine infinite bus system for electric generator control [217].

**Xingqiao Liu** et.al has presented a paper on three-motor synchronous decoupling control based on bp neural network. Multi-transducer driving multi-motor to constitute multi-motor synchronous system, it is a widely-used electrical controlled system in modern industrial applications, and has wide prospects in industrial, military and aeronautic applications. With advancement of Industrial automation degree in manufacture, the mode of multi-motor driving becomes more and more necessary when it is difficult for using single motor to satisfy the requirement of high-power drive equipment. Thus, it is inevitable for multi-transducer driving multi-motor system. The key of problem is focusing on the synchronous control of multi-motor synchronous system, because the synchronous performances of the system affect the productivity and the quality of product directly. However, the synchronous performances of multi-motor system will be affected by mismatch of drive characteristic, disturbance of load and so forth. Therefore, how to control the multi-motor synchronous system to realize coordinated operation, and decoupling control of speed and tension with high synchronous performance is a hotspot and difficulty of the research [218].

**M. Rahimpour** et.al has proposed a method online synchronous generator parameters estimation based on applying small disturbance on excitation system using ANN. This paper presents a technique for on-line estimation of synchronous generator parameters,

using an excitation disturbance. To illustrate and verify the proposed algorithm, some excitation disturbance tests are conducted on an actual hydro generator. Machine response to the applied disturbance is processed by proposed technique using artificial neural network method (ANN). The estimated parameter values are compared with manufacture's data [219].

**Hongwei Fang** et.al has proposed a fuzzy neural network based fault detection scheme for synchronous generator with internal fault. A fuzzy neural network (FNN) based interturn short circuit fault detection scheme for generator is proposed. The second harmonic magnitude of field current and the negative sequence components of voltages and currents are used as inputs for the FNN fault detector. The negative sequence voltage and current are obtained from the phase voltages and currents using the symmetrical component analysis method. And the second harmonic magnitude of field current is achieved by the FFT technique. The FNN fault detector with Gauss membership functions is trained off-line using the training data which comes from the Multi-Loop simulation program. The proposed fault detection scheme can perform the interterm short circuit fault detection, the fault type classification, and the fault location identification. Experimental results corroborate the effectiveness of the proposed scheme [220].

**Zhiqiang Cheng** et.al presents a method global sliding mode control for brushless dc motors by neural networks. A global sliding mode control scheme by neural networks is proposed for high performance drive systems of brushless DC motors with uncertain external disturbances and unknown loads. A global sliding mode manifold is designed in this approach, which guarantees that the system states can be on the sliding mode manifold at initial time and the system robustness is increased. A radial basis function neural network (RBFNN) is applied to learn the maximum of unknown loads and external disturbances. Based on the neural networks, the switching control parameters of sliding mode control can be adaptively adjusted with uncertain external disturbances and unknown loads. Therefore, the chattering of the sliding mode controller is eliminated without sacrificing its robustness. Simulation results proved the validity of the control scheme [221].

**Chia-Yu Hsu** et.al has given method of adaptive position tracking control of a bldc motor using a recurrent wavelet neural network. An adaptive position tracking control

(APTC) system, which is composed of a neural controller and a robust controller, is proposed in this paper. The neural controller uses the recurrent wavelet neural network structure to online mimic an ideal controller, and the robust controller is designed to achieve  $2L$  tracking performance with desired attenuation level. The adaptive laws of APTC system are derived based on the Lyapunov stability theorem and gradient decent method. Finally, the proposed APTC method is applied to a brushless DC (BLDC) motor. Experimental results verify that a favorable tracking response can be achieved by the proposed APTC method even under the change of position command frequency after training of RWNN [222].

**Jongman Hong** et.al has introduced a new inverter embedded technique for automated monitoring of magnet quality for permanent magnet synchronous motors (PMSM) that overcomes the limitations of existing techniques. The main concept is to use the inverter to perform a standstill test whenever the motor is stopped to detect local or uniform PM demagnetization. The machine is excited with a pulsating field at different angular positions, and the change in the current peaks caused by the change in the degree of magnetic saturation due to demagnetization is observed. An experimental study on a 10hp PMSM verifies that local and uniform PM demagnetization can be detected with high sensitivity [223].

**Peter Scavenius Andersen** et.al addresses the causes of synchronous torques in split-phase induction motors. First, an analytical model is outlined to describe the processes involved in producing synchronous torques. This involves the consideration of the motor MMFs interacting with the slot permeances. The results from the implementation of the model are given for several different motor designs to calculate the synchronous torques. These highlight the way that the synchronous torque is a function of the MMF and slotting relationships. Measurement of the synchronous torque is not straightforward; however, a method of assessment is developed in this paper by using a deceleration test and other tests. The test results are fully described in this paper, and they illustrate that even with correct bar/slot combinations and skew, synchronous torques still exist in the machine [224].

**Wang Hong-jun** et.al has an idea of designing of fuzzy-neuro controller implicated to a synchronous generator excitation control system. A fuzzy-neuro controller has been

designed to stabilize the frequency and voltage output of a synchronous generator. The structure of the proposed control system consists of two PI like fuzzy controllers and two neural networks. With this control scheme, difficulty for tuning scale factors of the fuzzy controller is reduced. Simulation results show that the system is robust to drastic changes on the load [225].

---

# CHAPTER 2

## FUZZY LOGIC AND ITS CONTEMPORARY MODELS

---

### **Introduction**

From beginning artificial intelligence is widely used in various domains so as to get a better solution. In majority of the cases, researchers got much better results when they applied artificial intelligence algorithms in various engineering problems. Engineering problems have shown remarkable enhancement in performance and also efficiency when different artificial intelligence techniques were applied in comparison to conventional techniques. There are three basic domains in artificial intelligence e.g fuzzy logic, artificial neural network and genetic algorithm.

There is a wide variety of engineering application. These algorithms and their techniques have been applied to almost every engineering discipline. Presently, these techniques are applied on data mining, image processing, bio informatics, digital signal processing, measurement of concrete beams, vibration analysis, machine vision, machine control, navigation and communication equipment.

This thesis deals with the application of different fuzzy logic models in machine control and error estimation and control performance evaluation.

### **2.1 Fuzzy Logic**

Fuzzy Logic is extension of Boolean logic. It incorporates partial values of truth. Instead of sentences being "Completely True" or "Completely False," Here in fuzzy logic they are assigned a value which represents their degree of truthfulness. In fuzzy systems, values are indicated by a number called as truth value. It lies in the range from 0 to 1. 0.0 represents absolute falseness and 1.0 represents absolute truth. Fuzzification is generalization of theory from discrete to continuous. Fuzzy logic is important to artificial intelligence. Fuzzy logic allows computers to answer 'to a certain degree' unlike Boolean

logic (one extreme or the other). Computers are allowed to think more 'human-like'. Nothing in our perception is extreme. However, it is true only to a certain degree. In fuzzy logic, machines think in degrees. It can solve problems in the cases where there is no simple mathematical model. Fuzzy logic solves highly nonlinear processes. Fuzzy logic uses expert knowledge to make decisions [231].

Fuzzy logic was first invented as a representation scheme. It acts as calculus for uncertain or vague notions. It allows more human-like interpretations. Fuzzy logic has put reasoning in machines by resolving intermediate categories between notations like true/false, hot/cold etc. Fuzzy logic is a problem-solving control system methodology. It lends itself to implementation in systems ranging from small, simple, embedded micro-controllers to large, multi-channel, networked PC or workstation-based data acquisition control systems etc. It can be implemented in software, hardware, or a combination of both. Fuzzy logic provides a simple way to arrive at a definite conclusion. Conclusion is based upon ambiguous or vague, noisy, imprecise, or missing input information. Fuzzy logic's approach to control problems simply mimics how a person will make efficient decisions much faster.

In 1965, Professor L.A. Zadeh of the University of California, Berkeley presented his seminal paper outlining fuzzy theory. In this paper he introduced fuzzy set theory and operation, fuzzy logic based controller etc. In 1970, fuzzy logic theory began to produce result in Japan, China and Europe. In 1987 sixteen station subway railway system was built. It worked with a fuzzy logic-based automatic train operation control system in Sendai, Japan. The ride of train is so smooth that riders do not need to hold straps [131,187]. Fuzzy controller makes 70 percent fewer judgment errors [131]. Fuzzy logic is a powerful problem-solving methodology. It has myriad of applications in embedded information processing and control. Fuzzy provides remarkably simple and definite conclusions. Conclusions are made from vague, ambiguous and imprecise information. Fuzzy logic resembles human decision making. It has ability to work from approximate data. It finds precise solutions. Classical logic requires a deep understanding of a system, exact equations, and precise numeric values. Fuzzy logic provides an alternative way of thinking. Fuzzy logic allows modeling complex systems while using a higher level of abstraction that originates from knowledge and experience. Fuzzy logic expresses

knowledge with subjective concept like bright red, very hot, long time, very quick etc. are mapped into exact numeric ranges.

Fuzzy logic is new and novel paradigm for an alternative design methodology. The fuzzy logic is applied in developing both linear and non-linear control systems. Fuzzy logic provides an alternative solution to non-linear control. It is closer to real world. Membership functions, rules and the inference process results in improved performance, simpler implementation, and reduced design costs. It handles non-linearity very efficiently. By using fuzzy logic, designers can realize superior features, lower development costs, optimized and better end product performance. Products can be brought to market faster and also more cost-effectively. Fuzzy logic is gaining increasing acceptance for the past couple of years. There are over two thousand commercially available products which use fuzzy logic like washing machines, high-current trains etc. Every application can potentially realize the benefits of fuzzy logic. These benefits are simplicity, performance, productivity and lower cost [131].

Fuzzy logic consists of simple, rule-like if X and Y then Z. It does not model system mathematically. The fuzzy logic models are empirical. They rely on an operator's experience rather than their technical understanding of system. For example, instead of dealing with temperature control in terms like "SP =450F", "T <900F", or "200C <TEMP, terms like "IF (process is cool) AND (process is getting colder) THEN (add heat process)" or "IF (process is hot) AND (process is heating rapidly) THEN (cool)". These terms are imprecise. Also these terms are descriptive. Fuzzy logic is capable of mimicking unpredictable and non linear behavior at very high rate.

Fuzzy logic is a simple and flexible. Fuzzy logic handles problems with imprecise, vague and incomplete data. Fuzzy logic can model nonlinear functions of arbitrary complexity. If plant model is not available, or if the system is changing, then Fuzzy produces better solutions than conventional control techniques. Fuzzy systems match any set of input-output data. The fuzzy logic toolbox makes it easy by supplying adaptive techniques like adaptive neuro-fuzzy inference systems (ANFIS) and fuzzy subtractive clustering. Fuzzy logic models are called as fuzzy inference system. These models consist of number of conditions i.e "if-then" rules. For designer who understands the system better, these rules can be easily written. Flexible membership function scheme

make fuzzy systems quite straightforward to create. Also it simplifies the design of systems. It ensures that it can be very easily updated and can be maintained over time. Fuzzy logic has several unique features. It is inherently robust. It does not require precise, noise-free inputs. It can be programmed to fail safely if a feedback sensor quits or gets destroyed. The output control is a smooth control function for a wide range of input variations. Fuzzy logic controller processes user-defined rules governing the target control system. Fuzzy logic can be modified and tweaked easily in order to improve or drastically alter the control system performance. Sensors can easily be incorporated into fuzzy logic system. Just appropriate governing rules need to be generated. Fuzzy logic is not limited to a few feedback inputs or control outputs. It is not necessary to measure or compute rate-of-change in parameters for implementation. Sensor data providing some indication of a system's actions and reactions is just sufficient. Sensors required are inexpensive and imprecise. Thus it keeps the overall system cost and its complexity low. Because of the rule-based operation, a large number of inputs can be very easily processed and also numerous outputs can be generated. Defining the rule base is complex especially if there are too many inputs and outputs and their interrelations need to be defined. For this purpose control system is broken into smaller chunks. Several smaller fuzzy logic controllers are used which are distributed on system. Each fuzzy logic controller has different responsibilities. Fuzzy logic can control nonlinear systems. Non linear systems are difficult or impossible to model mathematically.

It is quite important to define the control objectives and control criteria. What is to be controlled? What has to be done to control the system? What kind of response should be there? What are the possible failure modes in the systems? It is necessary to determine the input and output relationships. A minimum number of variables are chosen for input to the fuzzy logic inference engine typically error and rate-of-change-of-error. Using the rule-based structure of fuzzy logic, the control problem is broken down into a series of IF X AND Y THEN Z rules. Rules must define the desired system output response for the given system input conditions. Number and complexity of rules depends on the number of input parameters be processed. It also depends upon the number fuzzy variables associated with each parameter. It is preferred to use at least one variable and its time derivative. A single instantaneous error parameter should be used along with its rate of

change. Fuzzy logic membership functions need to be created which define the meaning (values) of input / output terms that are used in the rules. System need to be tested, evaluated for results. Tune the rules and membership functions. Until satisfactory results are obtained, retest the system.

Fuzzy logic requires some numerical parameters. Exact values of significant error and rate of change of significant error are not critical unless very responsive performance is needed. Empirical tuning determines it.

### 2.1.1 Type-1 Fuzzy Set

Let  $X$  be a collection of objects. It is called universe of discourse. A fuzzy set  $A \in X$  is characterized by membership function  $\mu_A(x)$  represents the degree of membership. Degree of membership maps each element between 0 and 1. It is defined as

$$A = \{(x, \mu_A(x)); x \in X\}$$

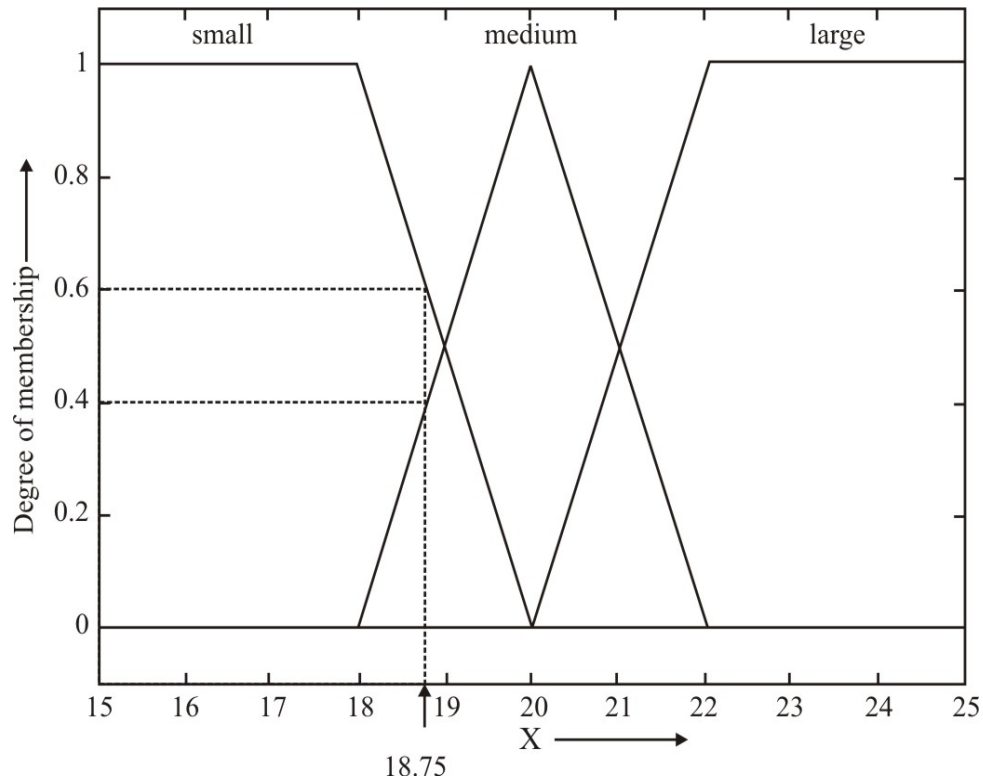


Figure 2.1: Fuzzy logic membership function

Figure 2.1 shows the membership functions of three fuzzy sets i.e. “small”, “medium” and “large” for a fuzzy variable X. The universe of discourse is all possible values of X. It is  $X = [15;25]$ . At X of 18.75, the fuzzy set is a “small” with membership value of 0.6.

Thus,  $\mu_{small}(18.75)=0.6$ ,  $\mu_{medium}(18.75)=0.4$ , and  $\mu_{large}(18.75)=0.4$

The support of a fuzzy set A is the crisp set of all points  $x \in X$  such that  $\mu_A(x) > 0$ . The core of a fuzzy set is of all points  $x \in X$  such that  $\mu_A(x) = 1$ . A T norm denoted by \*. It is a two place function from  $[0,1] \times [0,1]$  to  $[0,1]$ . It includes fuzzy intersection, drastic product, algebraic product and bounded product as

$$x * y = \min(x, y) \tag{2.1}$$

And

$$x * y = xy \tag{2.2}$$

$$x * y = \begin{cases} x : y = 1 \\ y : x = 1 \\ 0 : x, y < 1 \end{cases} \tag{2.3}$$

- There are various types of membership function in fuzzy logic. Some standard membership functions are given here. Membership functions contain the membership values of elements in fuzzy set. Membership values can lie between 0 and 1.

### Triangular Membership Function

It is given as

$$triangle(x, a, b, c) = \begin{cases} 0 & x \leq a \\ \frac{x-a}{b-a} & a \leq x \leq b \\ \frac{c-x}{c-b} & b \leq x \leq c \\ 0 & c \leq x \end{cases} \tag{2.4}$$

$$triangle(x, a, b, c) = \max\left(\min\left(\frac{x-a}{b-a}, 1, \frac{c-x}{c-b}\right), 0\right) \tag{2.5}$$

Here a, b and c represent the x coordinates of the three vertices of  $\mu_A(x)$  in a fuzzy set A. Here the ‘a’ represents lower boundary and ‘c’ represents upper boundary where membership degree is zero, ‘b’ is the centre where membership degree is 1.

### Trapezoidal Membership Function

It is given as

$$\text{trapezoid}(x, a, b, c) = \max\left(\min\left(\frac{x-a}{b-a}, 1, \frac{d-x}{d-c}\right), 0\right) \quad (2.6)$$

$$\text{trapezoid}(x, a, b, c, d) = \begin{cases} 0, & x \leq a \\ \frac{x-a}{b-a}, & a \leq x \leq b \\ 1, & b \leq x \leq c \\ \frac{d-x}{d-c}, & c \leq x \leq d \\ 0, & d \leq x \end{cases} \quad (2.7)$$

### Gaussian Membership Function

It is given as

$$\text{gaussian}(x; c, \theta) = e^{-\frac{1}{2}\left(\frac{x-c}{\theta}\right)^2} \quad (2.8)$$

### Bell Membership Function

It is given as

$$\text{bell}(x, a, b, c) = \frac{1}{1 + \left|\frac{x-c}{a}\right|^{2b}} \quad (2.9)$$

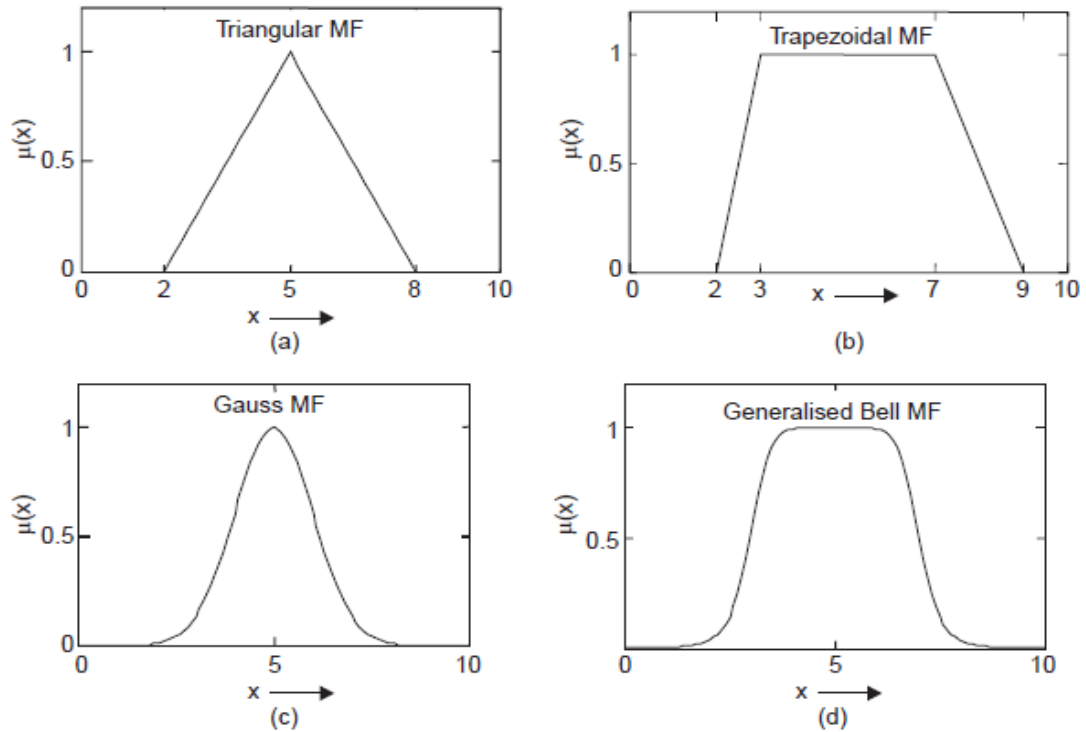


Figure 2.2: Various types of fuzzy logic membership functions  
 (a)Triangular Membership (b)Trapezoidal Membership  
 (c)Gauss Membership (d)Generalized Bell Membership

Figure 2.2 shows various fuzzy logic membership functions which are widely used for various fuzzy logic based control systems, where different mathematical relations can be considered as different membership functions.

Fuzzy inference systems (FIS) are rule-based systems. It is based on fuzzy set theory and fuzzy logic. FIS are mappings from an input space to an output space. FIS allows constructing structures which are used to generate responses i.e outputs for certain stimulations i.e inputs. Response of FIS is based on stored knowledge i.e relationships between responses and stimulations. Knowledge is stored in the form of a rule base. Rule base is a set of rules. Rule base expresses relations between inputs of system and its expected outputs [15, 97,149].

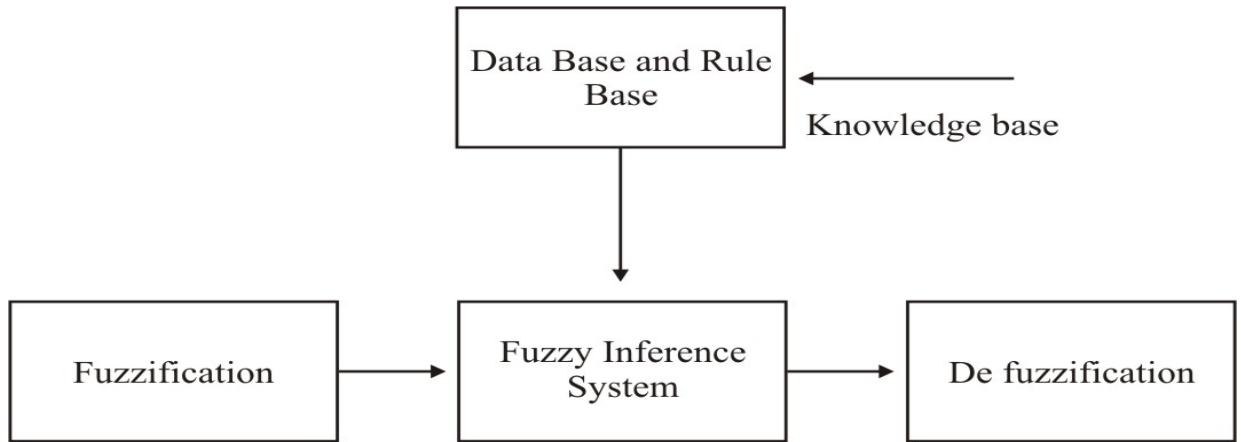


Figure 2.3: Block diagram of fuzzy logic System

In Figure 2.3 the simple block diagram of fuzzy logic system having provision primarily for converting process inputs into fuzzy sets of inputs with the help of fuzzification block. The data base and rule base block helps in significantly differentiating the inputs and outputs from other less significant data. Then FIS i.e the fuzzy inference system block and defuzzification block implements the inferred control action [7]. All varieties of decisions can be implemented using this control structure for optimal solution. Two types of inferencing engines named as Sugeno FIS and Mamdani FIS helps the FLC in collecting the knowledge, rules and memberships of various inputs and output variables. Knowledge is obtained by eliciting information from specialists. These systems are usually known as fuzzy expert systems. Another common denomination for FIS is fuzzy knowledge-based systems. It is also called as data-driven fuzzy systems. FIS are usually divided in two categories i.e. multiple input and multiple output (MIMO) systems and Multiple Input and Single Output (MISO) systems, the system returns several outputs based on the inputs which it receives. Multiple input and single output (MISO) systems are those where only one output is returned from multiple inputs. MIMO systems are decomposed into a set of MISO systems which work in parallel. In terms of inference process there are two main classes of FIS i.e. the Mamdani-type FIS and the Takagi-Sugeno- Kang (TSK) type FIS. TSK FIS is also called as Sugeno FIS.

In Mamdani based fuzzy inference system, inputs and output have an If-Then rules. An example of a rule in a Mamdani fuzzy model is:

IF X is negative big AND Y is negative small THEN Z is zero.

In Figure 2.4 Mamdani based inference system has been shown implementing the rules corresponding to input  $x$  in  $U$  which after fuzzification going to the fuzzy inference engine, where a corresponding rule from fuzzy rule base is implemented to take decisions. The defuzzifier converts the decisions taken in the form of fuzzy sets in  $V$  as output  $y$  in  $V$ .

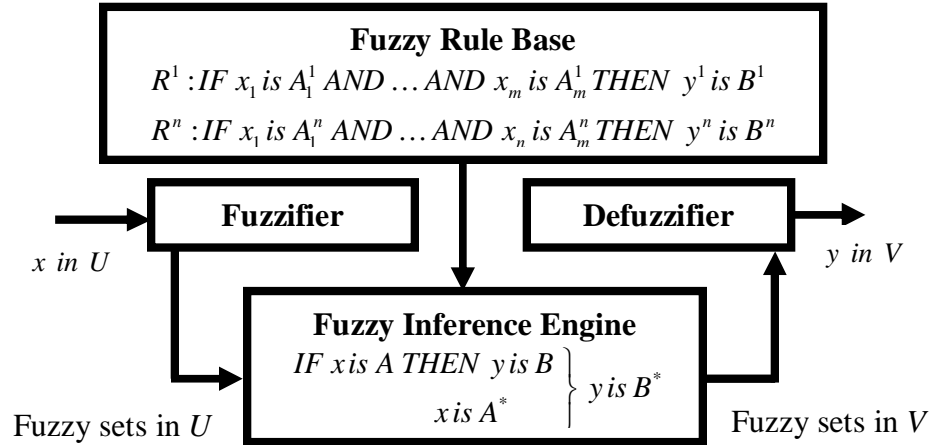


Figure 2.4: Mamdani based fuzzy inference system

Sugeno-type systems are used to model any inference system in which output membership functions are either linear or constant. This fuzzy inference system was introduced in 1985. It is also called as Takagi-Sugeno-Kang. Sugeno output membership functions ( $z$ ) are either linear or constant. A typical rule in a Sugeno fuzzy model is:

If Input 1 =  $x$  and Input 2 =  $y$ , then Output is  $z = ax + by + c$

For a zero-order Sugeno model, the output level  $z$  is a constant ( $a=b=0$ ). The implementation of Sugeno type fuzzy inference system has been shown in Figure 2.5

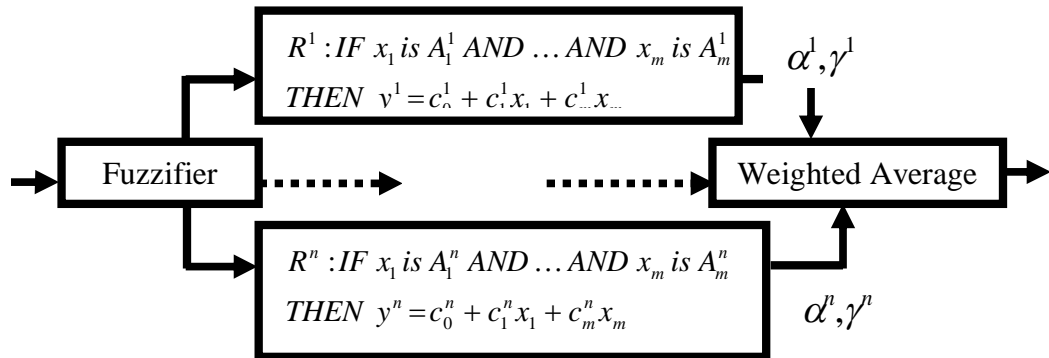


Figure 2.5: Sugeno type fuzzy inference system

Both Sugeno and Mamdani FIS can be used to perform the similar tasks. Rule base and fuzzification remain same for the variables. There are various defuzzifiers that can be chosen for a Mamdani FIS. These defuzzifiers also originate similar results in a Sugeno FIS. There is a certain overlap between both types of systems. Mamdani FIS is more widely used. It is used for decision support applications, because its intuitive and interpretable nature. Consequents of the rules in a Sugeno FIS do not have a direct semantic mean. This means that they are not linguistic terms. Also, this interpretability is partially lost. Sugeno FIS rules consequents can have many parameters per rule as per input values. Thus, Sugeno FIS gets translated into more degrees of freedom in its design as compared to Mamdani FIS. Thus it provides more flexibility. Many parameters can be used in the consequents of the rules of a Sugeno FIS. A zero order Sugeno FIS can reasonably approximate a Mamdani FIS. In computational terms, a Sugeno FIS is more efficient than a Mamdani FIS. It is so because Sugeno FIS does not involve computationally expensive defuzzification process. Also Sugeno FIS always generates continuous surfaces. The continuity of the output surface is quite important. Any existence of discontinuities will result in similar inputs originating substantially different outputs. It will be a situation which is undesirable from the control/ monitoring perspective. Because of continuous structure of output functions, a Sugeno FIS is also better and adequate for functional analysis than a Mamdani FIS.

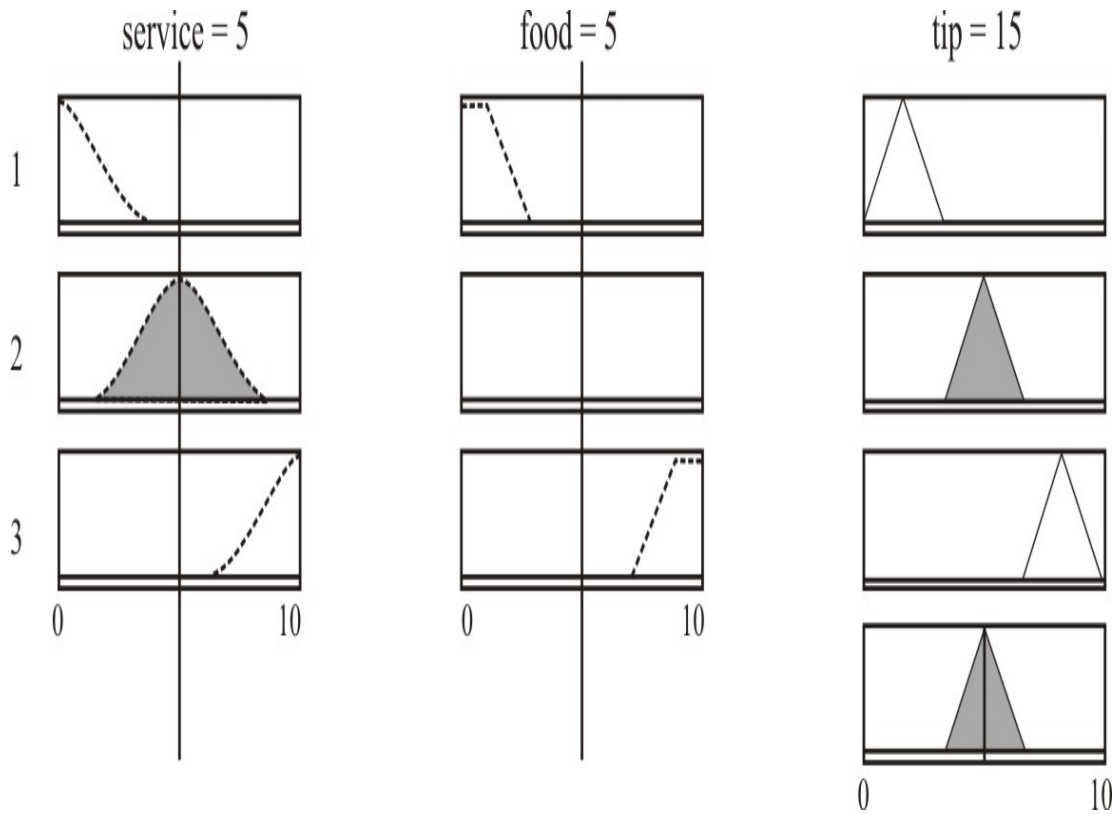


Figure 2.6: Fuzzy rule base in the case of a Mamdani fuzzy inference system

The above diagram in Figure 2.6 shows the inputs and output membership functions. The input memberships function i.e service in hotel and food quality helps in taking decisions regarding output i.e tip to the service providers. The Mamdani FIS takes the decisions for tip as per service and food. The Figure 2.7 shows the surface view for taking different output decisions corresponding two input membership values. The 3D surface view shown by Mamdani fuzzy inference system depicts the decision [20].

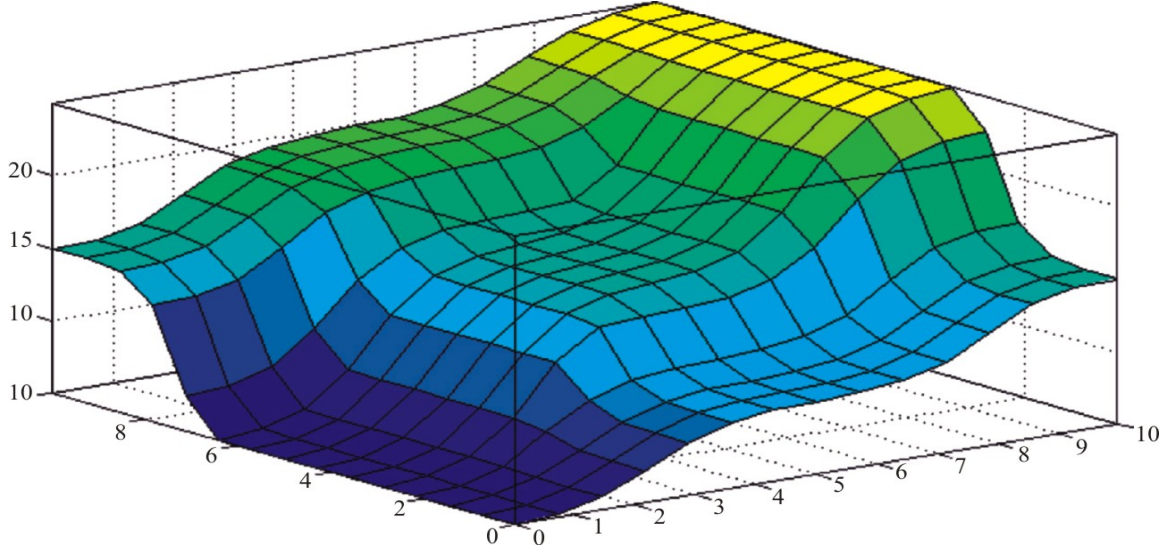


Figure 2.7: Surface view in the case of a Mamdani fuzzy inference system

Defuzzification converts the fuzzy outputs back to crisp values [231]. There are different defuzzification methods given as

1. Max Membership  $\mu_c(z^*) \geq \mu_c(z)$  for all  $z \in Z$

2. Centroid 
$$z^* = \frac{\int \mu_c(z) \cdot z dz}{\int \mu_c(z) dz} \quad (2.11)$$

3. Weighted average 
$$z^* = \frac{\sum \mu_c(z) \cdot z}{\sum \mu_c(z)} \quad (2.12)$$

4. Mean-Max 
$$z^* = \frac{a+b}{2} \quad (2.13)$$

5. Center of Sum 
$$z^* = \frac{\int z^* \sum_{k=1}^n \mu_c(z) dz}{\int \sum_{k=1}^n \mu_c(z) dz} \quad (2.14)$$

6. Center of Largest Area 
$$z^* = \frac{\int \mu_c(z) z dz}{\int \mu_c(z) dz} \quad (2.15)$$

### 2.1.2 Type-2 Fuzzy Sets

Further development on type-1 fuzzy set is type-2 fuzzy set. Type-2 fuzzy set models uncertainty and imprecision in a much better way. Type-2 fuzzy set is introduced at the first time at 1975 by Zadeh. Later it was developed by Mendel with characterizing type-2 fuzzy set as a Footprint of Uncertainty (FOU). FOU is limited by superior and inferior type-1 membership functions. Development of Fuzzy set from type-1 to type-2 in mostly shows better results. Membership function in type-2 fuzzy logic set acts as Footprint of Uncertainty (FOU). FOU is limited by two type-1 membership function i.e. upper membership function (UMF) and lower membership function (LMF). Type-2 membership function is shown in Figure 2.8.

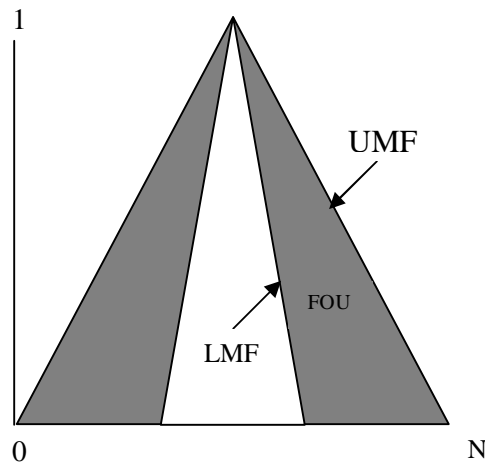


Figure 2.8: Membership function interval type-2 fuzzy logic set

Operation at interval type-2 fuzzy set is identical with an operation on type-1 fuzzy set, however on interval type-2 fuzzy system, fuzzy operator is implemented at two type-1 membership function which limits the FOU, UMF and LMF to produce firing strength. Operation on interval type-2 fuzzy logic is shown in Figure 2.9. The effectiveness of type-2 fuzzy controller lies in the implementation of various algorithms designed to ensure optimal control and compensation of different parameters which are acting as controller inputs. In complex control fuzzy systems type-2 fuzzy systems are combined with conventional fuzzy controllers ensures the implementation of fuzzy control algorithms and other contemporary artificial intelligence control techniques [109].

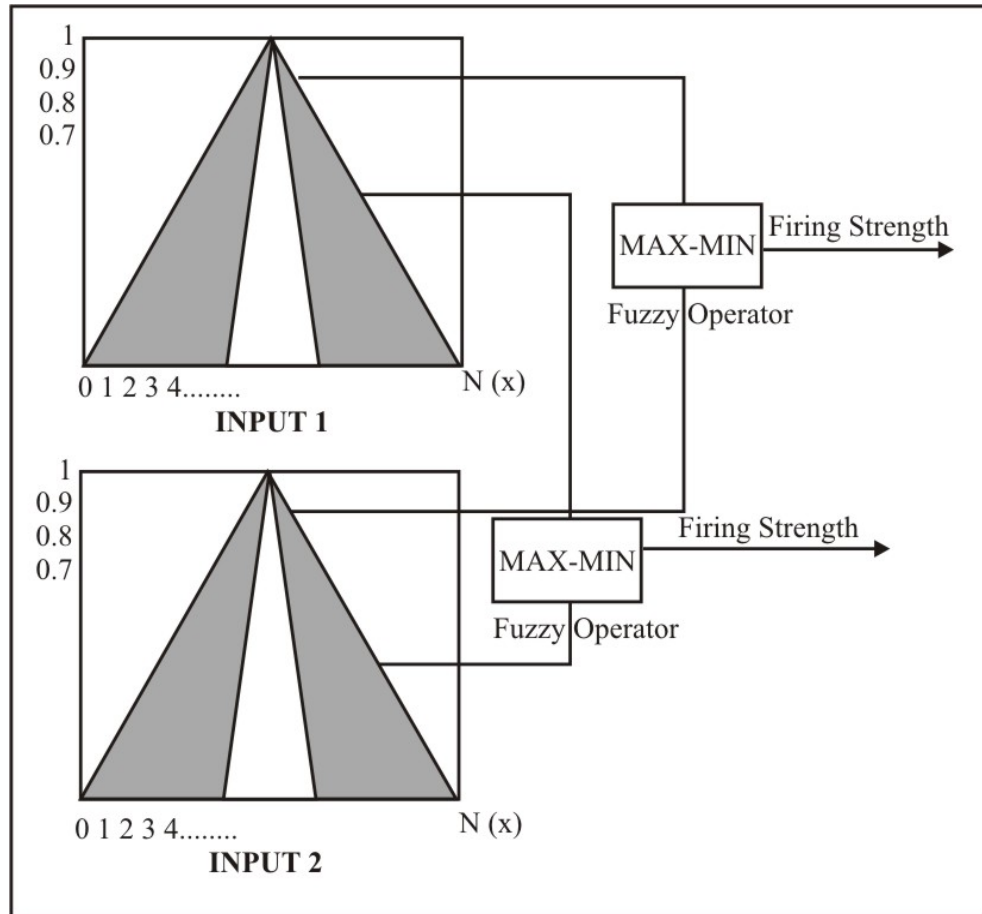


Figure 2.9: Operation on interval type-2 membership function

On Mamdani FIS it needs five steps to produce an output: Fuzzification, Membership function operation, Implication function, Aggregation, and Defuzzification. A simple example of Mamdani Fuzzy Inference System on “dinner for two” on interval type-2 fuzzy logic system is shown in Figure 2.10. Defuzzification is a mapping process from fuzzy logic control action area to a non-fuzzy i.e crisp value in the control action area. Defuzzification on an interval type-2 fuzzy logic system that use centroid method has been proposed by Karnik and Mendel, known as Karnik-Mendel Algorithm. The Karnik-Mendel Algorithm flow chart is shown at Figure 2.11. The type-2 fuzzy logic system block diagram as shown in Figure 2.12 effectively utilizes the facilities of type-2 fuzzy logic and effectively implements Karnik-Mendel Algorithm

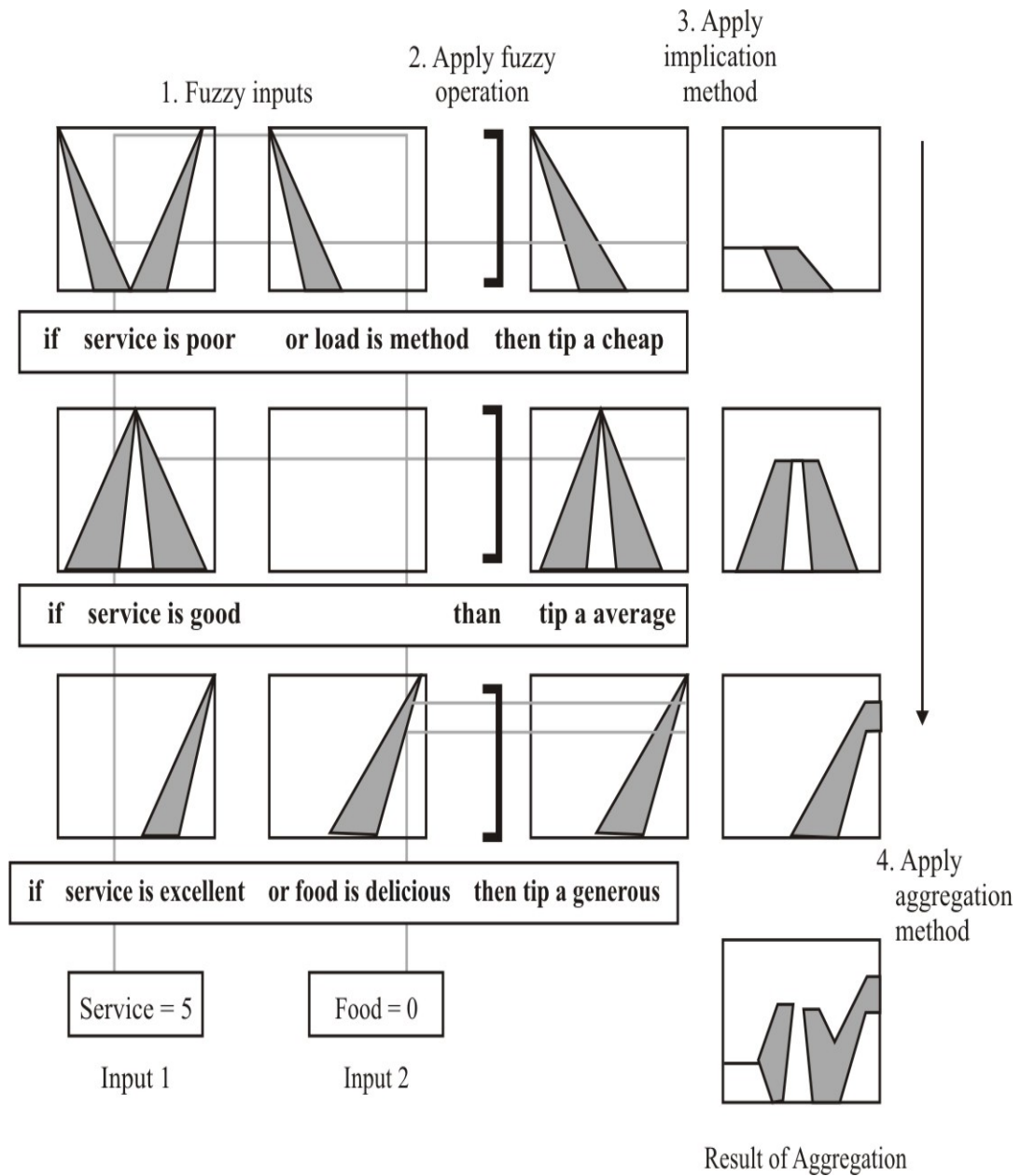


Figure 2.10: Mamdani fuzzy inference system on interval type-2 fuzzy logic

The implementation of selected approximations for determining the character of control process for different forms of inputs, the type-2 fuzzy logic system requires a decision point which is determined by the Karnik Mandel algorithm. This decision point is the centroid point. The location of the centroid point could be found by following this algorithm as shown in Figure 2.11 starting from the initialization and calculation of the value of C.

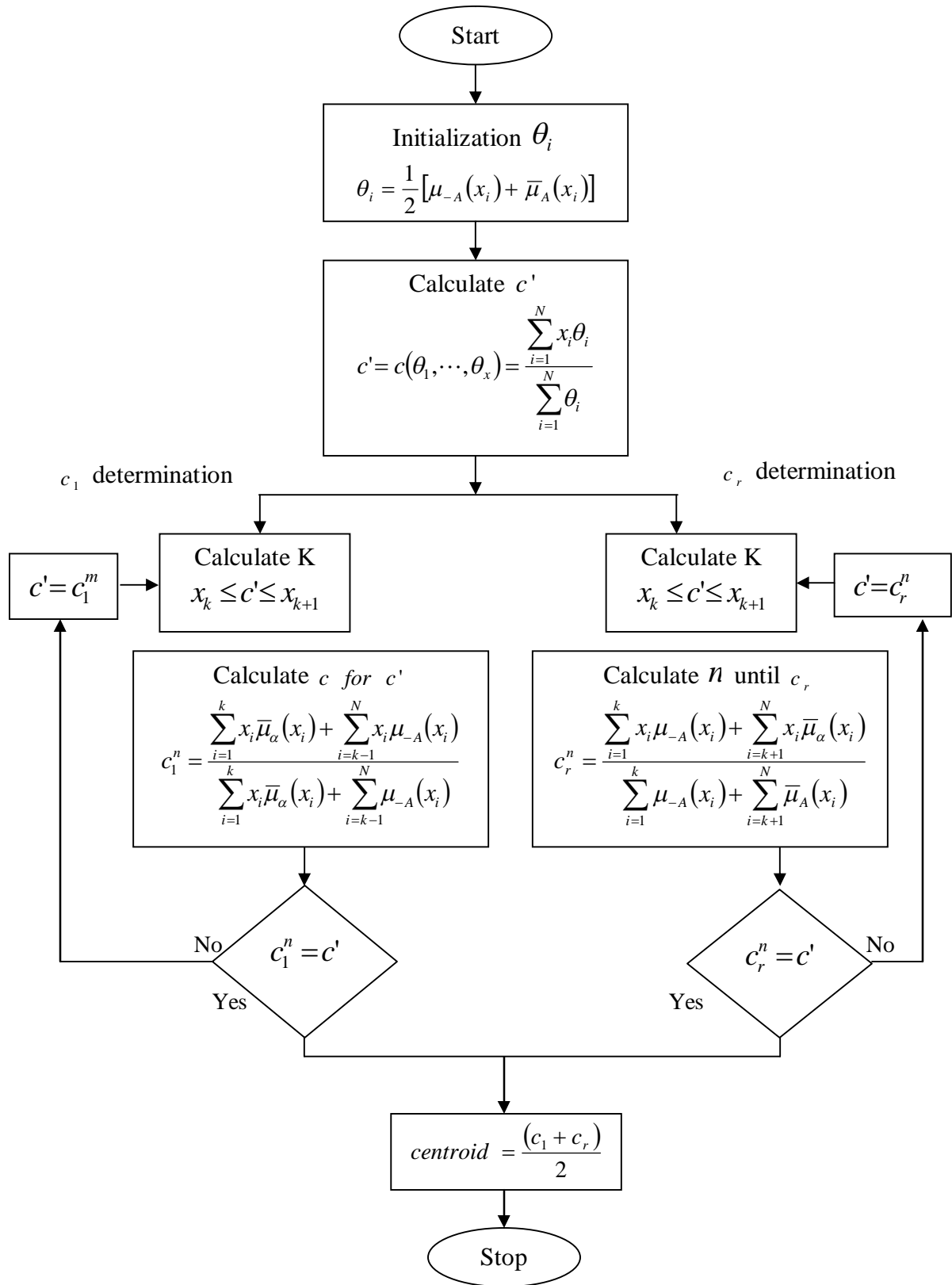


Figure 2.11: Karnik-Mendel algorithms to locate centroid on interval type-2 fuzzy logic system [224].

Where,

$K = 1, \dots, N$

$C_r$  is the centroid having largest element

$C_l$  is the centroid having smallest element

$\theta_i$  is slope and  $\theta_i \in [\mu_{-A}(x_i), \bar{\mu}_A(x_i)]$

$\mu_{-A}$  is lower membership function

$\bar{\mu}_A$  is upper membership function

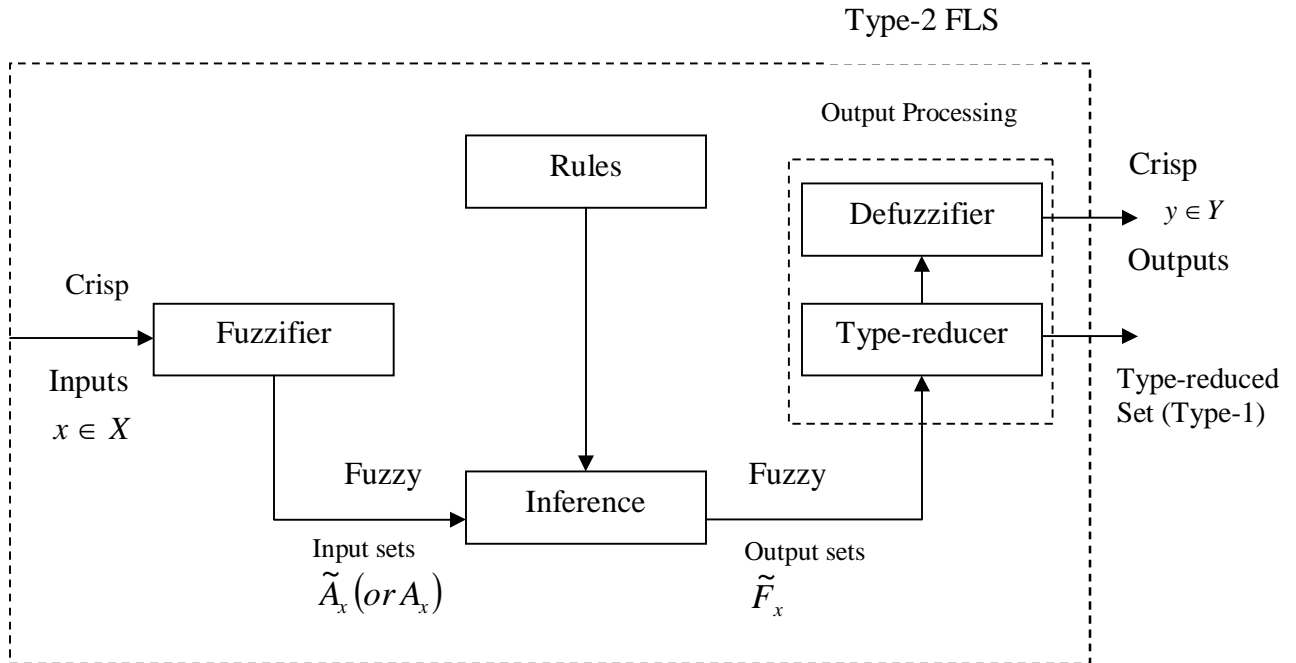


Figure 2.12: Type-2 fuzzy logic system

### 2.1.3 Artificial Neural Network

Artificial neural network (ANN) is named after the network of nerve cells in the human brain. McCulloch and Pitts have developed the neural networks for different computing machines. There are extensive applications of all kinds of ANN in the field of communication, control, instrumentation and forecasting. The ANN is capable of performing on nonlinear input and output systems in the workspace due to its large parallel interconnection between different layers and its nonlinear processing characteristics. An artificial neuron basically consists of a computing element that computes the weighted sum of the input signal and the connecting weight. The sum is added with the bias or threshold and the resultant signal is then processed for nonlinear function of sigmoid or hyperbolic tangent type. Every neuron is associated with three

parameters whose learning can be adjusted; these are 1) the connecting weights, 2) the bias, 3) the slope of the nonlinear function. The structure of a neural network (NN) may be single layer or it may be multilayer. In multilayer structure, there can be one or many artificial neurons in each layer. In the practical cases, there may be a number of layers to each and every parameter under consideration. Each neuron of the one layer is connected to each neuron of the next layer. The functional-link ANN is another type of single layer NN. In these networks, the input data is allowed to pass through a functional expansion block where the input data are nonlinearly mapped to more number of points. This is achieved by using trigonometric functions, products or power terms of the input. The output of the functional expansion is then passed through that single neuron [232].

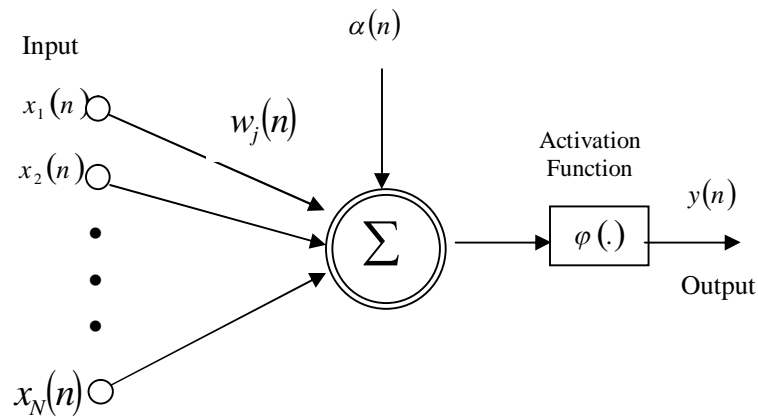


Figure 2.13: Structure of a single neuron

The basic structure of an artificial neuron is presented in Figure 2.13. The neuron is involved in the computation of the weighted sum of inputs and threshold. The resultant signal is then passed through a nonlinear activation function. This is also known as a perceptron which is built around a nonlinear neuron. The output of the neuron may be represented as

$$y(n) = \varphi \left[ \sum_{j=1}^N w_j(n)x_j(n) + \alpha(n) \right] \quad (2.16)$$

where

$\alpha(n)$  is the threshold to the neurons in the first layer.

$w_j(n)$  is the weight associated with the  $j^{\text{th}}$  input.

$N$  is the number of inputs to the neuron

$\varphi(\cdot)$  is the nonlinear activation function. Different types of nonlinear functions are shown in the Figure 2.14.

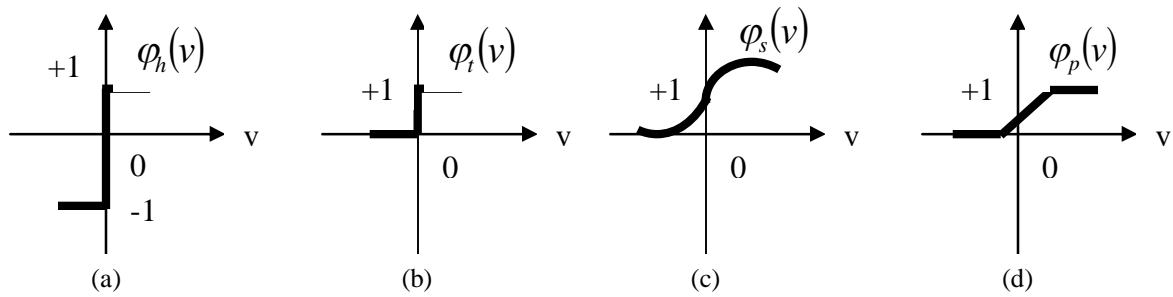


Figure 2.14: Different types of nonlinear activation function,  
 (a) Signum function or hard limiter,  
 (b) Threshold function,  
 (c) Sigmoid function,  
 (d) Piecewise linear

Signum Function: For this type of activation function, we have

$$\varphi(v) = \begin{cases} 1 & \text{if } v > 0 \\ 0 & \text{if } v = 0 \\ -1 & \text{if } v < 0 \end{cases} \quad (2.17)$$

Threshold Function: This function is represented as,

$$\varphi(v) = \begin{cases} 1 & \text{if } v \leq 0 \\ 0 & \text{if } v < 0 \end{cases} \quad (2.18)$$

Sigmoid Function: This function is S-shaped and is the most common form of the activation function used in artificial neural network. It is a function that exhibits a graceful balance between linear and nonlinear behaviour.

$$\varphi(v) = \frac{1}{1 + e^{-av}} \quad (2.19)$$

where  $v$  is the input to the sigmoid function,  $a$  is the slope of the sigmoid function.

For the steady convergence a proper choice of  $a$  is required.

### Multilayer Perceptron

In the multilayer neural network (MNN) or multilayer perceptron (MLP), the input signal moves in a forward direction in the considered MNN on a layer-by-layer basis. This network has been applied successfully to solve some difficult and diverse problems by training in a supervised manner with a highly popular algorithm known as the error back-propagation algorithm. Basic block diagram has been shown in Figure 2.15(a).

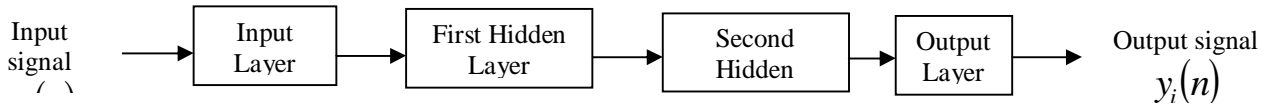


Figure 2.15(a) MLP block diagram

The basic MLP system has an input layer to accept input signal  $x_i(n)$  then the design of first hidden layer and second hidden layer performs the operation on the input signal for which they are formed. The output layer manipulates the output signal  $y_i(n)$ .

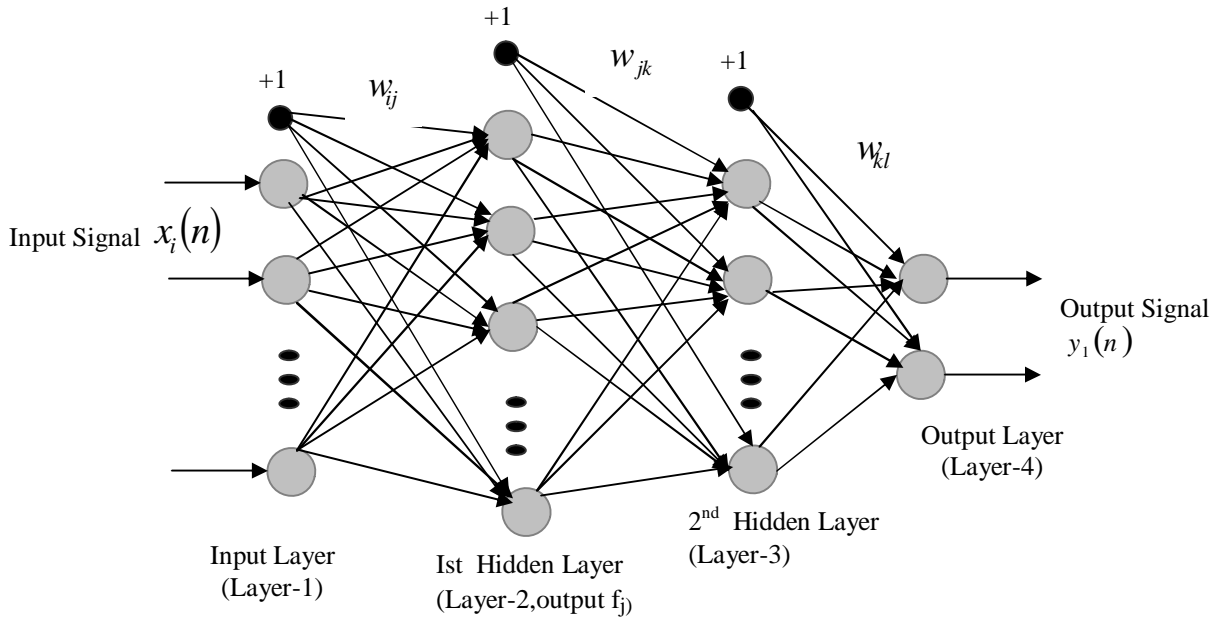


Figure 2.15 (b): MLP Structure

The scheme of MLP using four layers is shown in Figure 2.15(b).  $x_i(n)$  represent the input to the network,  $f_j$  and  $f_k$  represent the output of the two hidden layers and  $y_l(n)$  represents the output of the final layer of the neural network. The connecting weights between the input to the first hidden layer, first to second hidden layer and the second hidden layer to the output layers are represented by  $w_{ij}$ ,  $w_{jk}$  and  $w_{kl}$  respectively.

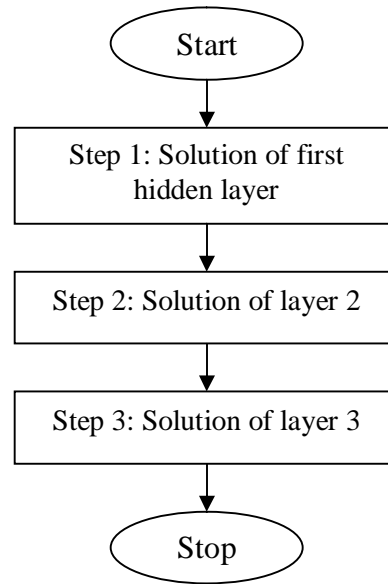


Figure 2.15(c) Flow chart for solving artificial neural network

The neuron works as per the instructions framed in the flow chart shown in Figure 2.15(c) If  $P_1$  is the number of neurons in the first hidden layer, every element of the output vector of first hidden layer can be found using Equation 2.20 if number of neurons is known and number of neurons are  $T_1$  in the first hidden layer.

$$o_j = \varphi_j \left[ \sum_{i=1}^N w_{ij} x_i(n) + \alpha_j \right] \quad (2.20)$$

For  $i= 1, 2, 3 \dots N$

$j= 1, 2, 3, T_1$

where  $\alpha_j$  is the threshold to the neurons of the first hidden layer.

$N$  is the number of inputs and  $\varphi_j(N)$  nonlinear activation function.  $n$  is the time index dropped for simpler equation. Now consider  $T_2$  be the number of neurons in the second hidden layer. Then output of second layer can be given by:

$$f_k = \varphi_j \left[ \sum_{j=1}^{P_1} w_{jk} f_j + \alpha_k \right] \quad (2.21)$$

where  $\alpha_k$  is the threshold to the neurons of the second hidden layer. The final output of first layer can be found by

$$y_1(n) = \varphi_k \left[ \sum_{k=1}^{P_2} w_{kl} f_k + \alpha_1 \right] \quad (2.22)$$

where  $\alpha_i$  is the threshold to the neuron of the final layer and  $T_3$  is the number of neurons in the output layer. The output of the MLP may be expressed as

$$y_1(n) = \varphi_n \left[ \sum_{k=1}^{P_2} w_{kl} \varphi_k \left( \sum_{j=1}^{P_1} w_{jk} \varphi_j \left\{ \sum_{i=1}^N w_{ij} x_i(n) + \alpha_j \right\} + \alpha_k \right) + \alpha_l \right] \quad (2.23)$$

#### 2.1.4 Neuro-Fuzzy System

Upcoming neuro-fuzzy systems are represented as special multilayer feed-forward neural networks models like Adaptive Neuro-Fuzzy Inference System (ANFIS). Fuzzifications of neural network architectures are also considered, for example self-organizing feature maps. In those neuro-fuzzy networks, connection weights and propagation and activation functions differ from common neural networks. Although there are different approaches, here the use of the term neuro-fuzzy system for approaches which display the following properties is validated.

1. Neuro-fuzzy system is based on a fuzzy system which is trained by a learning algorithm derived from neural network theory. The heuristical learning procedure operates on local information, and causes only local modifications in the underlying fuzzy system.
2. Neuro-fuzzy system can be viewed as a 3-layer feed-forward neural network. The first layer represents input variables, the middle hidden layer represents fuzzy rules and the third layer represents output variables. Fuzzy sets are encoded as connection weights which too are fuzzy. It is not necessary to represent a fuzzy system like this to apply a learning algorithm to it. However, it can be convenient, because it represents the data flow of input processing and learning within the

model. Sometimes five layer architecture is used, where the fuzzy sets are represented in the units of the second and fourth layer.

3. A neuro-fuzzy system can be always (i.e. before, during and after learning) interpreted as a system of fuzzy rules. It is also possible to create the system out of training data from scratch, as it is possible to initialize it by prior knowledge in form of fuzzy rules. All neuro-fuzzy models not necessarily specify learning procedures for fuzzy rule creation.
4. The learning procedure of a neuro-fuzzy system takes the semantical properties of the underlying fuzzy system into account. This results in constraints on the possible modifications applicable to the system parameters. All neuro-fuzzy approaches do not have this property.

#### 2.1.4.1 Neuro-fuzzy modeling

Neuro-fuzzy modeling allows a fuzzy system to be refined by neural training, thus avoid lengthy trial-and-error phases in defining both membership functions and inference rules. An approach to obtain simple neuro-fuzzy models is proposed, which reduces the number of rules by means of a systematic procedure that consists in successively removing a rule and updating the remaining rules in such a way that the overall input-output behavior is kept approximately unchanged over the entire training set. A formulation of the proper update is described and a criterion for choosing the rules to be removed is also provided. Initial experimental results show the effectiveness of the proposed method in reducing the complexity of a neuro-fuzzy system by using its input-output data.

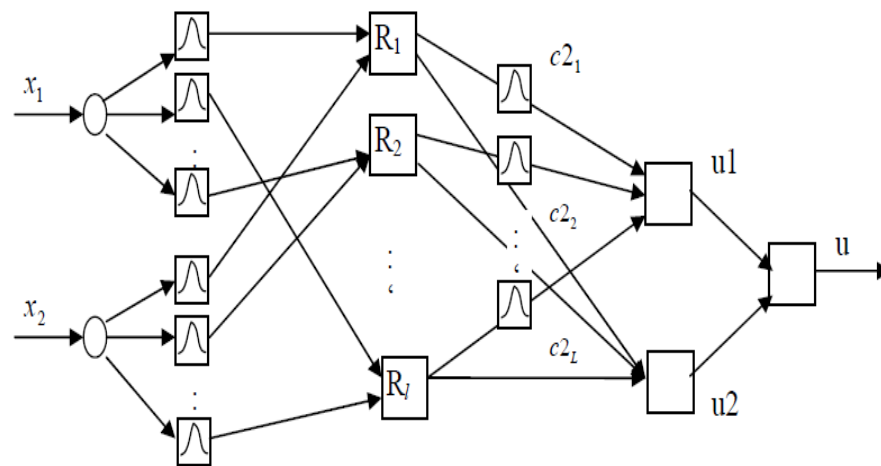


Figure 2.16: Schematic of neuro-fuzzy system

In Figure 2.16 the schematic of neuro-fuzzy has been shown. This is the graphical representation of the processing of knowledge in the neuro-fuzzy based model. This model is able to learn and optimize the control requirement. In Figure 2.17 the general architecture of ANFIS represents how the different layers are performing according to the weights assigned to them as in layer1,layer 2,layer 3,layer 4 and layer 5.The Figure 2.18 shows the schematic of ANFIS in MATLAB.

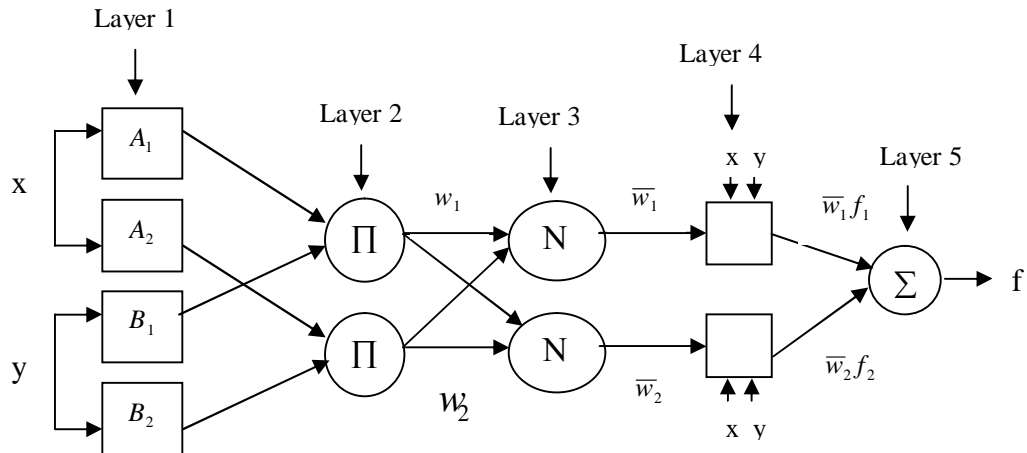


Figure 2.17: General architecture of ANFIS

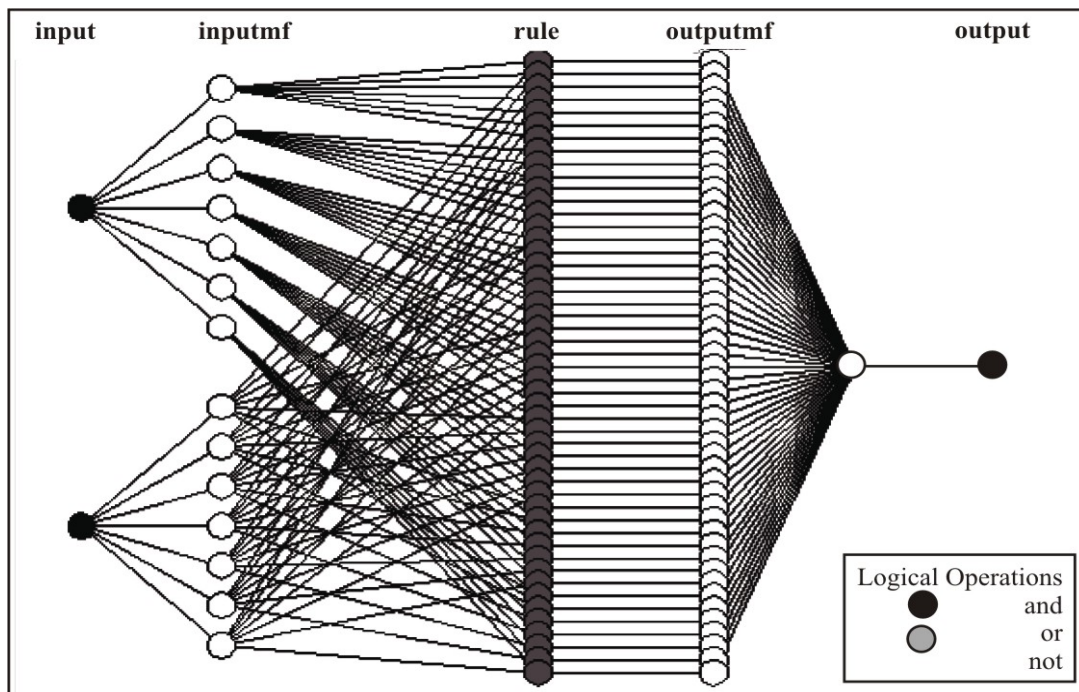


Figure 2.18: Schematic of ANFIS in MATLAB

Fuzzy hardware developments have been a major force in driving the applications of fuzzy set theory and fuzzy logic in both science and engineering. An important research trend is the design of improved fuzzy hardware. There is an increasing interest in both analog and digital implementations of fuzzy controllers in particular and fuzzy systems in general. Specialized analog and digital VLSI implementations of fuzzy systems, in the form of dedicated architectures, aim at the highest implementation efficiency. This particular efficiency is asserted in terms of processing speed and silicon utilization. Processing speed in particular has caught the attention of developers of fuzzy hardware manufacturers and researchers in the field of artificial intelligence.

The basic design flow as shown in Figure 2.19 is divided into two parts. One is structural description and other is layout generation. The system specifications are to be considered as inputs in the form of analog, digital, linear or non linear functions. Then the fuzzy equivalence for them is drawn from the fuzzy hardware. Finally the system is integrated after the decisions are predicted by fuzzy cells.

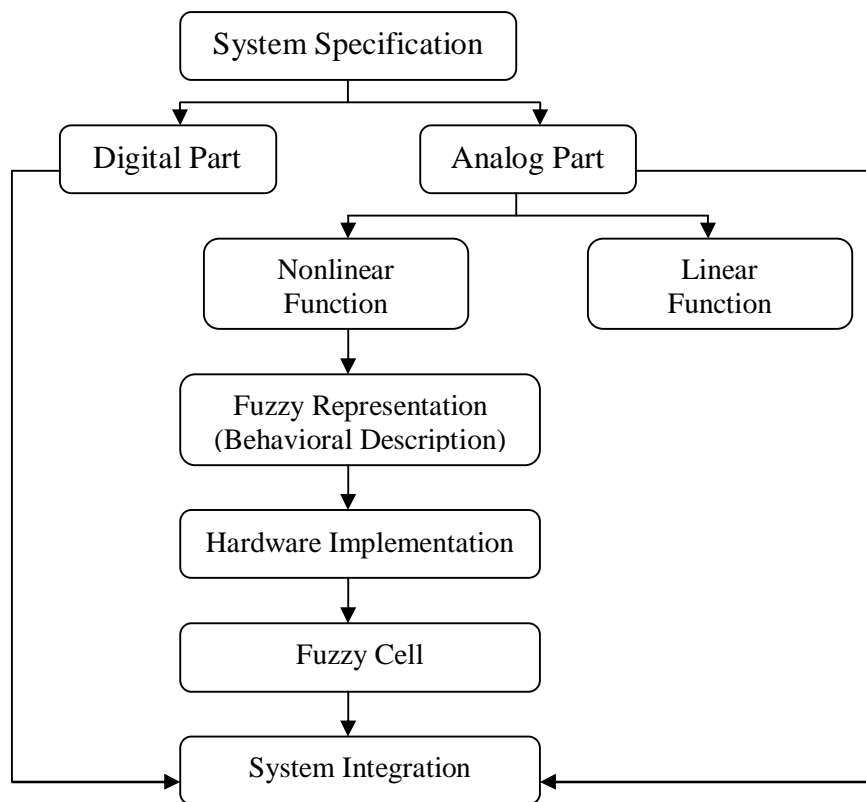


Figure 2.19: Design process for system with fuzzy hardware

The two steps i.e structural description and layout generation are shown in Figure 2.20 and Figure 2.21 respectively.

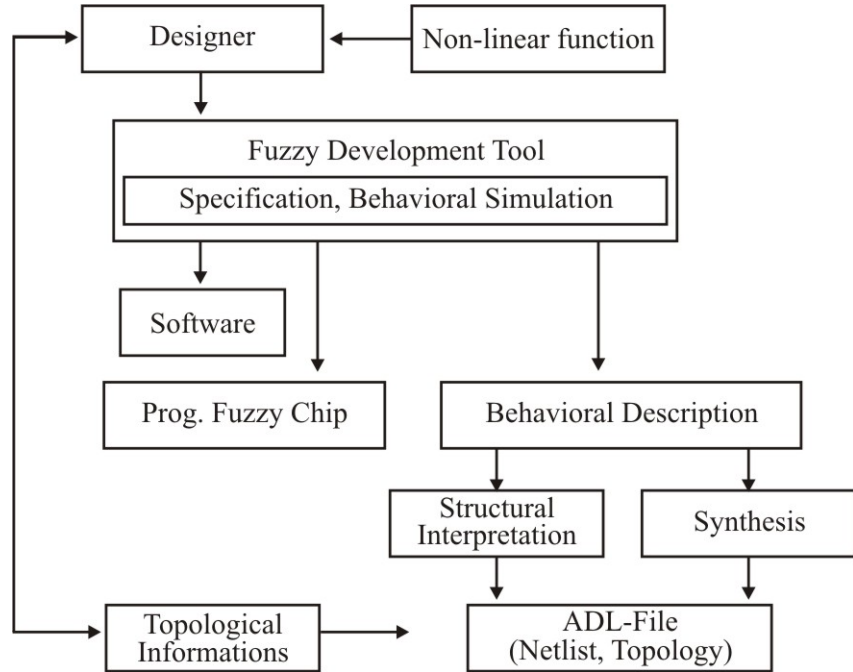


Figure 2.20: Structural description of fuzzy hardware

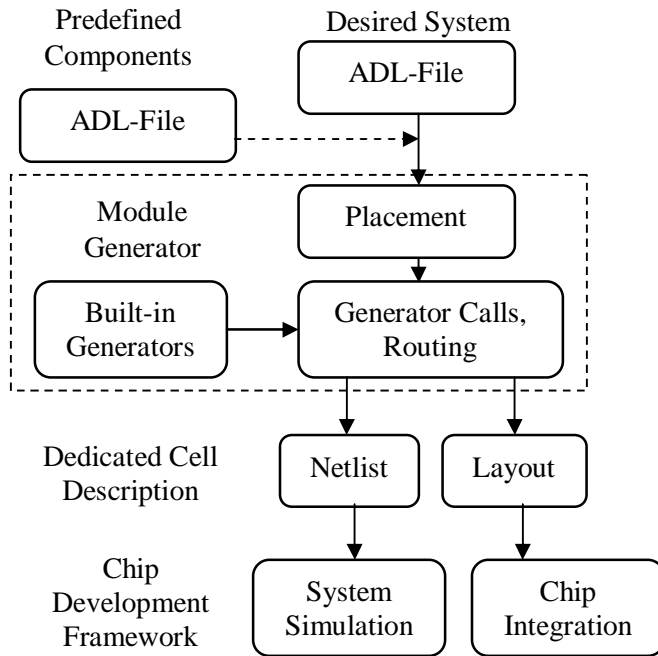


Figure 2.21: Layout generation for fuzzy hardware

With this basic structural description and layout generation many companies are manufacturing dedicated devices to facilitate mankind. The hardware design process for implementing intelligent techniques of fuzzy and neuro-fuzzy utilizes microcontrollers. The first fuzzy logic enhanced MCU was developed by Motorola's 68Hc12. This new 16-bit microcontroller family includes four fuzzy logic instructions in addition to the memory and on-chip peripheral functions as expected in a general purpose microcontroller. The fuzzy logic instructions use existing CPU logic to perform computations including addition, subtraction, multiplication, multiply-and-accumulate, and comparisons, so the speed and efficiency of fuzzy logic programs is greatly improved without increasing the cost of the MCU. A fuzzy inference kernel on the HC12 takes 1/5 as much code space and executes more than 10 times faster compared to an HC11 general purpose MCU. The fuzzyTECH is a family of complete software development systems based on fuzzy logic and neuro-fuzzy technologies. For MCU implementations, fuzzyTECH offers assembly code generation to ensure maximum computational performance using as little memory resources as possible.

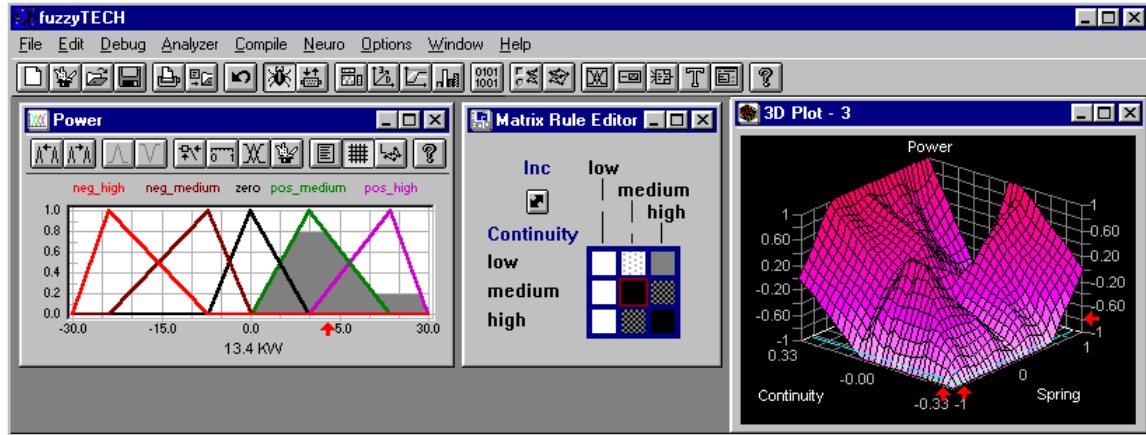


Figure 2.22: fuzzyTech software screenshot

The fuzzyTECH MCU-HC12 Edition is a version of fuzzyTECH dedicated to the Motorola 68HC12 family of microcontrollers. In Figure 2.22 the fuzzyTECH SOFTWARE screen shot is shown. This is very user friendly software.

In many fuzzy logic applications, an implemented control strategy can best be optimized on the running process. The fuzzyTECH supports this "on-the-fly" optimization of a running fuzzy logic system with its RTRCD-HC12 Module, an add-on

to the fuzzyTECH MCU-HC12 Edition. The RTRCD Module uses the background debug mode of the HC12 MCU to:

1. Visualize the complete fuzzy logic inference in real time in fuzzyTECH's analyzers and dynamic editors.
2. Carry out any modification done in fuzzyTECH on the HC12 in real time without interfering with the running process.

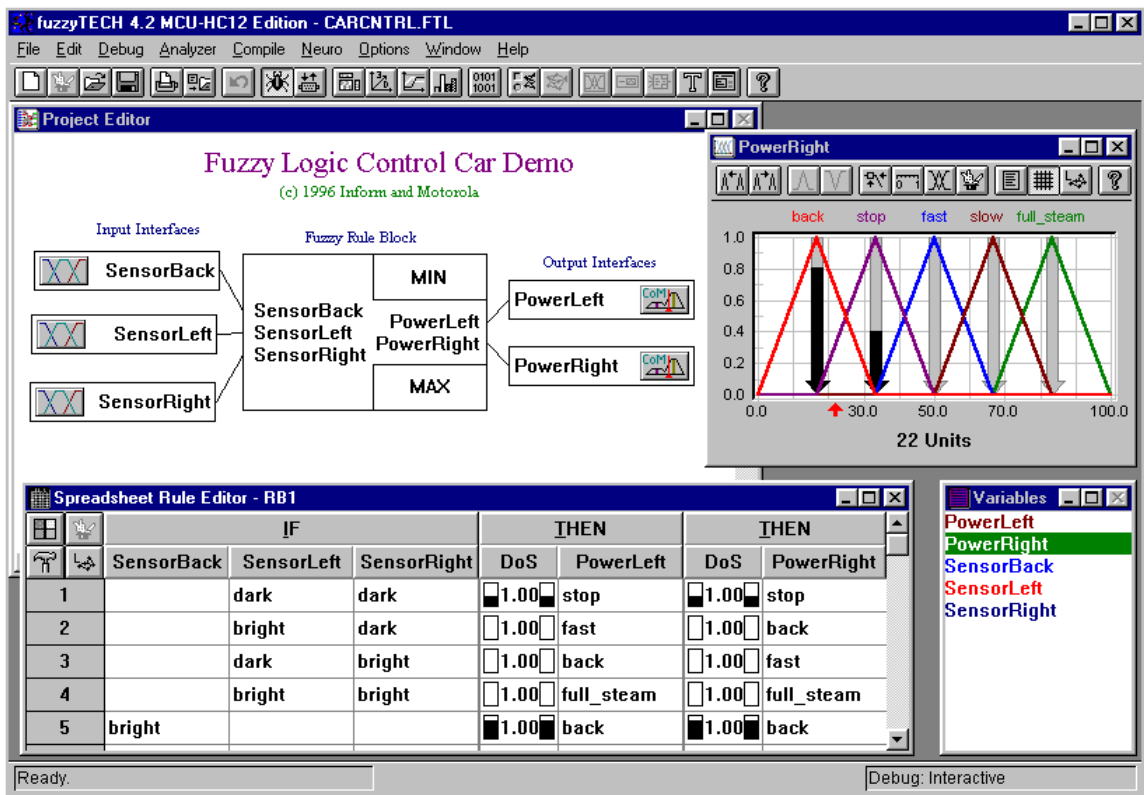


Figure 2.23: Fuzzy car controller using fuzzyTECH

Figure 2.23 shows the graphical design of the fuzzy logic tank controller in the fuzzyTECH development system. The upper left window shows the structure of the fuzzy logic controller. The three inputs of the fuzzy logic system, SensorBack, SensorLeft, and SensorRight, are the light intensities measured by the optical sensors. They feed into the rule block that contains the linguistic control strategy. The two output variables of the fuzzy logic system, PowerLeft and PowerRight, feed directly into the PWM registers of the HC12 MCU.

## 2.2 Robustness and Fuzzy Logic

The concept of stability of systems is of paramount importance and from an application point of view an unstable system is of no use. One of the most important tasks a control engineer is required to do, in connection with the design and analysis of a control system, is to ensure its stability. As with many other general statements, there are exceptions, but in the present context, it may be stated that all the control designs must result in a closed-loop stable system. Many physical systems are inherently open-loop unstable, and some systems are even designed intentionally to be open-loop unstable. Most modern fighter aircraft are open-loop unstable by design, and the pilot cannot fly it without stabilization with feedback control. Feedback not only stabilizes an unstable plants, it also takes care of the transient performance by a judicious choice of controller parameters.

## 2.3 Fuzzy Control

This section describes the classical control scheme and fuzzy control scheme. In classical control scheme we have open loop and closed loop control architecture. Figure 2.24 shows the classical feedback control structure of a plant. In fuzzy control scheme the conventional controller is replaced by fuzzy logic controller. The fuzzy control scheme is shown in Figure 2.25.

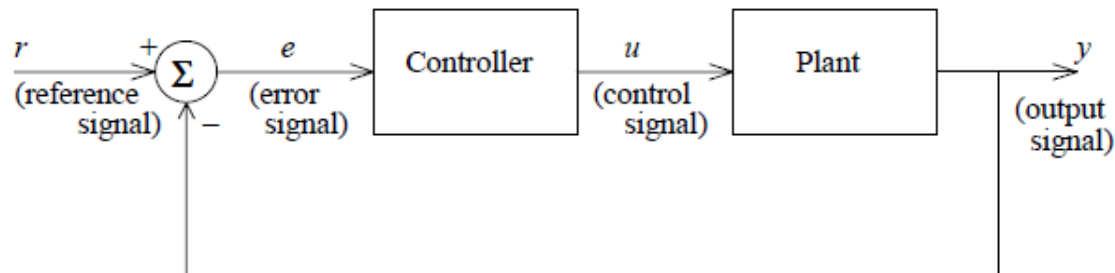


Figure 2.24: Classical feedback control structure

The majority of fuzzy logic control systems are knowledge-based systems in that either their fuzzy models or their fuzzy logic controllers are described by fuzzy IF-THEN rules, which have to be established based on expert's knowledge about the systems, controllers, performance, etc. Moreover, the introduction of input-output intervals and

membership functions is more or less subjective, depending on the designer's experience and the available information. However the emphasize once again is on the determination of the fuzzy sets, all mathematics etc. are rigorously followed. Also, the purpose of designing and applying fuzzy logic control systems is above all to tackle those vague, ill-described, and complex plants and processes that can hardly be handled by classical systems theory, classical control techniques, and classical two-valued logic. This is the first type of fuzzy logic control system in which the fuzzy logic controller directly performs the control actions and thus completely replaces a conventional control algorithm. Yet, there is another type of fuzzy logic control system in which the fuzzy logic controller is involved in a conventional control system and thus becomes part of the mixed control algorithm just to enhance or improve the performance of the overall control system.

The fuzzy logic controller provides an algorithm, which converts the expert knowledge into an automatic control strategy. Fuzzy logic is capable of handling approximate information in a systematic way and therefore it is suited for controlling non linear systems and is used for modeling complex systems, where an inexact model exists or systems where ambiguity or vagueness is common.

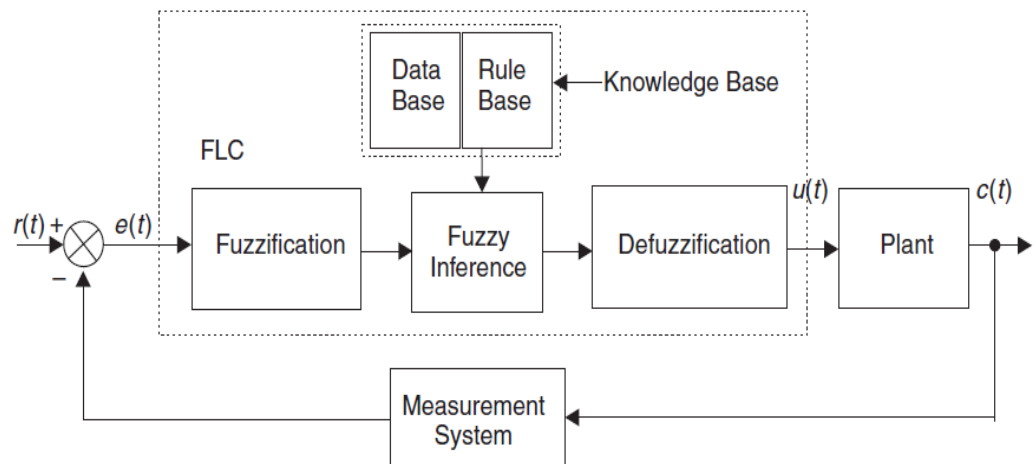


Figure 2.25: Fuzzy logic control structure

The fuzzy control systems are rule-based systems in which a set of fuzzy rules represent a control decision mechanism for adjusting the effects of certain system stimuli. With an

effective rule base, the fuzzy logic control structure as shown in Figure 2.25 can replace a skilled human operator. The rule base reflects the human expert knowledge, expressed as linguistic variables, while the membership functions represent expert interpretation of those variables.

Designing a good fuzzy rule base is the key to obtain satisfactory control performance for a particular operation. Classical analysis and control strategy are incorporated in the rule base. The control literature has worked towards reducing the size of the rule base and optimizing the rule base using different optimization techniques like GA, PSO for intelligent controller. At last defuzzified output is obtained from the fuzzy inputs. Table 2.1 shows the linguistic variables for making rule base in a fuzzy control system.

Table 2.1: Linguistic variables for fuzzy control

<b>Error <math>e(t)</math></b>	<b>Change in Error <math>\Delta e(t)</math></b>	<b>Controller Output <math>u(t)</math></b>
NB: Negative Big	NB: Negative Big	NB: Negative Big
NM: Negative Medium	NM: Negative Medium	NM: Negative Medium
NS: Negative Small	NS: Negative Small	NS: Negative Small
ZO: Zero	ZO: Zero	ZO: Zero
PS: Positive Small	PS: Positive Small	PS: Positive Small
PM: Positive Medium	PM: Positive Medium	PM: Positive Medium
PB: Positive Big	PB: Positive Big	PB: Positive Big

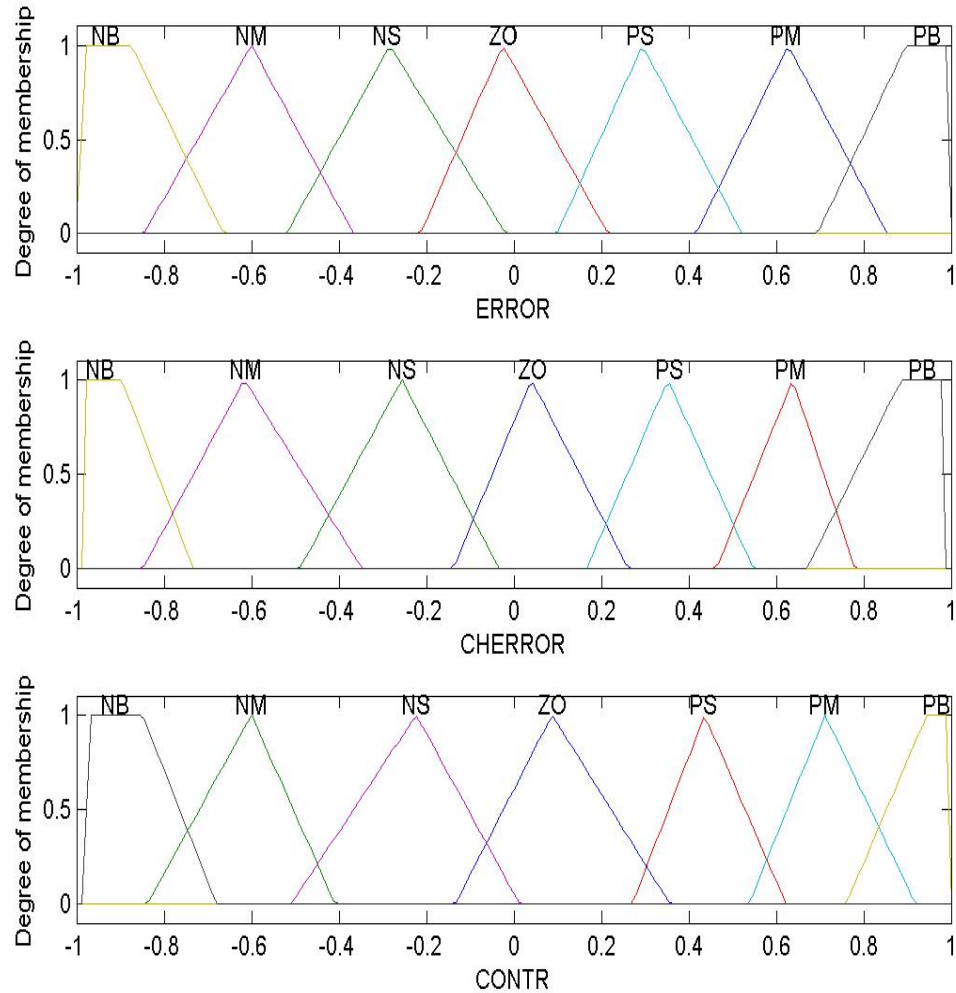


Figure 2.26: Membership functions for inputs and output.

Figure 2.26 shows the membership function for inputs and output. Here there are two inputs, i.e error  $e(t)$  and change in error  $\Delta e(t)$ . The output is the controller output  $u(t)$ .

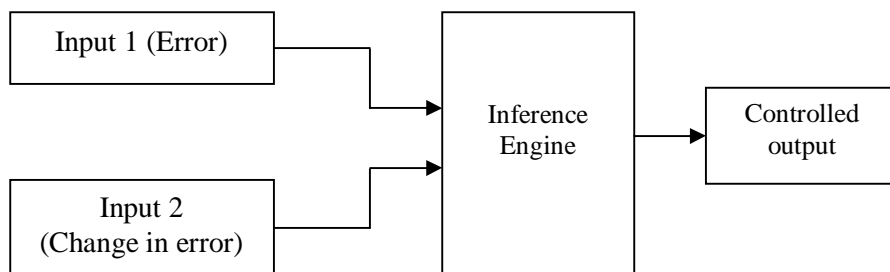


Figure 2.27: Mamdani based fuzzy control system

Mamdani based fuzzy inference system for the desired control application is shown in Figure 2.27. Input 1 is error and input 2 is change in error. The final controlled output is used to take control action. The surface plot and the input-output rule matrix are shown in Figure 2.28 and Table 2.2 respectively.

Table 2.2: Rule matrix for Mamdani fuzzy inference system

u(t)		e(t)						
		NB	NM	NS	ZO	PS	PM	PB
$\Delta e(t)$	NB	NB	NB	NB	NB	NM	NS	ZO
	NM	NB	NB	NB	NM	NS	ZO	PS
	NS	NB	NB	NM	NS	ZO	PS	PM
	ZO	NB	NM	NS	ZO	PS	PM	PB
	PS	NM	NS	ZO	PS	PM	PB	PB
	PM	NS	ZO	PS	PM	PB	PB	PB
	PB	ZO	PS	PM	PB	PB	PB	PB

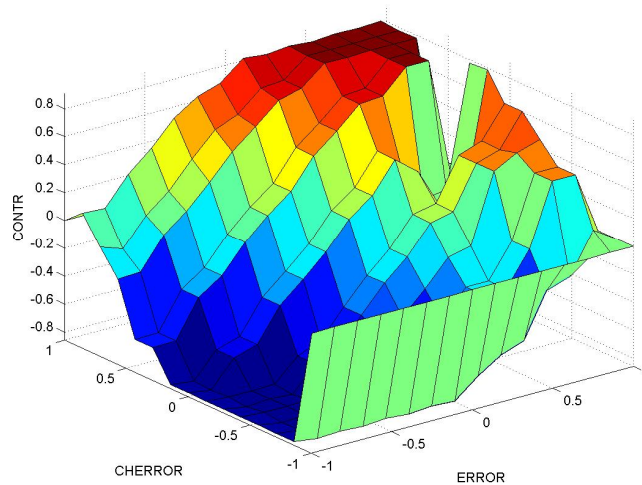


Figure 2.28: Surface plot of inputs and output.

### 2.3.1 Self Organizing Fuzzy Logic Controller

Self organizing fuzzy logic controller has a two level hierarchical control system which comprises of

1. A learning element at the top level
2. A Fuzzy Logic Controller at the bottom level

The learning element comprises of a performance index table combined with a rule generation and modification algorithm, which creates new rules or modifies the existing rules. The structure of self organizing fuzzy logic controller is shown in Figure 2.29.

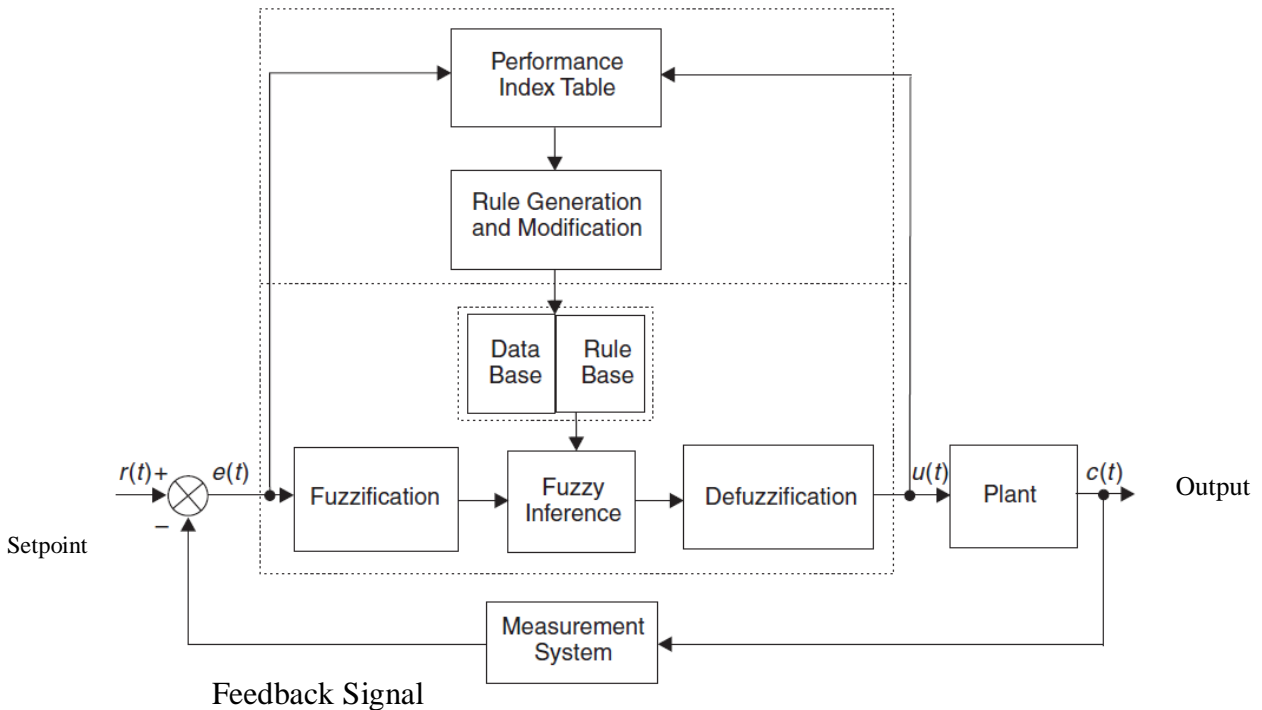


Figure 2.29: Self organizing fuzzy logic control system.

In the decade after Dr. Zadeh's seminal paper on fuzzy sets many theoretical developments in fuzzy logic took place in the United States, Europe, and Japan. From the mid-Seventies to the present, however, Japanese researchers have been a primary force in advancing the practical implementation of the theory; they have done an excellent job of commercializing this technology. Fuzzy logic affects many disciplines. In videography, for instance, Companies like Fisher, Sanyo, and others make fuzzy logic camcorders, which offer fuzzy focusing and image stabilization. Mitsubishi manufactures a fuzzy air conditioner that controls temperature changes according to human comfort indexes. Matsushita builds a fuzzy washing machine that combines smart sensors with fuzzy logic. The sensors detect the color and kind of clothes present and the quantity of dirt and fuzzy

microprocessors selects the most appropriate combination from 600 available combinations of water temperature, detergent amount, and wash and spin cycle times. The Japanese City of Sendai has a 16-station subway system that is controlled by a fuzzy computer. The ride is so smooth that the riders do not need to hold straps, and the controller makes 70 percent fewer judgmental errors in acceleration and braking than human operators do. Nissan introduced a fuzzy automatic transmission and a fuzzy anti-skid braking system in one of their recent luxury cars. Tokyo's stock market has stock-trading portfolios based on fuzzy logic that outperformed the Nikkei Exchange average. In Japan, there are fuzzy golf diagnostic systems, fuzzy toasters, fuzzy rice cookers, fuzzy vacuum cleaners, and many other industrial fuzzy control processes.

With increasing complexities in system engineering, the focus of fuzzy control is moving from elementary control problems to higher levels in the system hierarchy such as supervisory control, monitoring and diagnosis, and logistic support. It is to be noted that telecommunications, which is one of the major future industries, has started investigating fuzzy control for communication systems and that several pilot projects have been initiated for tackling routing and overload handling problems. So far, the majority of existing applications are purely software-based. However, general purpose fuzzy logic processors or coprocessors will be found to be useful in extremely time critical applications like pattern recognition task in complex plant automation and in mass produced automotive electronics. The first generation of fuzzy control in the existing applications exploits only a very small fragment of fuzzy logic theory. In many cases of more complex, ill-structured problems, this first generation technology is not sufficiently equipped to represent and implement the knowledge needed for powerful solutions. Besides, there is strong need for a more systematic design and analysis methodology for fuzzy control applications, spanning the whole life-cycle from perception to all the way up to deployment and maintenance. It must provide answers to make a proper choice of alternative design issues after a thorough analysis of the problem, and must be able to associate variations of parameters to system-performance. At this stage, one should not expect a universal design and optimization strategy for fuzzy control, which will be of some practical use. Such a universal theory does not exist for conventional control engineering either. Instead, we have to proceed from the few isolated islands where we

already know exactly how to design a fuzzy control algorithm to clusters of problems and related design methodologies. From the above discussions it is apparent that fuzzy control has tremendous scope in the knowledge based systems approach to closed loop control system, which may be defined as:

A knowledge based system for closed loop control is a system which enhances the performance, reliability and robustness of control by incorporating knowledge which cannot be captured in the analytical model used for controller design and that is taken care of by manual modes of operation or by other safety and ancillary logic mechanism.

## **2.4 Hierarchical Modeling**

Hierarchical modeling of fuzzy logic concepts that has been used within the recently developed model of intelligent systems, called Object- Oriented Abstraction i.e OBOA [80]. The model is based on a multilevel, hierarchical, general object-oriented approach. Current methods and software design and development tools for intelligent systems are usually difficult extend, and it is not easy to reuse their components in developing intelligent systems. The OBOA model tries to reduce these deficiencies. The model starts with a well-founded software engineering principle, making clear distinction between generic, low-level intelligent software components, and domain-dependent, high-level components of an intelligent system. Here the concentration is on modeling and implementation of fuzzy logic concepts within the hierarchical levels of the OBOA model. The fuzzy components described are extensible and adjustable.

In conventional fuzzy logic controllers, the computational complexity increases with the dimensions of the system variables; the number of rules increases exponentially as the number of system variables increases. Hierarchical fuzzy logic controllers (HFLC) have been introduced to reduce the number of rules to a linear function of system variables. However, the use of hierarchical fuzzy logic controllers raises new issues in the automatic design of controllers, namely the coordination of outputs of sub-controllers at lower levels of the hierarchy. A method which is described for the automatic design of an HFLC using an evolutionary algorithm is called Differential Evolution (DE). A sufficiently versatile method that can be applied to the design of any HFLC architecture exists. The feasibility of the method is demonstrated by developing a two-stage HFLC for

controlling a cart-pole with four state variables. The merits of the method are automatic generation of the HFLC and simplicity as the number of parameters used for encoding the problem is greatly reduced as compared to conventional methods.

The hierarchical fuzzy logic systems not only provide a complex and flexible architecture for modeling nonlinear systems. It also reduces the size of rule base to some extent. But there is no systematic method for designing of the hierarchical T-S fuzzy systems yet. The problems in designing of hierarchical fuzzy logic system include:

1. Selecting a proper hierarchical structure: Selecting the inputs for each partial fuzzy model: Determining a rule base for each fuzzy logic T-S model.
2. Optimizing the parameters used in the fuzzy membership Functions and the then-part of TS fuzzy model.

## 2.5 Control Evaluation

A performance index is a quantitative measure of the performance of a system and is chosen so that emphasis is given to the important system specifications. The performance index must be a number that should be positive or zero. The best system is defined as the system that minimizes the indices. There are four performance indices available in classical control literature. These performance indices are Integral Square Error (ISE), Integral Absolute Error (IAE), Integral Time Absolute Error (ITAE), and Integral Time Square Error (ITSE). The desirable feature of performance indices is the selectivity and its power to distinguish between optimum and non optimum system. These indices are easier to implement and mathematically convenient both for analysis and computation.

Typical criteria to minimize a loss function of the form

$$I = \int_0^{\infty} t^n |e(t)|^m dt \quad (2.24)$$

Table 2.3: Different performance indices in classical control system

Performance Index	Name	Formula
IAE	Integral of Absolute magnitude of Error	$IAE = \int_0^T  e(t)  dt$
ITAE	Integral Time Absolute Error	$ITAE = \int_0^T t  e(t)  dt$

## **2.6 Conclusion**

Chapter 2 discusses fuzzy logic, the importance of fuzzy logic in non linear control and engineering applications. There are different types of fuzzy sets which are described in this chapter. In recent times neuro-fuzzy modeling has been used in a variety of control applications. In servo control precise control is required with no overshoot and minimum settling time. The fuzzy and neuro fuzzy control algorithms are important in this regard. This chapter also discusses the commercial aspects of fuzzy logic and discusses the hardware and software used to implement embedded fuzzy and embedded neuro fuzzy control applications. In recent times fuzzy logic system and neuro fuzzy system has a wide variety of applications from bioinformatics, digital image processing, adaptive filtering, communication system, adaptive control. Recent development in hierarchical modeling of fuzzy system is also discussed where there are multiple rule base and multiple fuzzy inference system which acts in a cascade manner. Neural network possesses advantages in the areas of classification, learning and optimization whereas fuzzy logic has advantages in imprecise data handling and human reasoning and intuition. Many researchers tried to combine both the discipline to get a hybrid structure which is known as neuro-fuzzy system. This kind of hybrid structure gives a more accurate reading. Every control system's performance evolution is done by stability analysis and error estimation. Different methods of error estimation in classical control technique are also discussed in this chapter.

---

## CHAPTER 3

# SYNCHRONOUS GENERATOR: CASE STUDY

---

### **Introduction**

Alternator i.e the synchronous generator came in to commercial limelight in August 24, 1891. So it is considered as its birth date. The first large-scale demonstration of transmission of ac power was carried out on the same day. It made possible the transmission from Lauffen, Germany, to Frankfurt, about 110 miles. It was demonstrated during an international electrical exhibition in Frankfurt. The demonstration convinced about the feasibility of transmitting ac power over long distances, and the city of Frankfurt agreed to install it. The first power plant was commissioned in 1894.

The Lauffen-Frankfurt demonstration of alternating power delivery was instrumental in the adoption by New York's Niagara Falls power plant of the same technology. The Niagara Falls power plant became operational in 1895. Southern California Edison's history book reports that its Mill Creek hydro plant is the oldest active polyphase i.e three-phase plant in the United States. Located in San Bernardino County, California, its first units went into operation on September 7, 1893, placing it almost two years ahead of the Niagara Falls project. One of those earlier units is still preserved and displayed at the plant. It is interesting to note that although tremendous development in machine ratings, insulation components, and design procedures has occurred now for over one hundred years, the basic constituents of the machine have remained practically unchanged.

### **3.1 Synchronous Generator**

Electric generators convert mechanical energy into electrical energy. The mechanical energy is produced by prime movers. Prime movers are mechanical machines. They convert primary energy of a fuel or fluid into mechanical energy. They are also called turbines or engines. Figure 3.1 shows the basic prime mover generator system, where turbine drives an electric generator directly or through transmission line

[228]. The fossil fuels commonly used in prime movers are coal, gas, oil, or nuclear fuel. Essentially, the fossil fuel is burned in a combustor; thus, thermal energy is produced. Thermal energy is then taken by a working fluid and turned into mechanical energy in the prime mover. Steam is the working fluid for coal or nuclear fuel turbines. In gas turbines or in diesel or internal combustion engines, the working fluid is the gas or oil in combination with air. On the other hand, the potential energy of water from an upper-level reservoir may be turned into kinetic energy that hits the runner of a hydraulic turbine, changes momentum and direction, and produces mechanical work at the turbine shaft as it rotates against the “braking” torque of the electric generator under electric load. Wave energy is similarly converted into mechanical work in special tidal hydraulic turbines. Wind kinetic energy is converted by wind turbines into mechanical energy.

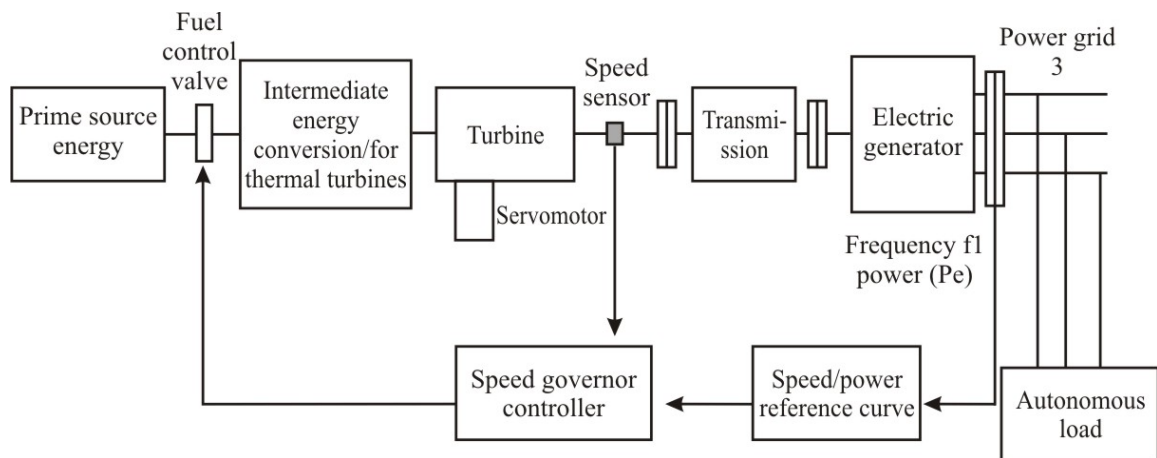


Figure 3.1: Basic prime-mover generator system

Synchronous generator runs at a constant speed and draws its excitation from a power source external or independent of the load or transmission network it is supplying. A synchronous generator has an exciter that enables the synchronous generator to produce its own reactive power and to also regulate its voltage. Synchronous generators can operate in parallel with the utility. It requires a speed reduction gear.

Customers worried about future blackouts and having increased power reliability should only consider cogeneration and regeneration power plants that have synchronous generators. The electric generators which are classified as per their principle of operation

and secondly as per the application domain, where they are used. Figure 3.2 by principle shows the classification of synchronous generators [228]. Additionally, systems with synchronous generators can provide up to 100% of the facility's power, whereas induction generators can only supply about 1/3 of the facility's power requirements.

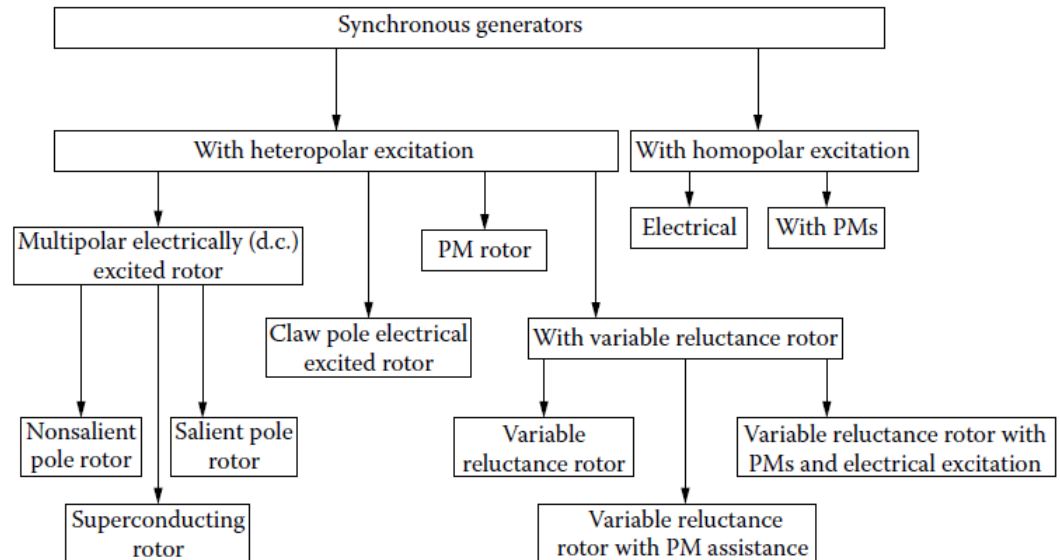


Figure 3.2: Classification of synchronous generator system [228]

Synchronous machine is an ac rotating machine whose speed under steady state condition is proportional to the frequency of the current in its armature. The magnetic field created by the armature currents rotates at the same speed as that created by the field current on the rotor, which is rotating at the synchronous speed, and a steady torque results. Synchronous machines are commonly used as generators especially for large power systems, such as turbine generators and hydroelectric generators in the grid power supply. Because the rotor speed is proportional to the frequency of excitation, synchronous motors can be used in situations where constant speed drive is required. Since the reactive power generated by a synchronous machine can be adjusted by controlling the magnitude of the rotor field current, unloaded synchronous machines are also often installed in power systems solely for power factor correction or for control of reactive kVA flow. Such machines, known as synchronous condensers, may be more economical in the large sizes than static capacitors.

An excited SG is driven on no load at speed  $\omega_r$ . When a balanced three-phase load is connected to the stator, the presence of EMFs at frequency  $\omega$  will naturally produce currents of the same frequency. The phase shift between the EMFs and the phase current  $\Psi$  is dependent on load nature (power factor) and on machine parameters, not yet mentioned. The sinusoidal EMFs and currents are represented as simple phasors in Figure 3.3. Because of the magnetic anisotropy of the rotor along axes  $d$  and  $q$ , it helps to decompose each phase current into two components: one in phase with the EMF and the other one at  $90^\circ$  with respect to the former  $I_{-Aq}, I_{-Bq}, I_{-Cq}$  and  $I_{-Ad}, I_{-Bd}, I_{-Cd}$  respectively.

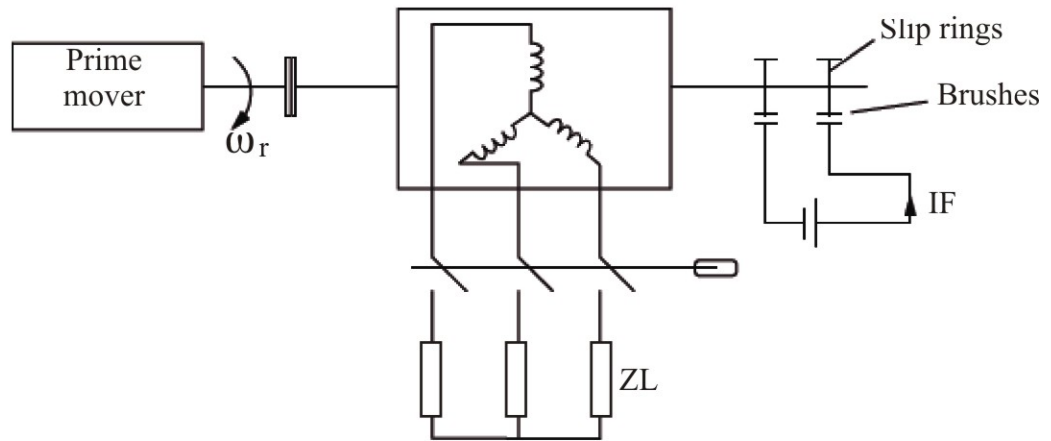


Figure 3.3: The synchronous generator on load

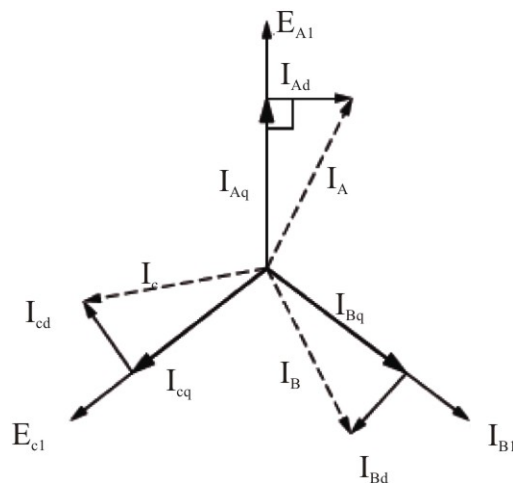


Figure 3.4: EMF and current phasors

Synchronous generators in parallel are the basis of electric power system. Synchronous generators are connected to the power grid one by one. Here we assume that power grid is of infinite power, and fixed voltage, frequency, and phase. When the Synchronous generators is connected to the power grid without large current and power transients, the amplitude, frequency, sequence, and phase of the Synchronous generators no-load voltages have to coincide with the same parameters of the power grid. As the power switch does not react instantaneously, some transients will always occur. However, they have to be limited. Automatic synchronization of the Synchronous generators to the power grid is today performed through coordinated speed (frequency and phase) and field current control.

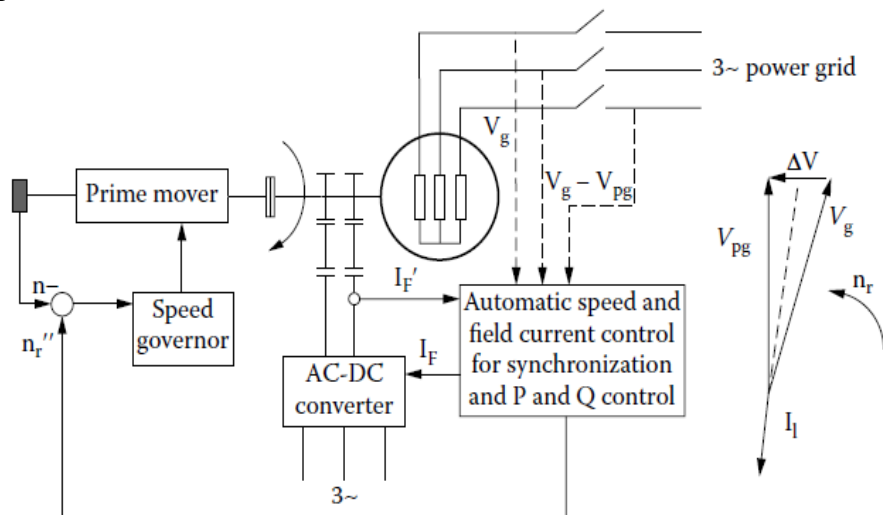


Figure 3.5: Synchronous generator connected with grid

A generator is an electromechanical machine composed of a static part the stator and a rotating part the rotor whose relative position is changed periodically by rotating the angle. Synchronous machines can be catalogued into two types according to air gaps between stator and rotor:

1. Synchronous machine with uniform air gaps and concentric cylindrical rotor, such as surface mount permanent machine
2. Synchronous machine with non uniform air gaps, such as salient pole of machine, interior permanent machine (IPM), etc.

Excitation system performs control and protective functions for generator. The direct current required for field excitation is furnished by the excitation system. The source of power can be a shaft-mounted exciter, a motor-generator set, or a static rectifier. Turbine and governors is the prime mover for generator. They convert the primary energy of fuel into mechanical energy. Power system stabilizers are used to add damping to the generator power oscillations by controlling its excitation using an auxiliary stabilizing signal. To provide damping, the stabilizer must add a component of electrical torque in phase with rotor speed deviation.

In a conventional synchronous machine the armature winding is almost invariably on the stator and is which is a three phase winding. The field winding is usually on the rotor and excited by DC current, or permanent magnets. The DC power supply required for excitation usually is supplied through a DC generator known as exciter, which is often mounted on the same shaft as the synchronous machine. Various excitation systems using ac exciter and solid state rectifiers are used with large turbine generators. There are two types of rotor structures: round or cylindrical rotor and salient pole rotor as illustrated schematically in the diagram below. Generally, round rotor structure is used for high speed synchronous machines, such as steam turbine generators, while salient pole structure is used for low speed applications, such as hydroelectric generators. Figure 3.6 shows the stator and rotor of a hydroelectric generator and the rotor of a turbine generator [227,228].

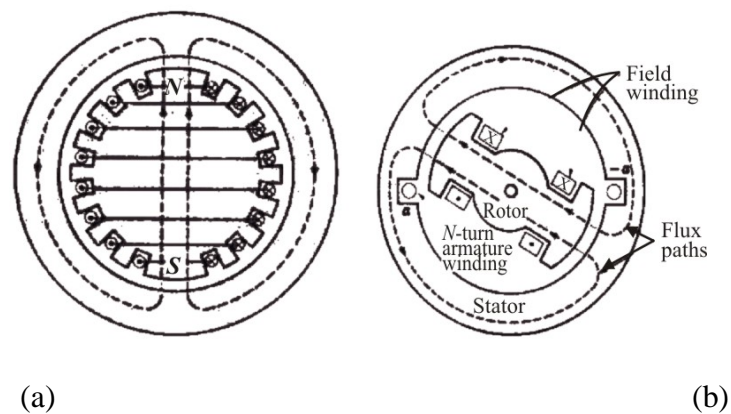


Figure 3.6: (a) Schematic Illustration of Synchronous Machines of Salient rotor  
(b) Round or cylindrical rotor

Let us consider a synchronous machine with two magnetic poles. The idealized radial distribution of the air gap flux density is sinusoidal along the air gap. When the rotor rotates for one revolution, the induced EMF, which is also sinusoidal, varies for one cycle as illustrated by the waveforms in the diagram below. If we measure the rotor position by physical or mechanical degrees or radians and the phase angles of the flux density and EMF by electrical degrees or radians, in this case, it is ready to see that the angle measured in mechanical degrees or radians is equal to that measured in electrical degrees or radians, i.e.  $\theta = \theta_m$

Where  $\theta$  is the angle in electrical degree and  $\theta_m$  is the mechanical angle. As the rotor rotates for one revolution  $\theta_m = 2\pi$ , the induced EMF varies for two cycles  $\theta = 4\pi$  and hence  $\theta = 2\theta_m$

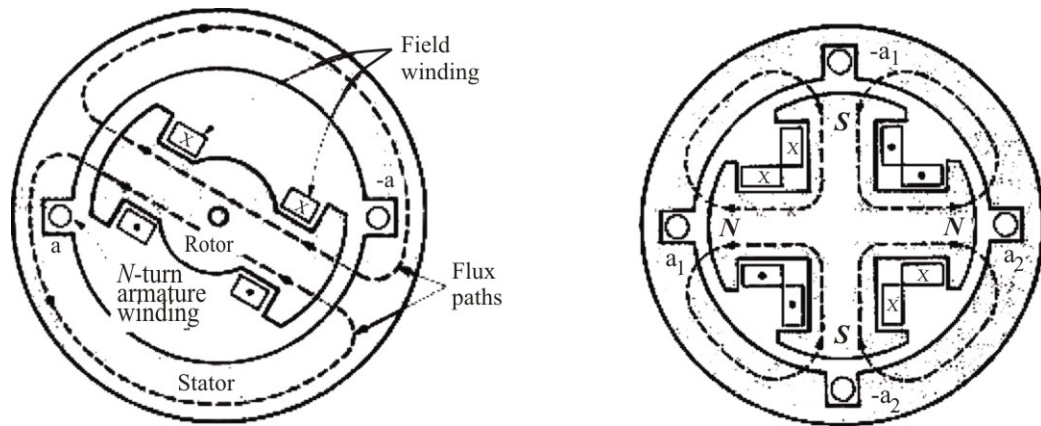


Figure: 3.7: Flux density distribution in air gap & induced EMF in phase winding

- (a) Two Pole and
- (b) Four pole synchronous machine

For a general case, if a machine has P poles, the relationship between the electrical and mechanical units of an angle can be readily deduced as

$$\theta = \frac{P}{2} \theta_m \tag{3.1}$$

Taking derivatives on the both side of the above equation, we obtain

$$\frac{d\theta}{dt} = \frac{P}{2} \frac{d\theta_m}{dt} \tag{3.2}$$

$$\omega = \omega_m \quad (3.3)$$

where  $\omega$  is the angular frequency of EMF in electrical radians per second and the angular speed of the rotor in mechanical radians per second. When  $\omega$  and  $\omega_m$  are converted into cycles per second or Hz and revolutions per minute respectively, we have

$$f = \frac{pn}{120} \quad (3.4)$$

$$n = \frac{120f}{p} \quad (3.5)$$

Where  $\omega = 2\pi f$  and  $\omega_m = \frac{2\pi n}{60}$ . And  $n$  is rotor speed in rev/min. The frequency of the induced EMF is proportional to the rotor speed.

The magnetic field distribution of a distributed phase winding can be obtained by adding the fields generated by all the coils of the winding. The diagram below plots the profiles of MMF and field strength of a single coil in a uniform air gap. If the permeability of the iron is assumed to be infinite, by ampere's law, the MMF across each air gap would be  $NI_a/2$ , where  $N$  is the number of turns of the coil and  $I_a$  the current in the coil. The MMF distribution along the air gap is a square wave. Because of the uniform air gap, the spatial distribution of magnetic field strength is the same as that of MMF.

It can be shown analytically that the fundamental component is the major component when the square wave MMF is expanded into a fourier series, and it can be written as

$$F_{a1} = \frac{4Ni_a}{2\pi} \cos \theta \quad (3.6)$$

When the field distributions of a number of distributed coils are combined, the resultant field distribution is close to a sine wave, as shown in the diagram. The fundamental component of the resultant MMF can be obtained by adding the fundamental components of these individual coils.

$$F_{a1} = \frac{4N_{ph}k_p}{\pi p} i_a \cos \theta \quad (3.7)$$

$N_{ph}$  is the total number of turns of the phase winding.  $K_p$  is the distribution factor of the winding.  $K_p$  is the ratio between fundamental MMF of a distributed winding and fundamental MMF of a concentrated MMF.  $P$  is the number of poles.

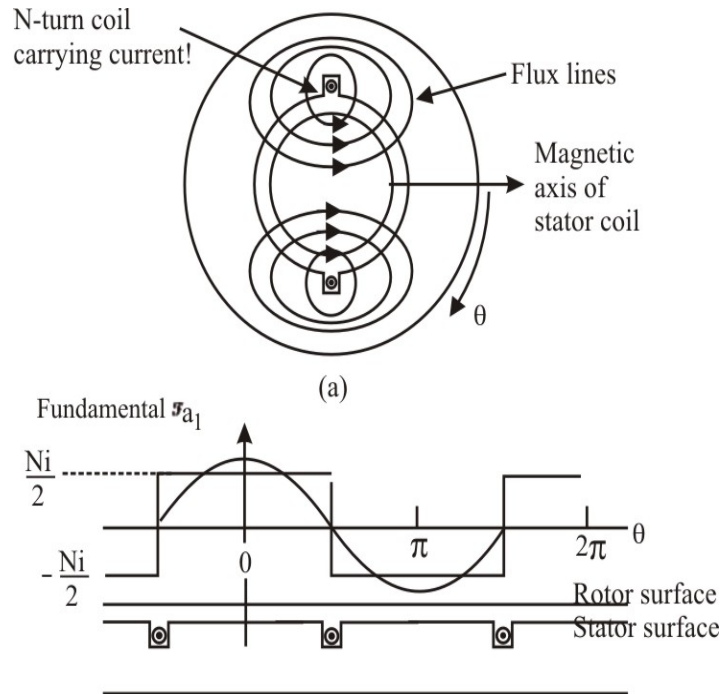


Figure 3.8 (a): Rotating Magnetic Field

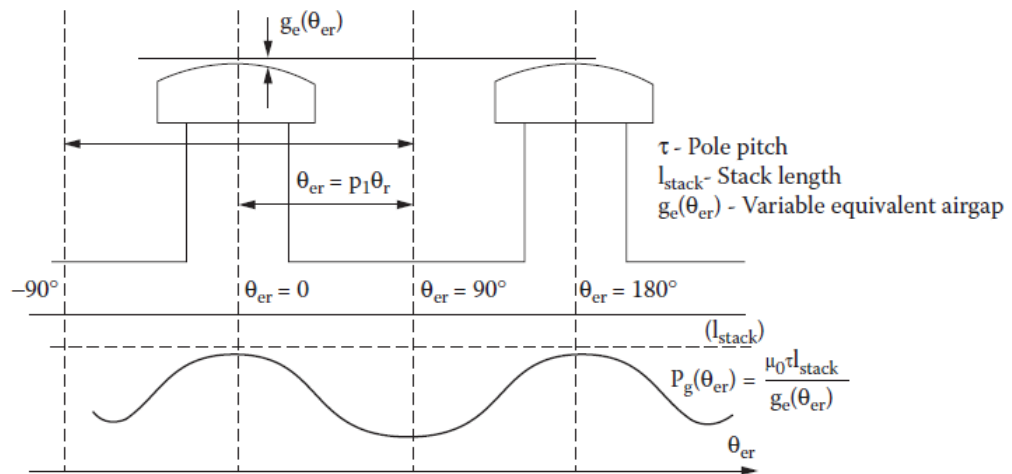


Figure 3.8 (b): The airgap permeance per pole versus rotor position



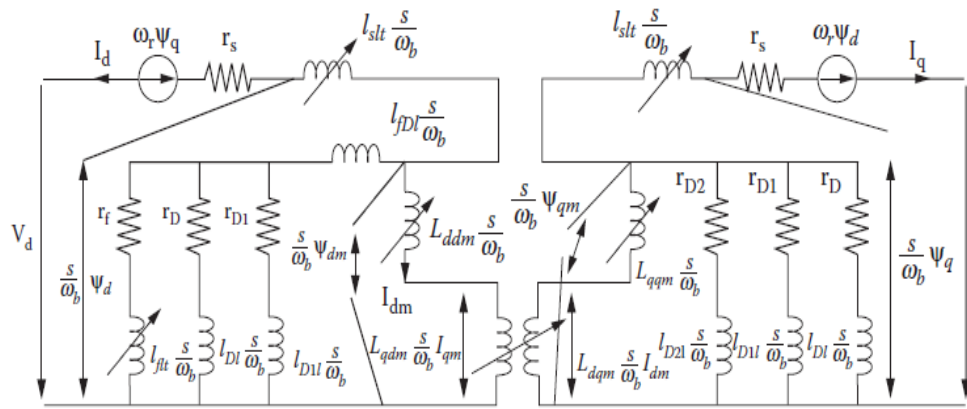
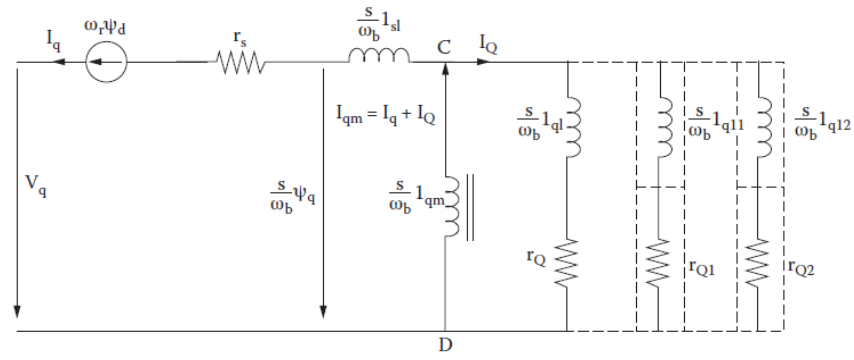


Figure 3.9: Equivalent circuit diagram of synchronous generator

(a) along d axis and along q axis

(b) circuit for cross coupling saturation

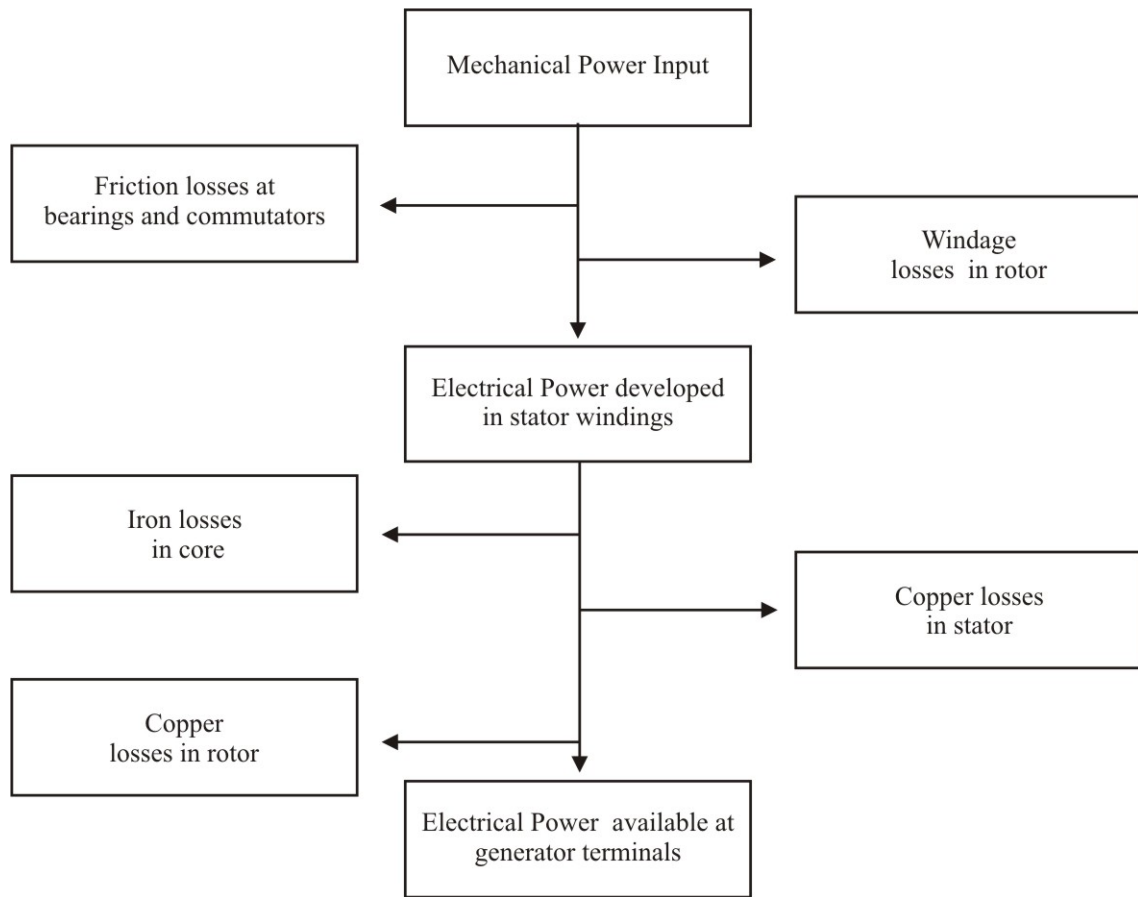


Figure 3.10: Power flow diagram of synchronous generator

The power flow, shown in Figure 3.10, within the generator is tracked by balancing the input and the output taking into account the heat and magnetic power losses. The losses are quantified by performing several standard tests on the generator. The current flowing in the generator can be calculated using the equivalent circuit representing the generator physical elements. The steady-state developed torque and power are then evaluated and plotted to reveal the generator characteristics. The expected efficiency of those particular parameters can also be plotted. In many cases, the armature resistance and copper losses are ignored to simplify the procedures.

### 3.3 Steady state power angle characteristics

The maximum power a synchronous machine can deliver is determined by the maximum torque which can be applied without loss of synchronism with the external system to which it is connected. The purpose of this section is to derive expressions for the steady-

state power limits of synchronous machines in simple situations for which the external system can be represented as impedance in series with a voltage source. Since both the external system and the machine itself can be represented as an impedance in series with a voltage source, the study of power limits becomes merely a special case of the more general problem of the limitations on power flow through a series impedance. The impedance will include the synchronous impedance of the synchronous machine as well as an equivalent impedance of the external system (which may consist of transmission lines and transformer banks as well as additional synchronous machines).

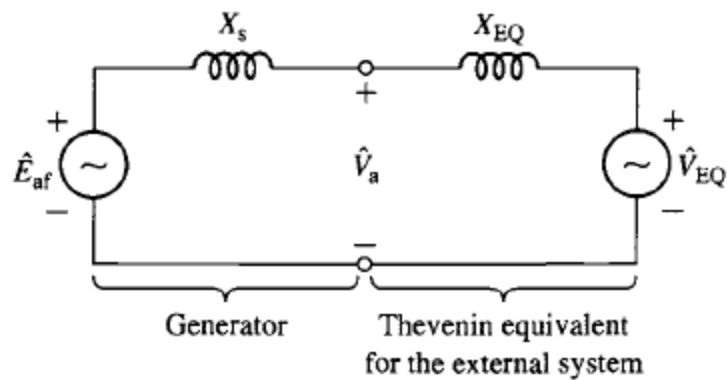


Figure 3.11: Synchronous machine connected to an external system

The terminal voltage vs power angle and  $E_{af}$  vs power curve of a three-phase, 75-MVA, 13.8-kV synchronous generator with saturated synchronous reactance  $X_s = 1.35$  per unit and unsaturated synchronous reactance  $X_{s,u} = 1.56$  per unit is connected to an external system with equivalent reactance  $X_{EQ} = 0.23$  per unit and voltage  $V_{EQ} = 1.0$  per unit, both on the generator base is plotted. It achieves rated open-circuit voltage at a field current of 297 amperes. The Figure  $\delta$  shows the curves.

$$P_{\max} = \frac{E_{af} V_{EQ}}{X_s + X_{EQ}} \quad (3.10)$$

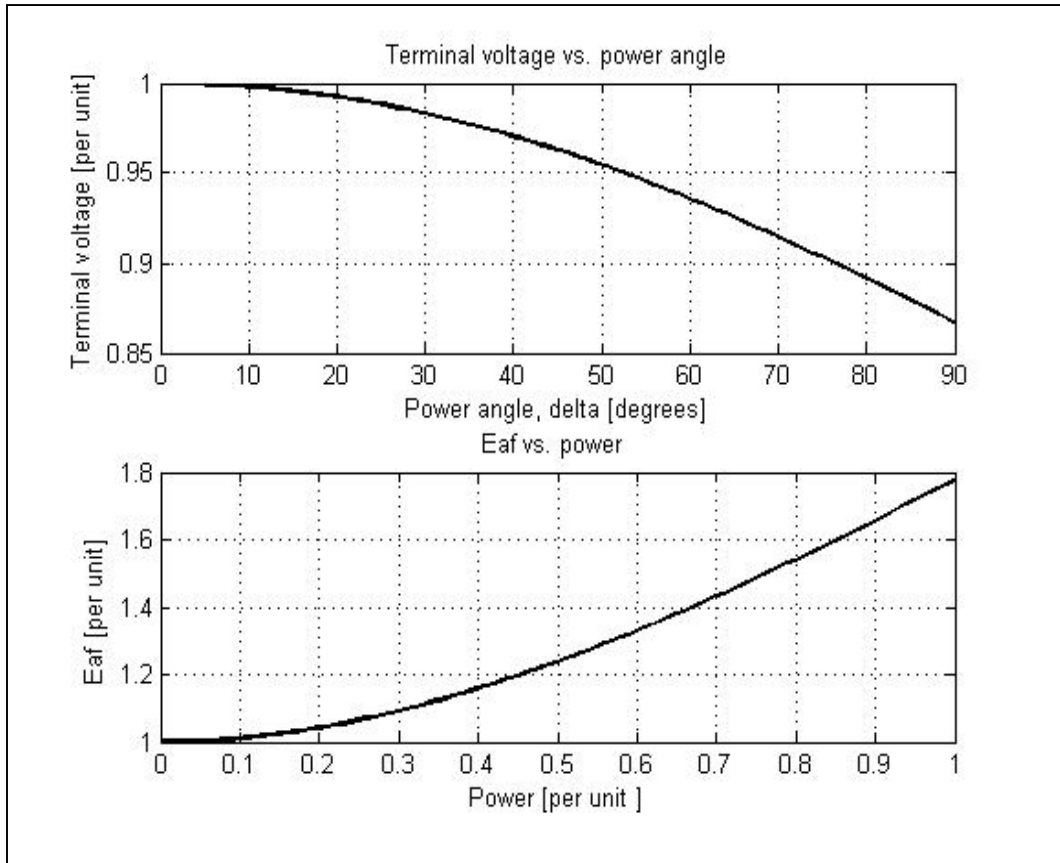


Figure 3.12: Graph between  $E_{af}$  vs power and terminal voltage vs power angle of the synchronous generator

In the internal generated voltage of a synchronous generator, the voltage induced is dependent upon flux and speed of rotation, hence from what we have learnt so far, the induced voltage can be found as follows:

$$E_A = \sqrt{2}\pi N_c \phi f \quad (3.11)$$

$$\text{For simplicity we can write } E_A = k\phi\omega \quad (3.12)$$

$$\text{Where } k = \frac{N_c P}{\sqrt{2}} \quad (\omega \text{ is in rad/sec}) \quad (3.13)$$

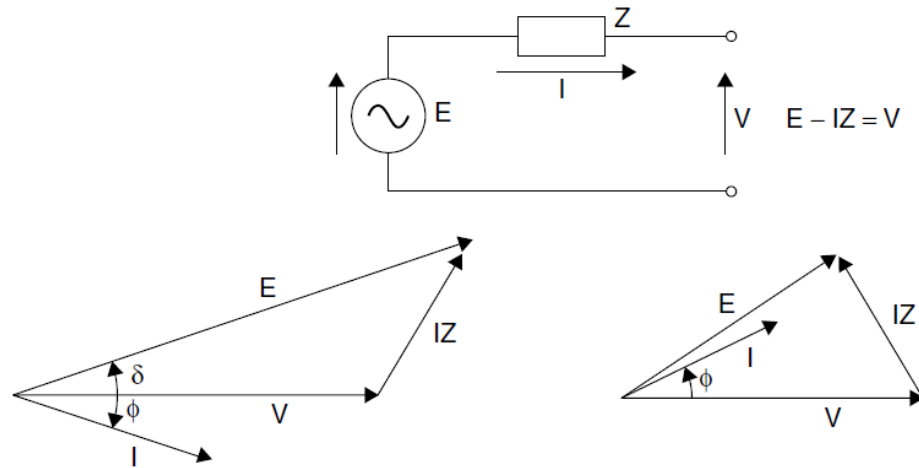


Figure 3.13: Phasor Models

(a) Lagging power factor (over excited)

(b) Leading power factor (under excited)

### 3.4 Power and torque in synchronous generators

A generator converts mechanical energy into electrical energy. Input power is a mechanical prime mover, e.g. diesel engine, steam turbine, water turbine or anything similar. Regardless of the type of prime mover, the rotor velocity must remain constant to maintain a stable system frequency.

$$\text{Input:} \quad P_{in} = \tau_{app} \omega_m \quad (3.14)$$

Losses: Stray losses, friction and windage losses, core loss

$$\text{Converted power:} \quad P_{conv} = \tau_{ind} \omega_m = 3E_A I_A \cos \gamma \quad (3.15)$$

where  $\gamma$  is the angle between  $E_A$  and  $I_A$ .

Losses: Copper losses

Output:

$$P_{out} = \sqrt{3} V_T I_L \cos \theta \quad \text{or} \quad P_{out} = 3V_\phi I_A \cos \theta \quad (3.16)$$

$$Q_{out} = \sqrt{3} V_T I_L \sin \theta \quad \text{or} \quad Q_{out} = 3V_\phi I_A \sin \theta \quad (3.17)$$

Simplifying the phasor diagram, an assumption may be made whereby the armature resistance  $R_A$  is considered to be negligible and assuming that load connected to it is lagging in nature. Based upon the simplified phasor diagram:

$$I_A \cos \theta = \frac{E_A \sin \delta}{X_s} \quad (3.18)$$

which gives another form of output power expression since  $R_A$  assumed to be zero

$$P = \frac{3V_\phi E_A \sin \delta}{X_s} \quad (3.19)$$

From the above equation, it can be seen that power is dependent upon:

- The angle between  $V_\phi$  and  $E_A$  which is  $\delta$ .
- $\delta$  is known as the torque angle of the machine.
- Maximum torque may be found when  $\sin \delta$  is 1 which gives the maximum power (a.k.a. static stability limit) to be:

$$P_{\max} = \frac{3V_\phi E_A}{X_s} \quad (3.20)$$

The basic torque equation:

$$\tau_{ind} = kB_R \times B_s = kB_R \times B_{net} = kB_R B_{net} \sin \delta \quad (3.21)$$

An alternative expression can be derived from the power expression since  $P_{out}=P_{conv}$  when  $R_A$  assumed to be zero. Because  $P_{conv}=\tau_{ind}\omega_m$ , the induced voltage is:

$$\tau_{ind} = \frac{3V_\phi E_A \sin \delta}{\omega_m X_s} \quad (3.22)$$

### 3.5 Stability Analysis

The eigen values of the system matrix  $A$  describe machine's stability properties at the linearization point. If the eigen values are on the left half plane, the system will return to its stationary state after a small perturbation and the system is stable. Eigen values on the right half plane mean that the system is unstable. However, an unstable system may be stabilized using feedback. The original system is still unstable, but the whole system, which consists of the original system and the feedback, may be stable. Therefore, the response does not grow towards infinity [229,230,109].

When a transformation is represented by a square matrix  $A$ , the eigen value equation can be represented as  $(A - \lambda I)x = 0$  (3.23)

Where  $A$  is the square matrix,  $I$  is the identity matrix,  $|\lambda I - A| = 0$  (3.24)

$\lambda$  is the eigen values. For a state space model with n states, A is a nXn matrix and there will be n solutions.

For a two state systems

$$\begin{aligned}\lambda I - A &= \begin{bmatrix} \lambda & 0 \\ 0 & \lambda \end{bmatrix} - \begin{bmatrix} a_{11} & a_{12} \\ a_{21} & a_{22} \end{bmatrix} \\ &= \begin{bmatrix} \lambda - a_{11} & -a_{12} \\ -a_{21} & \lambda - a_{22} \end{bmatrix}\end{aligned}\tag{3.25}$$

$$\det \begin{bmatrix} \lambda - a_{11} & -a_{12} \\ -a_{21} & \lambda - a_{22} \end{bmatrix} = 0$$

$$\Rightarrow 0 = (\lambda - a_{11})(\lambda - a_{22}) - (-a_{21})(-a_{12})$$

$$\Rightarrow \lambda^2 - (a_{11} + a_{22})\lambda + a_{11}a_{22} - a_{12}a_{21} = 0$$

$$\lambda = \frac{a_{11} + a_{12} \pm \sqrt{(a_{11} + a_{22})^2 - 4(a_{11}a_{22} - a_{12}a_{21})}}{2}\tag{3.26}$$

$$a_{11} + a_{22} < 0 \text{ and } a_{11}a_{22} > a_{12}a_{21}$$

If the roots are negative then the system is stable.

Figure 3.14 shows the plot for frequency response and the stability analysis can be depicted from the plot for synchronous generator. Figure 3.15 shows the depreciation in gain margin and phase margin in the frequency response of the synchronous generator. The stability analysis is essential for the system for predicting the best performance of the system

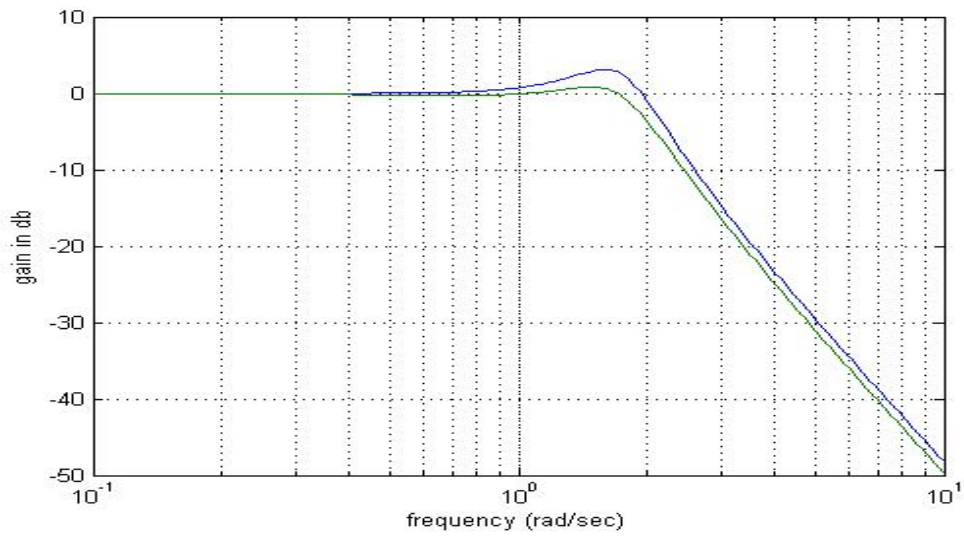


Figure 3.14: Frequency response and stability analysis of synchronous generator

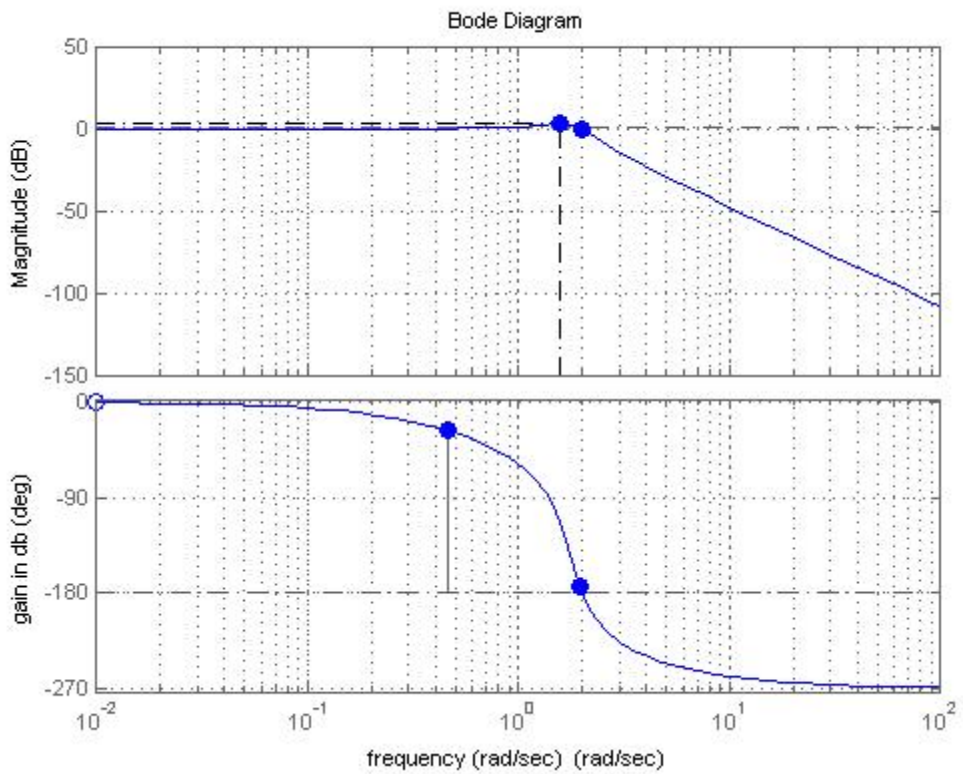


Figure 3.15: Synchronous generator frequency response depreciating GM & PM.

### 3.6 Mathematical Modeling of Synchronous Generator

The mathematical model of synchronous generator has been discussed in the following sub sections. This mathematical model helps in taking various control decisions keeping the stability in to consideration.

#### 3.6.1 Reference frame theory

Reference frame theory is quite important to the analysis of different electric machines analysis. Here the reference frame theory has been given. An approach for electric machine analysis has been given by Park in 1920. Variables which replaced the variables (voltages, currents and flux linkages) associated with the stator windings of a synchronous machine with variables associated with windings rotating with the rotor. In other words, he transformed, or referred, the stator variables to a frame of reference in the rotor. Park's transformation, which revolutionized electric machine analysis, has the unique property of eliminating all time-varying inductance from the voltage equations of the synchronous machine which happen because of electric circuits in relative motion, electric circuits with varying magnetic reluctance. The model of two pole salient pole synchronous superconducting machine with damper windings is shown in Figure 3.17. d-axis is aligned with the N-pole of the rotor and q- axis is 90 degree apart from d-axis.

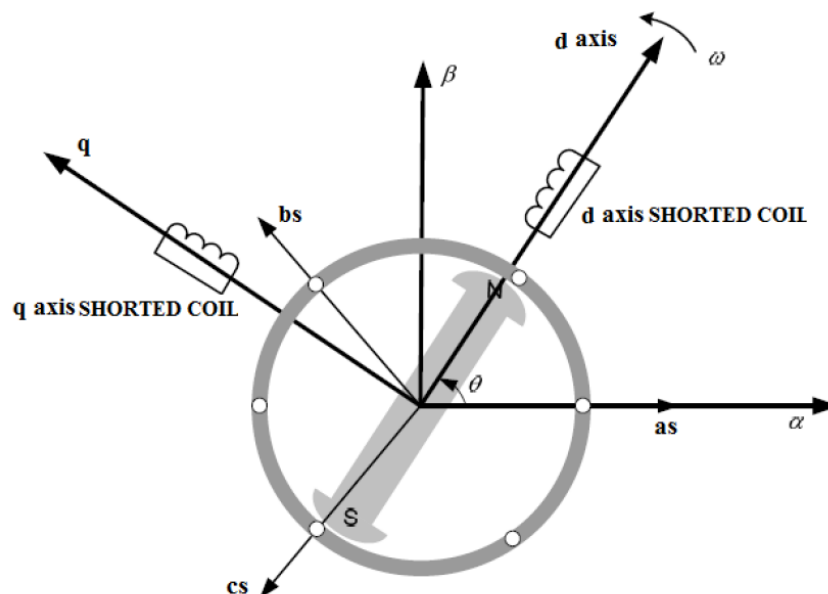
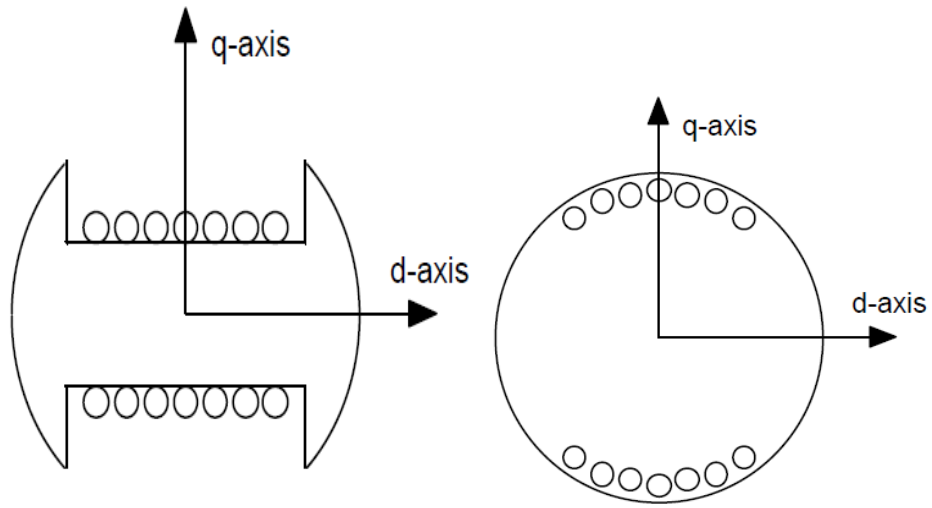
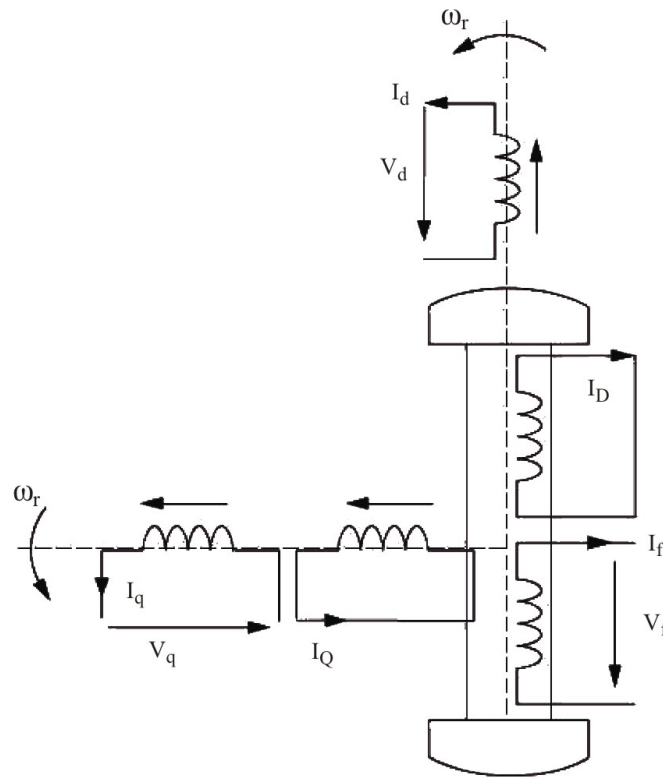


Figure 3.16: d-q model of synchronous generator



(a)



(b)

Figure 3.17 (a) d-q axis representation in case of synchronous generator  
 (b) d-q model of synchronous generator

### 3.6.2 Model of a basic two pole salient pole synchronous machine

A multi-pole machine having any number of pairs of poles can be treated as a two-pole machine electrically, because armature i.e stator windings are identically arranged with respect to each pair of poles. As the rotor has two axes of mechanical rectangular symmetry, we call them the 'd-axis' and 'q-axis'. d-axis or direct-axis is the axis from the axial centre point in the pole direction. q-axis or quadrature-axis is the axis from the axial centre point in the direction 90 degree ahead i.e leading of the d-axis.

The field winding named 'd-axis field coil' is a closed circuit field windings connected to a source of d.c. voltage, and with an inductance to produce flux only in the direction of the d-axis. The flux may flow into the left-hand side i.e. the +q-axis component and right-hand side i.e. the -q-axis component of the d-axis. Typical hydraulic-turbine- driven generators (vertical type with salient poles) have most of the times the squirrel-cage windings in the pole face i.e damper windings, which consists of copper bars through the pole connected at their ends as a closed circuit. Thermal or nuclear-turbine-driven generators i.e horizontal type with cylindrical non-salient poles has field windings only and do not have such damper windings. However eddy currents are forced to flow into the pass of the rotor solid steel for the duration of transient or current-unbalanced conditions.

The stator has three stator windings in name for phases a, b and c connected at their ends commonly as the neutral terminal. The three windings are arranged electrically by 120° symmetrically to each other. This is justify from the assumption that the stator windings are sinusoidal distributed along with the air gap as far as all the mutual effects of the rotor are concerned, because the generator windings are distributed so as to minimize harmonics in its design.

### 3.6.3 Relative angular position between rotor and stator

The stator is immovable. Rotor is rotating counter clockwise at an angular speed of

$$\omega = \frac{d\theta}{dt}$$

Relative position between rotor and stator is measured by the rotating angle of rotor d-axis. Rotating position of each coil in time can be written as follows on a d-axis basis.

Stator: A phase coil:  $\theta_a = \theta = \omega t = 2\pi ft$   
 B phase coil:  $\theta_b = \theta + 240^\circ = \theta - 120^\circ = \omega t - 120^\circ$   
 C phase coil:  $\theta_c = \theta + 120^\circ = \omega t + 120^\circ$

Rotor: Field Coil :  $0^\circ$   
 Damper d axis coil :  $0^\circ$   
 Damper q axis coil :  $90^\circ$

### 3.6.4 Generator model

To handle the machine behaviour properly there is requirement of model of generator. These advanced models for transients include

1. Phase-variable model
2. d-q variable model
3. d-q model neglecting stator transients

#### 3.6.4.1 Phase variable model

The model of synchronous generator is described by a set of three stator circuits coupled through motion with two or a multiple of two orthogonally placed  $d$  and  $q$  damper windings and a field winding along axis  $d$ . Stator and rotor circuits are magnetically coupled to each other. Synchronous machine is operated as a generator so that the voltage equation in the machine variable are expressed in matrix form as

$$v_{abc} = -r_s i_{abc} + p \lambda_{abc} \quad (3.27)$$

$$v_{dqr} = -r_r i_{dqr} + p \lambda_{dqr} \quad (3.28)$$

Here the subscripts s and r subscripts denote variables associated with stator and rotor windings, respectively. Flux linkage equation are given as

$$\begin{bmatrix} \lambda_{abc} \\ \lambda_{dqr} \end{bmatrix} = \begin{bmatrix} L_s & L_{sr} \\ (L_{sr})^T & L_r \end{bmatrix} \begin{bmatrix} -i_{abc} \\ i_{dqr} \end{bmatrix} \quad (3.29)$$

$$L_s = \begin{bmatrix} L_{ls} + L_a - L_b \cos 2\theta_r & -0.5L_a - L_b \cos 2(\theta_r - \frac{\pi}{3}) & -0.5L_a - L_b \cos 2(\theta_r + \frac{\pi}{3}) \\ -0.5L_a - L_b \cos 2(\theta_r - \frac{\pi}{3}) & L_{ls} + L_a - L_b \cos 2(\theta_r - \frac{2\pi}{3}) & -0.5L_a - L_b \cos 2(\theta_r + \pi) \\ -0.5L_a - L_b \cos 2(\theta_r + \frac{\pi}{3}) & -0.5L_a - L_b \cos 2(\theta_r + \pi) & L_{ls} + L_a - L_b \cos 2(\theta_r + \frac{2\pi}{3}) \end{bmatrix}$$

(3.30)

$$L_{sr} = \begin{bmatrix} L_{mq} \cos \theta_r & L_{mq} \cos \theta_r & L_{md} \sin \theta_r & L_{md} \sin \theta_r \\ L_{mq} \cos(\theta_r - \frac{2\pi}{3}) & L_{mq} \cos(\theta_r - \frac{2\pi}{3}) & L_{md} \sin(\theta_r - \frac{2\pi}{3}) & L_{md} \sin(\theta_r - \frac{2\pi}{3}) \\ L_{mq} \cos(\theta_r + \frac{2\pi}{3}) & L_{mq} \cos(\theta_r + \frac{2\pi}{3}) & L_{mq} \sin(\theta_r + \frac{2\pi}{3}) & L_{md} \sin(\theta_r + \frac{2\pi}{3}) \end{bmatrix} \quad (3.31)$$

$$L_r^T = \begin{bmatrix} L_{kq1}^T + L_{mq} & L_{mq} & 0 & 0 \\ L_{mq} & L_{kq2}^T + L_{mq} & 0 & 0 \\ 0 & 0 & L_{fd}^T + L_{md} & L_{ld} \\ 0 & 0 & L_{md} & L_{kd}^T + L_{md} \end{bmatrix} \quad (3.32)$$

### 3.6.4.2 Torque equation in machine variables

The energy stored in the coupling field of a synchronous machine may be expressed

$$T_e = \left( \frac{P}{2} \right) \left[ (k_s^r)^{-1} i_{qdos}^T \right]^T \left[ -0.5 \frac{\partial}{\partial \theta_r} (L_s - L_{ls} I) (k_s^r)^{-1} i_{qdos}^T + \frac{\partial}{\partial \theta_r} (L_{sr}^T) i_{dqr}^T \right] \quad (3.33)$$

### 3.6.4.3 The d–q variable model

d–q model eliminates the dependence of inductances on rotor position. *d–q* model express both stator and rotor equations in rotor reference. These are aligned to rotor *d* and *q* axis because, with the cross saturation is neglected, there is no coupling between the two axis. Rotor windings *f*, *D*, *Q* are already aligned along *d* and *q* axes. The rotor circuit voltage equations are expressed in rotor coordinates. The voltage equation of the stator winding of a synchronous machine can be expressed in arbitrary reference frame. Park's voltage equations are given as

$$V_{qs}^r = -r_s i_{qs}^r + w_s \lambda_{ds}^r + \rho \lambda_{ds}^r \quad (3.34)$$

$$V_{ds}^r = -r_s i_{ds}^r + w_s \lambda_{qs}^r + \rho \lambda_{ds}^r \quad (3.35)$$

$$V_{kq1}^r = -r_{kq1} i_{kq1}^r + \rho \lambda_{kq1}^r \quad (3.36)$$

$$V_{kq2}^r = -r_{kq2} i_{kq2}^r + \rho \lambda_{kq2}^r \quad (3.37)$$

$$V_{fd}^r = -r_{fd} i_{fd}^r + \rho \lambda_{fd}^r \quad (3.38)$$

$$V_{kd}^{r'} = -r_{kd}' i_{kd}^{r'} + \rho \lambda_{kd}^{r'} \quad (3.39)$$

Flux linkage equations are given as

$$\lambda_{qs}^r = -L_{ls} i_{qs}^r + L_{mq} (-i_{qs}^r + i_{kq1}^{r'}) \quad (3.40)$$

$$\lambda_{ds}^r = -L_{ls} i_{ds}^r + L_{md} (-i_{ds}^r + i_{kd1}^{r'} + i_{fd}^{r'}) \quad (3.41)$$

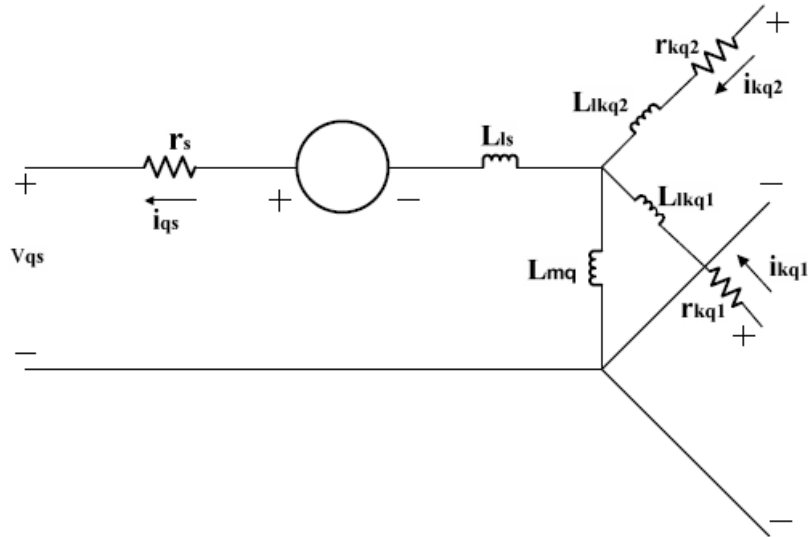
$$\lambda_{kq1}^r = -L_{lkq1} i_{kq1}^{r'} + L_{mq} (-i_{qs}^r + i_{kq1}^{r'}) \quad (3.42)$$

$$\lambda_{kq2}^r = -L_{lkq2} i_{kq2}^{r'} + L_{mq} (-i_{ds}^r + i_{kq1}^{r'}) \quad (3.43)$$

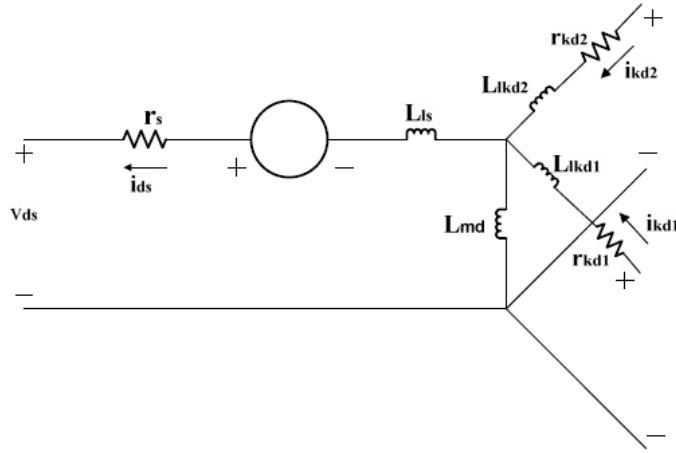
$$\lambda_{fd}^{r'} = L_{ffd}' i_{fd}^{r'} + L_{md} (-i_{ds}^r + i_{fd}^{r'}) \quad (3.44)$$

$$\lambda_{kd}^{r'} = L_{lkd}' i_{kd}^{r'} + L_{md} (-i_{ds}^r + i_{fd}^{r'}) \quad (3.45)$$

The voltage and flux linkage equations have their equivalent circuit as shown. The equivalent circuits of generator in reference form are shown as sub section of the circuit in Figure 3.18. The values of flux linkages are considered as per the flux linkage equations. Also the corresponding voltages are considered as per the voltage equations given above.



(a) q- axis



(b) d- axis

Figure 3.18: Equivalent circuit of generator in reference frame

In the synchronous generator at steady state the expressions for active and reactive power are made more complicated by rotor saliency. Round rotor case is given here.

The phasor equation  $E_q = V + jX_d I$ . It is illustrated in Figure 3.19

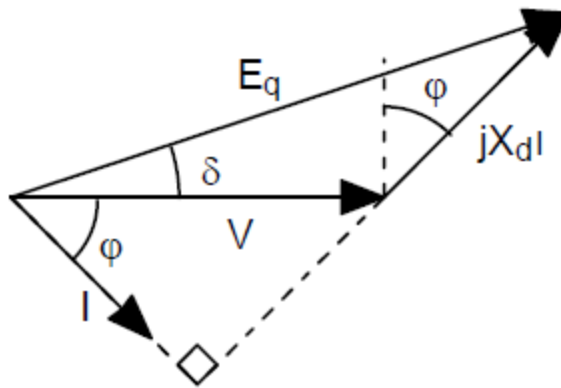


Figure 3.19: Round rotor machine phasor equation

Here  $\cos\Phi$  is the power factor of the load. Here the load is inductive, I lags V and  $\Phi > 0$ .

The power supplied to the load is (per phase):

$$S = P_e + jQ_e \tag{3.46}$$

$$S = VI \cos \varphi + jVI \sin \varphi \tag{3.47}$$

Scaling the phasor diagram with  $V/X_d$  is represented in Figure 3.20.

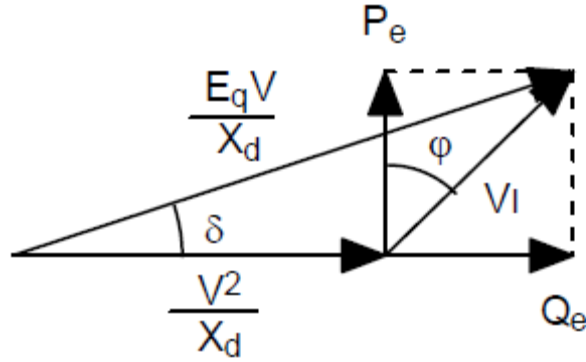


Figure 3.20: Phasor diagram of power flow of synchronous generator

Active and reactive power can now be expressed as:

$$P_e = VI \cos \varphi = \frac{E_q V}{X_d} \sin \delta \quad (3.48)$$

$$P_e = VI \sin \varphi = \frac{E_q V}{X_d} \cos \delta - \frac{V^2}{X_d} \quad (3.49)$$

The direct-axis (or d-axis) is defined as the main flux direction of the rotor. The d-q mathematical model showing the phasor as shown in Figure 3.21. The voltage induced in the stator  $E_q$  leads the d-axis by  $90^\circ$ , which is the quadrature-axis (or q-axis) direction. The fundamental (phasor) voltage equation for a salient pole generator is:

$$E_q = V + jX_d I_d + jX_q I_q \quad (3.50)$$

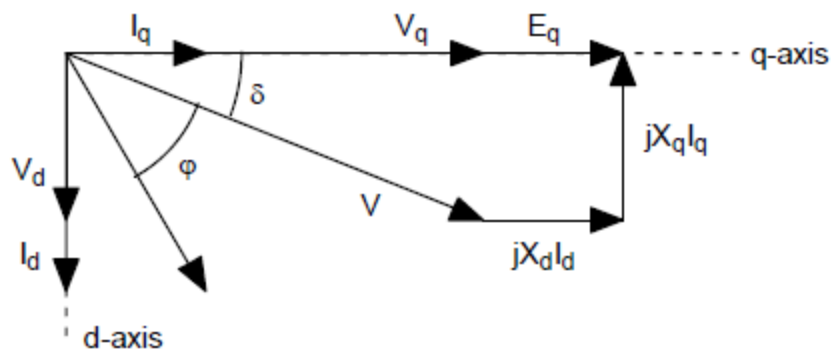


Figure 3.21: d-q mathematical model of the synchronous generator

The consideration of the synchronous generator mathematical model discussed above helps in making of effective simulink model as shown in Figure 3.22.

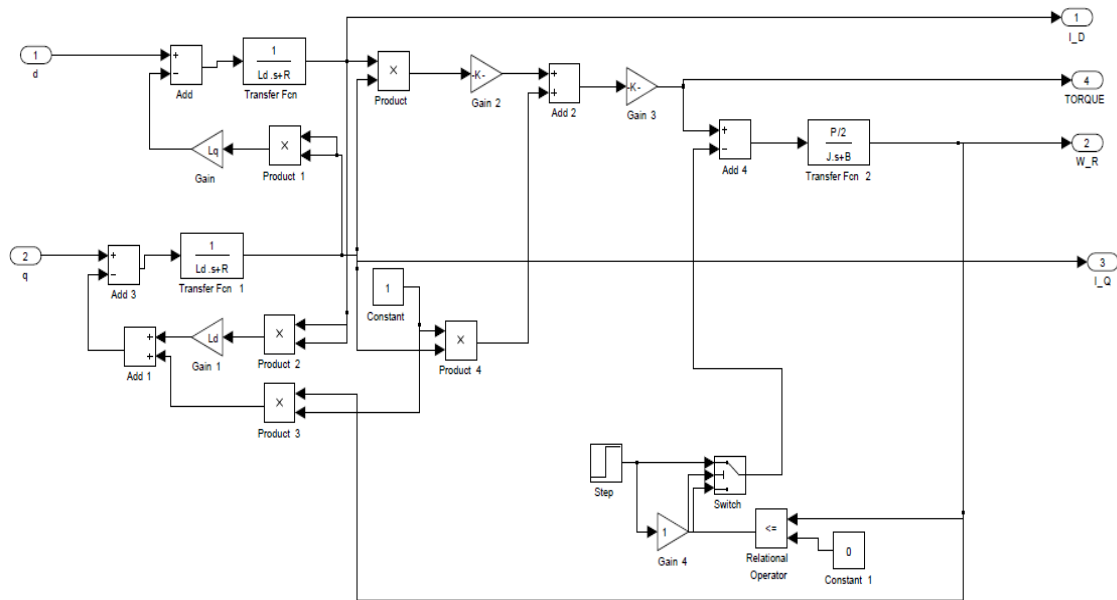
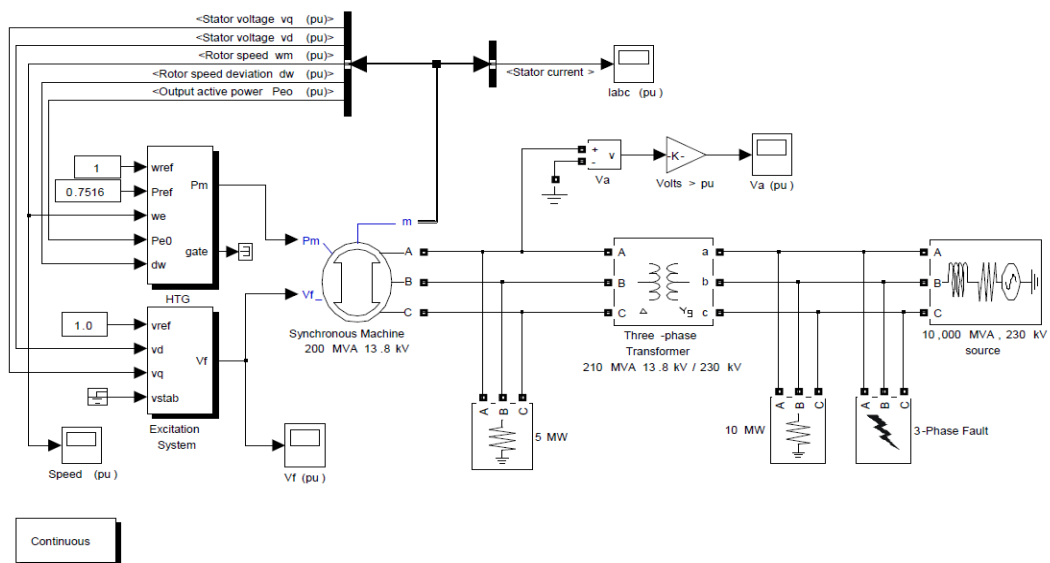


Figure 3.22: Simulink model of synchronous generator

The model of synchronous generator which has been implemented using matlab simulations gives us the output results as shown in Figure 3.23 and Figure 3.24 shows the transient and steady state parameters for synchronous generator model.



(a)

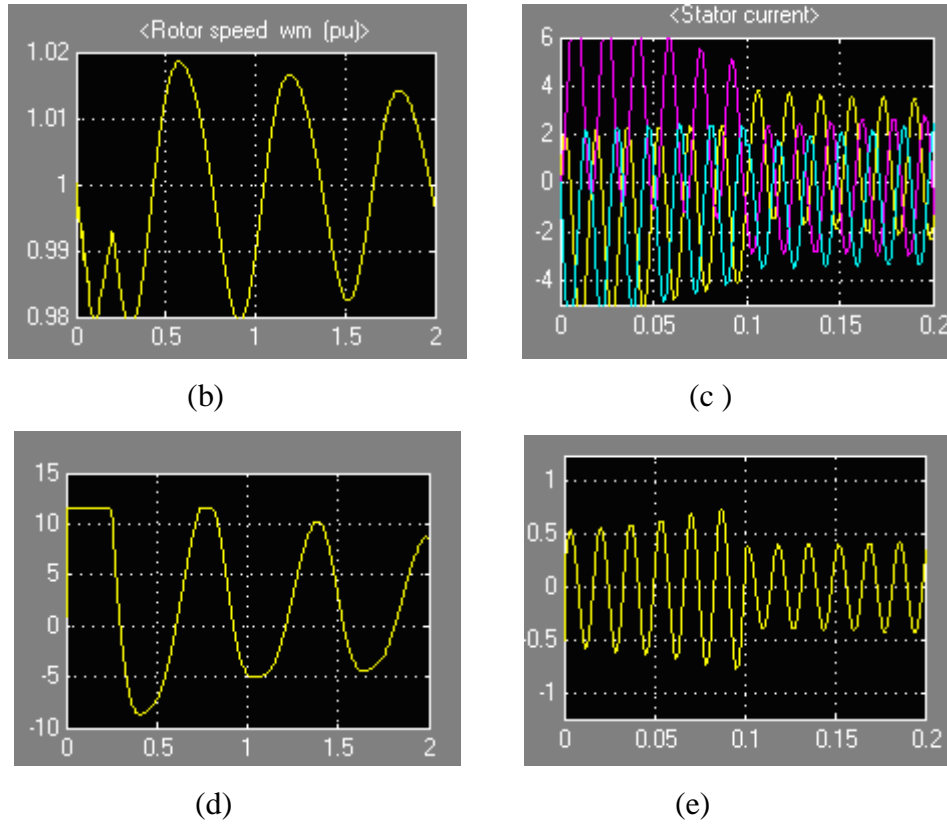


Figure 3.23: (a) Simulation of synchronous generator using simulink  
 (b) Rotor Speed of synchronous generator  
 (c) Field voltage of synchronous generator  
 (d) Stator current of synchronous generator  
 (e)  $V_a$  of synchronous generator

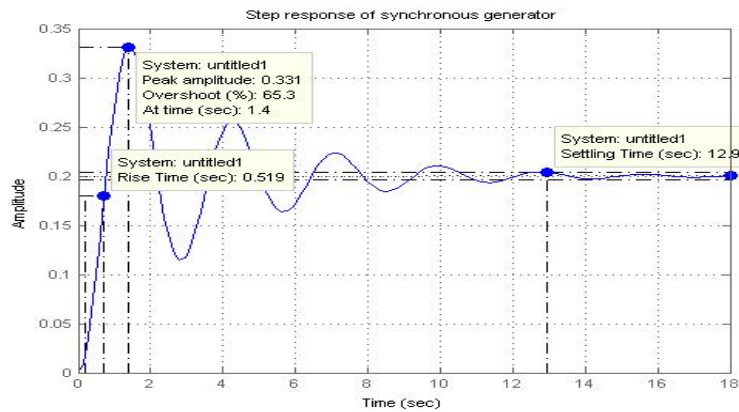
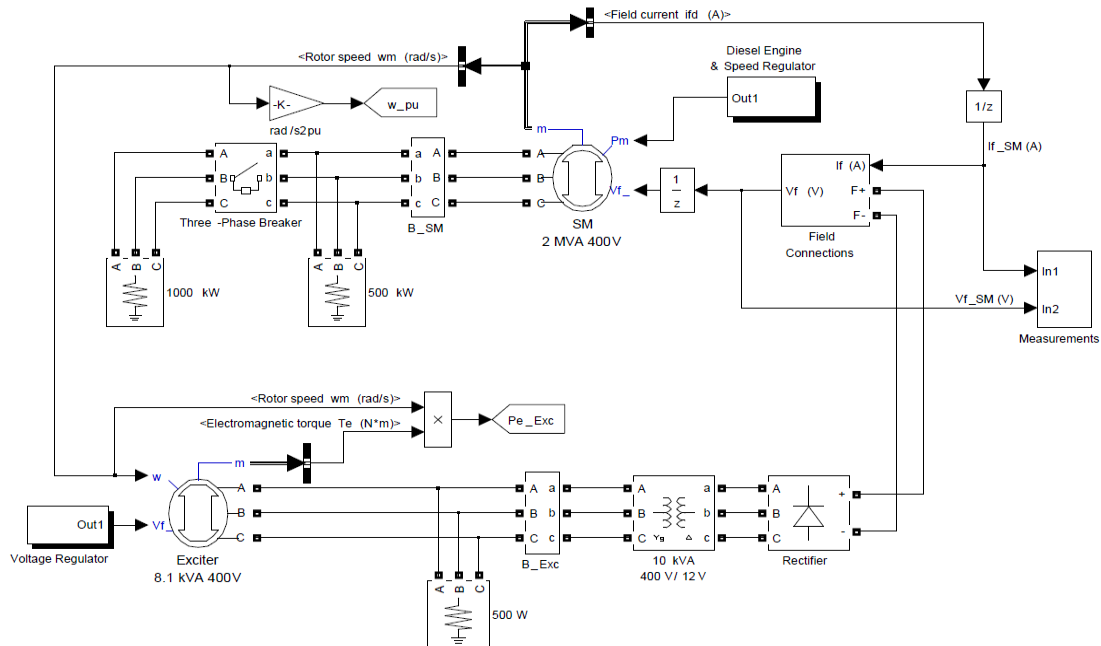


Figure 3.24: Different transient and steady state parameters of synchronous generator at step increase in torque

### 3.7 Coupling of synchronous generator with exciter system

In large alternators, excitation system is provided by a small synchronous machine connected on the same shaft as the main synchronous machine. Current rectification is performed by rotating diode bridges which are mounted on the synchronous machine shaft, thus avoiding slip rings for providing DC power to the synchronous machine field. The synchronous machine is a 2 MVA, 400V, 50 Hz, 1500 rpm machine driven by a diesel motor. A nominal field current ( $I_{fn}$ ) of 100A is considered. It results in a nominal field voltage of 9.2837 V. The Exciter is an 8.1 kVA, 400 V, 50Hz, 1500 RPM synchronous machine. A 400V / 12 V transformer is used to adapt the 400 V output voltage of the exciter to the rectifier. Output of the rectifier bridge is connected directly to the synchronous machine field terminals. Filtering is not required because of the large field inductance. The field terminal voltages of the synchronous machine model are measured by the Field Connections subsystems. The  $V_f$  synchronous machine input and terminals interface is simulated by a current source driven by the DC current output of the bridge or DC field current. The voltage appearing across this current source corresponds to the field voltage which must be applied to the  $V_f$  Synchronous Machine block input. Voltage regulation of the synchronous machine is performed by controlling the field voltage of the exciter. This is performed by the Voltage Regulator (PI type) which compares the measured voltage (positive sequence voltage) to a 1 pu reference.



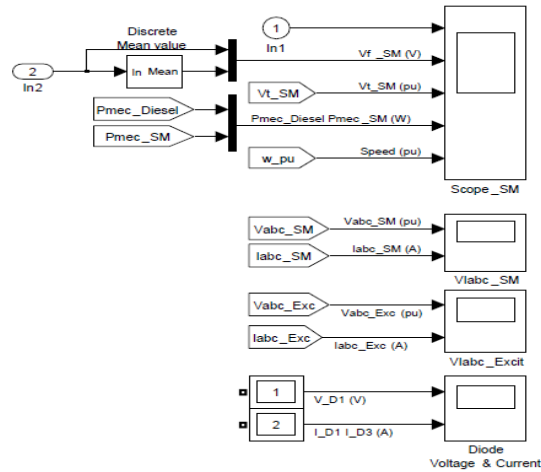


Figure 3.25 : Simulink representation of synchronous generator with exciter system

Figure 3.25 shows the simulink model for synchronous generator with exciter system. The output waveforms are shown in Figure 3.26 for voltage and current of diodes, Figure 3.27 and Figure 3.28 for three phase voltage and current waveforms for SM and exciter.

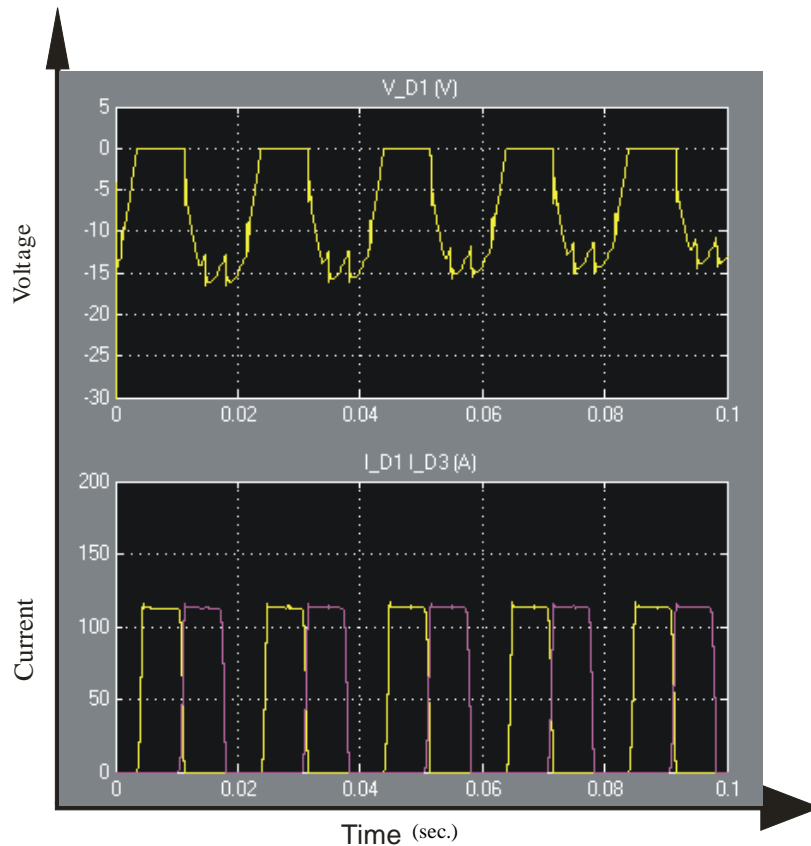


Figure 3.26: Voltage (V) of diode  $D_1$  and current (p.u) of diode  $D_1$  and  $D_3$

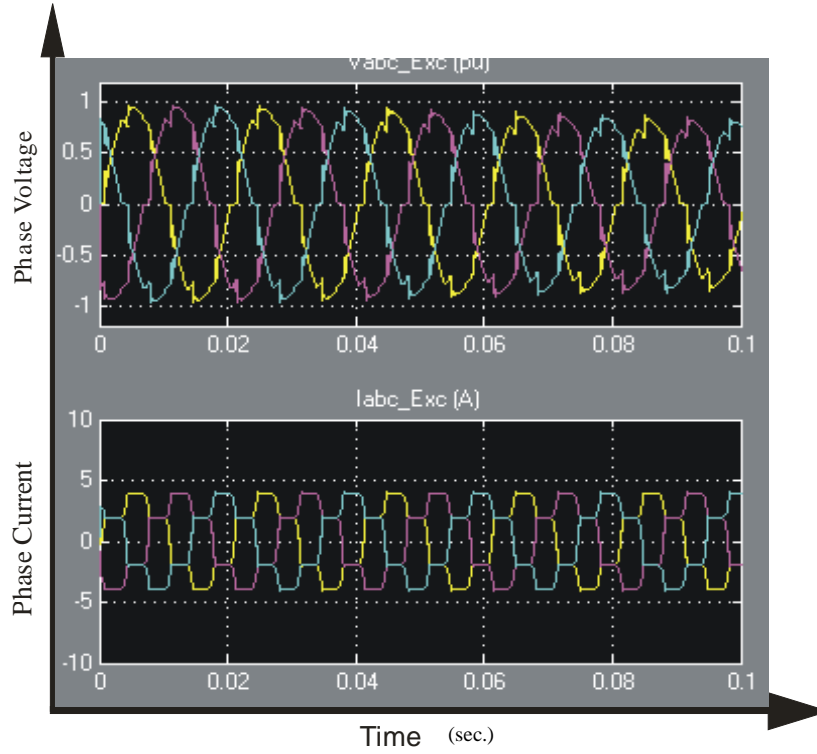


Figure 3.27: Three phase voltage (volt) and current (p.u)

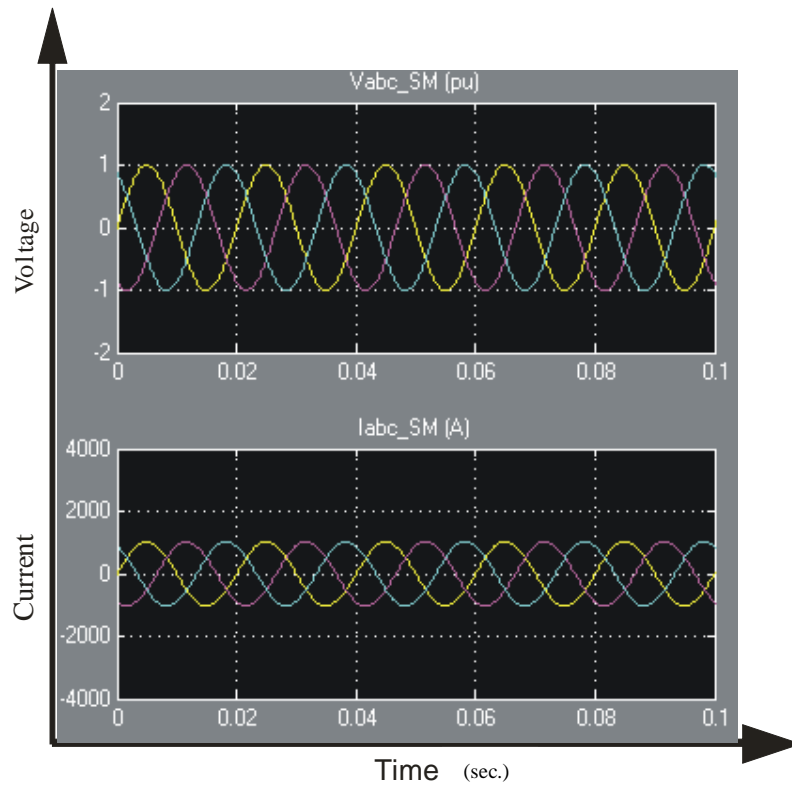


Figure 3.28: Three phase voltage (volt) and current (p.u)

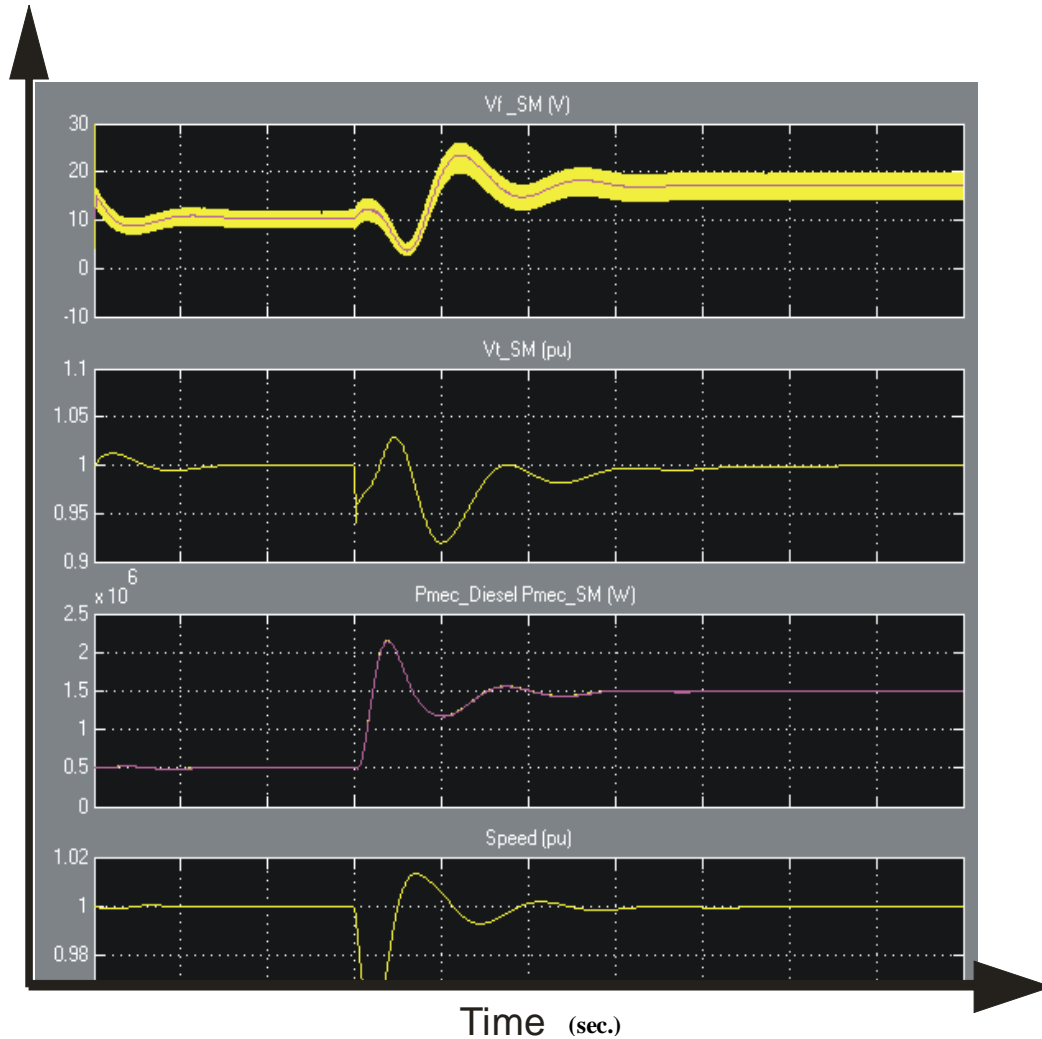


Figure 3.29: Speed regulation of synchronous generator connected with exciter system

When a synchronous motor is started, the excitation DC voltage is not applied to the field winding. The motor is started in induction machine mode with currents induced in the damper and field windings. A resistor is connected across the field winding in order to produce an acceptable field current and to limit voltage induced across the field winding. Then when speed reaches a preset value near synchronous speed, the field winding is connected to the DC voltage source and the motor synchronizes on the system frequency. The simulink model for synchronous machine on no load has been developed in Figure 3.30. The corresponding output resulting waveforms are achieved after successful running of model.

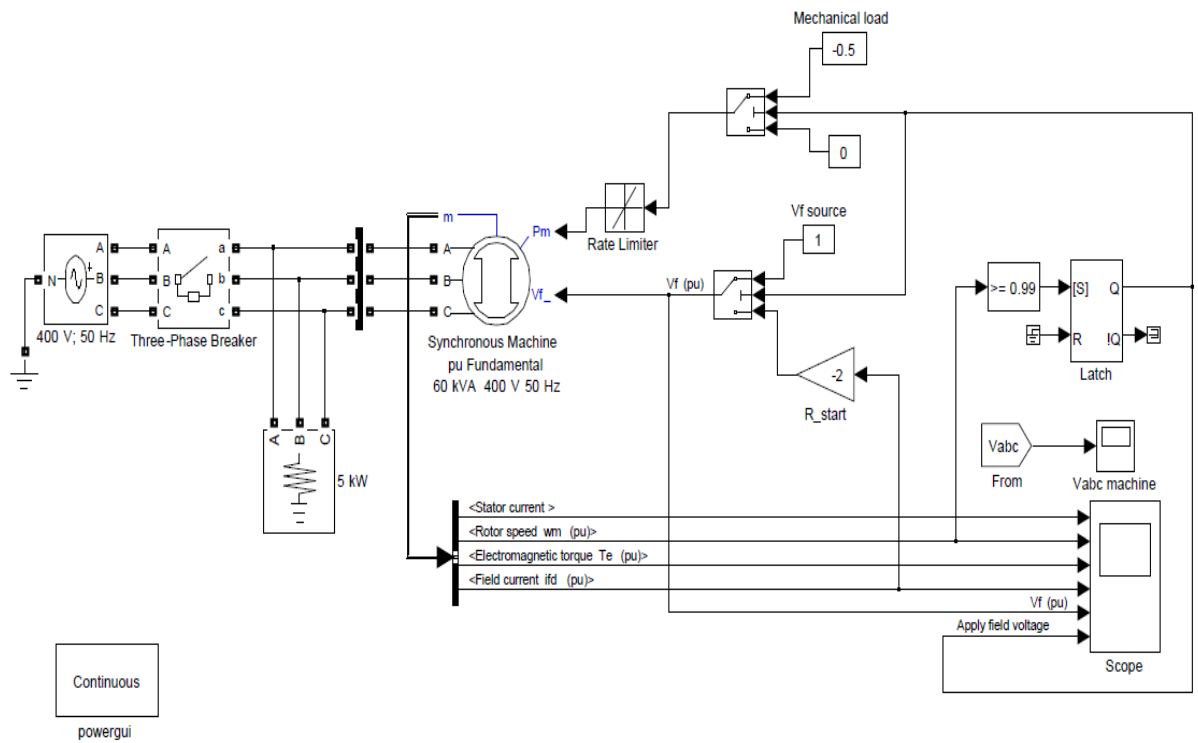


Figure 3.30: Synchronous machine without load

When there is no load on the machine the corresponding output graphs for starting current, rated speed and field voltage are shown in Figure 3.31. When it is just started all the waveforms follow the behavior which is expected from the simulink modeled circuit. All the waveforms are reaching at its steady state after the simulations.

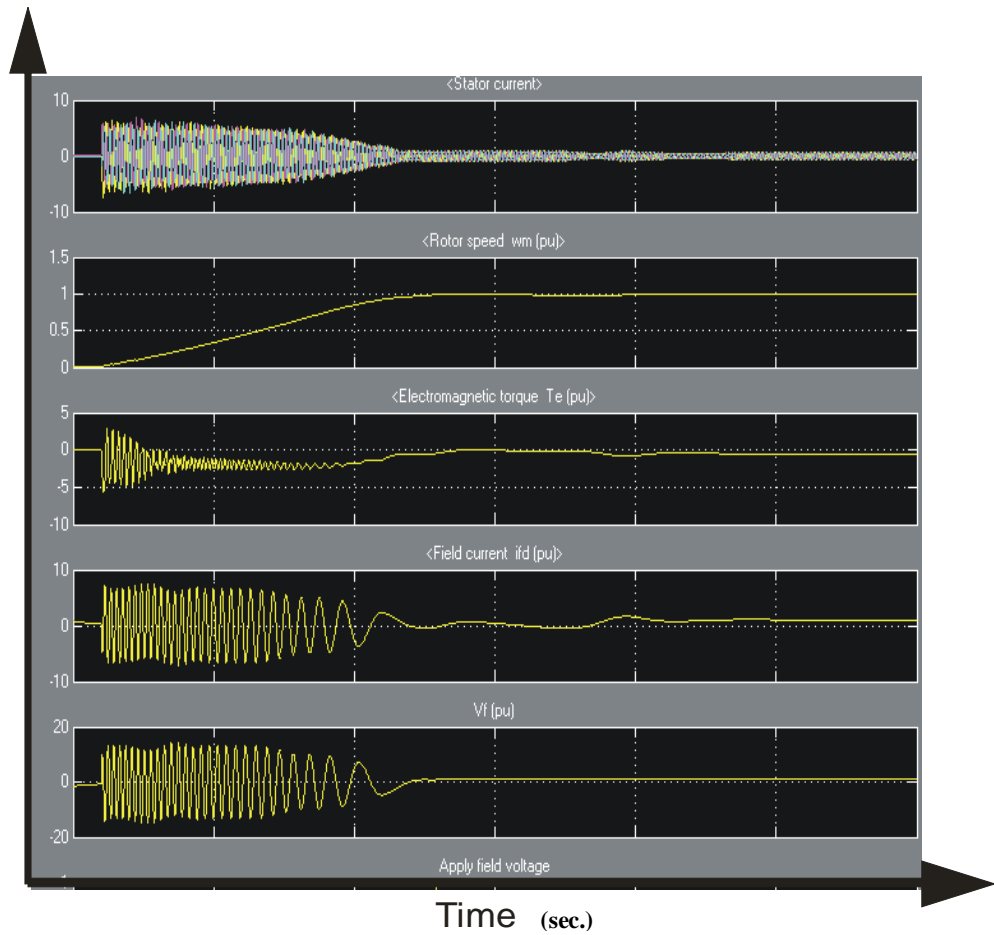


Figure 3.31: Graphs for stator current, rotor speed, torque, field voltage when the synchronous machine is started

### 3.8 Speed control of synchronous generator system: proposed system

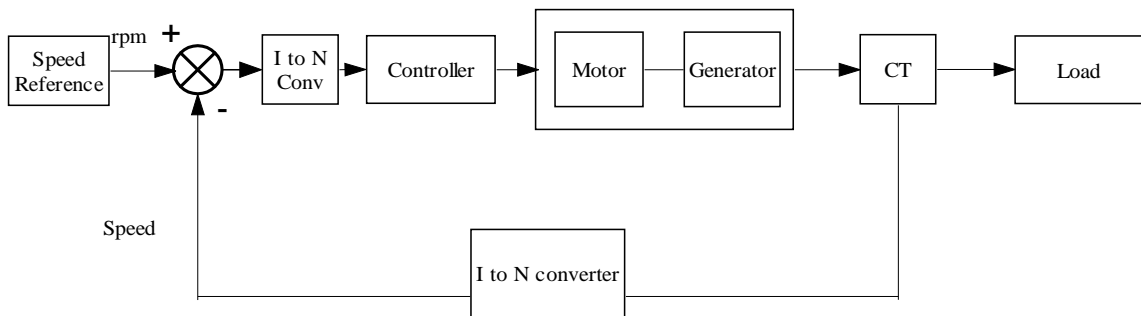


Figure 3.32: Control block diagram of proposed speed control system

The block diagram in Figure 3.32 shows the scheme followed to control the speed of the synchronous generator system. The proposed scheme keeps the reference model in

control by manipulating all the control parameters of the torque and field control. The control block diagram for this synchronous generator system serves as the basic model for taking the actions for controlling the speed.

The fuzzy logic controller provides an algorithm, which converts the expert knowledge into an automatic control strategy. Fuzzy logic is capable of handling approximate information in a systematic way and therefore it is suited for controlling non linear systems and is used for modeling complex systems, where an inexact model exists or systems where ambiguity or vagueness is common. The fuzzy control systems are rule-based systems in which a set of fuzzy rules represent a control decision mechanism for adjusting the effects of certain system stimuli. With an effective rule base, the fuzzy control systems can replace a skilled human operator. The rule base reflects the human expert knowledge, expressed as linguistic variables, while the membership functions represent expert interpretation of those variables.

Figure 3.33 provides a flow chart for control system design and evaluation. This step by step approach provides a complete view for the control system designer. Fuzzy control is essentially an intelligent way to control the servo applications. The following system describes different fuzzy logic control architecture and evaluates type-1 and type-2 membership function as well as the hierarchical control for the same system. All the uncertainties of the system are considered either as per the information from the existing plant or from the experience with the existing plant, the plant data also utilized for developing the efficient model. Here the plant comprises of the motor, generator, controller and current to speed converter as shown in Figure 3.32.

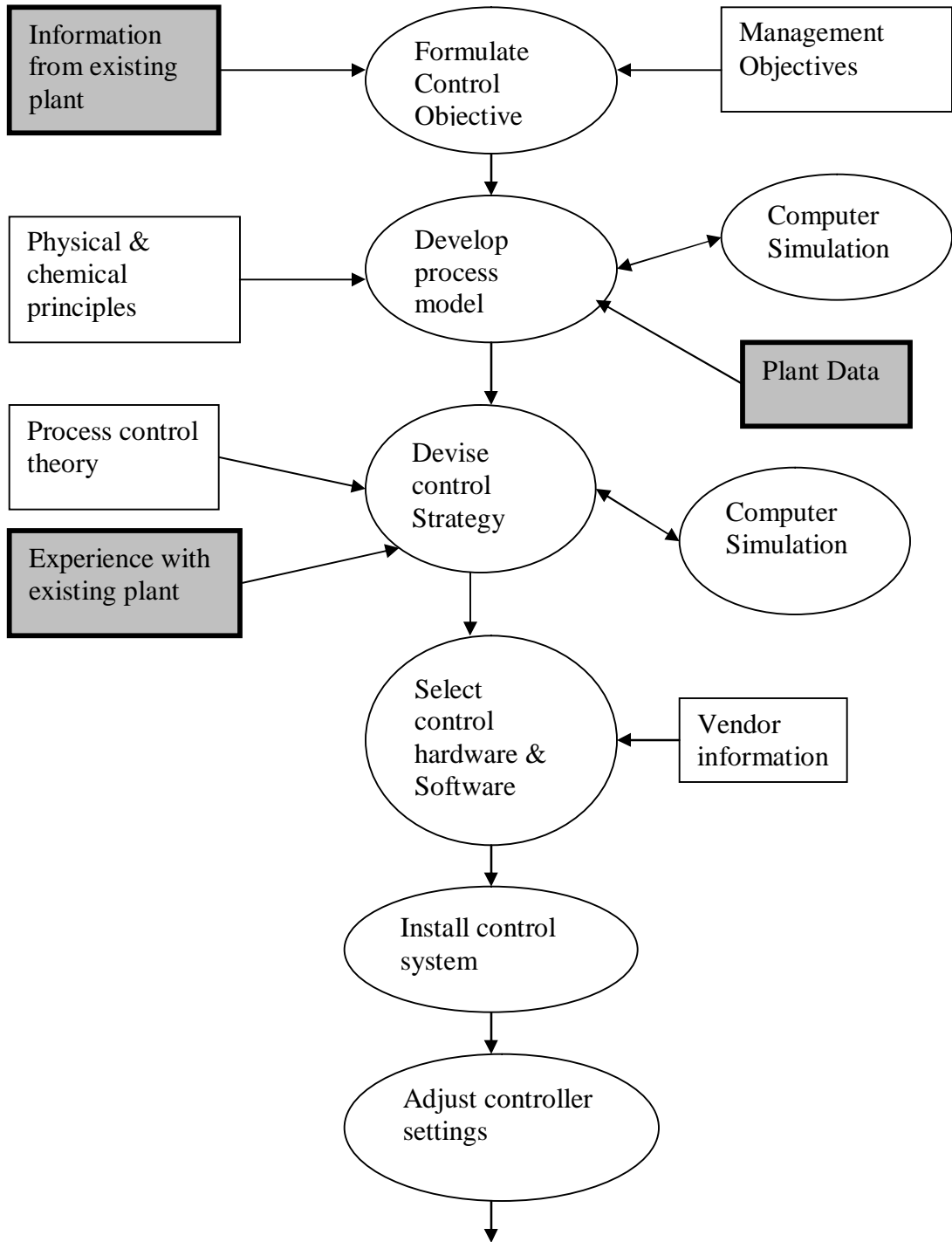


Figure 3.33: Flow chart of control system design and evaluation

Another method of vector control of synchronous machine is described and proposed fuzzy control scheme of synchronous machine is given in the Figure 3.34 .

$$v_{ds} = R_s i_{ds} + \frac{d\phi_{ds}}{dt} - \omega \phi_{qs} \quad (3.51)$$

$$v_{qs} = R_s i_{qs} + \frac{d\phi_{qs}}{dt} + \omega \phi_{ds} \quad (3.52)$$

$$v_f = R_f i_f + \frac{d\phi_f}{dt} \quad (3.53)$$

$$J \frac{d\Omega}{dt} = C_e - C_r - B\Omega \quad (3.54)$$

$$\phi_{ds} = L_{ds} i_{ds} + M_{fd} i_f \quad (3.55)$$

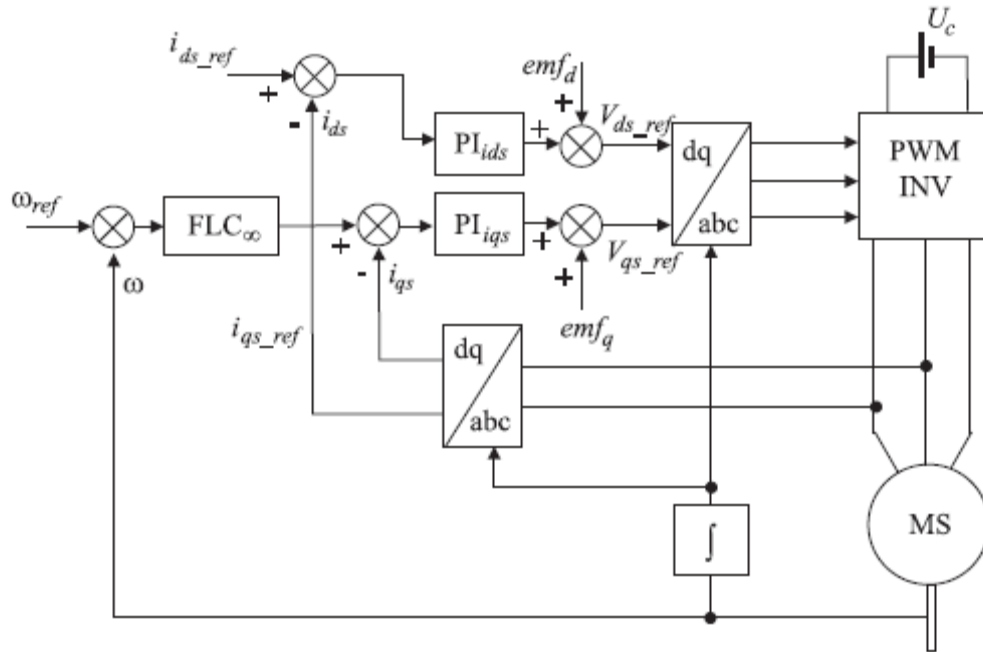


Figure 3.34: Schematic diagram of fuzzy of synchronous generator

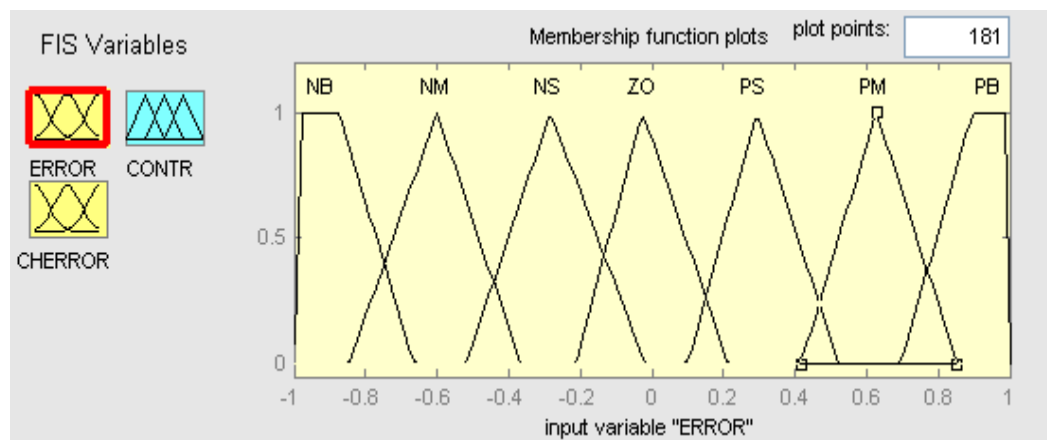
The schematic diagram of the speed control system under study is shown in Figure 3.34. The power circuit consists of a continuous voltage supply which can be provided by a six rectifier thyristors and a three phase GTO thyristors inverter whose

output is connected to the stator of the synchronous machine. The field current  $i_f$  of the synchronous machine, which determines the field flux level, is controlled by voltage  $V_f$ . The self-control operation of the inverter-fed synchronous machine results in a rotor field oriented control of the torque and flux in the machine. The principle is to maintain the armature flux and the field flux in an orthogonal or decoupled axis. The flux in the machine is controlled independently by the field winding and the torque is affected by the fundamental component of armature current  $I_{qs}$ . In order to have an optimal functioning, the direct current  $i_{ds}$  is maintained equal to zero

Three phases SM parameters: Rated output power 3 HP, Rated phase voltage 60 V, Rated phase current 14 A, Rated field voltage  $V_f = 1.5$  V, Rated field current  $I_f = 30$  A, Stator resistance  $R_s = 0.325$ , Field resistance  $R_f = 0.05$ , Direct stator inductance  $L_{ds} = 8.4$  mH, Quadrature stator inductance  $L_{qs} = 3.5$  mH, Field leakage inductance  $L_f = 8.1$  mH, Mutual inductance between inductor and armature  $M_{fd} = 7.56$  mH, The damping coefficient  $B = 0.005$  Nm/s, The moment of inertia =  $0.05$  kgm<sup>2</sup>, Pair number of poles = 2.

### 3.8.1 Type-1 membership function for fuzzy control

Figure 3.35 shows the membership function for inputs. Error  $e(t)$  and change in error  $de(t)$  is taken as inputs where as fuzzy controller output  $u(t)$  is taken as output. Triangular membership functions are taken for the fuzzy control purpose. The diagram shown in Figure 3.36 is the fuzzy membership functions for output variables in type-1 system.



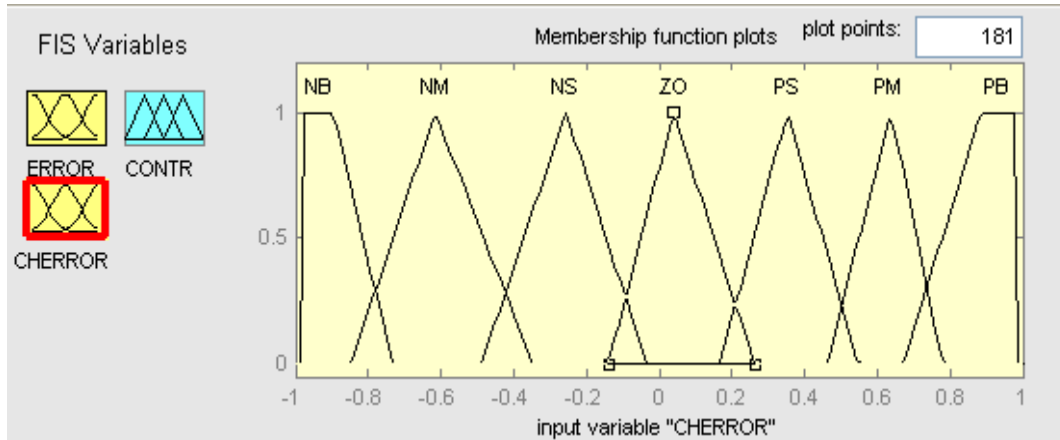


Figure 3.35: Membership function for type-1 fuzzy inputs,  $e(t)$  and  $de(t)$

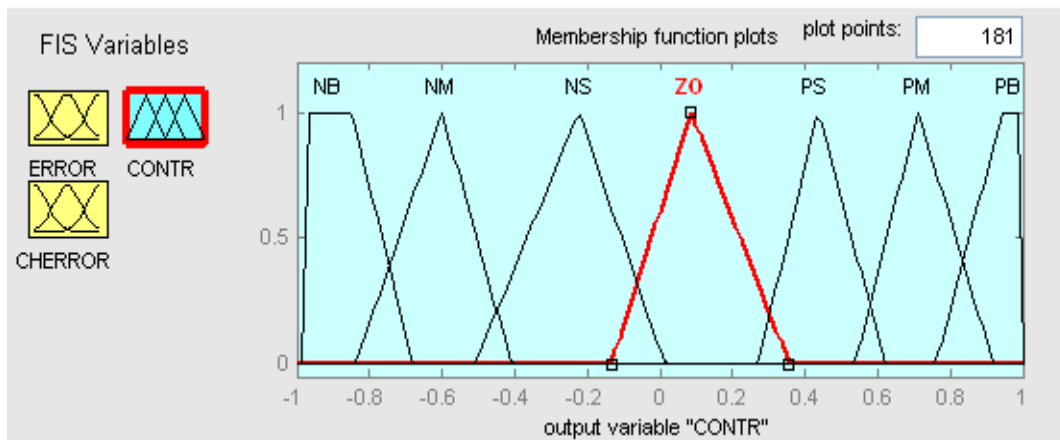


Figure 3.36: Membership function for type-1 fuzzy output

Table 3.1: Linguistic variable for type-1 fuzzy control

Error $e(t)$		Change in error $\Delta e(t)$		Controller output $u(t)$	
NB	Negative Big	NB	Negative Big	NB	Negative Big
NM	Negative Medium	NM	Negative Medium	NM	Negative Medium
NS	Negative Small	NS	Negative Small	NS	Negative Small
ZO	Zero	ZO	Zero	ZO	Zero
PS	Positive Small	PS	Positive Small	PS	Positive Small
PM	Positive Medium	PM	Positive Medium	PM	Positive Medium
PB	Positive Big	PB	Positive Big	PB	Positive Big

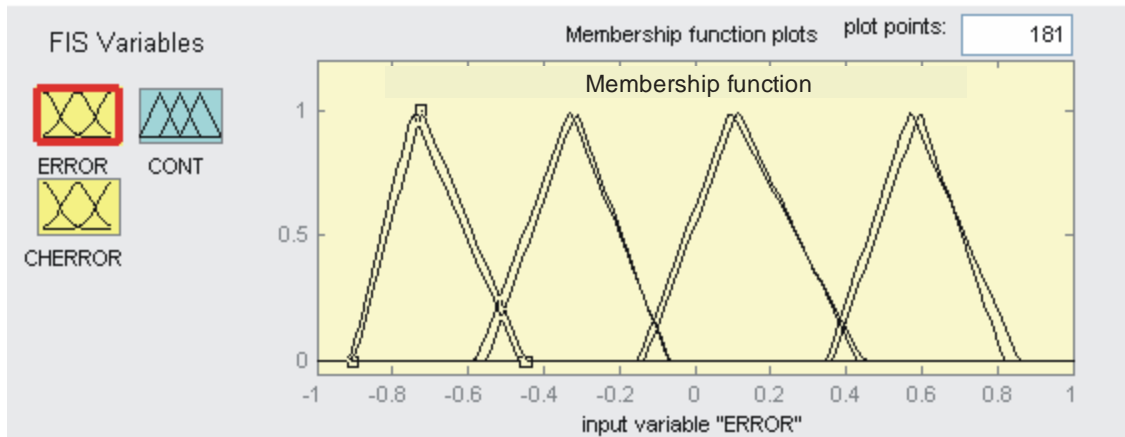
Table 3.2: If-then rule base for fuzzy control

u(t)		e(t)						
		NB	NM	NS	ZO	PS	PM	PB
$\Delta e(t)$	NB	NB	NB	NB	NB	NM	NS	ZO
	NM	NB	NB	NB	NM	NS	ZO	PS
	NS	NB	NB	NM	NS	ZO	PS	PM
	ZO	NB	NM	NS	ZO	PS	PM	PB
	PS	NM	NS	ZO	PS	PM	PB	PB
	PM	NS	ZO	PS	PM	PB	PB	PB
	PB	ZO	PS	PM	PB	PB	PB	PB

Table 3.1 shows the linguistic variables of fuzzy control and Table 3.2 shows the rule base for fuzzy control.

### 3.8.2 Type-2 membership function for fuzzy control.

Figure 3.37 shows the membership function for type -2 fuzzy inputs i.e. error and change in error. Figure 3.38 shows the membership function for type-2 fuzzy output variable To support type -2 fuzzy two mmf have been used in the fuzzy inference system.



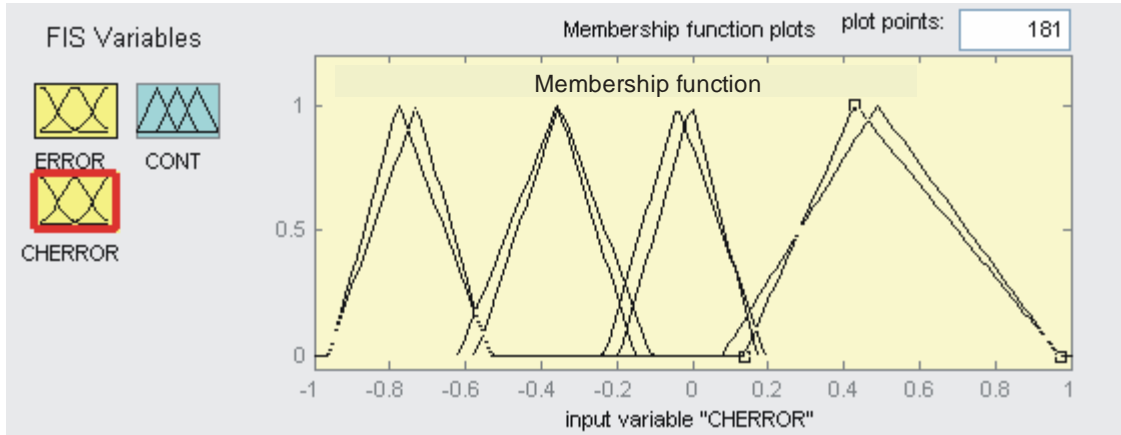


Figure 3.37: Membership function for type-2 fuzzy inputs  $e(t)$  and  $de(t)$

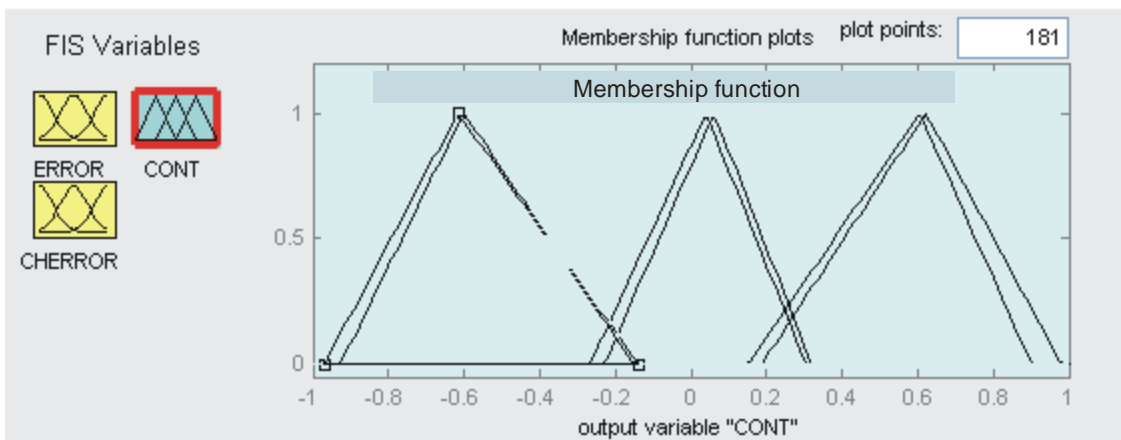


Figure 3.38: Membership function for type- 2 fuzzy output  $u(t)$

Figure 3.39 shows model of the fuzzy control based synchronous generator, in the fuzzy controller the type-1 and type-2 fuzzy membership and fuzzy inference system has been applied. This block diagram also evaluates the IAE and ITAE control criteria of the entire system. The IAE and ITAE values are found out for both type-1 and type-2 fuzzy sets. The corresponding output graphs for type-I is shown in Figure 3.40 and for type-II is shown in Figure 3.41

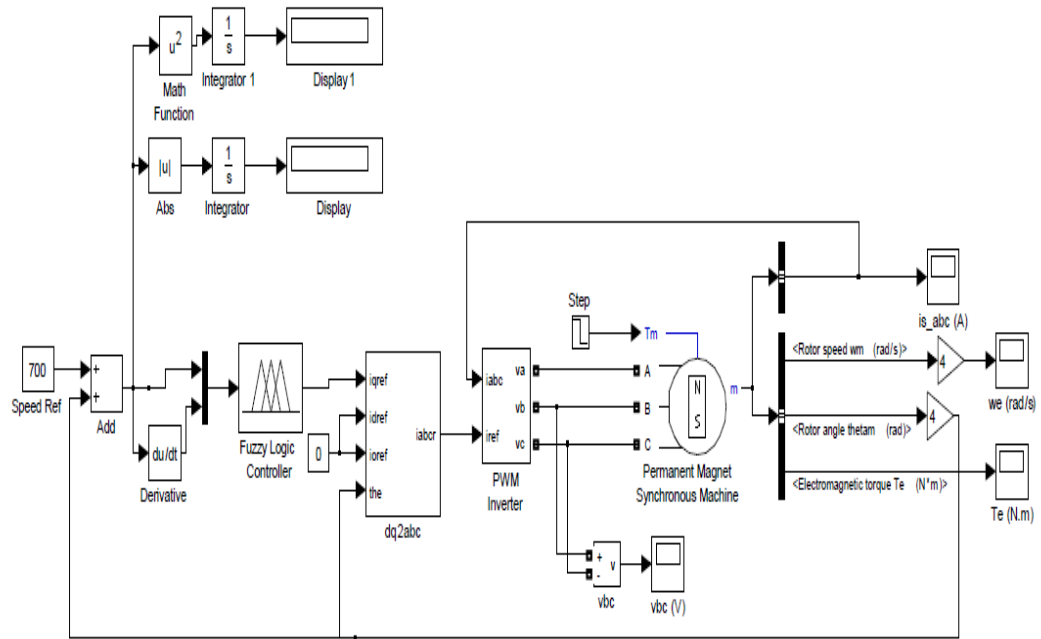


Figure 3.39: Fuzzy type-1 control of synchronous generator

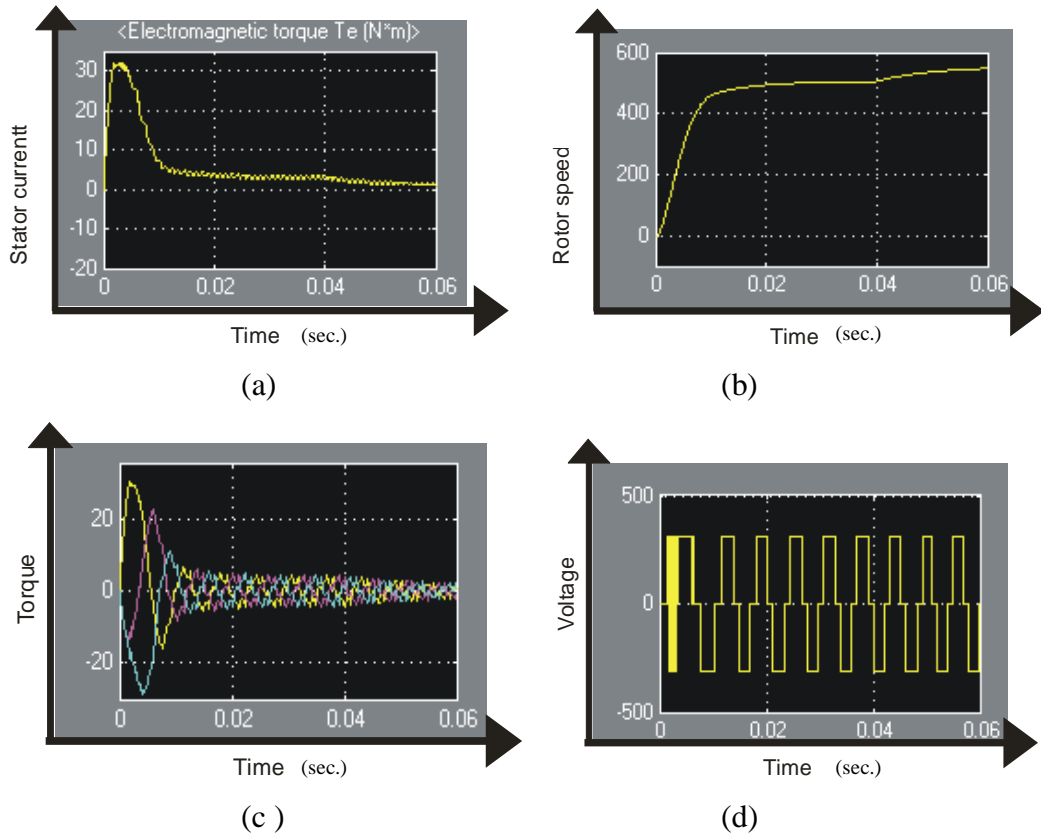
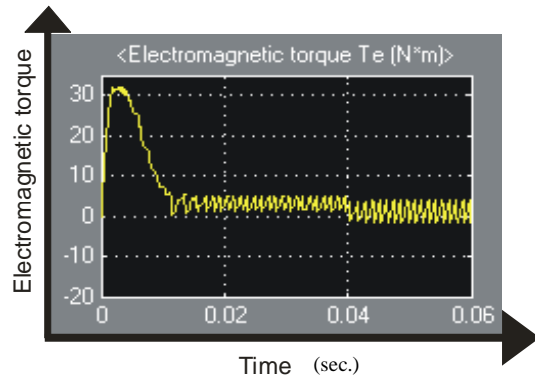
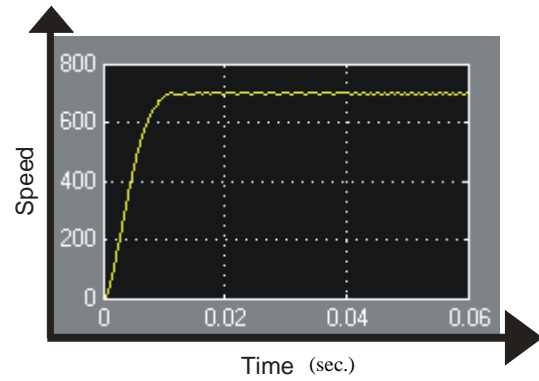


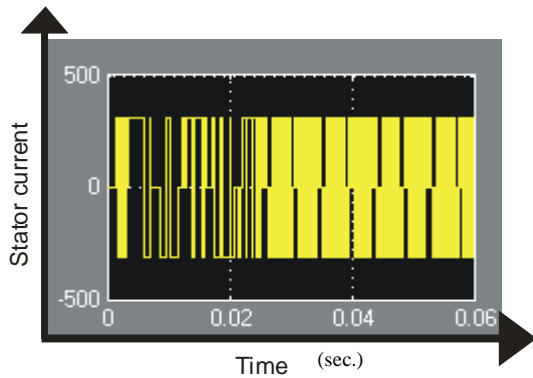
Figure 3.40: Graphs for (a) Stator current, (b) Rotor speed, (c) Torque, (d) Voltage for type-1 fuzzy membership functions



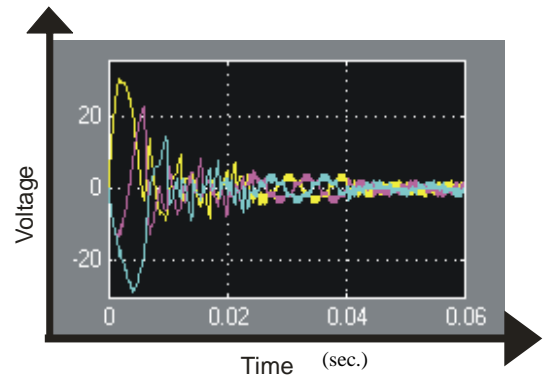
(a)



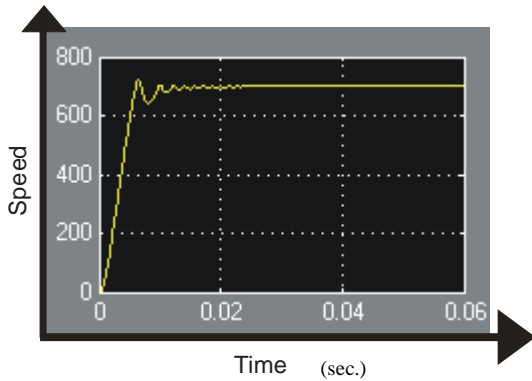
(b)



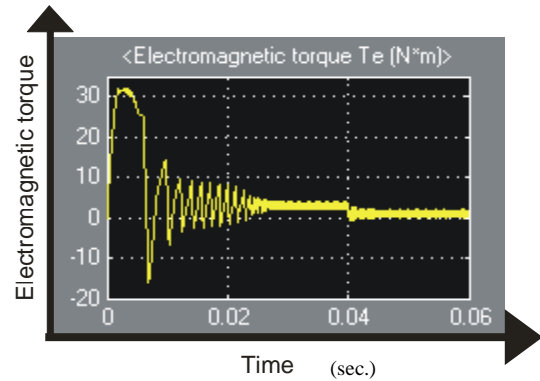
(c)



(d)



(e)



(f)

Figure 3.41: Graphs for type-2 fuzzy (a,f) Electromagnetic torque  
 (b,e) Speed  
 (c,d) Stator current and voltage

### 3.8.3 Fuzzy speed control of synchronous generator with load

A three-phase, four-wire alternator rated 2000 kVA, 1600 kW, 0.8 power factor, 600 V, 1800 rpm is connected to a 1600 kW, 400 kvar inductive load. The stator neutral point is grounded. The internal impedance of the generator ( $Z_g = 0.0036 + j*0.16$  pu) represents the armature winding resistance  $R_a$  and direct axis transient reactance  $X'd$ . The total inertia constant of the generator and prime mover is  $H = 0.6$  s, corresponding to  $J = 67.5$  kgm<sup>2</sup>. Speed regulation is modeled with simulink blocks implementing a PI regulator. The machine is excited with a constant voltage. A three-phase breaker is used to switch out a 800 kW resistive load. The breaker is initially closed and it is opened at  $t = 0.2$  s, resulting in a 50% load shedding. Figure 3.42 shows simulink model for fuzzy speed control of synchronous generator on load.

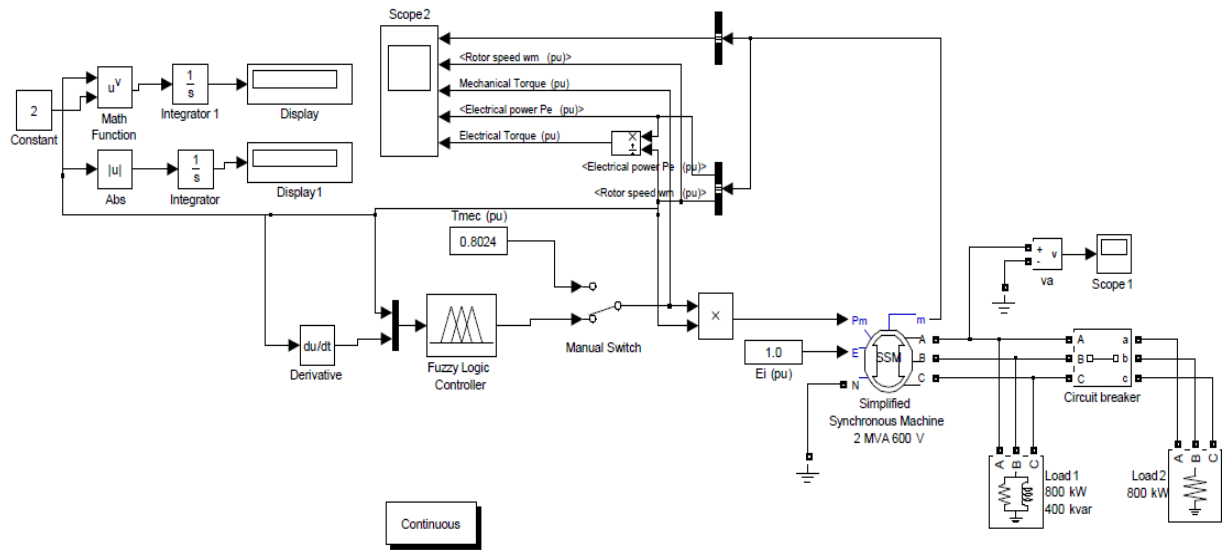


Figure 3.42: Fuzzy speed control of synchronous generator with load

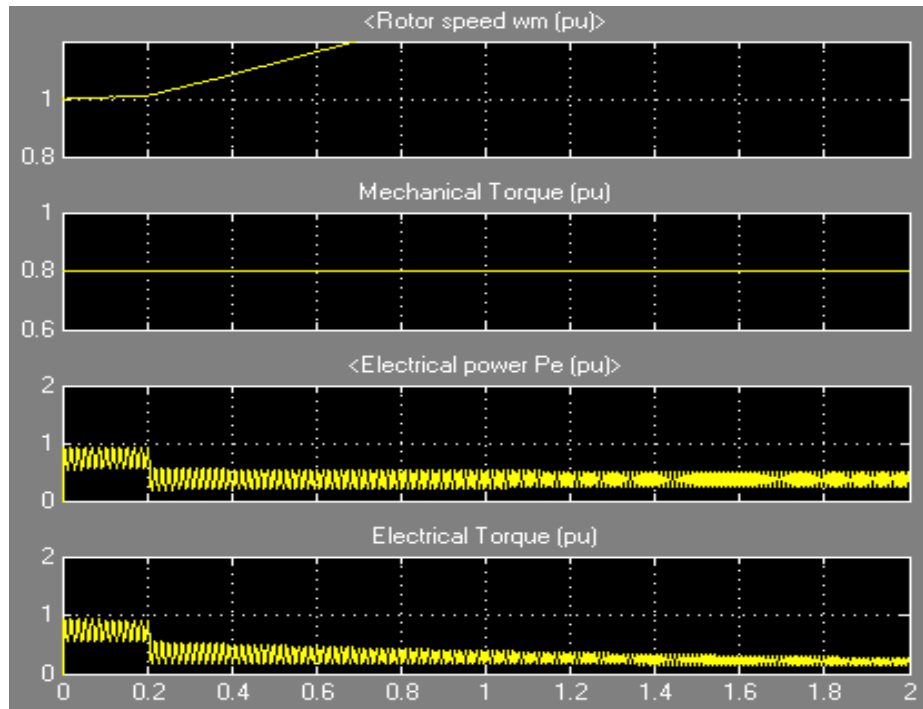


Figure 3.43: Graphs for rotor speed, torque, power and electrical torque

After  $t=0.2$ sec the system goes through a transition period as a result rotor speed is having oscillatory response. After  $t=0.2$  sec the rotor speed and other associated variables gets settled. Corresponding graphs for rotor speed, torque, power, electric torque and mechanical torque are shown in Figure 3.43 and Figure 3.45. Figure 3.44 shows graph for armature voltage

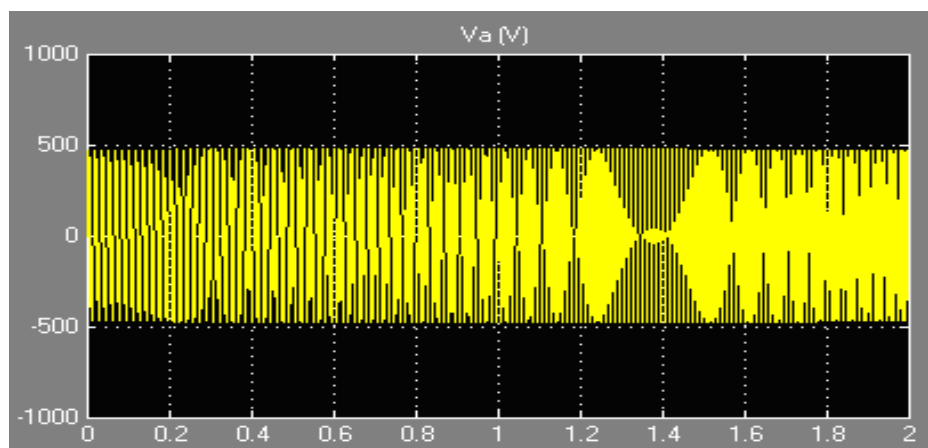


Figure 3.44: Graph for armature voltage

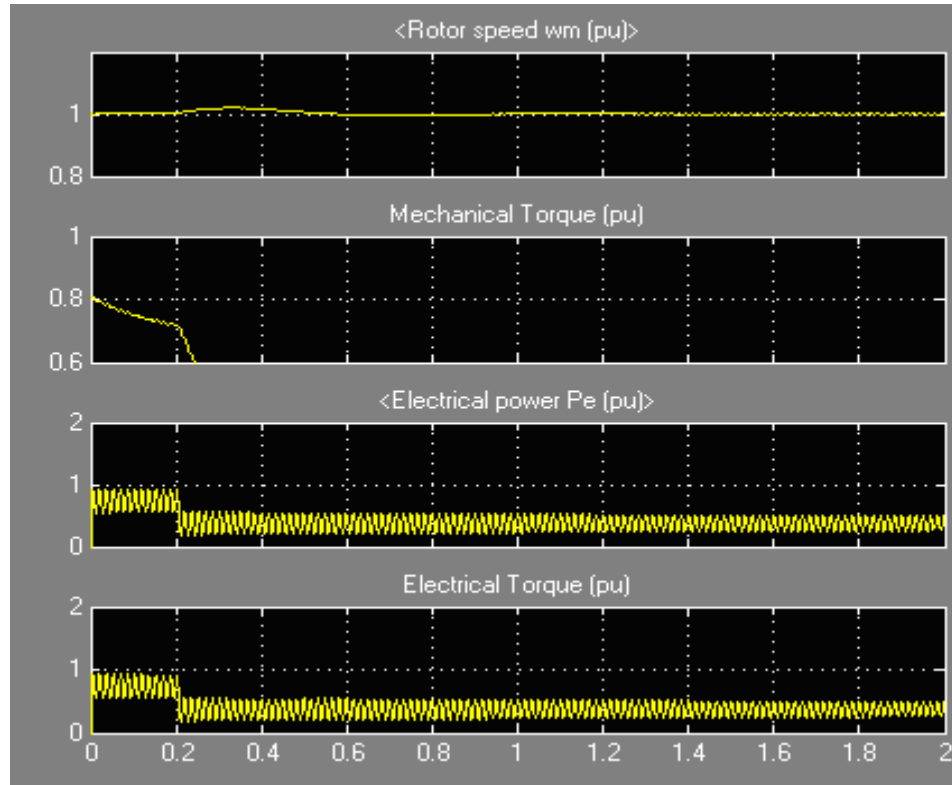


Figure 3.45: Graph for rotor speed, mechanical torque, electric power and torque

Graph in Figure 3.45 shows rotor speed, mechanical torque, electric power and torque as shown the mechanical torque settles at 0.6 p.u. The synchronous generator will react differently with different types of load applied at the output. Loads with different frequencies, reactive powers and voltages will produce different kinds of results. We will further investigate the different responses in this section. This section examines different loading condition; it shows the change in voltage and current with the change in the type of load. Different kind of loads and no load condition is tested in the generator system with fuzzy controller as the speed controller.

#### 3.8.4 No load condition

When no load is applied the change in voltage and current is shown in Figure 3.46. The voltage graph shows the frequency at 55 Hz and magnitude of 700V peak to peak. The current graph shows the 3 different color phases having a phase difference of 60 degrees. Figure 3.47 shows the torque and electrical power at constant magnitude. The Figure 3.48 shows torque,  $V_f$  and power graph.

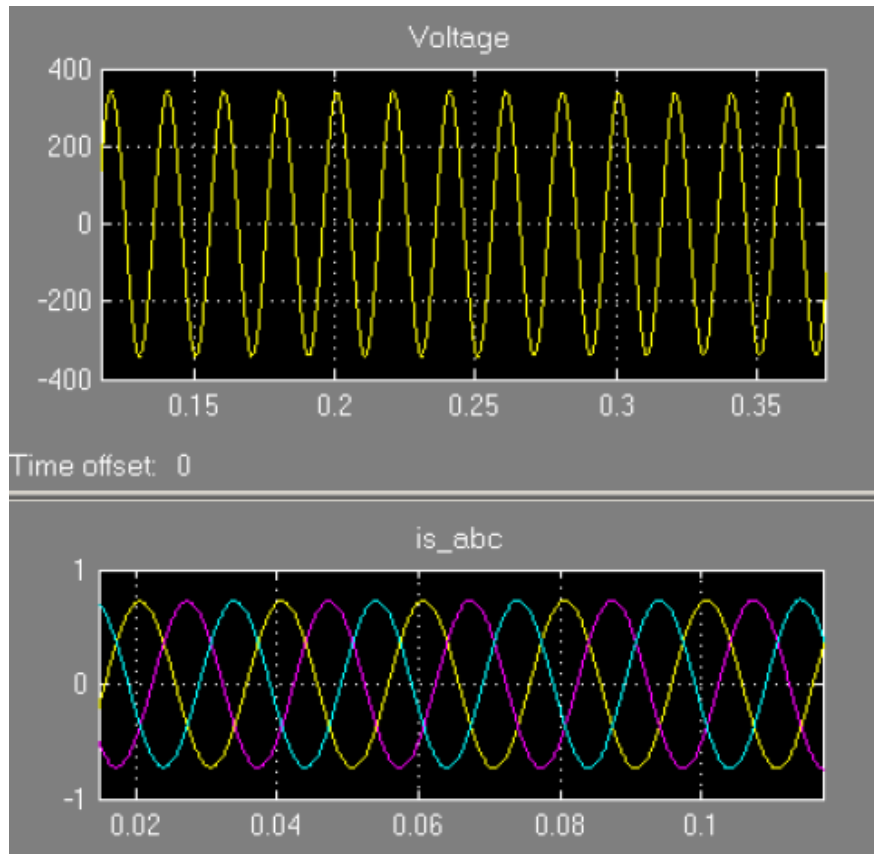


Figure 3.46: Variation in voltage and current when no load added

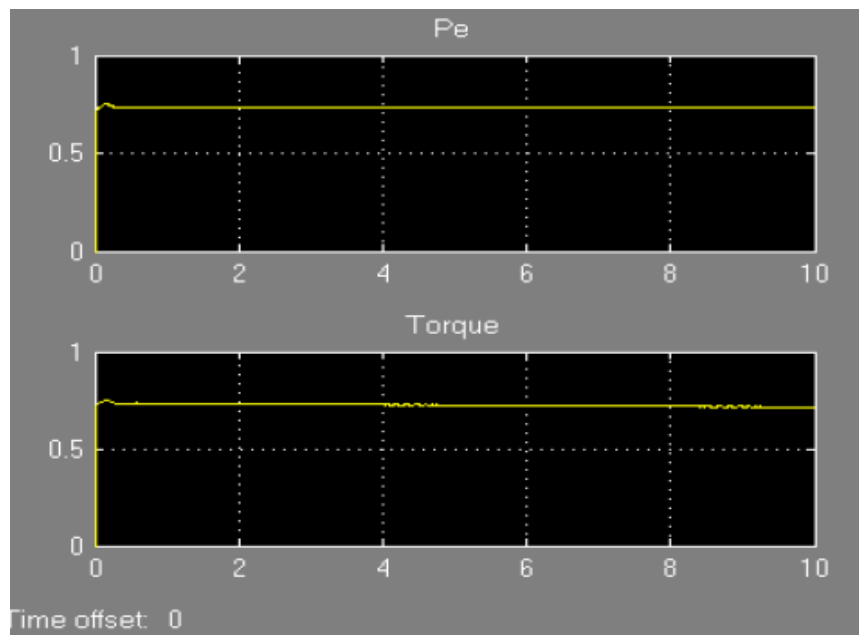


Figure 3.47: Variation in power and torque for no load condition

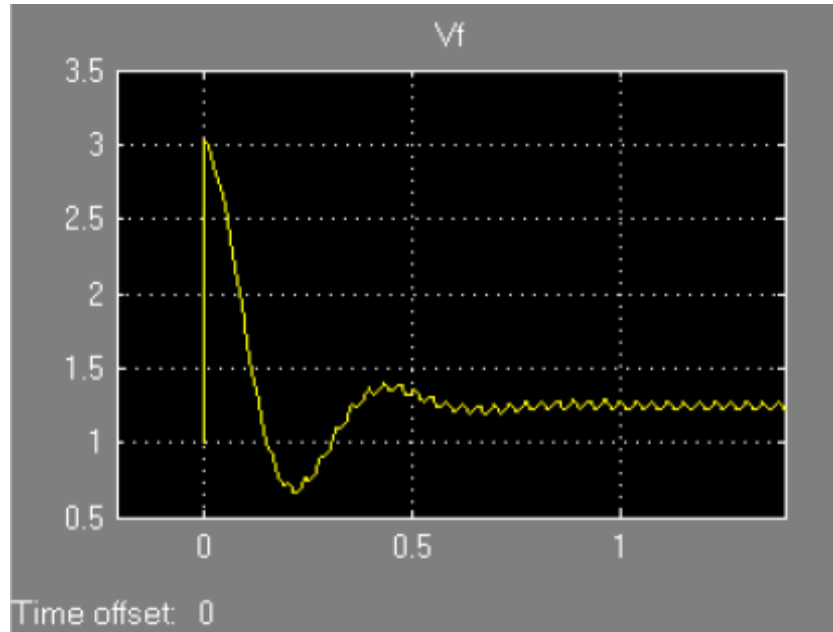


Figure 3.48: Variation in,  $V_f$  at no load condition

### 3.8.5 On load conditions

When a pure reactive load added to the generator system the voltage, current, power, torque and  $V_f$  waveforms are shown in following Figure 3.49 and Figure 3.50

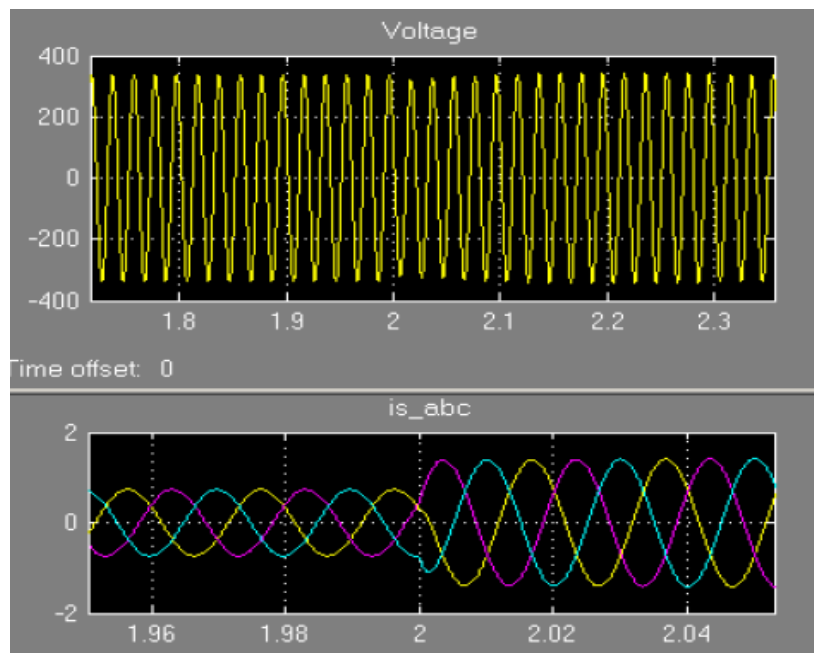


Figure 3.49: Variation in  $V_f$  and  $I_s$  at reactive load condition

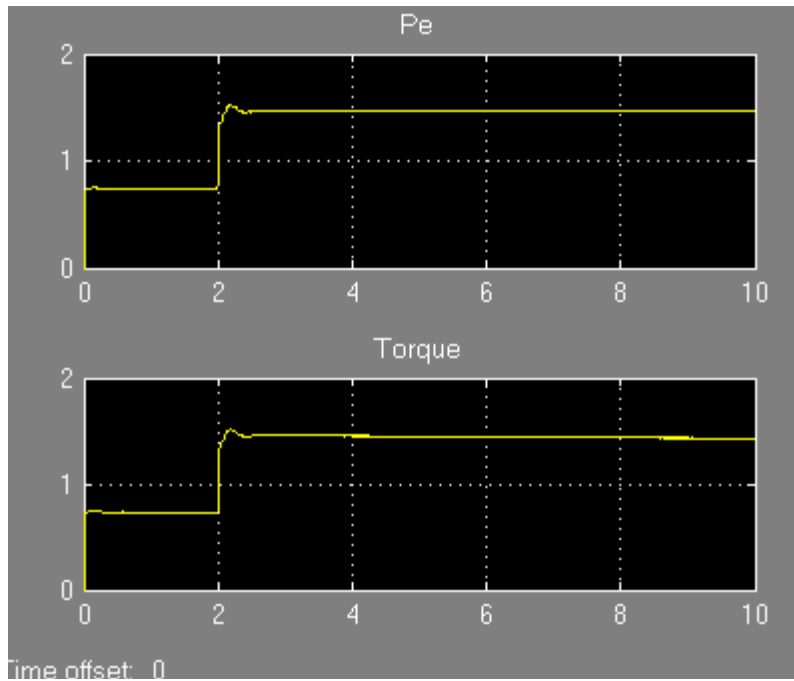


Figure 3.50: Variation in torque,  $V_f$  and power at reactive load condition

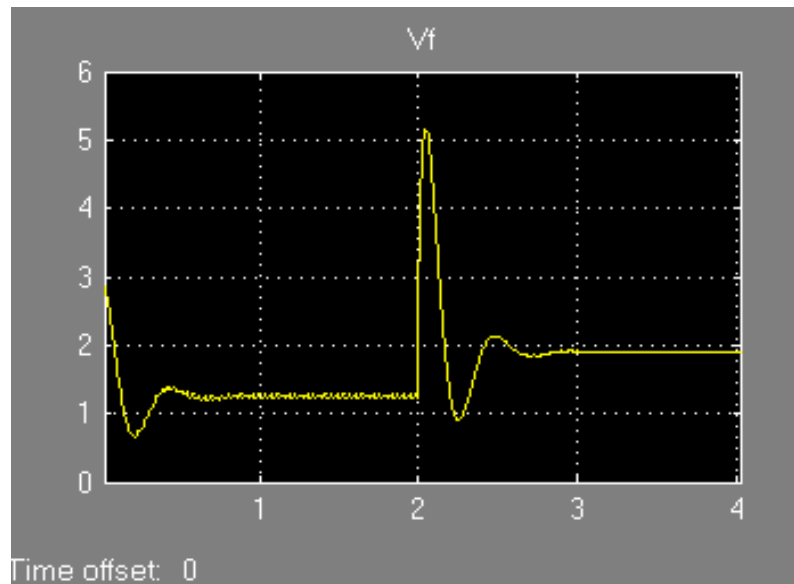


Figure 3.51: Variation in  $V_f$  at pure R load condition

The graph above shows the torque and electrical power of the generator. Both graphs are similar except for the state after  $t=2$ . After  $t=2$  the torque follows the applied input step change. There the overshoot is quite large which requires a greater integral action by the controller. For the electrical power, the magnitude remains constant after the step input

because the system enters steady state. The graph shows the response of  $V_f$  to the generator. After  $t=2$ , the magnitude of  $V_f$  increased by 50%.

When inductance reactive load added 50VAR the load now has a reactance of 50 VAR of inductance. At  $t=2$ , the three phase stator current,  $I_s$  has a shift in the magnitude equally with respect to the first phase. For the voltage, the magnitude fluctuates after  $t=2$ , but slowly goes to steady state as time increases. The frequency remains the same as shown in Figure 3.52.

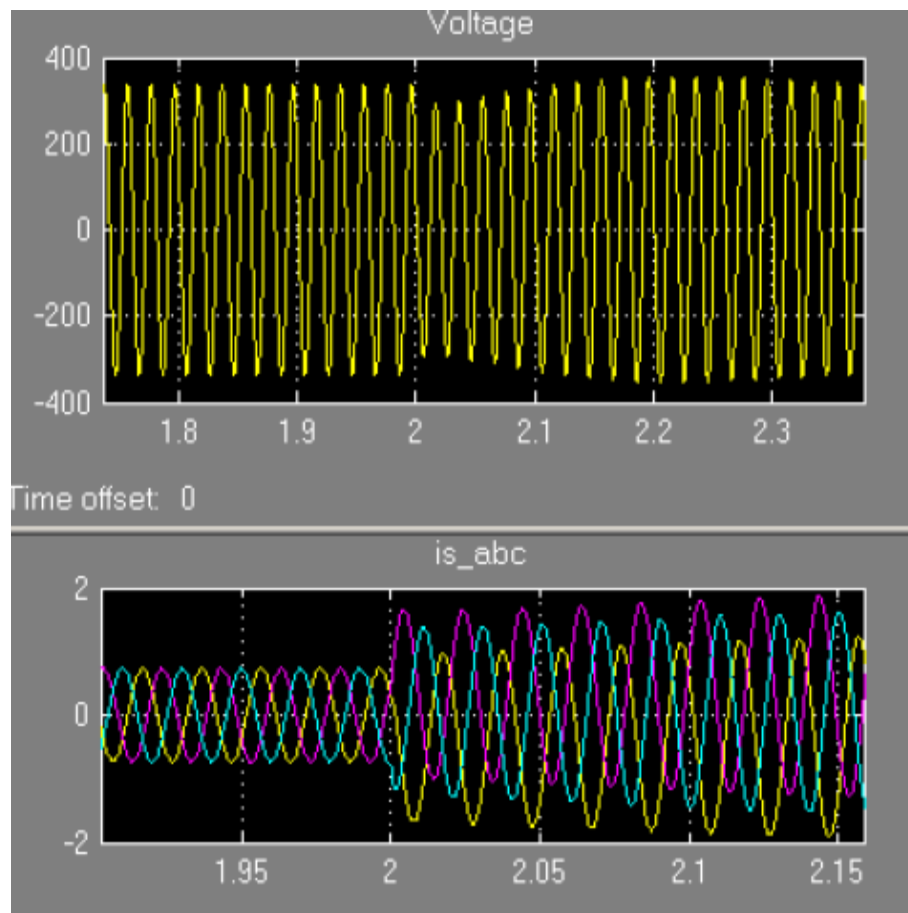


Figure 3.52: Variation in voltage and  $I_s$  at load condition added after 50 VAR

Graph in Figure 3.53 shows  $V_f$  has a larger overshoot at  $t=2$ , before settling down to steady state. Graphs in Figure 3.54 shows the variation in torque power after the steady state has been achieved. The transition time is well beyond 2.15 sec.

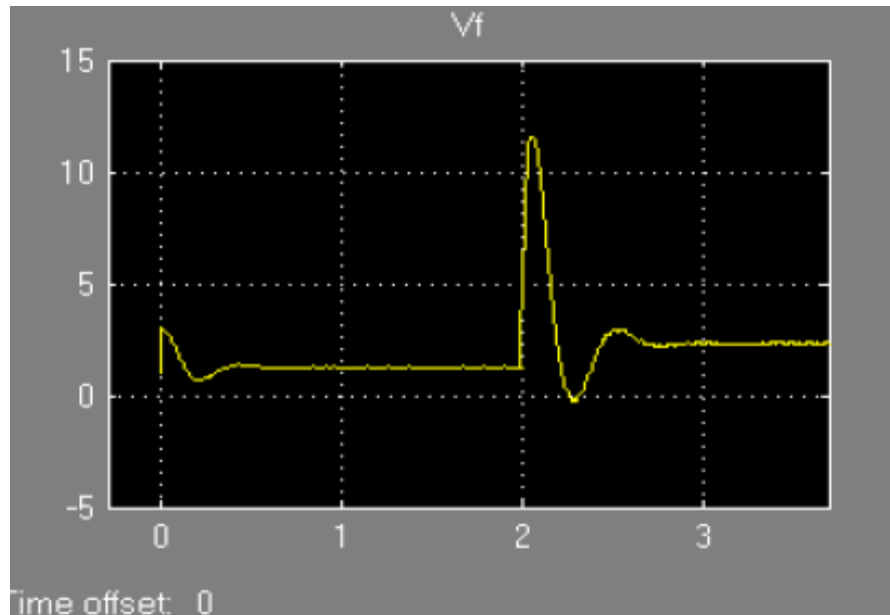


Figure 3.53: Variation in  $V_f$  at load condition added after 50 VAR

Graph in Figure 3.54 shows variation in torque power after  $t=2$ , before settling down when load is added at 50 VAR.

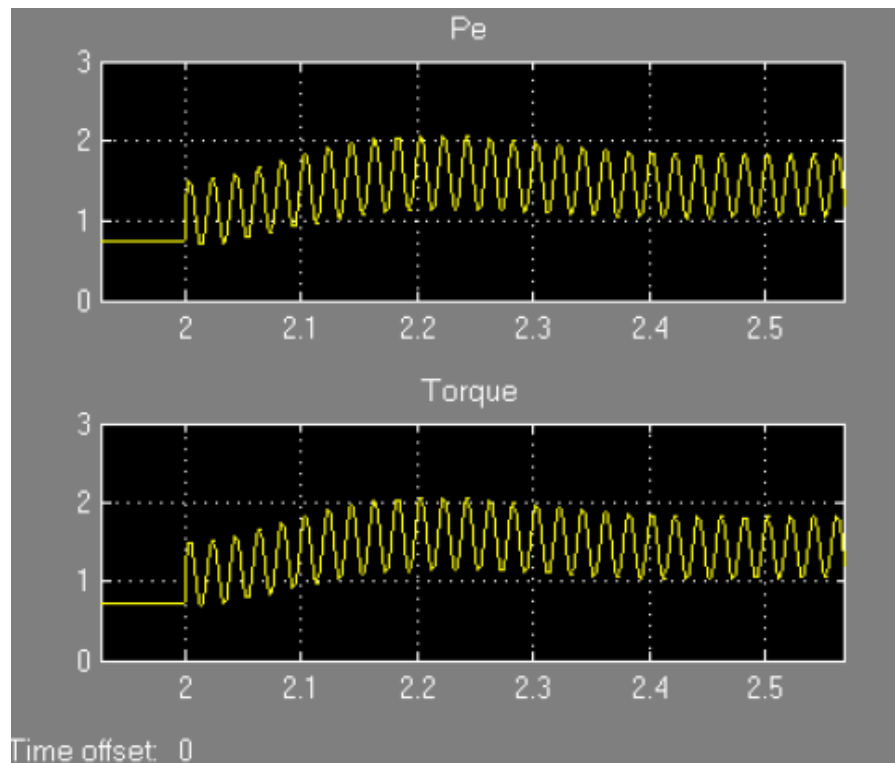


Figure 3.54: Variation in torque power at load added at 50VAR

When frequency load is added at 200Hz, the frequency is changed from 50 Hz to 200Hz. In Figure 3.55 the variation in  $V_f$  at load is shown. The frequency of the output voltage is 50 Hz. In Figure 3.56 at  $t=2$ , again the magnitude of the stator current increases to twice. But the magnitude of the output voltage remains constant even after  $t=2$ .

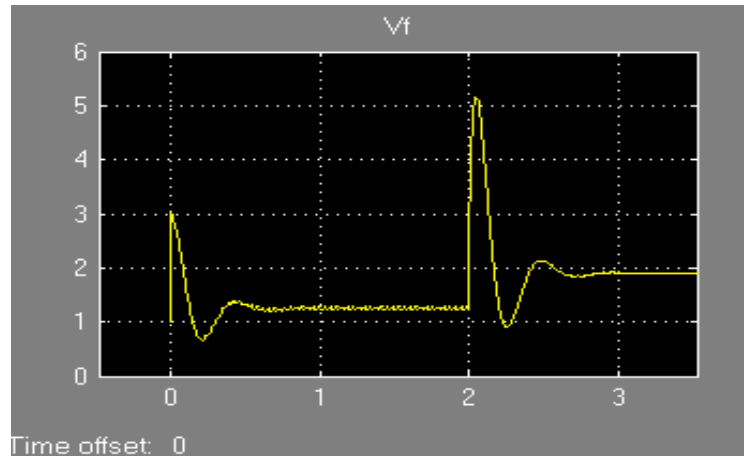


Figure 3.55: Variation in  $V_f$  at load condition added after 200 Hz

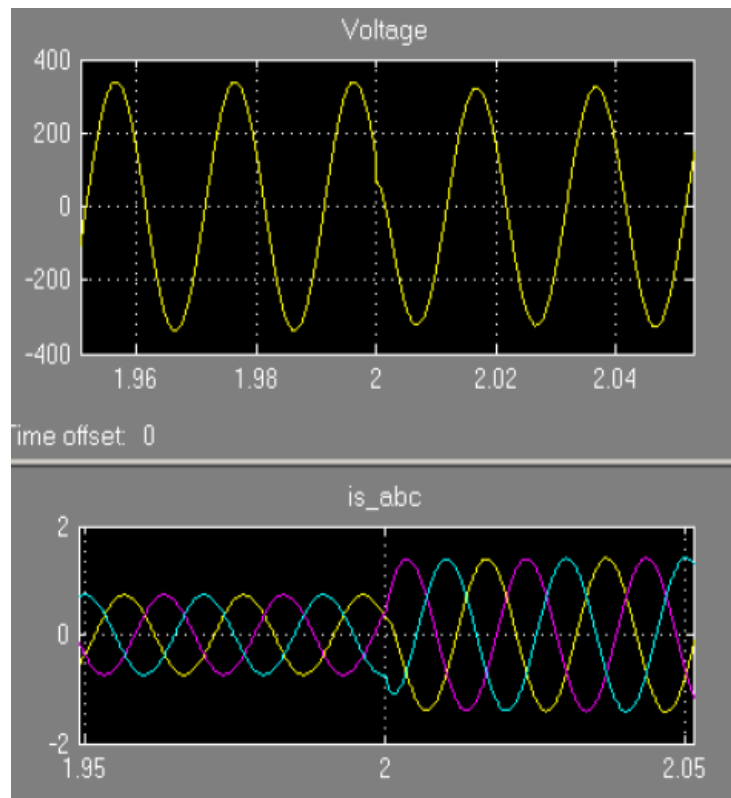


Figure 3.56: Variation in voltage and current at load condition added at 200Hz

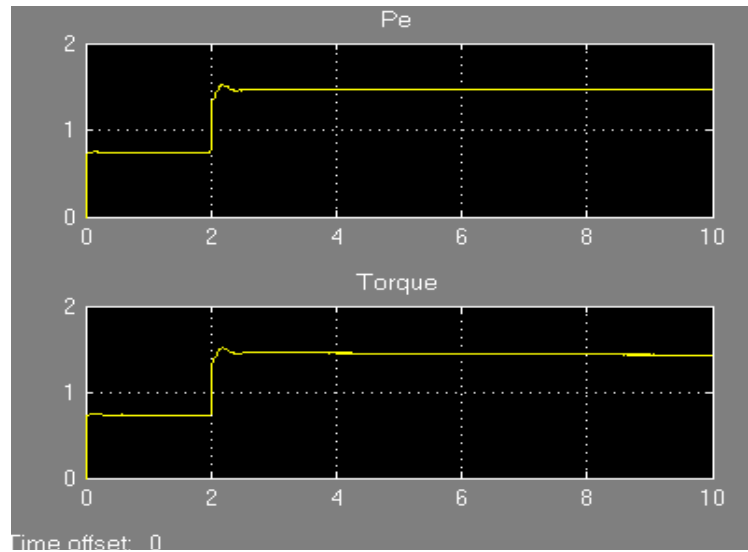


Figure 3.57: Variation in torque,  $V_f$  and power at 200Hz load

When active power load is added at 200W, the increase in the magnitude of the stator current is 1.8 times after  $t=2$ . The magnitude of the output voltage remains constant with increasing time as it should be. The graph shows the  $V_f$  increase in magnitude of 1 to 3 when  $t=2$ . The torque and  $P_e$  both are similar, they both increase steadily after  $t=2$  as shown in Figure 3.57

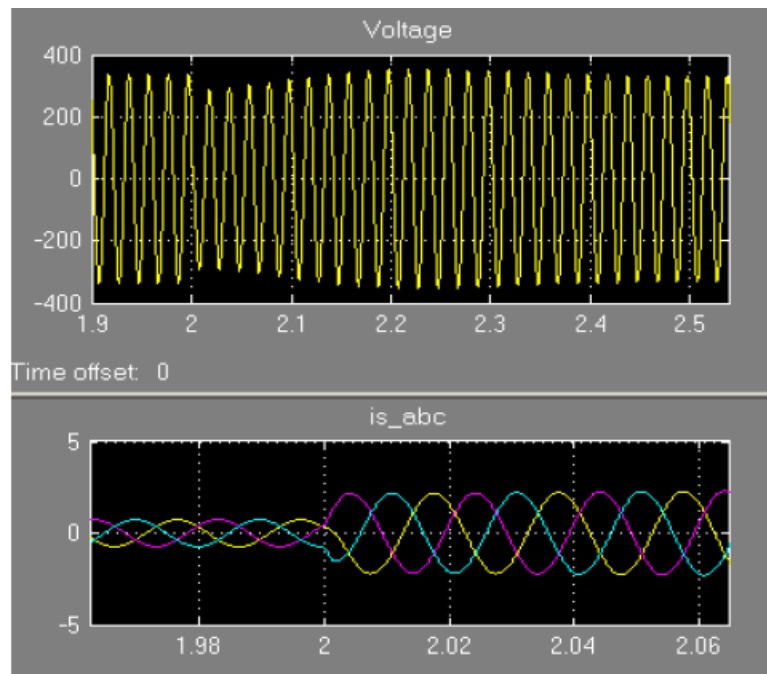


Figure 3.58: Variation in voltage and current at active load condition

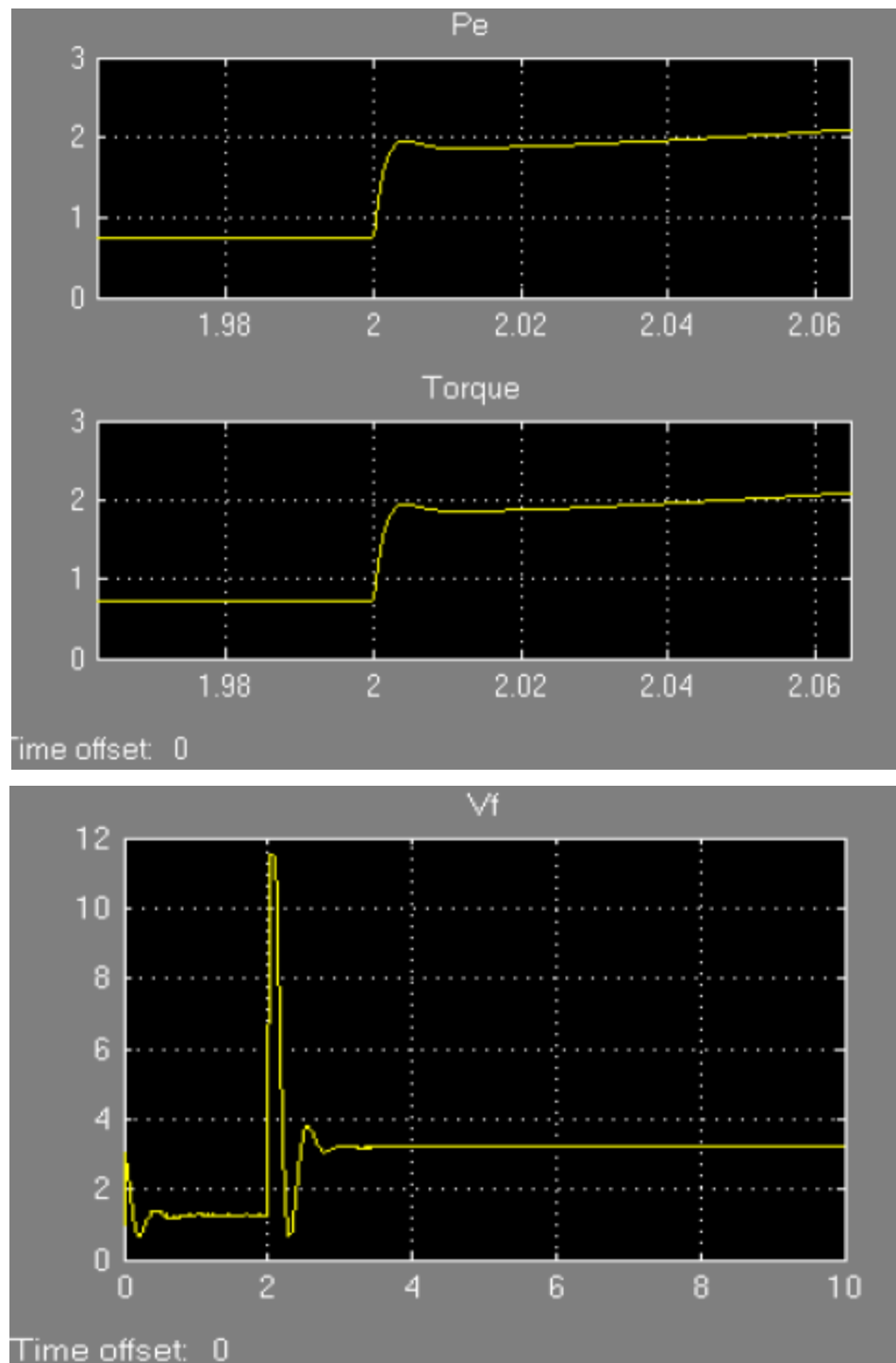


Figure 3.59: Variation in torque,  $V_f$  and power at 200W load condition

The variation of torque,  $V_f$  and power at 200W load has been shown in Figure 3.59.

### 3.9 Neuro-fuzzy control of synchronous generator

Fuzzy model reference learning controller (FMRLC) in synchronous generator terminal voltage and reactive power control is designed so that its learning controller has the ability to improve the performance of the closed-loop. A fuzzy model reference learning controller for synchronous generator terminal voltage control system by generating command inputs to the SG plant and utilizing feedback information from the SG. The FMRLC controller is superior to conventional self tuning controllers which continue to tune the controller parameters because it will tune and to some extent remember the values that it had tuned in the past.

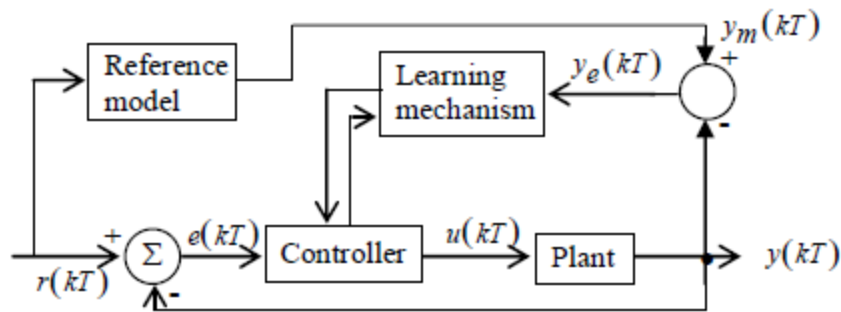


Figure 3.60: Fuzzy neuro controller for synchronous generator

Figure 3.60 shows the functional block diagram of the FMRLC. It is made up of four main parts; the plant, the fuzzy controller to be tuned, the reference model, and the learning mechanism (an adaptation mechanism). The FMRLC uses discrete time signals  $r(kT)$  and  $y(kT)$  with  $T$  as the sampling period. It also uses the learning mechanism to observe numerical data from a fuzzy control system. With this numerical data, it characterizes the fuzzy control system's current performance and automatically synthesizes or adjusts the fuzzy controller so that some given performance objectives are met. Here, the fuzzy control system loop operates to make  $y(kT)$  track  $r(kT)$  by manipulating  $u(kT)$ , while the adaptation control loop seeks to make the output of the plant  $y(kT)$  track the output of the reference model  $y_m(kT)$  by manipulating the fuzzy controller parameters. The synchronous generator which represents the plant has an input

$u(kT)$  from the fuzzy controller and terminal voltage output  $y(kT)$ . The input to the fuzzy controller is the error,  $e(kT) = r(kT) - y(kT)$

$$c(kT) = \frac{e(kT) - e(kT - T)}{T}$$

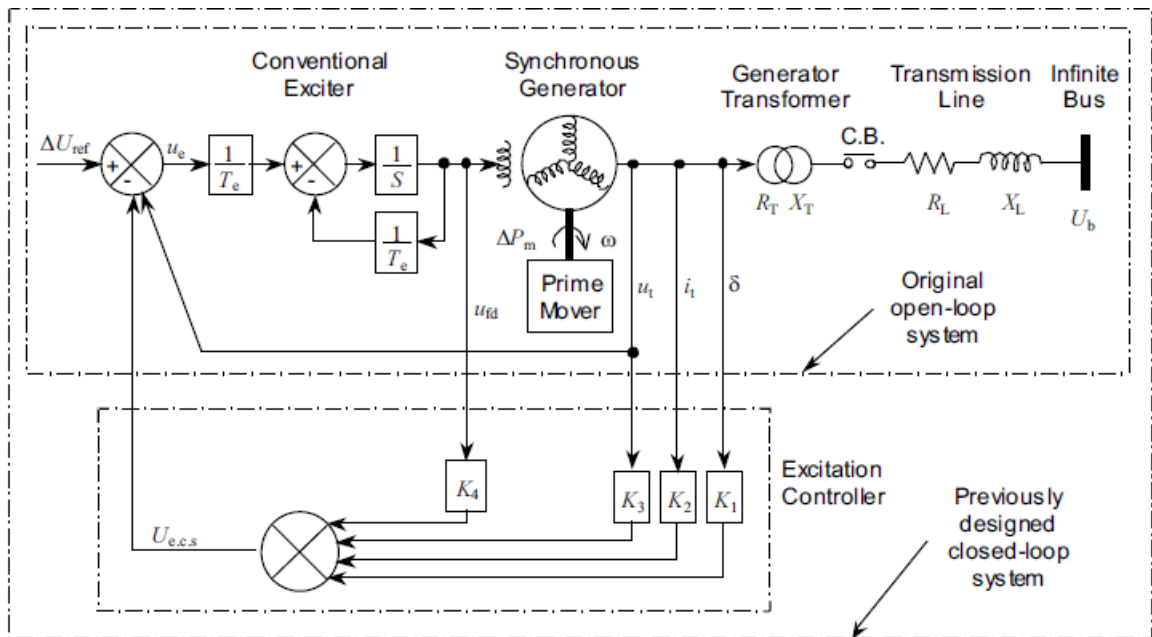


Figure 3.61: Detailed schematic diagram for adaptive controller for synchronous generator

Figure 3.61 shows separate components for infinite bus, transmission line, generator transformer, synchronous generator and the conventional exciter working for both original open loop system and previously designed closed loop system. The detailed schematic diagram for adaptive controller for synchronous generator is shown above .

The learning mechanism tunes the rule-base of the direct fuzzy controller so that the closed loop system behaves like the reference model. These rule-base modifications are made by observing data from the controlled process, the reference model, and the

fuzzy controller. The learning mechanism consists of two parts: a fuzzy inverse model and a knowledge base modifier. The fuzzy inverse model (having the same rule base with the fuzzy controller) performs the function of mapping  $y_e(kT)$  (representing the deviation from the desired behavior) to changes in the process inputs  $p(kT)$  that are necessary to force  $y_e(kT)$  to zero. The knowledge-base modifier performs the function of modifying the fuzzy controller's rule-base to affect the needed changes in the process inputs.

Table 3.3: Fuzzy rule base for inputs and output

u(t)		e(t)						
		NB	NM	NS	ZO	PS	PM	PB
$\Delta e(t)$	NB	NB	NB	NB	NB	NM	NS	ZO
	NM	NB	NB	NB	NM	NS	ZO	PS
	NS	NB	NB	NM	NS	ZO	PS	PM
	ZO	NB	NM	NS	ZO	PS	PM	PB
	PS	NM	NS	ZO	PS	PM	PB	PB
	PM	NS	ZO	PS	PM	PB	PB	PB
	PB	ZO	PS	PM	PB	PB	PB	PB

This table 3.3 shows all the possible rules which can be made in fuzzy rule base for above fuzzy based SG control system. Table 3.3 is same as Table 3.2 because of same reference comparison.

Now the techniques of neuro fuzzy will be applied to test for better control strategy. Figure 3.62 and Figure 3.63 shows the ANFIS training and ANN structure representing to synchronous generator controller which in neural network based.

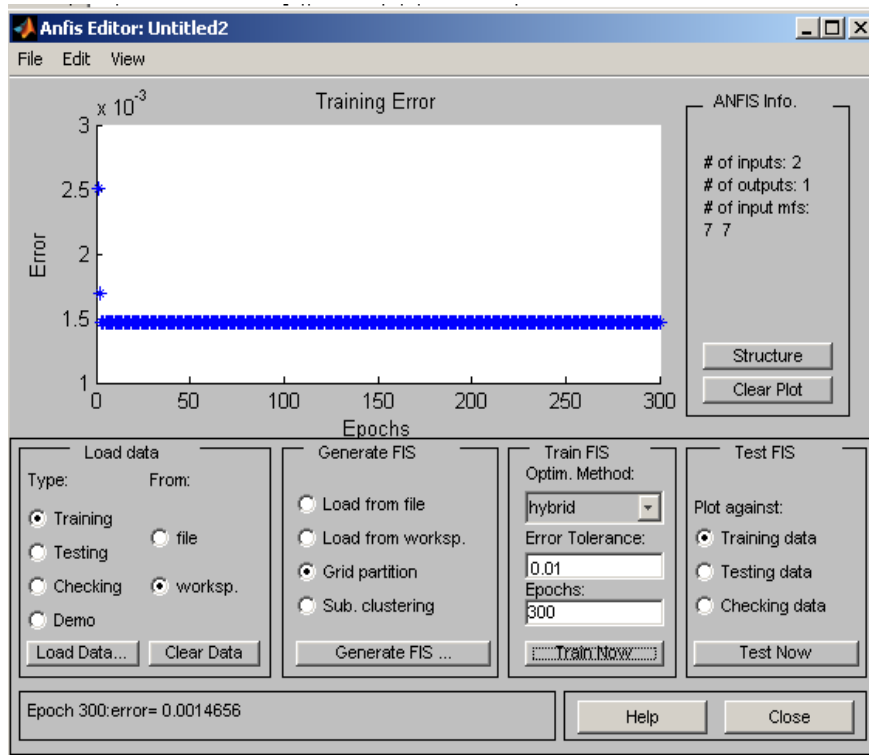


Figure 3.62: Graph between error and epoch of neural network

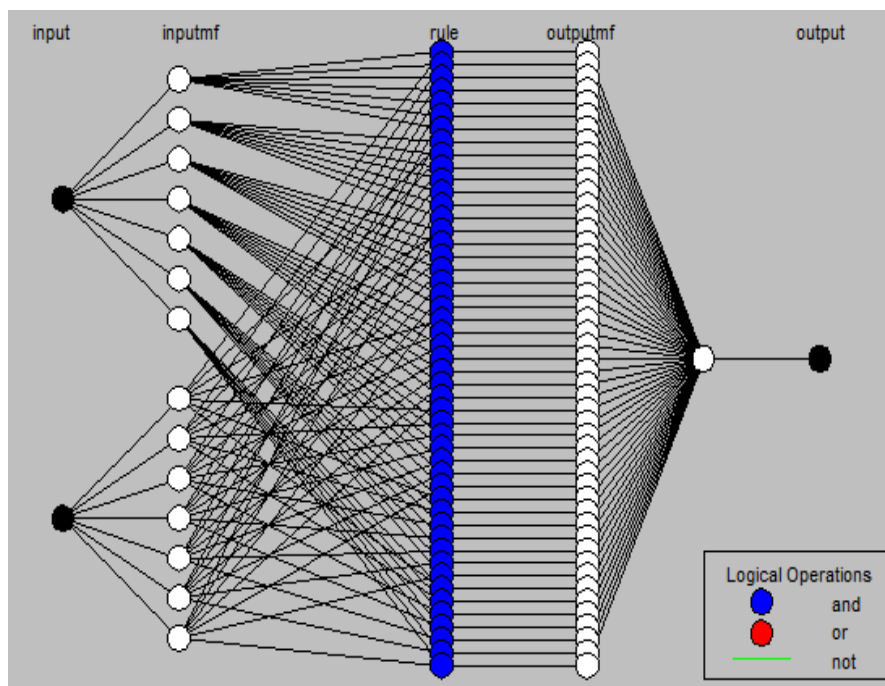


Figure 3.63: Fuzzy-neuro architecture implemented in synchronous generator

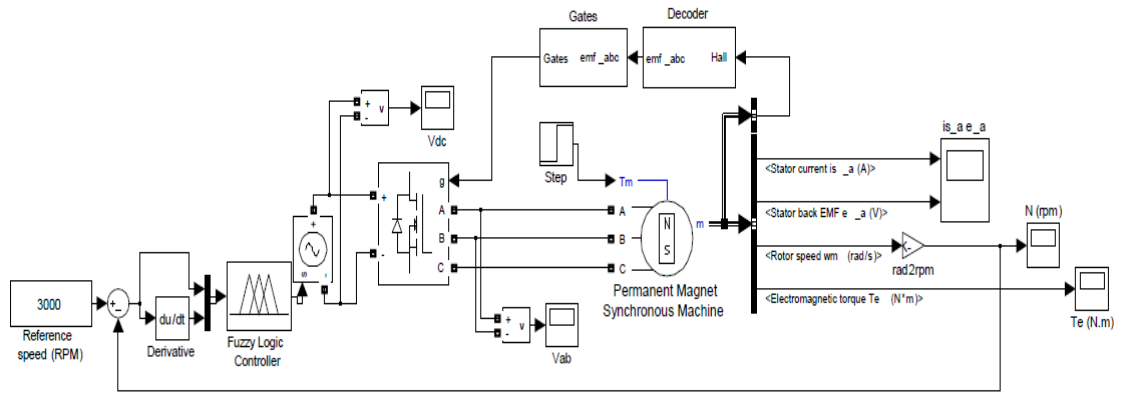
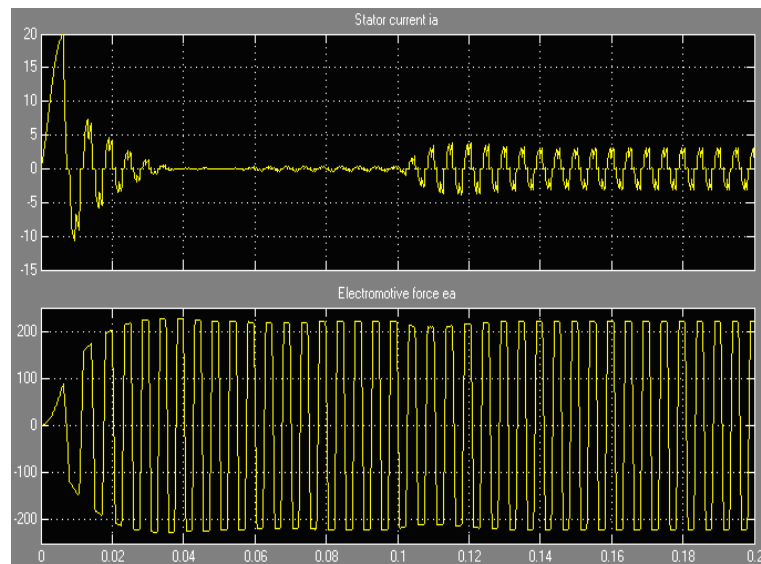


Figure 3.64: Simulink representation of neuro-fuzzy control of synchronous generator

The fuzzy neuro architecture implemented in the system has been shown in Figure 3.63 and the simulink representation of neuro fuzzy control of synchronous generator is shown in Figure 3.64



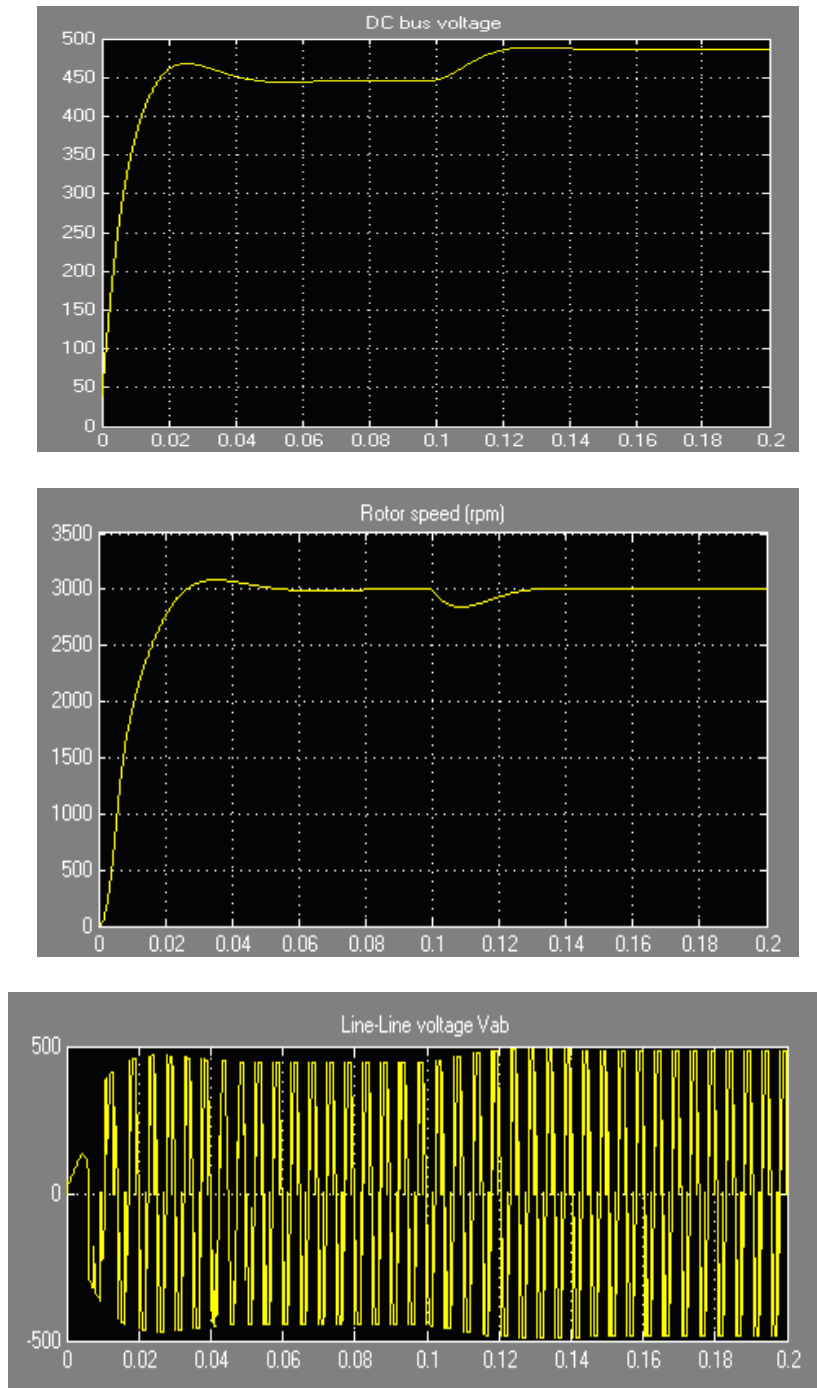


Figure 3.65: Response curves of stator current, rotor speed, and torque in fuzzy neuro control of synchronous generator

There is an inverse oscillation happening at  $t=0.1$  sec in the graph obtained for rotor speed. It might be due to component contributing dead time and lag in the system. The graphs in Figure 3.65 shows the response curves for stator current, rotor speed and torque

in fuzzy neuro based control strategy as implemented on SG. The system is stabilized after  $t=0.13$ .

### 3.10 Control parameters evaluation

From the above case studies we have calculated IAE i.e integral absolute error and ITAE i.e integral time absolute error parameters for each of the type of control architecture. The calculation for IAE and ITAE Table 3.4 gives in detail about the control parameters and gives a comparative study of the same. These performances indices of IAE and ITAE help in decision taking regarding selection of control architecture.

Table 3.4: IAE and ITAE calculations

S.No	Parameters	Type-1	Type-2	Neuro fuzzy	Multi layer
1	IAE	4.755	4.428	7.243	8.56
2	ITAE	0.3665	0.312	0.6035	0.77

### 3.11 Conclusion

Always the stability of any system and their transient & steady state responses play a role in selecting particular control scheme for designing and selecting specific control architecture. In the above sections the synchronous generator is efficiently controlled by contemporary control scheme of fuzzy logic and other models. The transient behavior and stability of the system have been analyzed using criterion of ITAE and IAE. The control schemes are compared on relative stability point of view also.

ITAE integrates the absolute error multiply by the time over considered time interval. It helps in consideration of an error which creeps into the system after a long time and effect the system performance considerably as compared to errors creeping into the system in the beginning of the process. It tunes the system to settle for stable performance. When the error is absolute over the entire period of considered time interval the criterion of IAE is used. It integrates absolute error over time. It provides usually less sustained oscillation and slower response to optimize the system performance.

---

# CHAPTER 4

## DC MOTOR: CASE STUDY

---

### **Introduction**

All land-based existing electrical power supply networks are AC systems of generation, transformation, transmission and distribution. Thus there is little need for large DC generators. AC motors are used in industries wherever they are suitable or can give appropriate characteristics by means of power electronic devices. Yet there remain important fields of application when the DC machines can offer economic and technical advantage. The wonderful thing about DC machines is its versatility.

DC machine operate as either a generator or a motor but at present its use as a generator is limited because of the widespread use of AC power. Large DC motors are used in machine tools, printing presses, conveyors, fans, pumps, hoists, cranes, paper mills, textile mills and so forth. Small DC machines (in fractional horsepower rating) are used primarily as control devices such as tacho-generators for speed sensing and servomotors for positioning and tracking. DC motors still dominate as traction motors used in transit cars and locomotives as the torque-speed characteristics of DC motor can be varied over a wide range while retaining high efficiency. The DC machine definitely plays an important role in industry. Electric motors exist to convert electrical energy into mechanical energy. This is done by two interacting magnetic fields - one stationary, and another attached to a part that can move. DC motors have potential for very high torque. It depends on physical size of motor. DC motors are simplest and oldest electric motors. Principles of electromagnetic induction were discovered by Oersted, Gauss, and Faraday in 1800. Later, Hans Christian Oersted and Andie Marie Ampere found that an electric current produces a magnetic field.

In 1831 Joseph Henry had improved on Faraday's experimental motor. He built a simple device whose moving part was a straight electromagnet rocking on a horizontal

axis. Henry considered his little machine to be merely a "philosophical toy". On the basis of his experiments, it was feasible to design both electric generators and electric motors.

Just a year after Henry's motor was demonstrated, William Sturgeon invented the commutator, and with it the first rotary electric motor. In many ways, a rotary analogue of Henry's oscillating motor. Sturgeon's motor, was simple, and could provide continuous rotary motion. It contained essentially all the elements of a modern DC motor.

DC machines are one of the most commonly used machines for electromechanical energy conversion. Converters are used continuously to convert electrical input to mechanical output or vice versa. An electric machine is therefore a link between an electrical system and a mechanical system. If the conversion is from mechanical to electrical, the machine is said to act as a generator. If the conversion is from electrical to mechanical, the machine is said to act as a motor. Therefore, the same electric machine can be made to operate as a generator as well as a motor. The limitations of the DC system however became more and more apparent as the power demand increased. In the case of DC systems the generating stations and the load centers have to be near to each other for efficient transmission of energy. AC system took over preferred system for the generation transmission and utilization of electrical energy. DC system however could not be obliterated due to the able support of batteries. Further, DC motors have excellent control characteristics. Even today the DC motor remains an industry standard as far as the control aspects are concerned.

#### **4.1 Features of DC motor**

DC motors are expensive because of brushes and commutator and has relatively low torque-volume and torque-inertia ratio. These are used in large power applications. Brushes and commutator which requires regular maintenance are no longer require regular checking and maintenance. DC motor is used in low power application.

DC motor operation is based on simple electromagnetism as shown in Figure 4.1. A current carrying conductor generates a magnetic field which when placed in an external magnetic field; it will experience a force proportional to the current in the conductor and to the strength of the external magnetic field. The internal configuration of

a DC motor is designed to harness the magnetic interaction between a current-carrying conductor and an external magnetic field to generate rotational motion.

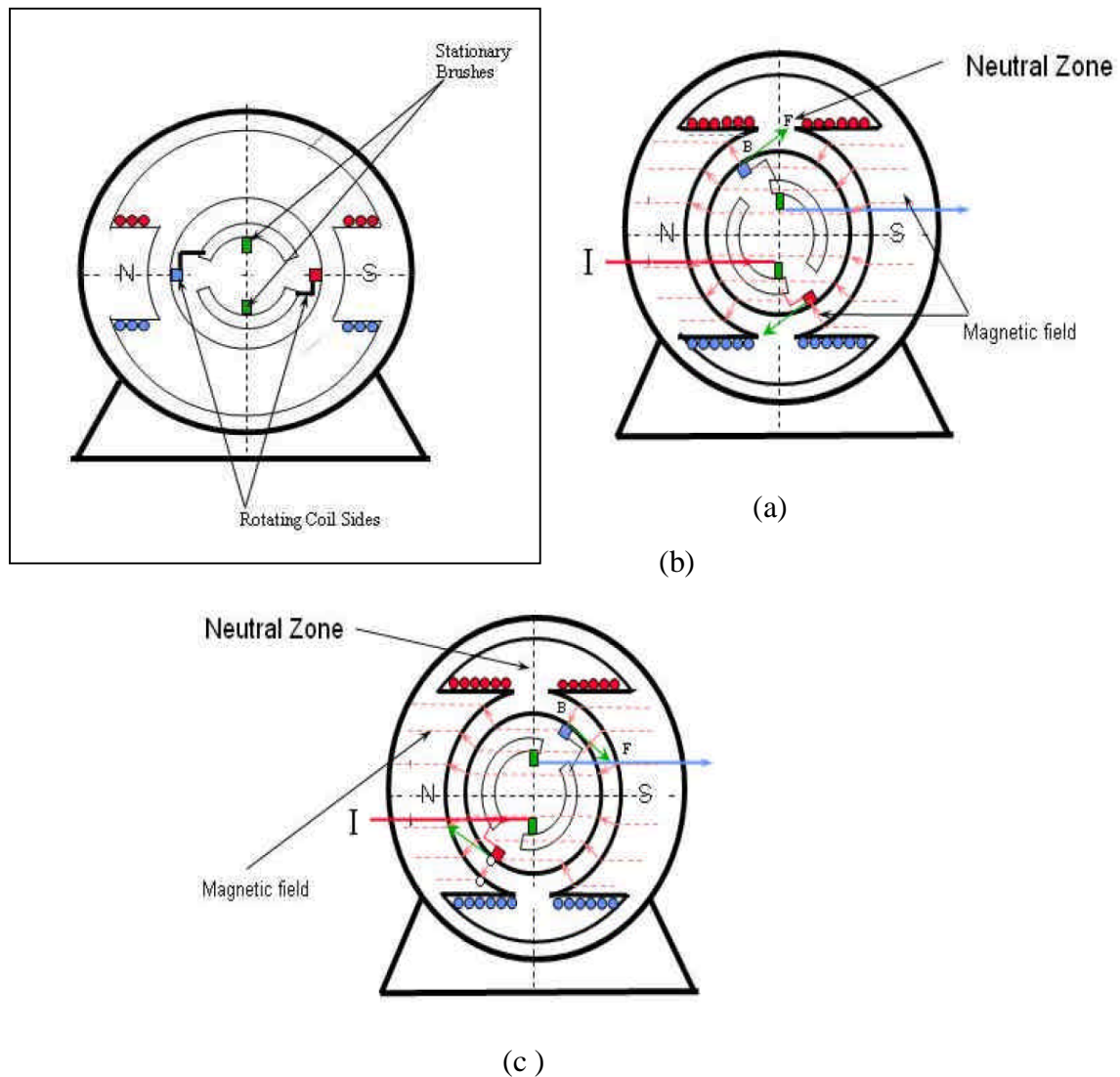


Figure 4.1: DC motor operation (current and magnetic field directions)

- (a) DC motor operation
- (b) Change in current direction when the conductor passes through neutral zone
- (c) Change in direction of magnetic field also changes as the conductor passes through neutral phase

When power is applied, the polarities of the energized winding and the stator magnet(s) are misaligned. Rotor rotates until it is almost aligned with stator's field

magnets. As the rotor reaches alignment, the brushes move to the next commutator contacts and energize the next winding. DC motors always have more than two poles. Three poles DC motor is very common. If the rotor is exactly at the middle of its rotation i.e perfectly aligned with the field magnets, it will get "stuck". The DC motor considered in our case study is shown in Figure 4.2.

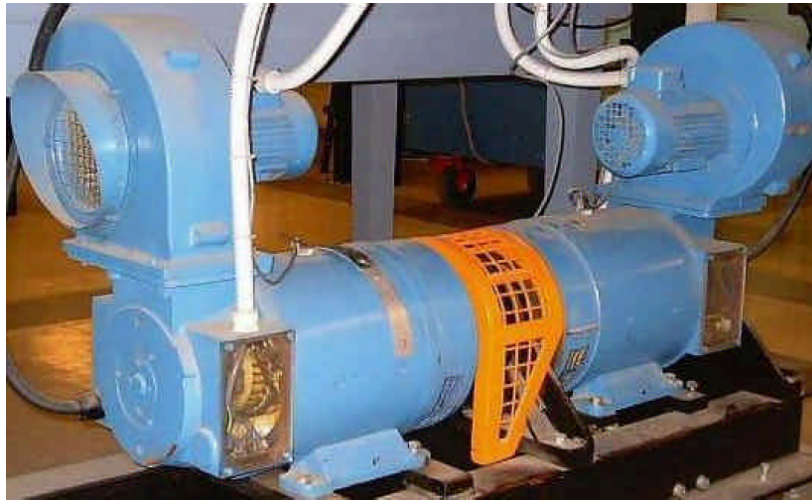


Figure 4.2 : Case study DC motor

## 4.2 DC motor modeling

Figure 4.3 shows the equivalent circuit model of armature control DC motor. This model helps in implementing and analyzing the DC motor.

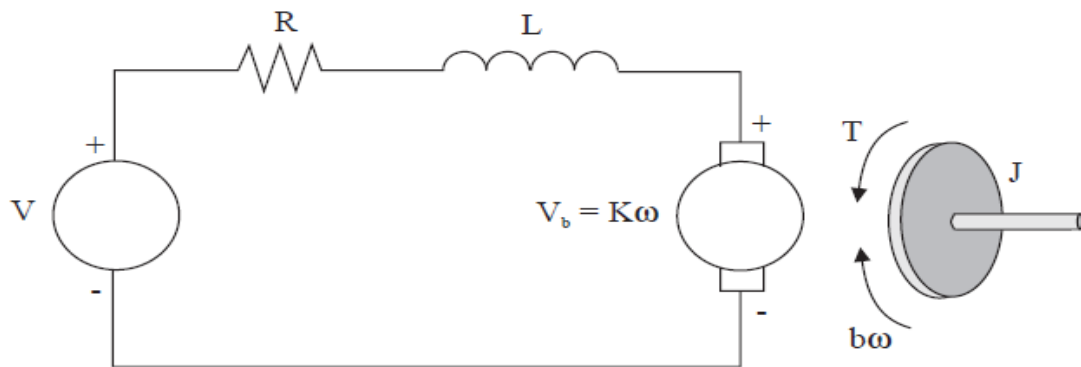


Figure 4.3: Armature controlled DC motor circuit

The rotor and the shaft are assumed to be rigid. Consider the following values for the physical parameters are given as below

Moment of inertia of the rotor  $J = 0.01 \text{ kg m}^2$

Damping (friction) of the mechanical system  $b = 0.1 \text{ Nms}$

Back electromotive force constant  $K = 0.01 \text{ Nm/A}$

Electric resistance  $R = 1 \text{ ohm}$ , Electric inductance  $L = 0.5 \text{ H}$

The input is the armature voltage  $V$  in Volts. Measured variables are angular velocity of the shaft  $\omega$  in radians per second, and the shaft angle  $\theta$  in radians.

$$\text{The motor torque is related to armature current by the equation } T = Ki \quad (4.1)$$

$$\text{The back EMF } V_b \text{ is related to angular velocity by } V_b = K\omega = K \frac{d\theta}{dt} \quad (4.2)$$

$$j \frac{d^2\theta}{dt^2} + b \frac{d\theta}{dt} = Ki \quad (4.3)$$

$$L \frac{di}{dt} + Ri = V - K \frac{d\theta}{dt} \quad (4.4)$$

$$js^2\theta(s) + bs\theta(s) = Ki(s) \quad (4.5)$$

$$Lsi(s) + Ri(s) = V(s) - ks\theta(s) \quad (4.6)$$

$$i(s) = \frac{V(s) - ks\theta(s)}{R + Ls} \quad (4.7)$$

$$js^2\theta(s) + bs\theta(s) = K \left( \frac{V(s) - ks\theta(s)}{R + Ls} \right) \quad (4.8)$$

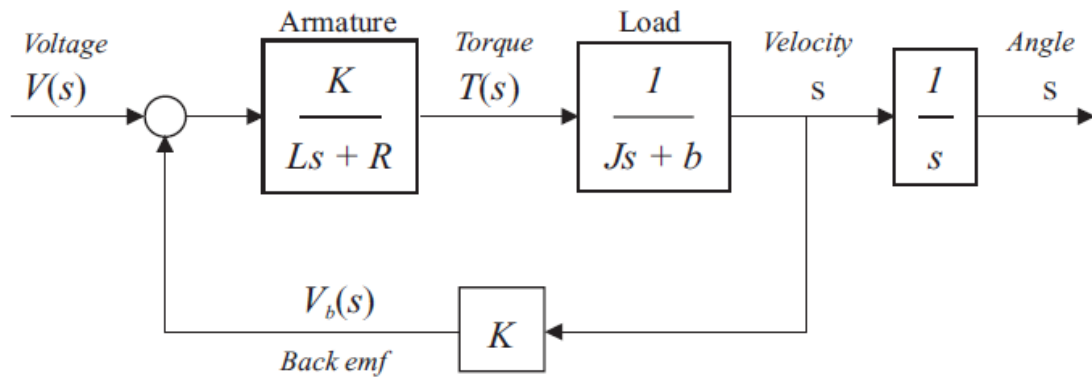


Figure 4.4: Block diagram representation of armature controlled DC motor

The block diagram in Figure 4.4 represents the implementation of mathematical model of armature control DC motor

Transfer function of armature controlled DC motor is given below.

$$\frac{\theta(s)}{V(s)} = \frac{K}{s[(R + Ls)(js + b) + K^2]}$$

$$\frac{\omega(s)}{V(s)} = \frac{K}{(R + Ls)(js + b) + K^2}$$

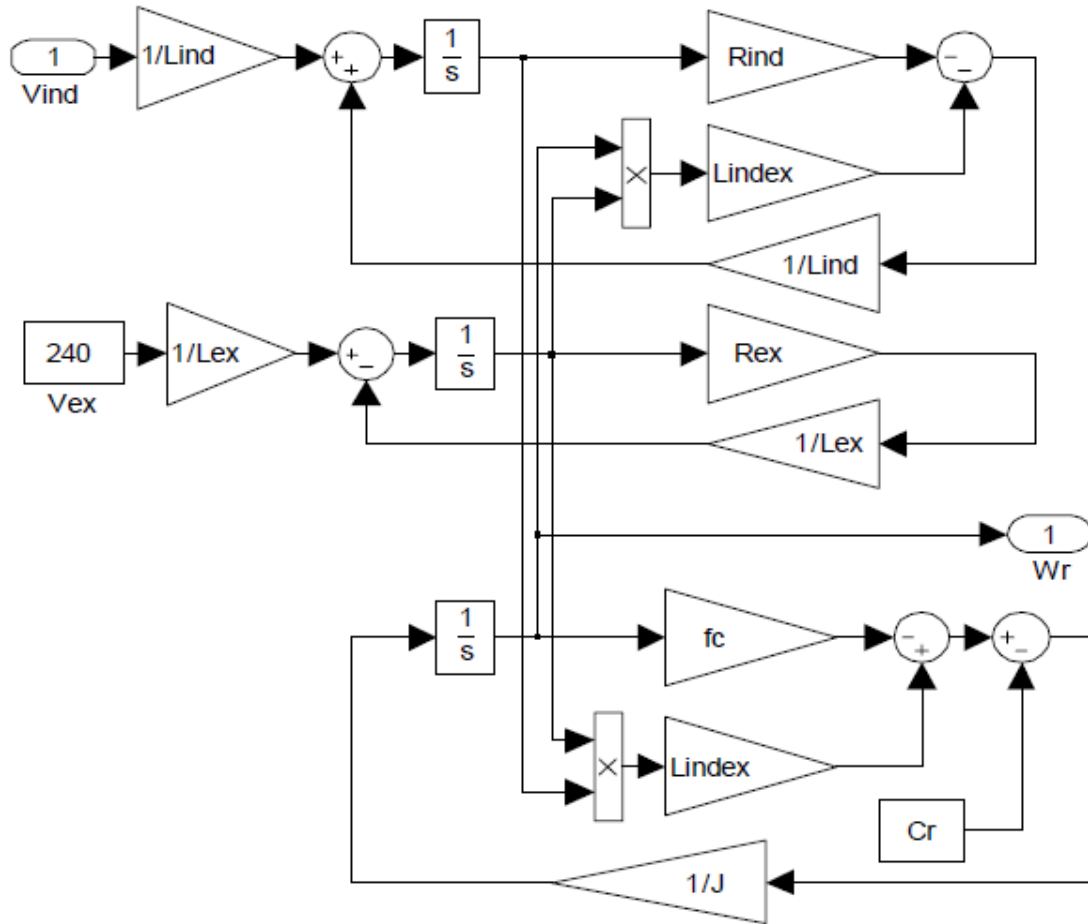


Figure 4.5: Functional block representation of armature controlled DC motor

The functional block diagram of DC motor is shown in Figure 4.5 and the corresponding simulink model is also shown in the Figure 4.6. The corresponding output response curves are shown in Figure 4.7 and Figure 4.8 when a step input is applied to the system. Figure 4.9 shows the simulink model for armature controlled DC motor when ramp input is applied. The corresponding output curve plots are shown in Figure 4.10 and Figure 4.11.

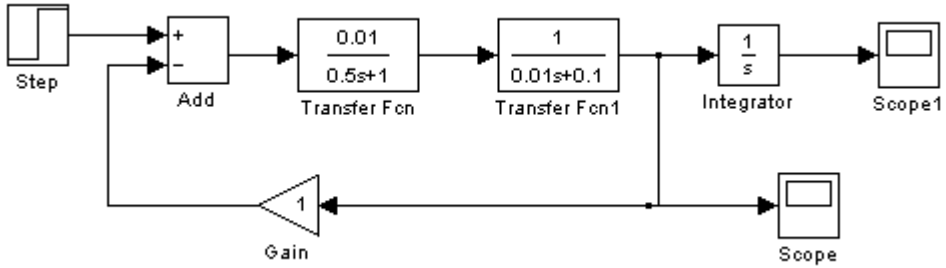


Figure 4.6: Simulink model of armature controlled DC motor for step input

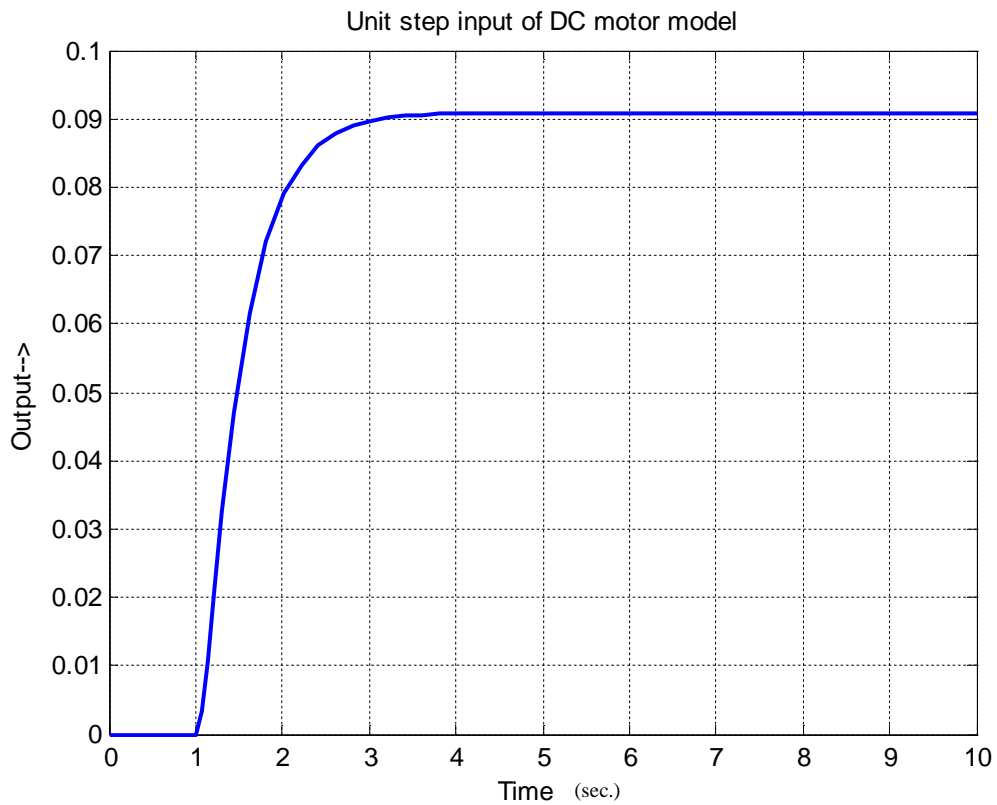


Figure 4.7: Graph of velocity for step input for an armature controlled DC motor

The graph of Figure 4.7 shows the velocity for step input change in DC motor. After 3.3 sec it gets stabilized at a value of 0.09m/sec.

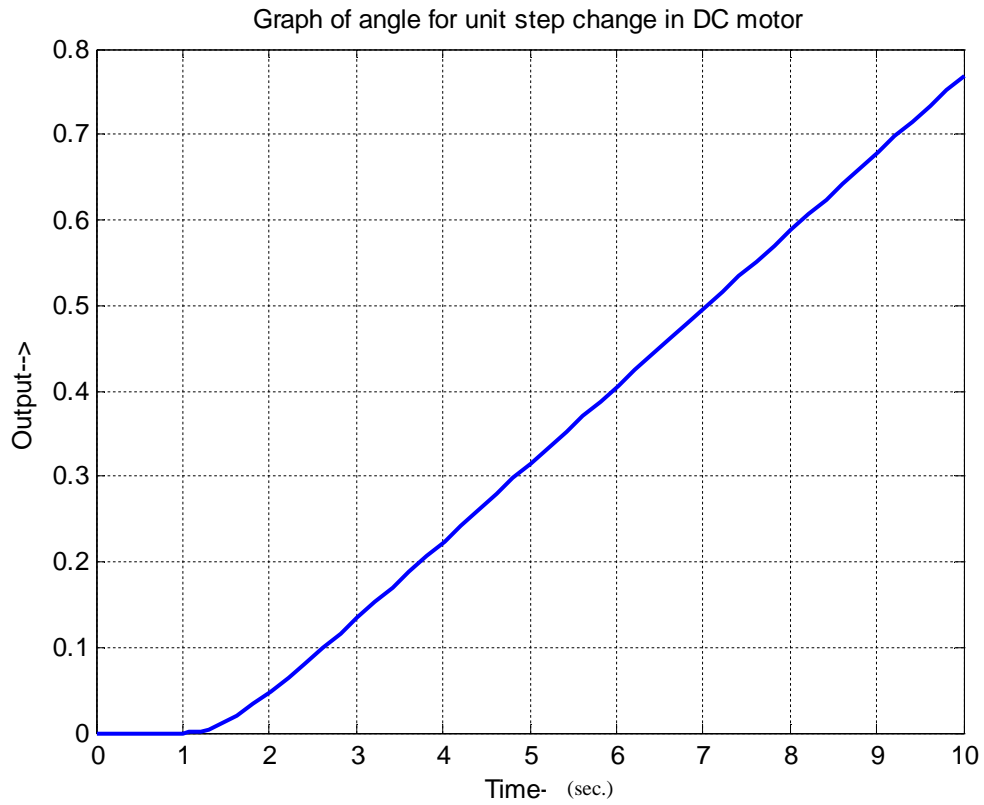


Figure 4.8: Graph of angle for step input for an armature controlled DC motor

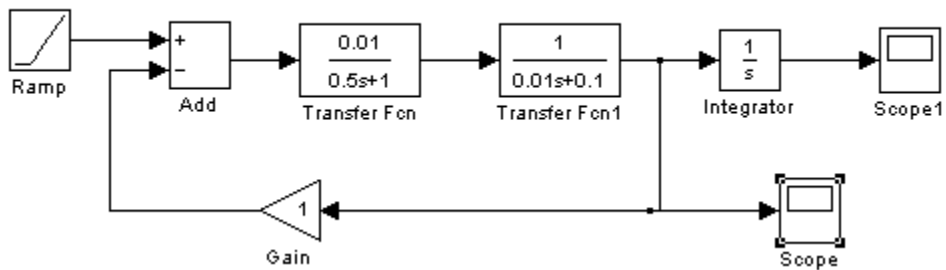


Figure 4.9: Simulink model of armature controlled DC motor for ramp input

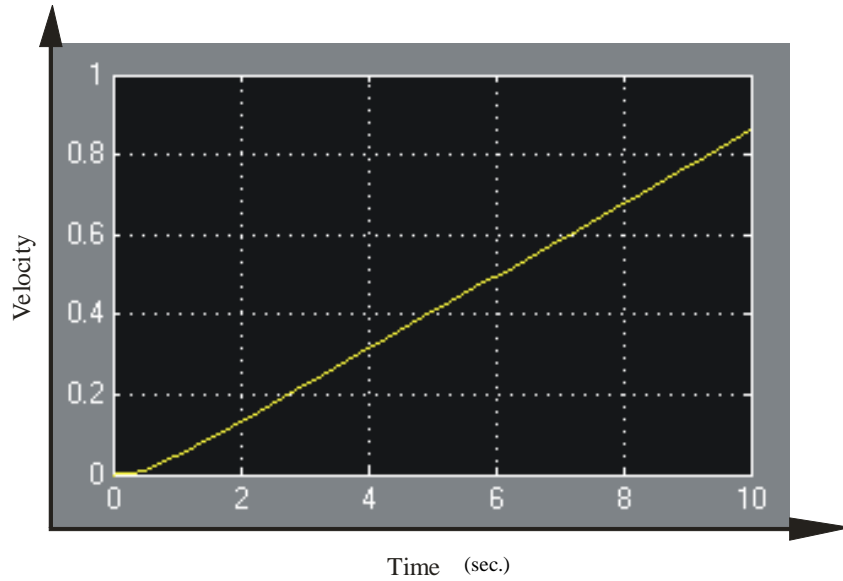


Figure 4.10: Graph of velocity for ramp input for an armature controlled DC motor

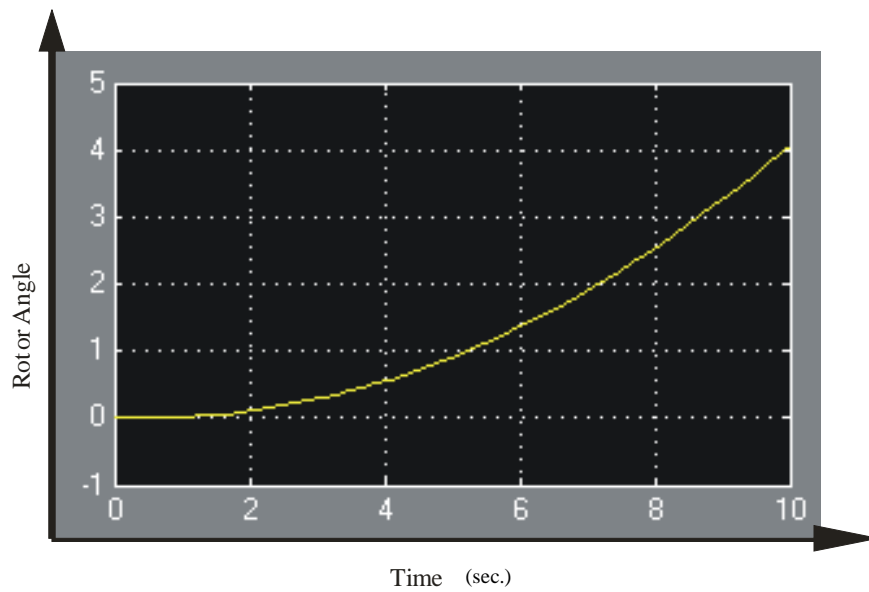


Figure 4.11: Graph of rotor angle for ramp input for an armature controlled DC motor

### 4.3 Separately excited shunt DC motor

The equivalent circuit diagram in separately excited DC motor has been shown in Figure 4.12 and equivalent circuit diagram for DC shunt motor is shown in Figure 4.13.

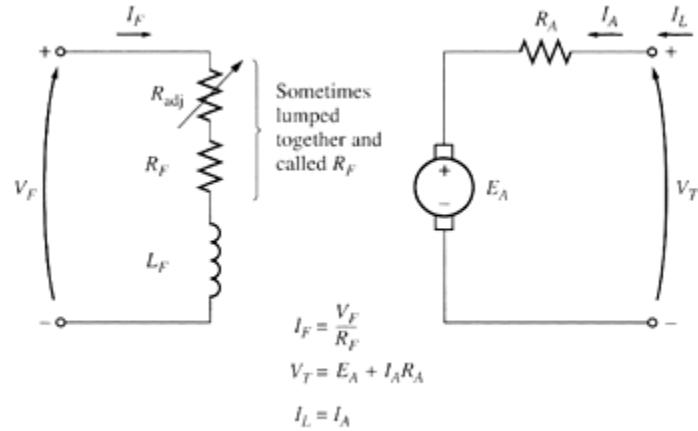


Figure 4.12: Equivalent circuit diagram for separately excited DC motor

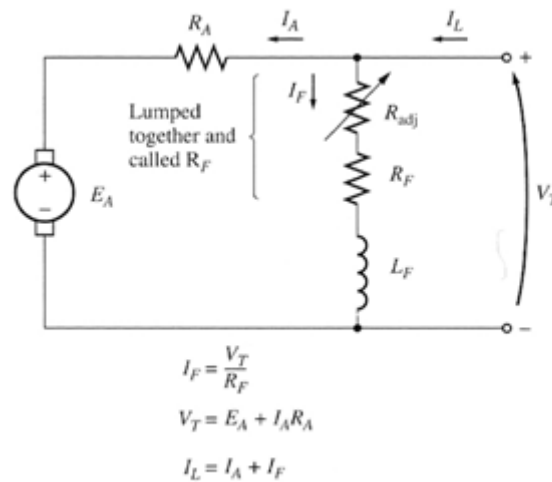


Figure 4.13: Equivalent circuit diagram for shunt DC motor

In the case of motor, the output quantities are shaft torque and speed. Terminal characteristic of a motor is a plot of its output torque versus speed. Suppose that the load on the shaft of a shunt motor is increased. Then the load torque  $\tau_{load}$  will exceed the induced torque  $\tau_{ind}$  in the machine, and the motor will start to slow down. When the motor slows down, its internal generated voltage drops ( $E_A = K\phi\omega$ ), so the armature current in the motor  $I_A = (V_T - E_A)/R_A$  increases. As the armature current rises, the induced torque in the motor increases ( $\tau_{ind} = K\phi I_a$ ) and finally the induced torque will equal the load torque at a lower mechanical speed of rotation. The output characteristic of

a shunt dc motor can be derived from the induced voltage and torque equations of the motor plus the KVL.

$$V_T = E_A + I_A R_A \quad (4.9)$$

The induced voltage  $E_A = K\phi\omega$  so

$$V_T = K\phi\omega + I_A R_A \quad (4.10)$$

Since  $\tau_{ind} = K\phi I_A$  current  $I_A$  can be expressed as:

$$I_A = \frac{\tau_{ind}}{K\phi} \quad (4.11)$$

Combining the  $V_T$  and  $I_A$  equations:

$$V_T = K\phi\omega + \frac{\tau_{ind}}{K\phi} R_A \quad (4.12)$$

Finally, solving for the motor's speed: 
$$\omega = \frac{V_T}{K\phi} - \frac{R_A}{(K\phi)^2} \tau_{ind} \quad (4.13)$$

Consider a 500-V, 100-hp, 2500 r/min, separately excited DC motor has following parameters:

Field resistance:  $R_f = 109\Omega$

Rated field voltage:  $V_{f0} = 300\text{ V}$

Armature resistance:  $R_a = 0.084\ \Omega$

Geometric constant:  $K_f = 0.694\text{ V/A (rad/sec)}$

Field voltage has been assumed constant at 300 V. Figure 4.14 shows the motor speed as a function of armature voltage with the motor operating under no-load and also under rated full-load torque as the armature voltage has been varied from 250 V to 500 V. Motor voltage is combined with field-current control in order to achieve the widest possible speed range. With such dual control, base speed can be defined as the normal-armature-voltage, full-field speed of the motor. Speeds above base speed are obtained by reducing the field current; speeds below base speed are obtained by armature-voltage control.

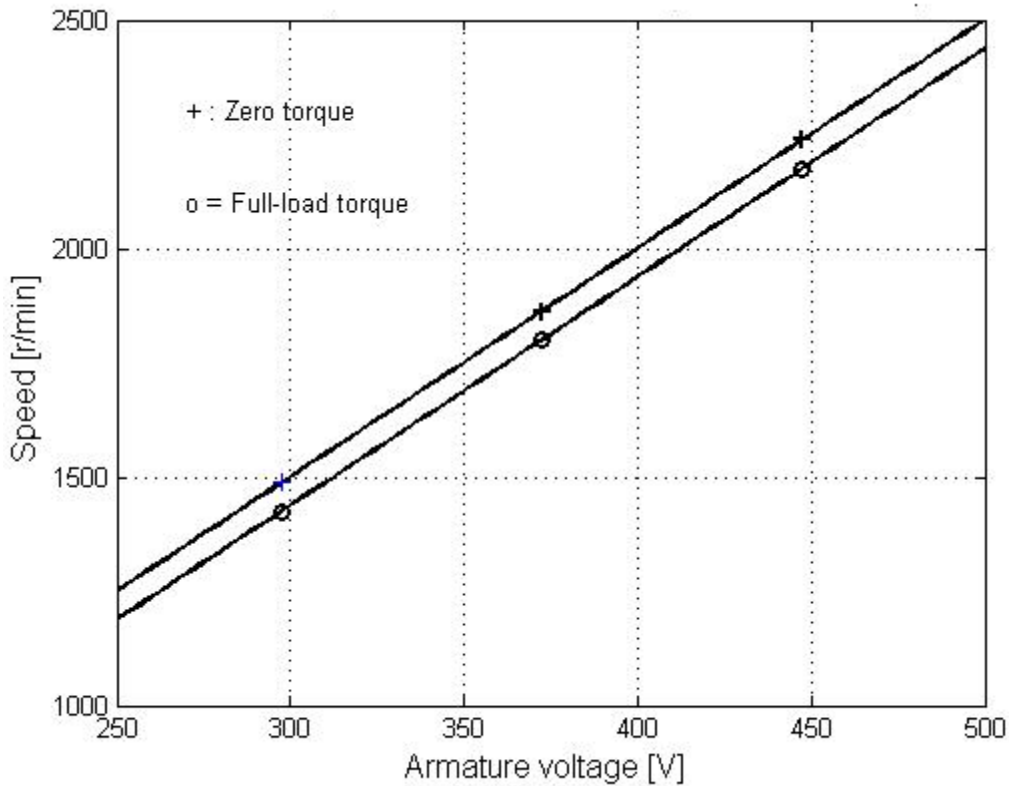


Figure 4.14: Graph of speed and armature voltage at different torques

In connection with field-current control, the range above base speed is that of a constant-power drive. The range below base speed is that of a constant-torque drive because, as in armature resistance control, the flux and the allowable armature current remain approximately constant. The overall output limitations are therefore as shown in Figure 4.15 (a) for approximate allowable torque and in Figure 4.15 (b) for approximate allowable power.

Constant-torque characteristic is needed in many applications in the machine tool industry, where many loads consist largely of overcoming the friction of moving parts and hence have essentially constant torque requirements. The speed regulation and the limitations on the speed range above base speed are those already presented with reference to field-current control; the maximum speed thus does not ordinarily exceed four times base speed and preferably not twice base speed. For conventional machines, the lower limit for reliable and stable operation is about one-tenth of base speed, corresponding to a total maximum-to-minimum range not exceeding 40:1. With armature

reaction ignored, the decrease in speed from no-load to full-load torque is caused entirely by the full-load armature-resistance voltage drop in the dc generator and motor. This full-load armature-resistance voltage drop is constant over the voltage-control range, since full-load torque and hence full-load current are usually regarded as constant in that range.

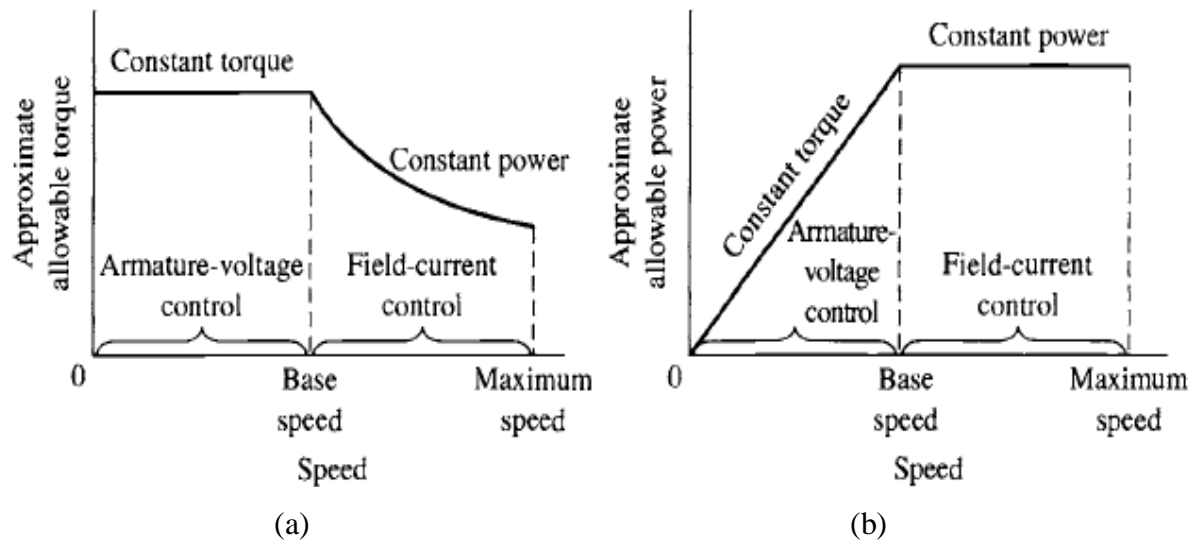


Figure 4.15: (a) Torque  
(b) Power limitations of combined armature-voltage and field-current methods of speed control.

A shunt DC motor is connected in similar way as a shunt generator. The field windings are connected in parallel (shunt) with the armature windings. Once the speed of a dc shunt motor is adjusted, the speed remains relatively constant even under changing load conditions. One reason for this is that the field flux remains constant. A constant voltage across the field makes the field independent of variations in the armature circuit. If the load on the motor is increased, the motor tends to slow down. When this happens, the counter emf generated in the armature decreases. This causes a corresponding decrease in the opposition to battery current flow through the armature. The armature current increases, which causes the motor to speed up. The conditions that established the original speed are reestablished and the original speed is maintained. Conversely, if the motor load is decreased, the motor tends to increase speed; counter emf increases, armature current decreases, and the speed decreases. In each case, all of this happens so rapidly that any actual change in speed is slight. There is instantaneous tendency to change rather than a large fluctuation in speed.

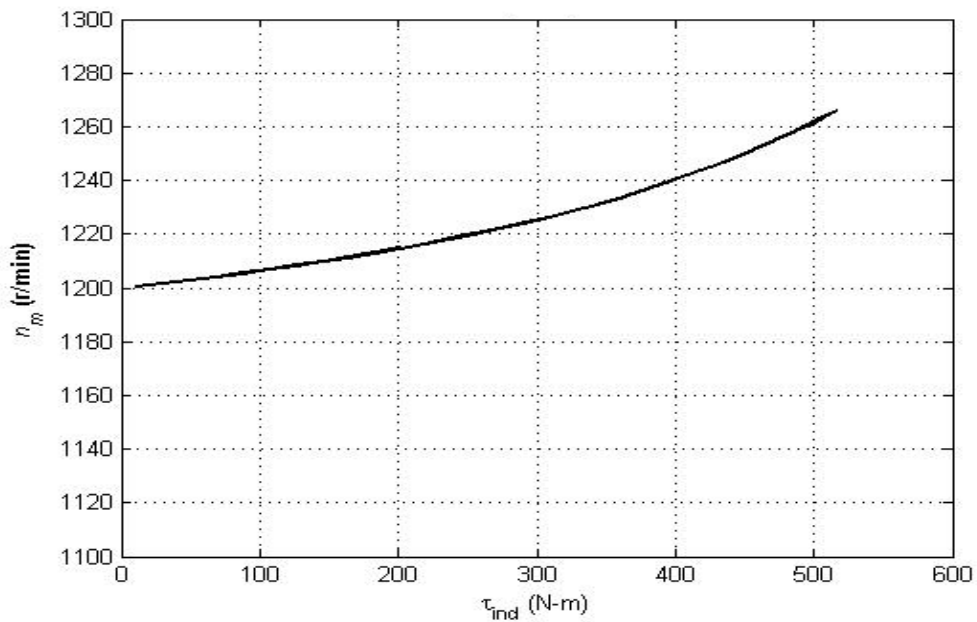


Figure 4.16: Speed v/s torque characteristics of a shunt DC motor

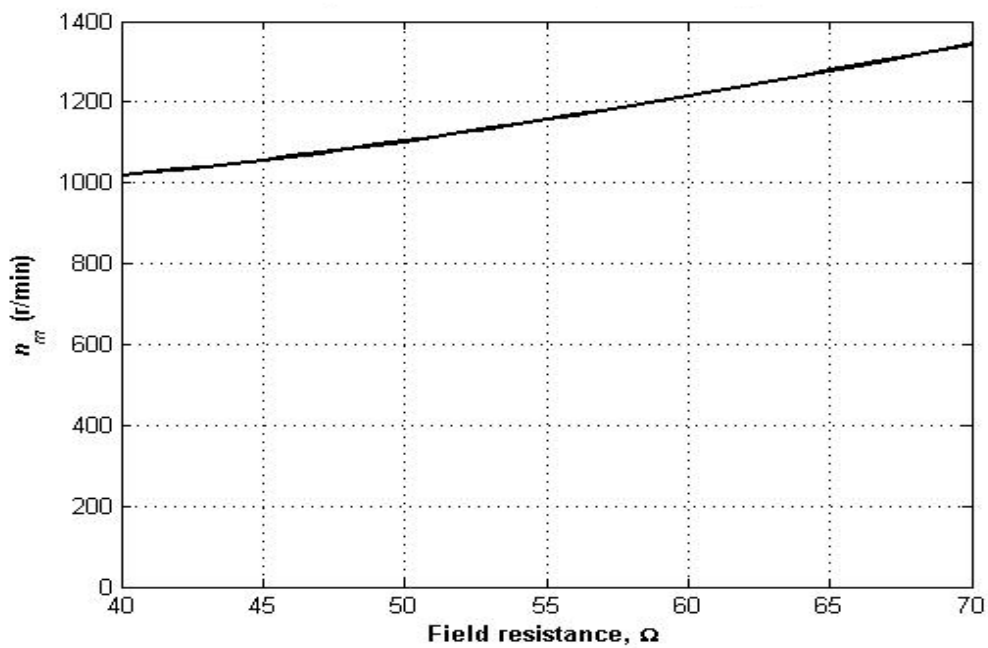


Figure 4.17: Speed v/s field resistance of a shunt DC motor

Figure 4.16 shows torque v/s speed characteristics and Figure 4.17 shows speed v/s field resistance behavior of DC shunt motor.

Series motor provides high starting torque and is able to move very large shaft loads when it is first energized. Since the series field winding is connected in series with the armature, it will carry the same amount of current that passes through the armature. The amount of current that passes through the winding determines the amount of torque the motor shaft can produce. Since the series field is made of large conductors, it can carry large amounts of current and produce large torques. Series motors used to power hoists or cranes may draw currents of thousands of amperes during operation. The series motor can safely handle large currents since the motor does not operate for an extended period. In most applications the motor will operate for only a few seconds while this large current is present. Figure 4.18 shows the plot for speed v/s torque for DC series motor

When voltage is applied, current begins to flow from negative power supply terminals through the series winding and armature winding. The armature is not rotating when voltage is first applied, and the only resistance in this circuit will be provided by the large conductors used in the armature and field windings. Since these conductors are so large, they will have a small amount of resistance. This causes the motor to draw a large amount of current from the power supply. When the large current begins to flow through the field and armature windings, it causes a strong magnetic field to be built. Since the current is so large, it will cause the coils to reach saturation, which will produce the strongest magnetic field possible.

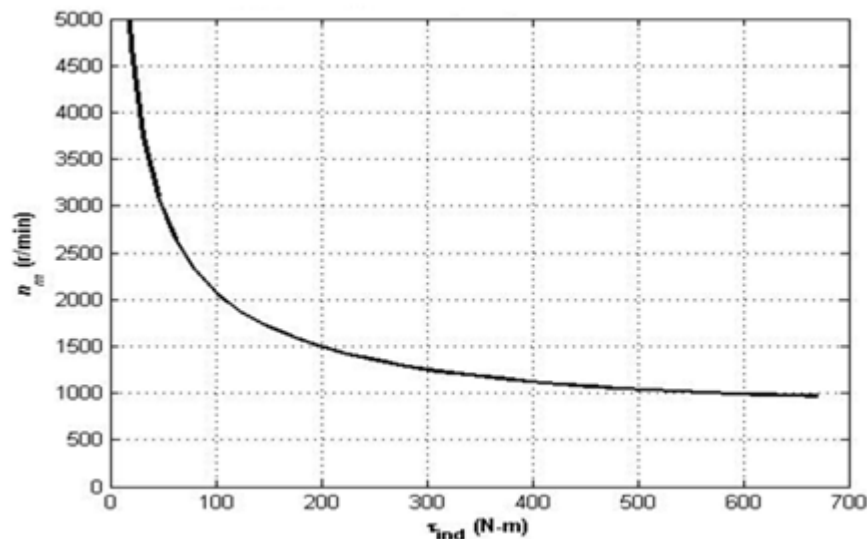


Figure 4.18: Speed v/s torque for a series DC motor

#### 4.4 Speed control of DC motor

The speed of a DC motor can be changed by controlling either field flux or the armature resistance or the terminal voltage applied to the armature circuit. The three most common speed control methods are field resistance control, armature voltage control and armature resistance control.

In the field resistance control method, a series resistance is inserted in the shunt-field circuit of the motor in order to change the flux by controlling the field current. It is theoretically expected that an increase in the field resistance will result in an increase in the no-load speed of the motor and in the slope of the torque-speed curve. The simulink model representation of DC motor speed control has been shown via two different methods as implemented in Figure 4.19 and Figure 4.20. The simulink implementation of the field resistance control method is shown in Figure 4.19. The DC motor block implements a separately excited DC motor. An access is provided to the field connections so that the motor model can be used as a shunt-connected.

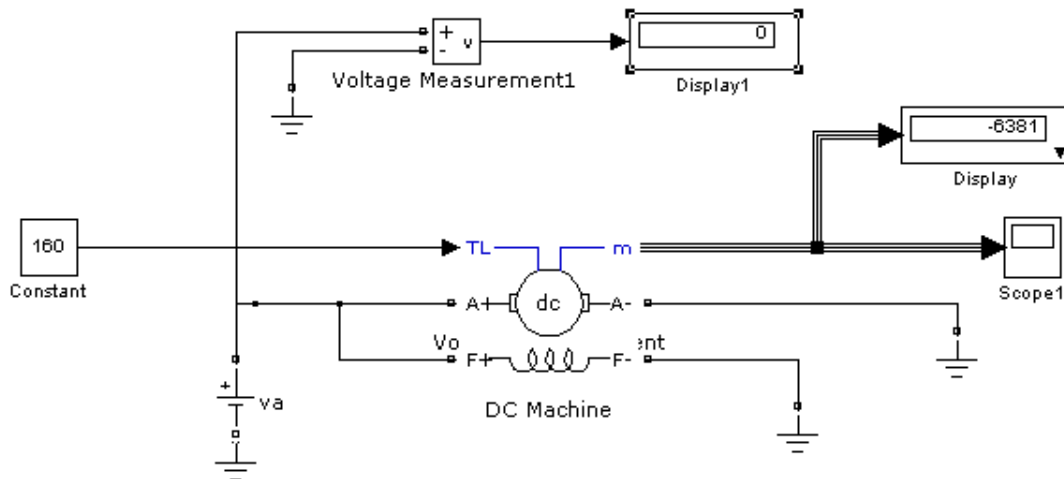


Figure 4.19: Simulink model of field resistance speed control method

The simulink implementation of armature voltage control method for speed control of DC is shown in Figure 4.20

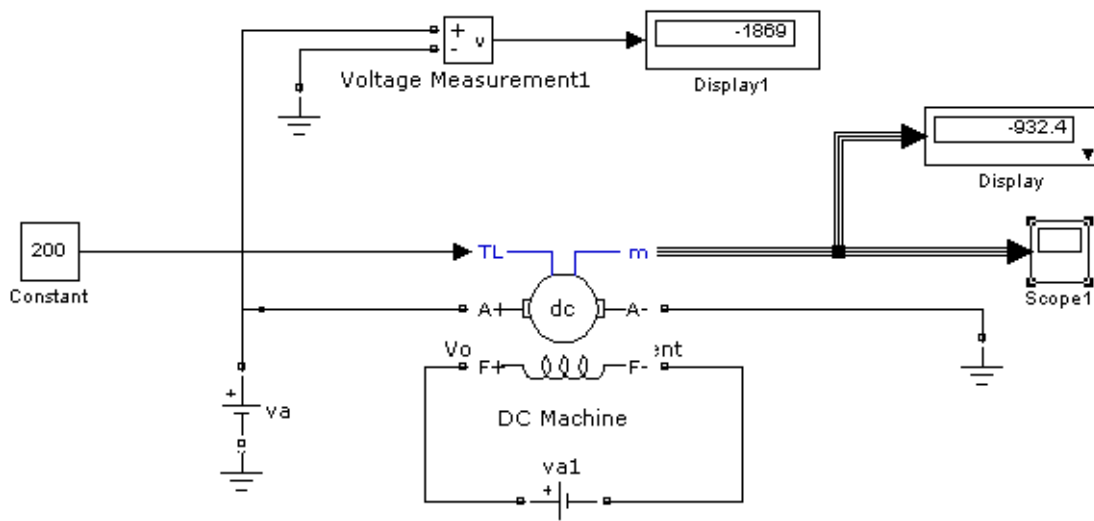


Figure 4.20: Simulink model of armature voltage speed control method

#### 4.5 Starting of a 5 HP 240V DC motor with a three-step resistance starter

DC Motor Rated Values

Induced EMF:  $E_o = 240 - 16.2 \times 0.6 = 230.3 \text{ V}$

$P_e = 230.3 \times 16.2 = 3731 \text{ W} = 5.0 \text{ HP}$

Field current:  $I_f = 240/240 = 1 \text{ A}$

$E_o = \omega \cdot L_a \cdot I_f \rightarrow \omega = (E_o / L_a \cdot I_f)$  speed  $\omega = 230.3 / 1.8 = 127.7 \text{ rad/s} = 1220 \text{ r/min}$

Nominal torque:  $T_e = P_e / \omega = 3731 / 127.7 = 29.2 \text{ N.m}$

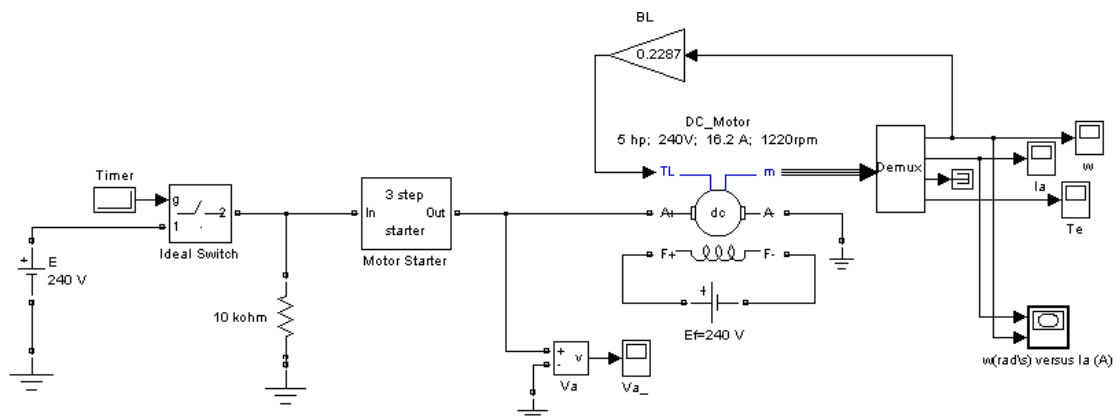


Figure 4.21: Simulink model of starting of a DC motor

Simulink model for starting of DC motor is shown in Figure 4.21. The speed vs armature current graph is shown in Figure 4.22. The resultant graphs for speed, armature current,

torque and armature voltage changing with time are shown in Figure 4.23, Figure 4.24, Figure 4.25 and Figure 4.26 respectively.

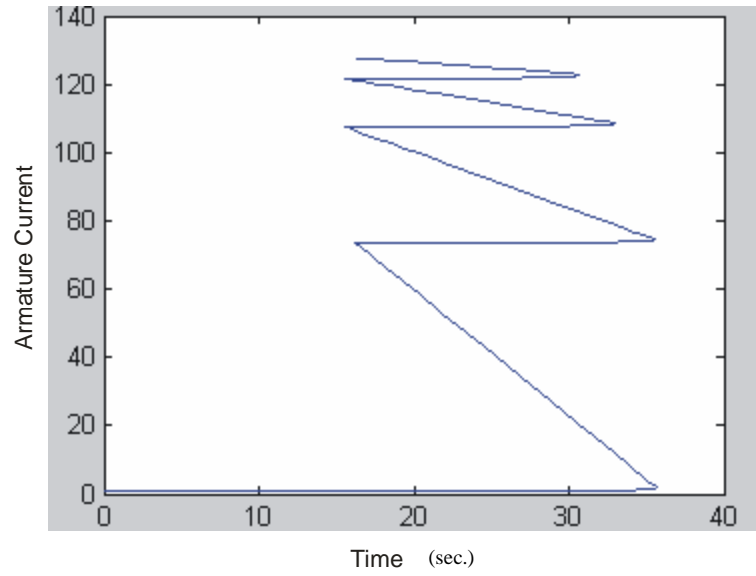


Figure 4.22: X-Y graph between speed (X-axis) vs armature current(Y-axis) of DC motor

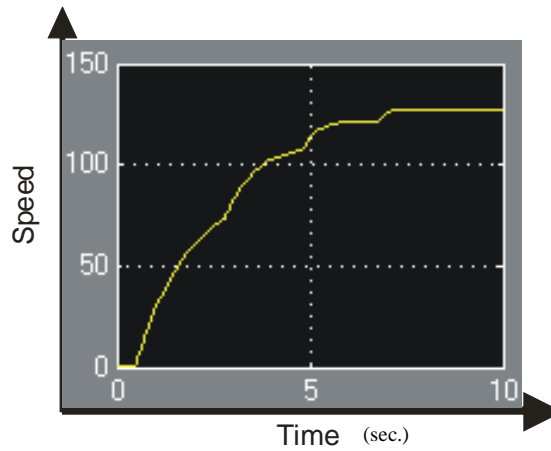


Figure 4.23: Speed vs time plot of DC motor

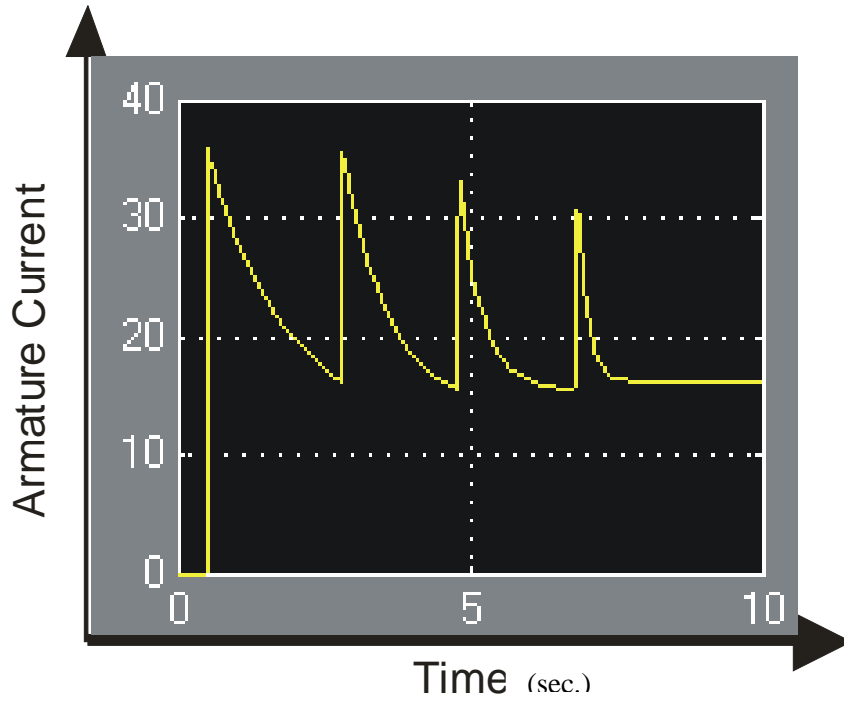


Figure 4.24: Armature current vs time plot of DC motor

Whenever there is change in speed the generator current also changes and tries to reach steady state as shown in Figure 4.24.

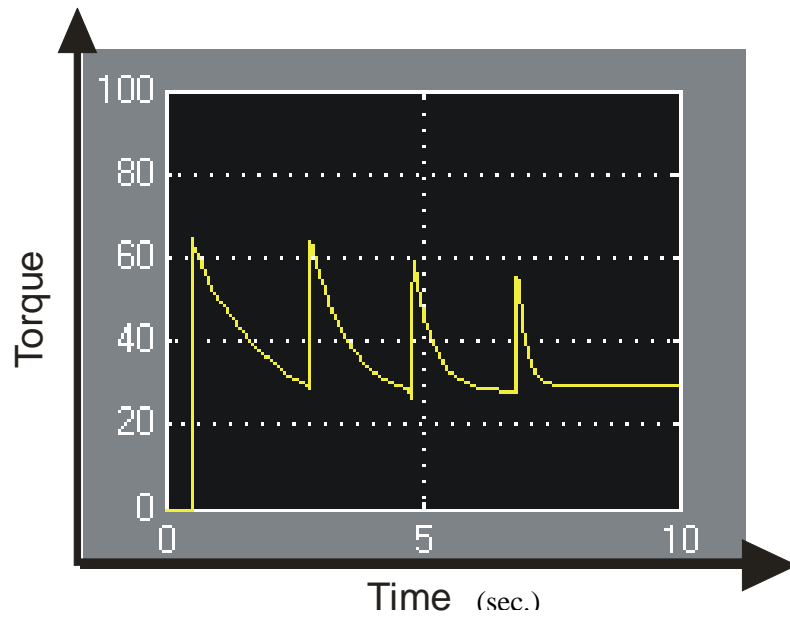


Figure 4.25: Torque vs time of DC motor

Figure 4.25 shows the torque response for the DC motor model developed using simulink.

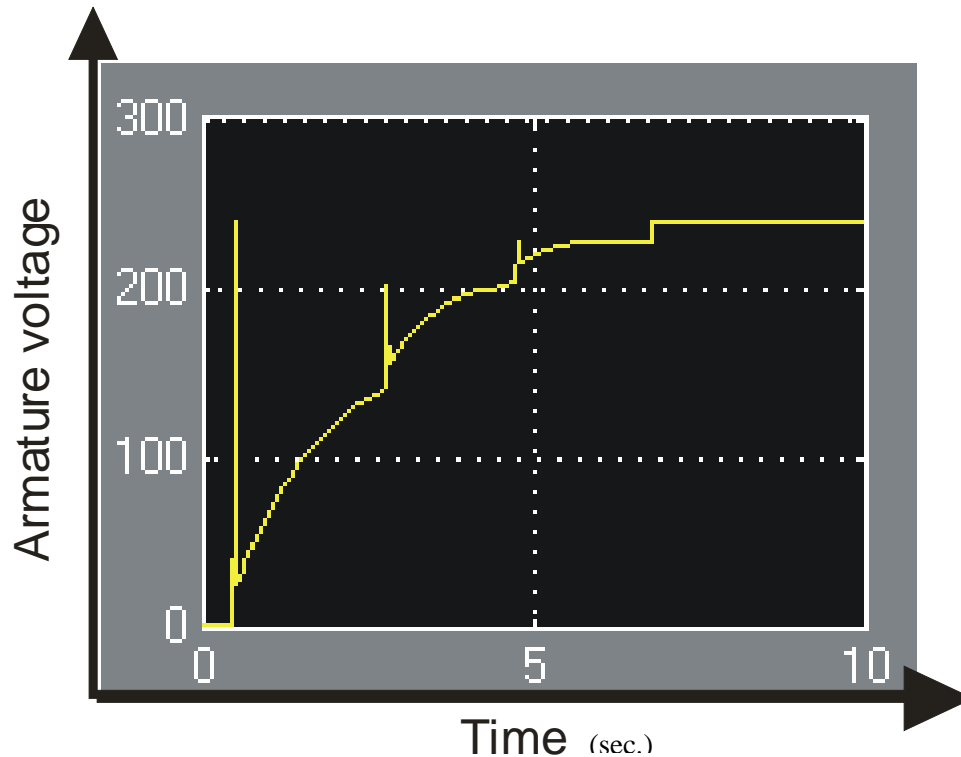


Figure 4.26: Armature voltage vs time of DC motor

Whenever armature voltage reference is changed as shown in Figure 4.26 the corresponding torque as shown in Figure 4.25 also changes and become stable when armature voltage becomes 220 volts.

This section describes field-current control because it involves control at a relatively low power level (the power into the field winding is typically a small fraction of the power into the armature of a dc machine), field-current control is frequently used to control the speed of a dc motor with separately excited or shunt field windings. The method is, of course, also applicable to compound motors. The shunt field current can be adjusted by means of a variable resistance in series with the shunt field. Alternatively, the field current can be supplied by power-electronic circuits which can be used to rapidly change the field current in response to a wide variety of control signals. Figure 4.27

shows in schematic form a switching scheme for pulse-width modulation of the field voltage. It consists of a rectifier which rectifies the ac input voltage, a DC-link capacitor which filters the rectified voltage, producing a dc voltage  $V_{dc}$  and a pulse-width modulator. In this system, because only a unidirectional field current is required, the pulse width modulator consists of a single switch and a free-wheeling diode rather than the more complex four-switch arrangement of Figure 4.27. Assuming the switch and diode to be ideal, the average voltage across the field winding will be equal to  $V_f = DV_c$ . Where D is the duty cycle

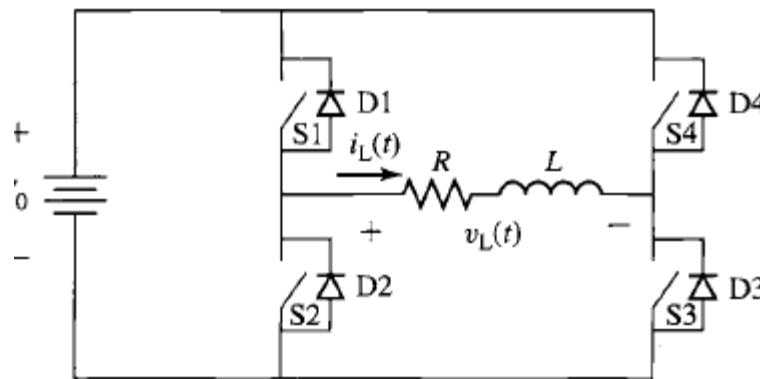


Figure 4.27: Switching scheme for PWM

#### 4.6 Speed control of a separately excited DC motor

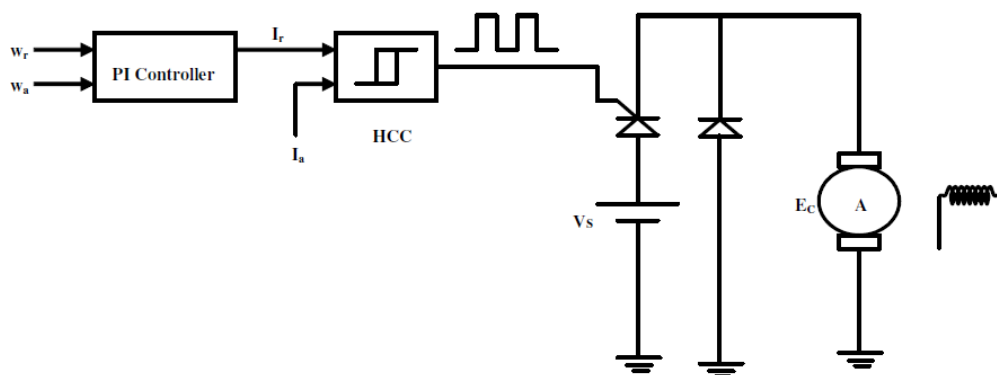


Figure 4.28: Speed control scheme of DC motor

Figure 4.28 shows the speed control circuit of an armature controlled separately excited dc motor using chopper circuit. Separately excited dc motor fed by a DC source through a chopper circuit. A single GTO thyristor with its control circuit and a free-wheeling diode form the chopper circuit. The motor drives a mechanical load characterized by inertia  $J$ , friction coefficient  $B$ , and load torque  $T_L$ . The control circuit consists of a speed control loop and a current control loop. A proportional-integral (PI) controlled speed control loop senses the actual speed of the motor and compares it with the reference speed to determine the reference armature current required by the motor. One may note that any variation in the actual speed is a measure of the armature current required by the motor. The current control loop consists of a hysteresis current controller (HCC). HCC is used to generate switching patterns required for the chopper circuit by comparing the actual current being drawn by the motor with the reference current. A positive pulse is generated if the actual current is less than reference armature current, whereas a negative pulse is produced if the actual current exceeds reference current. Hysteresis current control is a method of controlling a power electronic converter so that an output current is generated which follows a reference current waveform. A hysteresis current controller is implemented with a closed loop control. The difference between the desired current, and the current being injected is used to control the switching of the chopper circuit. When the error reaches an upper limit namely upper hysteresis limit, GTO is switched to force the current down. On the other hand when the error reaches the lower hysteresis limit, a positive pulse is produced to increase the current. The minimum and maximum values of the error signal are  $e_{\min}$  and  $e_{\max}$ . The range of the error signal,  $e_{\max}-e_{\min}$ , directly controls the amount of ripple in the output current and is called the hysteresis band. Thus the armature current is forced to stay within the hysteresis band determined by the upper and lower hysteresis limits.

Considering above strategy of speed control schemes of DC motor in developing a simulink model helps in taking better control action. Such simulink model for speed control of DC motor using speed controller and current controller has been shown in Figure 4.29. It results in the generation of control signal to effectively control the speed of DC motor.

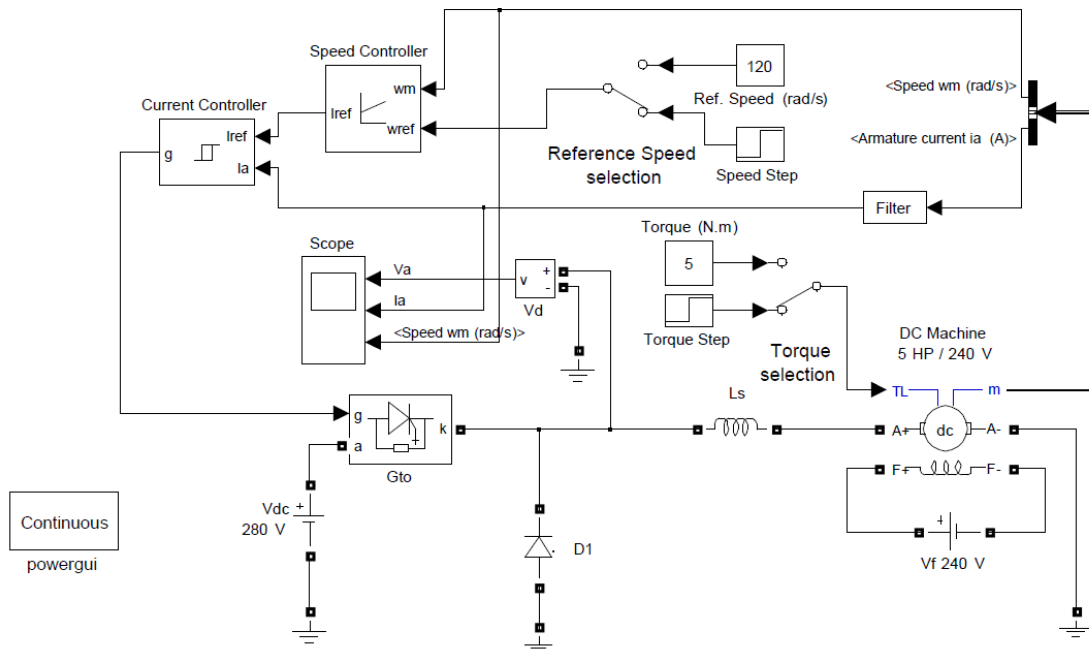


Figure 4.29: Simulink model of speed control of a DC motor using speed controller and current controller

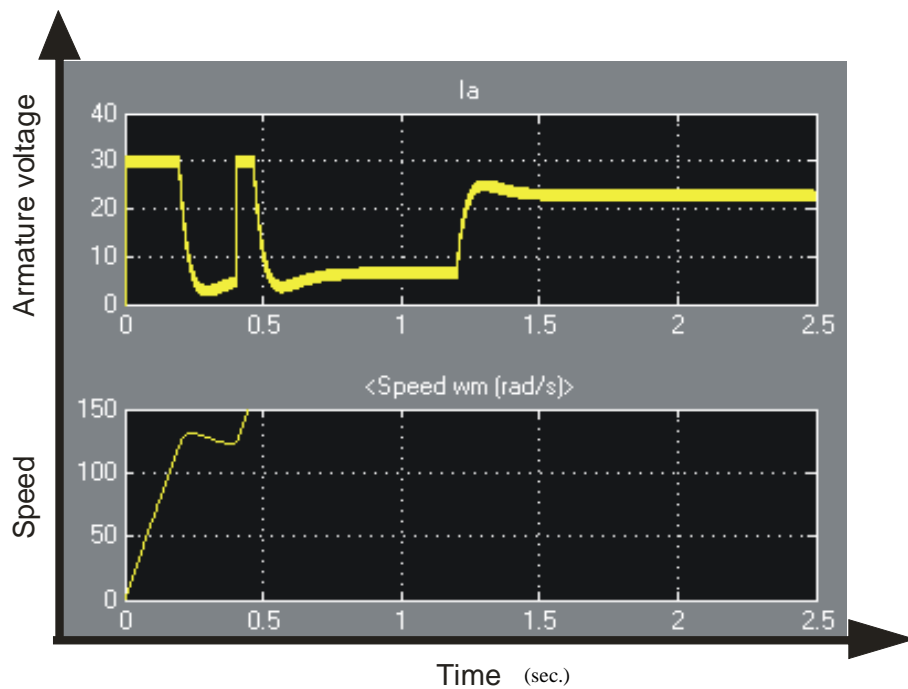


Figure 4.30: Graphs for armature current and speed of DC motor using speed controller and current controller

The armature current response is shown in graph of Figure 4.30 for which the speed response plot is given below at armature voltage supply of 220 volts. The armature current shown in Figure 4.30 stabilizes after  $t=1.25$  whereas in Figure 4.31 it stabilizes at  $t=0.5$ .

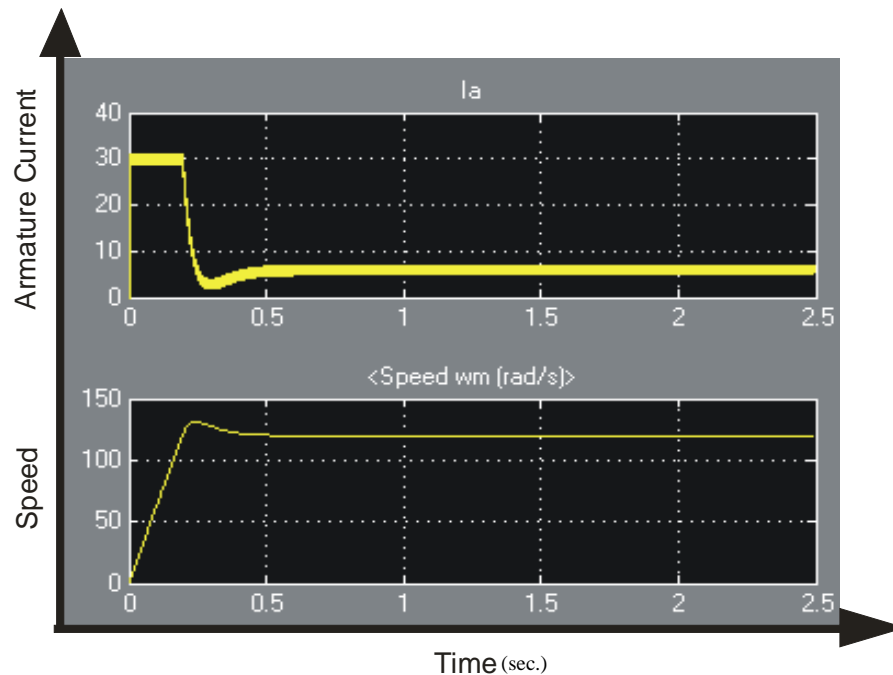


Figure 4.31: Graphs for armature current and speed of DC motor using speed controller and current controller

The Figure 4.30 and Figure 4.31 shows the graphs for armature voltage, armature current and speed of the motor as the result of the speed control and current controller strategy followed in Figure 4.29.

#### 4.7 Type-1 membership function for fuzzy control

Figure 4.32 shows the membership function for inputs of type-1 fuzzy and Figure 4.33 shows output of type-1 fuzzy system. Error  $e(t)$  and change in error  $de(t)$  is taken as inputs where as fuzzy controller output  $u(t)$  is taken as output. Triangular membership function is taken for the fuzzy control purpose. The fuzzy rule based has been developed for the fuzzy inference engine as per the conditions formulated in table 4.1 for error  $e(t)$

and change in error  $\Delta e(t)$  and controller output  $u(t)$ . The conditions are developed as per the fuzzy membership functions. Further if –then rule base are shown in table 4.2 concludes all the conditions for the development of the rules

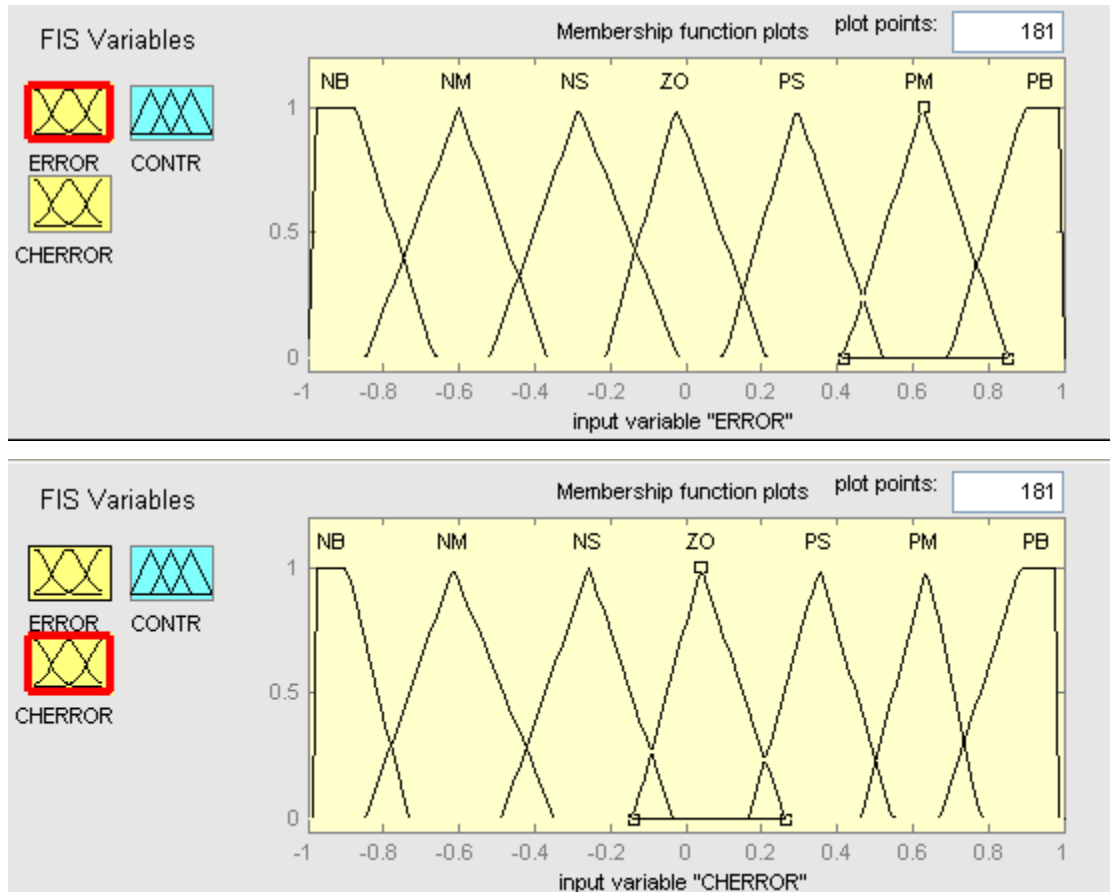


Figure 4.32: Fuzzy membership function for type I fuzzy inputs,  $e(t)$  and  $de(t)$

The triangular membership are represented by negative big NB, negative medium NM, negative small NS ,zero ZO, positive small PS, positive medium PM, positive big PB in the table 4.1 and if – then rules are developed accordingly. . Figure 4.34 finally shows the surface view of the decisions which can be taken by the fuzzy inference system.

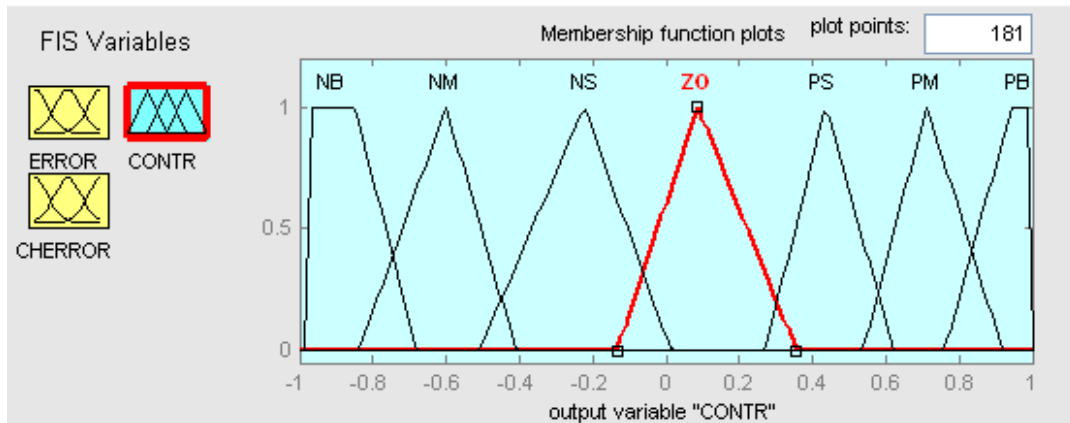


Figure 4.33: Fuzzy membership function for type I fuzzy output

The above Figure 4.33 shows the fuzzy membership function for type-1 fuzzy output.

Table 4.1: Fuzzy rule base and fuzzy inference system

Error $e(t)$		Change in error $\Delta e(t)$		Controller output $u(t)$	
NB	Negative Big	NB	Negative Big	NB	Negative Big
NM	Negative Medium	NM	Negative Medium	NM	Negative Medium
NS	Negative Small	NS	Negative Small	NS	Negative Small
ZO	Zero	ZO	Zero	ZO	Zero
PS	Positive Small	PS	Positive Small	PS	Positive Small
PM	Positive Medium	PM	Positive Medium	PM	Positive Medium
PB	Positive Big	PB	Positive Big	PB	Positive Big

Table 4.2: If-then rule base

$u(t)$		$e(t)$						
		NB	NM	NS	ZO	PS	PM	PB
$\Delta e(t)$	NB	NB	NB	NB	NB	NM	NS	ZO
	NM	NB	NB	NB	NM	NS	ZO	PS
	NS	NB	NB	NM	NS	ZO	PS	PM
	ZO	NB	NM	NS	ZO	PS	PM	PB
	PS	NM	NS	ZO	PS	PM	PB	PB
	PM	NS	ZO	PS	PM	PB	PB	PB
	PB	ZO	PS	PM	PB	PB	PB	PB

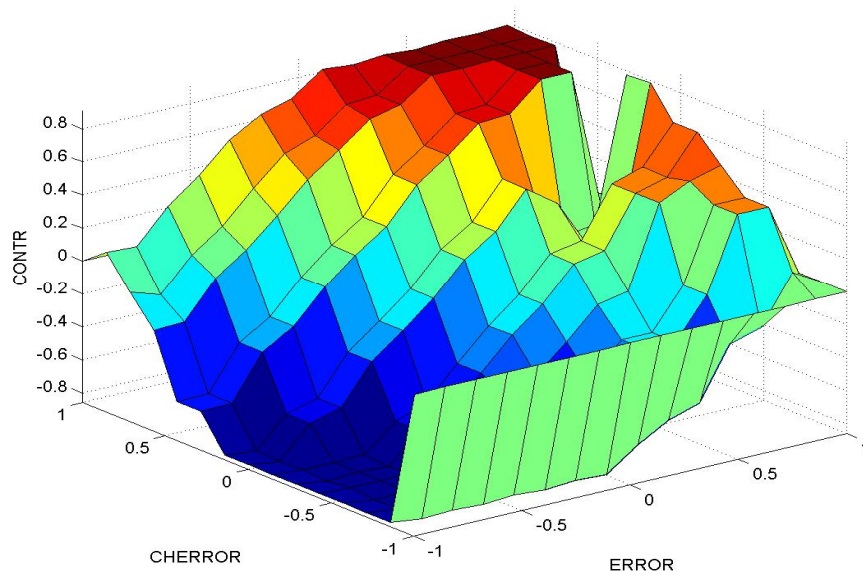


Figure 4.34: Surface view of fuzzy inference system

#### 4.8 Type-2 membership function for fuzzy control

The type-2 input membership functions are shown in the following Figure 4.35 for error  $e(t)$  and change in error  $de(t)$ . The triangular type-2 fuzzy membership incorporates more uncertainties around the boundaries of the membership function considered.

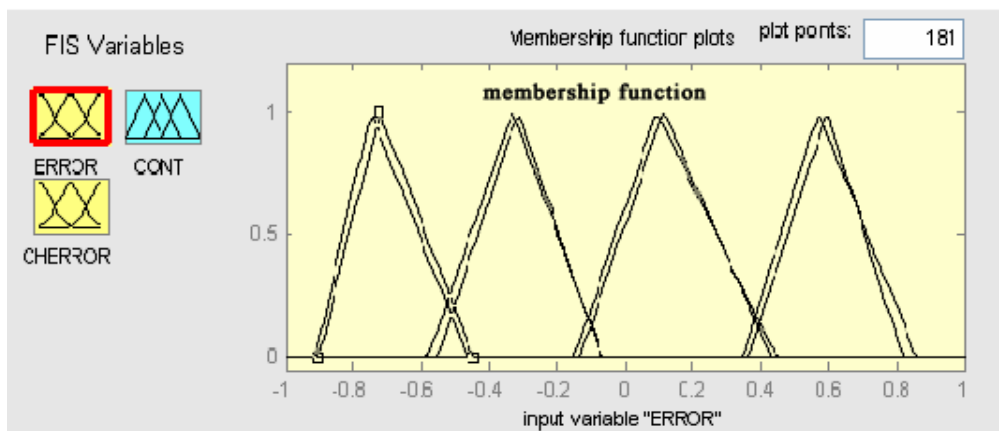


Figure 4.35: Fuzzy membership function for type-2 fuzzy inputs  $e(t)$  and  $de(t)$

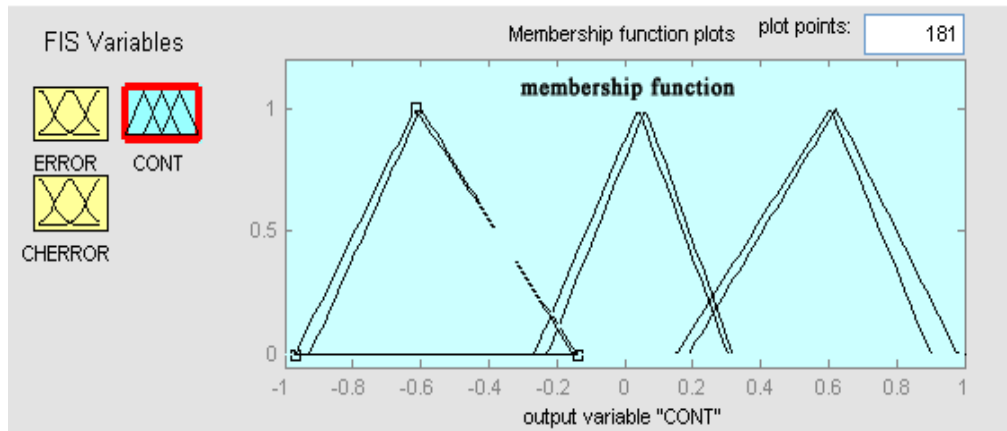


Figure 4.36: Fuzzy membership function for type II fuzzy output  $u(t)$

The Figure 4.36 shows the type-2 fuzzy output after considering more uncertainties for control purpose. Type-2 has incorporated all their random uncertainties which has probability of occurrence near the selected input triangular membership functions for error  $e(t)$  and change in error  $de(t)$ .

Another control scheme using fuzzy neuro controller has been successfully implemented in the following section. The artificial neural network (ANN) architecture is developed here.

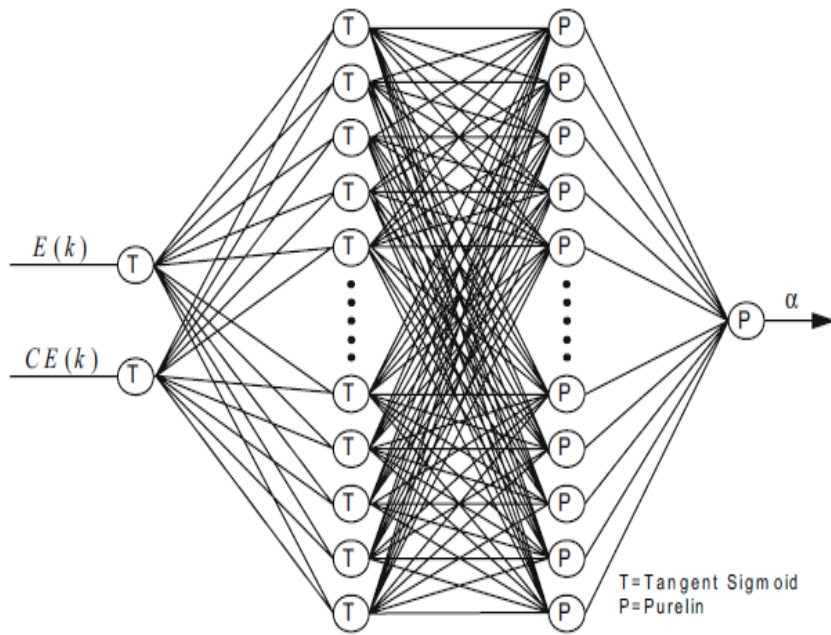


Figure 4.37: Artificial neural network used for training neuro fuzzy controller

Figure 4.37 shows the ANN architecture used in neuro-fuzzy control technique as applied on the DC motor for better control strategy. The neuro fuzzy speed control block diagram for DC motor has been shown in Figure 4.38.

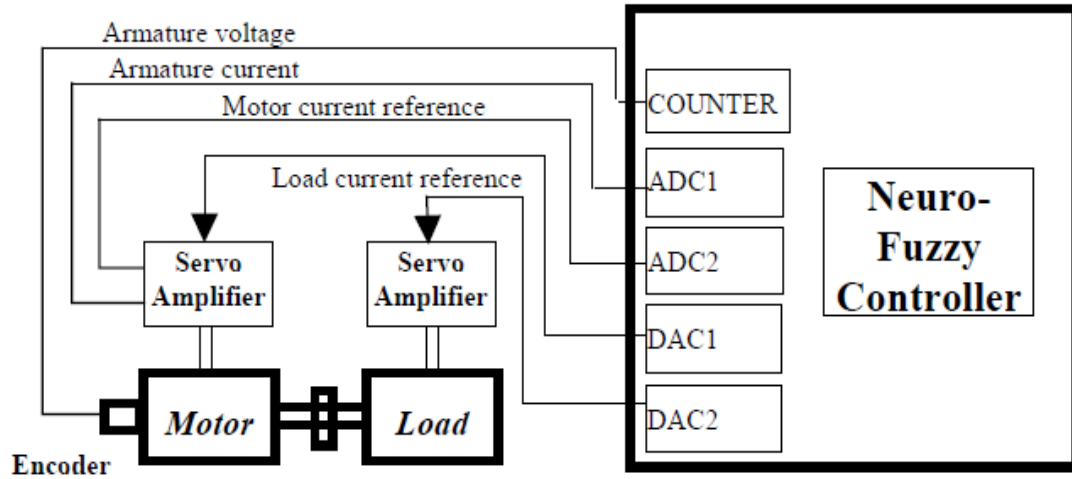


Figure 4.38: Neuro-fuzzy speed control block diagram for DC motor

To implement the neuro fuzzy speed controller the simulink model has been developed for speed control of DC motor

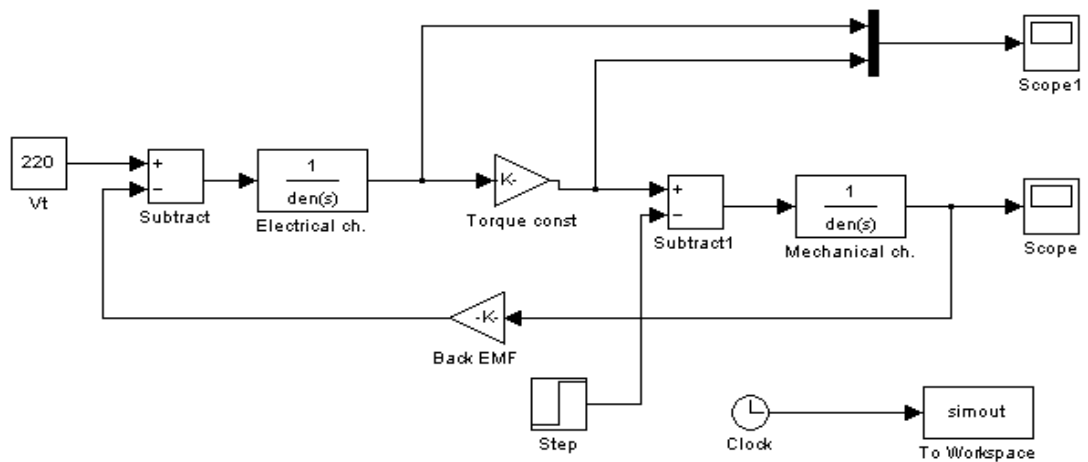


Figure 4.39: Simulink model of DC motor speed control

Figure 4.39 shows the Simulink representation of DC motor model. Figure 4.40 shows the output graph for armature current and torque and Figure 4.41 shows the graph for variation in angular speed with respect to time.

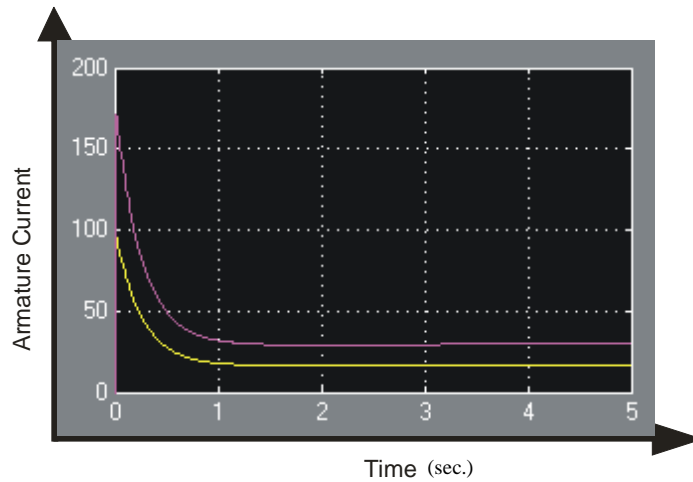


Figure 4.40: Graph for armature current and torque of DC motor

The specifications of DC motor are as follows:

$V_t = 220$ ; Terminal voltage in V

$R_a = 2.1975$ ; Armature resistance in ohm

$L_a = 0.0063$ ; Inductance in H

$K_m = 1.78$ ; Torque constant in Nm/A

$J = 0.0236$ ; Rotor inertia in Kg m<sup>2</sup>

$B = 0.015$ ; Damping factor

$W = 3$ ; Load torque Nm

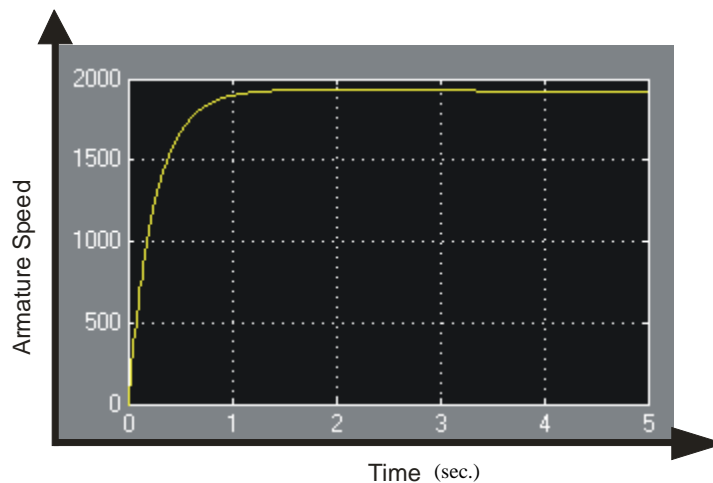


Figure 4.41: Graph for angular speed  $\omega$  (rad/sec) vs time of DC motor

### 4.9 Fuzzy controller for DC motor (Type-1)

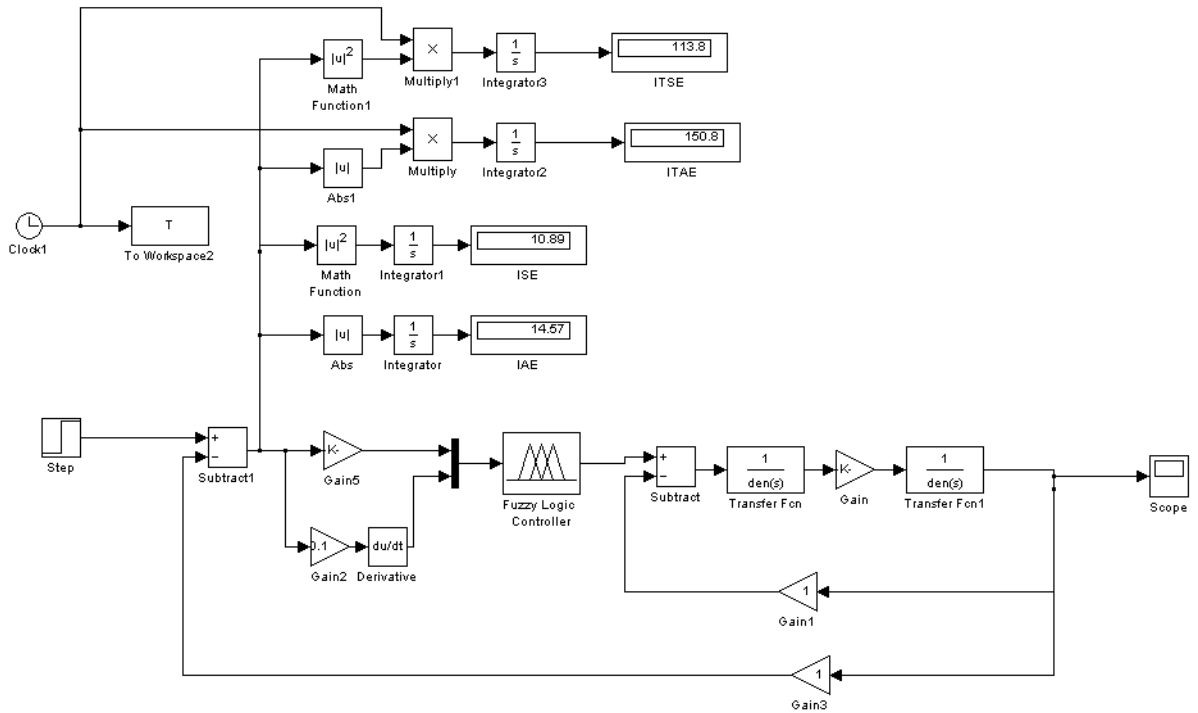


Figure 4.42: Simulink model of fuzzy type-1 and type-2 based speed control of DC motor

The simulink model of fuzzy type-1 and type-2 controlled DC motor is shown in Figure 4.42. The schematic remains same for type -1 and type-2 of the FLC i.e fuzzy logic controller only the structure changes. The speed response of this system is shown in Figure 4.43 for type-1 and Figure 4.42 shows the speed response for type-2 based system. The bode plot is shown in Figure 4.45

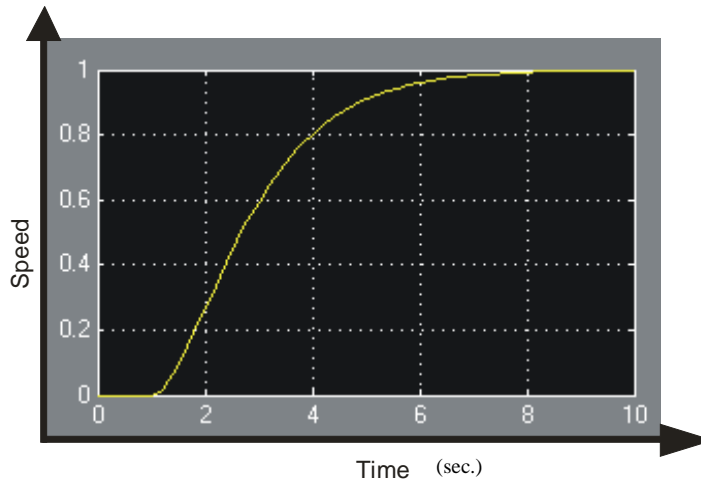


Figure 4.43: Speed response of DC motor using type-1 fuzzy controller

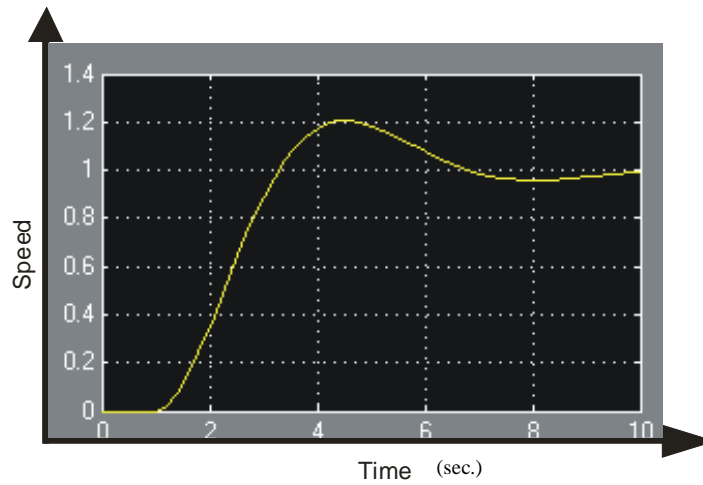


Figure 4.44: Speed response of DC motor using type-2 fuzzy controller

Figure 4.43 and Figure 4.44 shows speed response of DC motor using type-1 and type-2 fuzzy controller and shows that type-1 is faster settling system than type-2 contemporary schemes. Also type -1 shows no overshoot and zero steady state error.

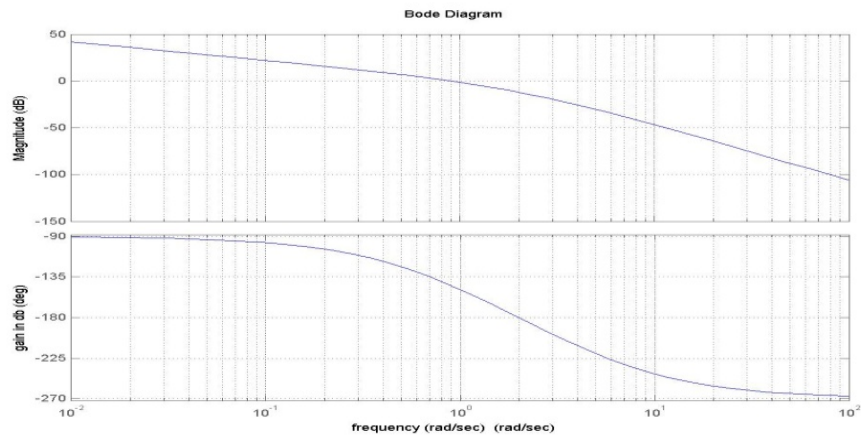


Figure 4.45: Bode magnitude and phase response of DC motor

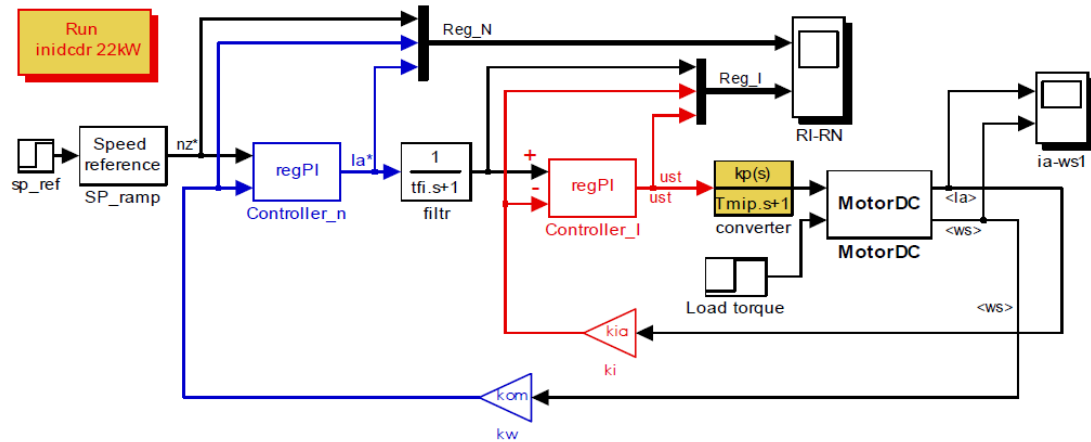


Figure 4.46: Simulink model of DC motor with PI controllers in current and velocity loop

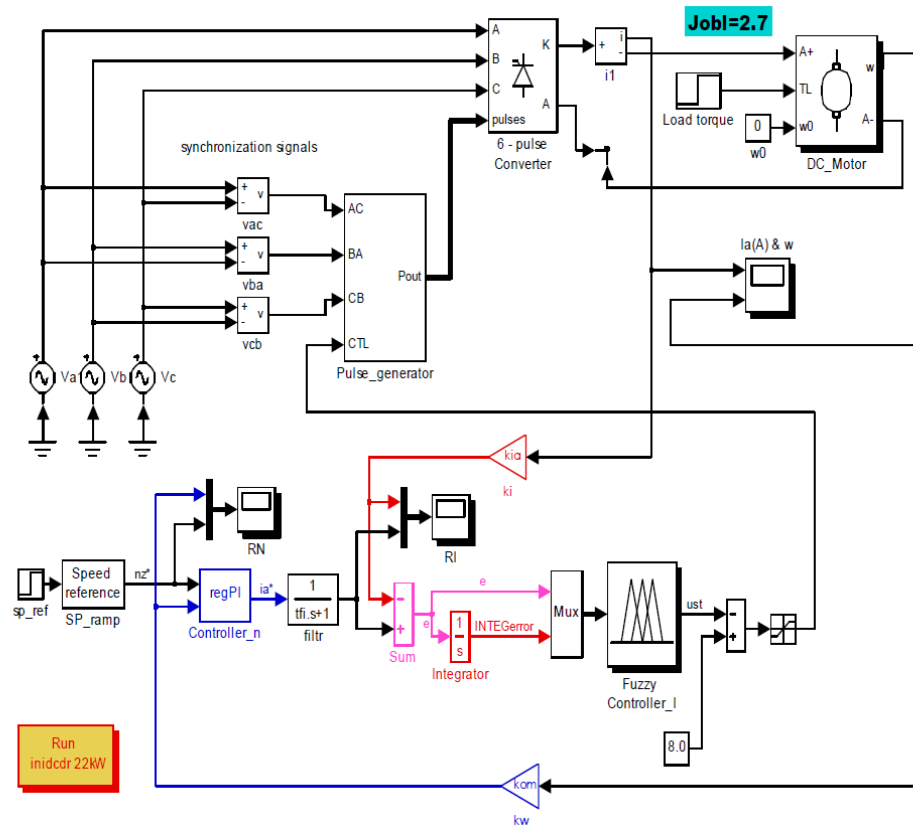


Figure 4.47: Simulink model of DC motor with fuzzy controllers in current and velocity loop

The simulink model in Figure 4.46 and Figure 4.47 shows the DC motor control with PI controllers in current and velocity loops.

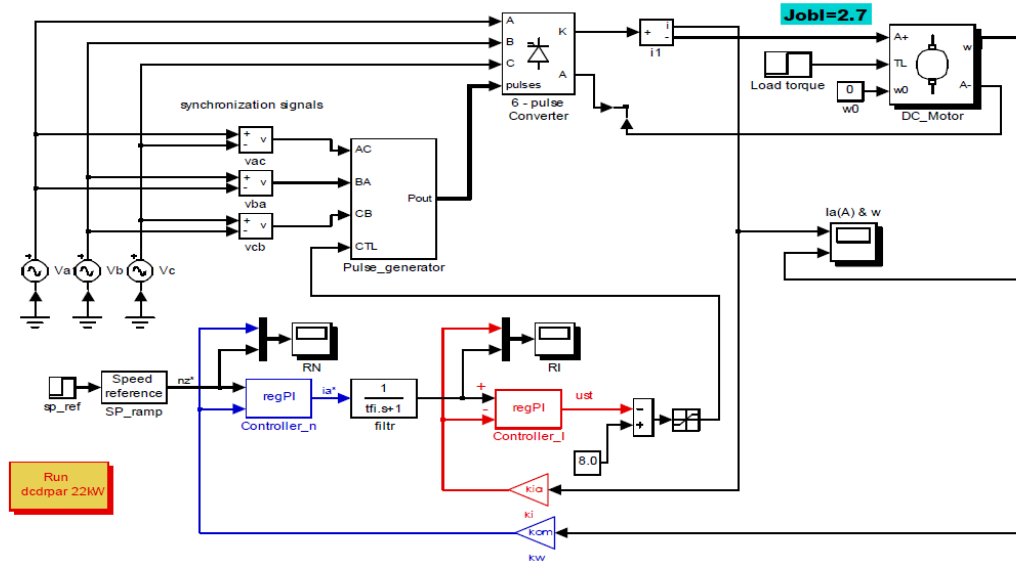


Figure 4.48: Simulink model of DC motor with PI controller in current loop

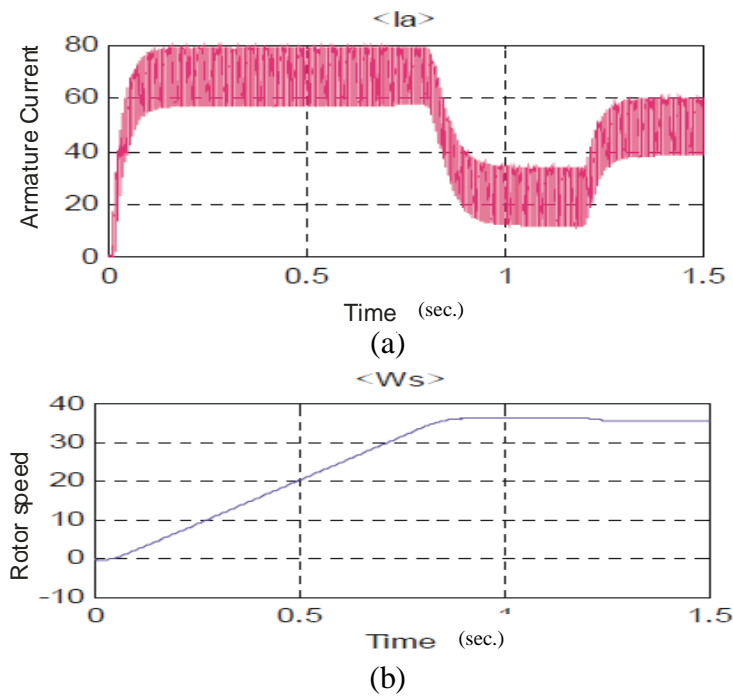


Figure 4.49: (a) Armature current plot  
(b) Rotor speed plot

The simulink models in Figure 4.48 has its resultant graphs for armature current and rotor speed as shown in Figure 4.49.

#### 4.10 Neuro-fuzzy control of DC motor

The DC motor control strategy has been formulated here considering the contemporary neuro-fuzzy technique. The basic model of ANN has been shown in Figure 4.50.

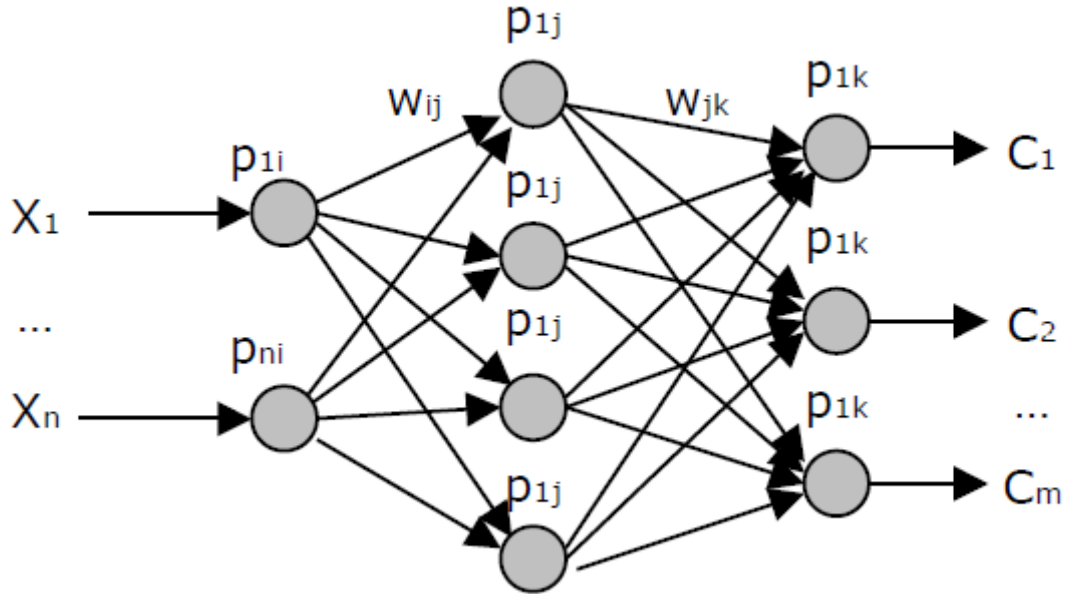


Figure 4.50: Architecture of artificial neural network

The following simulink model in Figure 4.51 helps in implementing the control strategy through ANN in DC motor. The training data have been generated on the basis of ideal input output characteristic of DC motor.

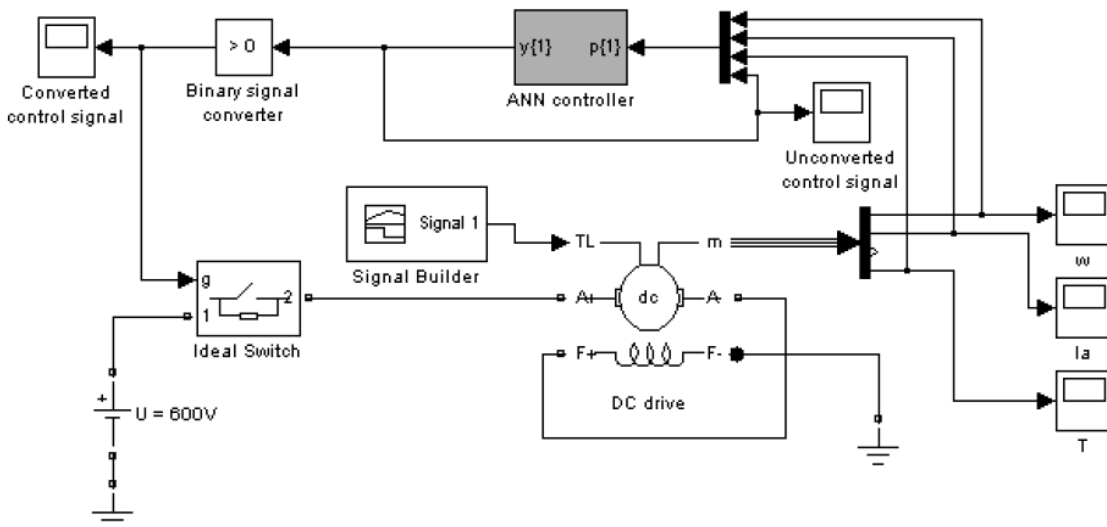


Figure 4.51: Simulink model of DC motor speed control using ANN controller

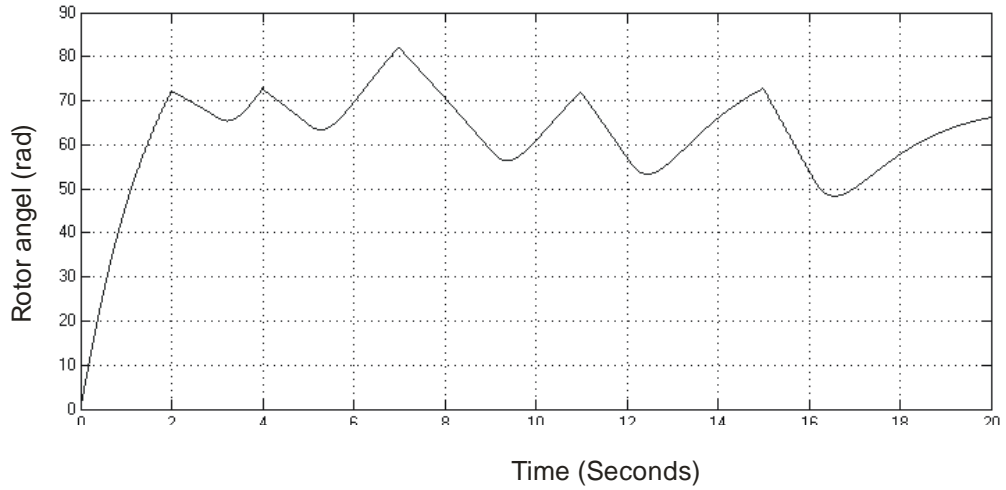


Figure 4.52: Angular speed controlled by neuro-fuzzy control

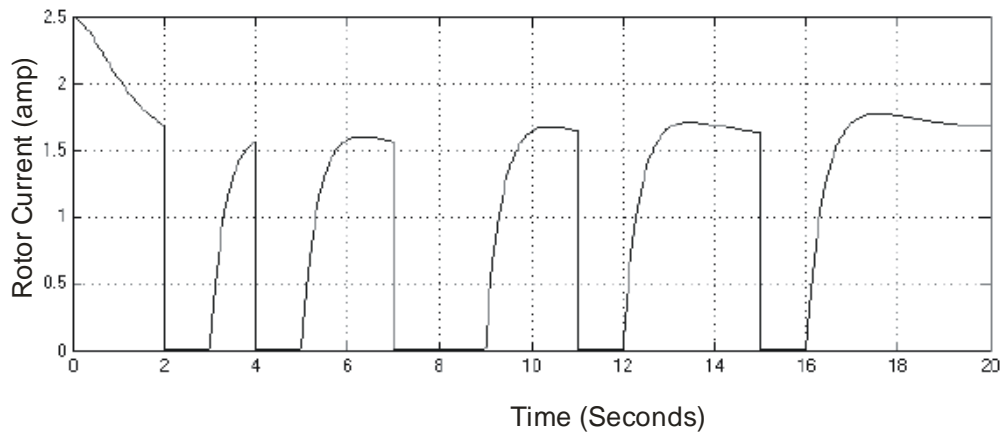


Figure 4.53: Current of DC motor controlled by neuro-fuzzy control

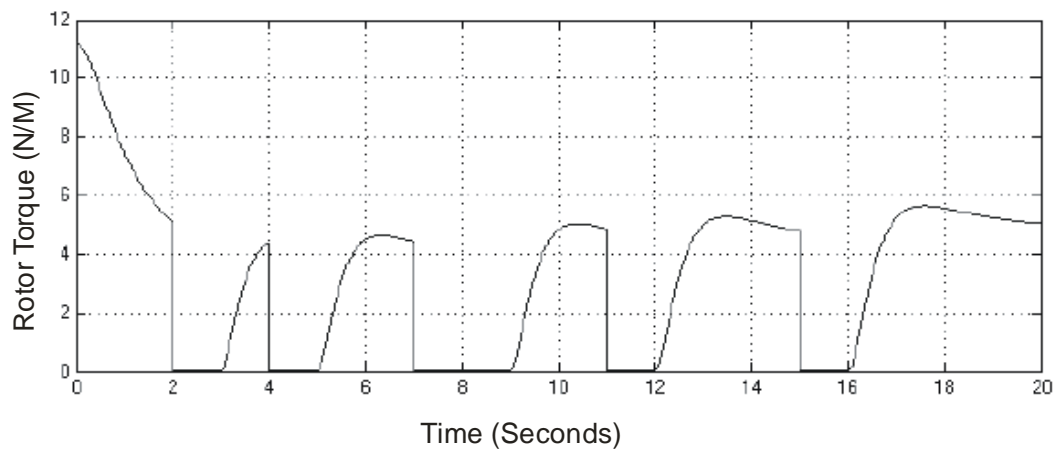


Figure 4.54: Torque of DC motor controlled by neuro-fuzzy control

The above waveforms for angular speed variations, current variations and torque variations are shown after the implementation of neuro-fuzzy control action in DC motor.

The torque output is controlled according to the changes in the armature current. The rotor angle also follows the change in the armature current.

#### 4.11 Speed control of DC motor at different load conditions

The responses of DC motor at no load and the graph of the motor show periodic pulses with no changes in the frequency.

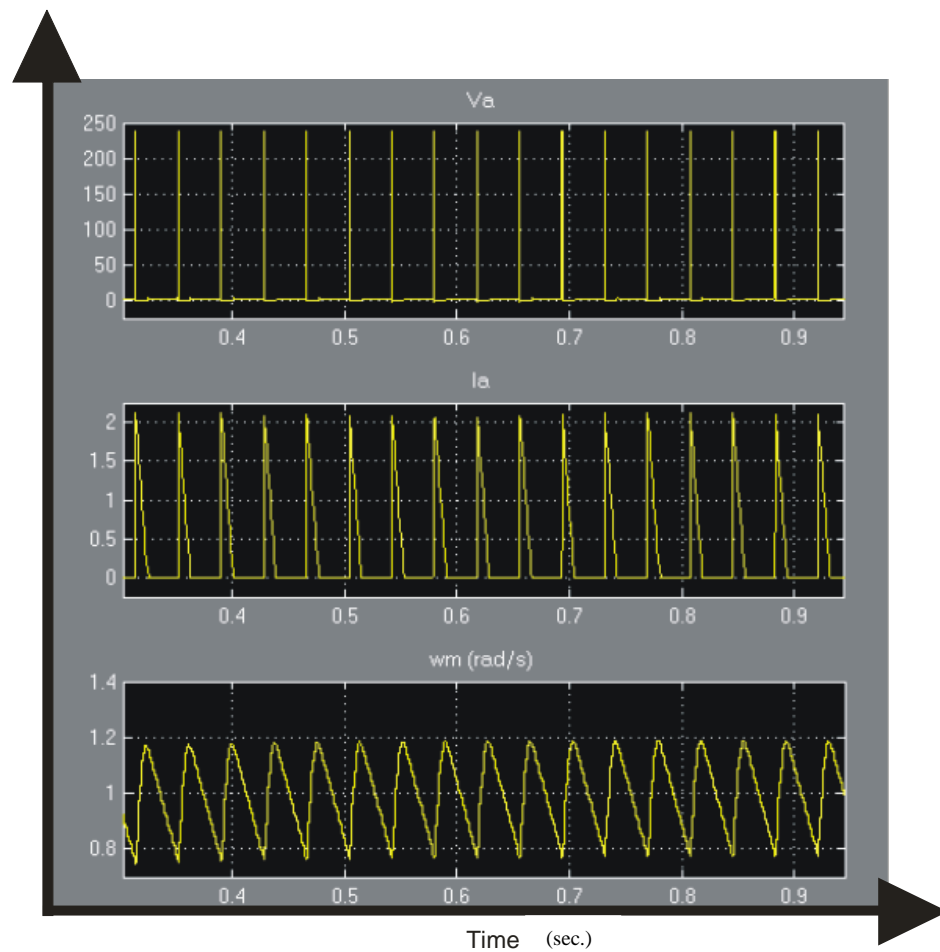


Figure 4.55: Armature voltage (Volts), armature current (Amp) and rotor speed (rpm) of DC motor with no load condition

The three graphs shown in Figure 4.55 for pure resistive load are the responses of the DC motor. The topmost graph shows the voltage being supplied to the armature circuit of the motor. The magnitude is 240V. But at  $t=2$  onwards, the frequency is

doubled. The middle graph shows the armature current. The waveform is similar armature voltage waveform. Since  $V$  is proportional to  $I$ . The bottom graph shows the speed of the motor. At every armature current peak, the speed will be at its peak and decreased gradually till the next  $I_a$  peak occurs. The plot as shown are acceptable because the rotor speed responds to the change in armature voltage and armature current.

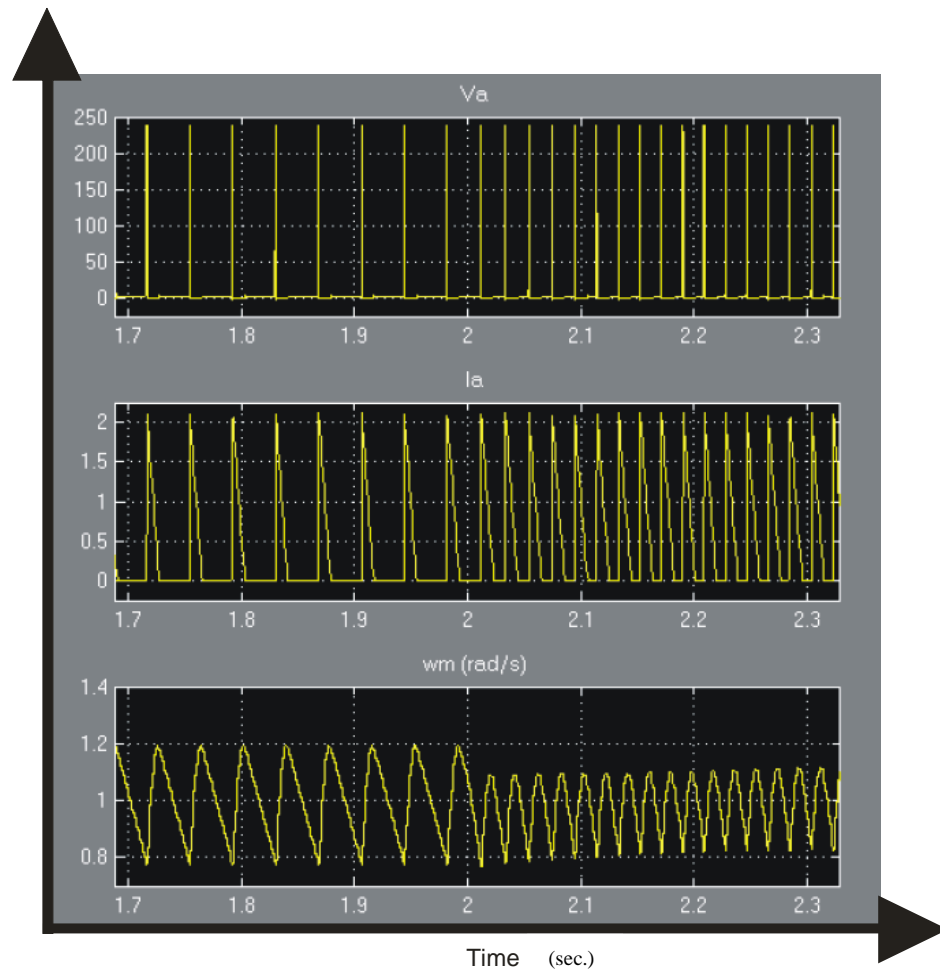


Figure 4.56: Armature voltage (Volts), armature current (Amp) and rotor speed (rpm) of DC motor with load.

The only changes in the graphs for reactive load at 50 VAR are the frequencies after  $t=2$  have been increased as shown in Figure 4.57. And as for the speed graph, the magnitude after  $t=2$  tend to fluctuates a bit before it goes to a constant value.

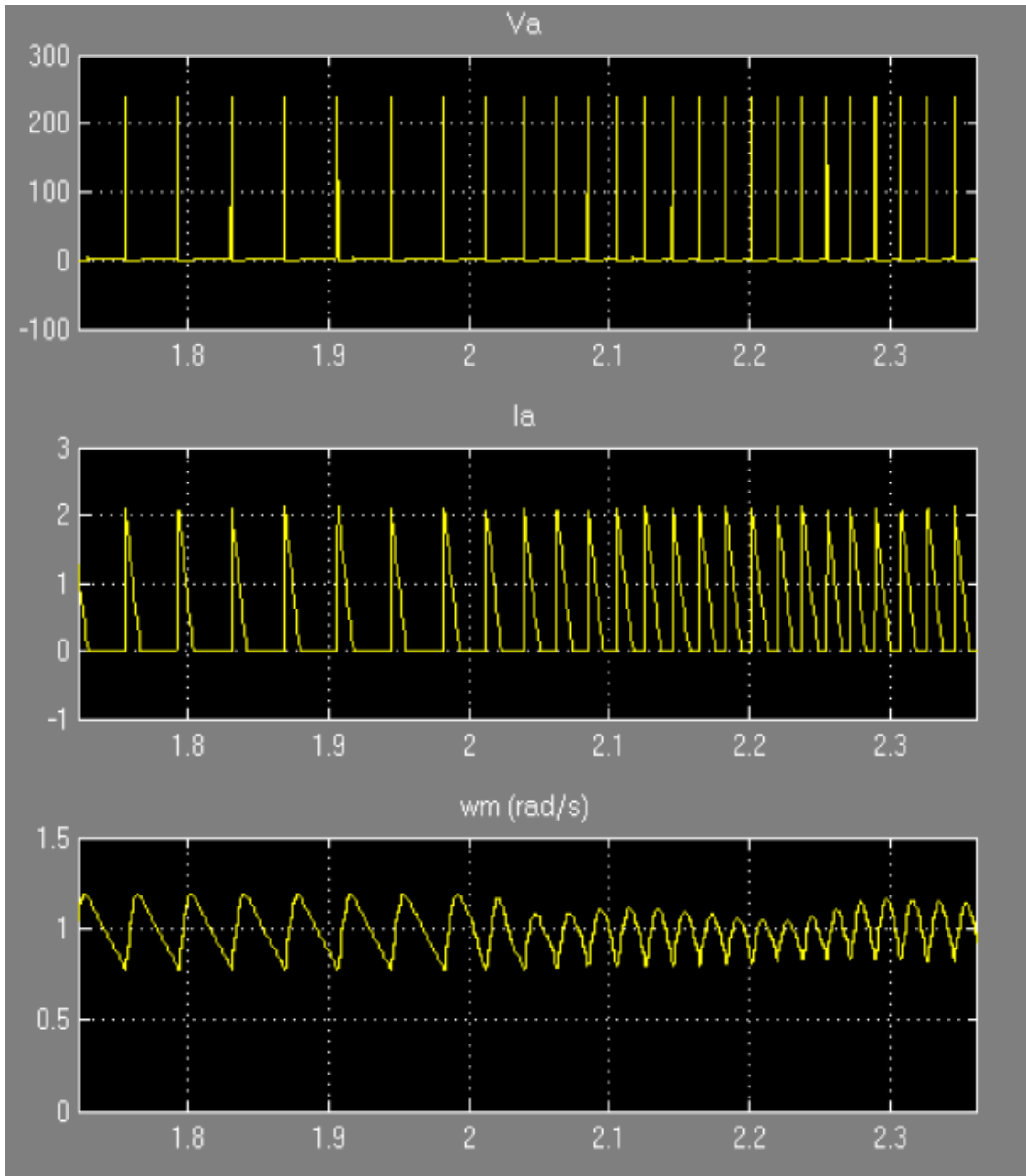


Figure 4.57: Armature voltage, armature current and rotor speed of DC motor with reactive load condition at 50 var

There is no change in DC motor response when frequency load at 200Hz is added as shown in Figure 4.58. Except for the frequency after  $t=2$  and the magnitude for the speed graph after  $t=2$ .

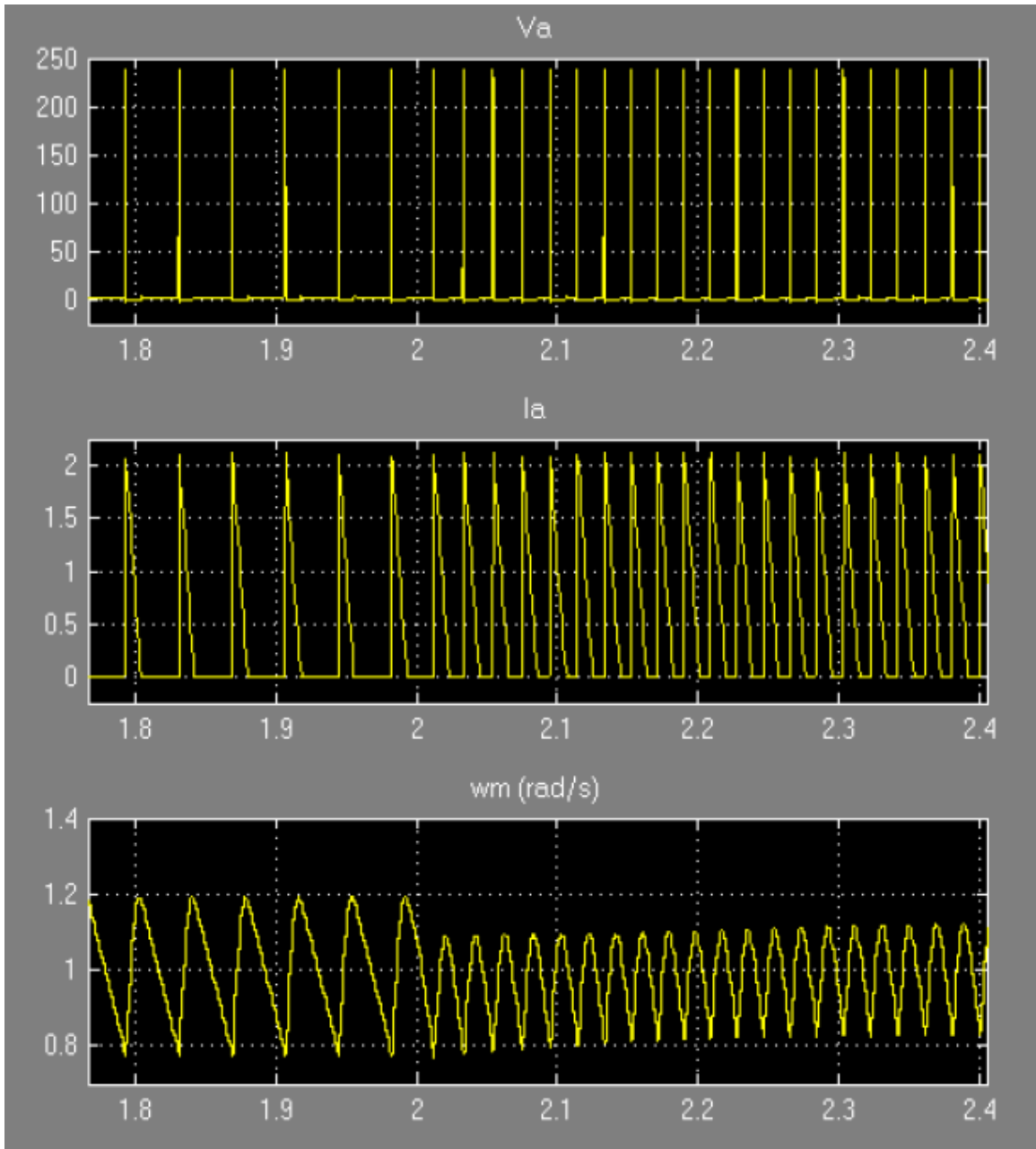


Figure 4.58: Armature voltage, armature current and rotor speed of DC motor with frequency load condition added 200Hz

The graph in Figure 4.59 shows the increase in frequencies when frequency load is added at 200Hz. After  $t=2$ . The magnitude of the armature current and speed graphs both have fluctuations.

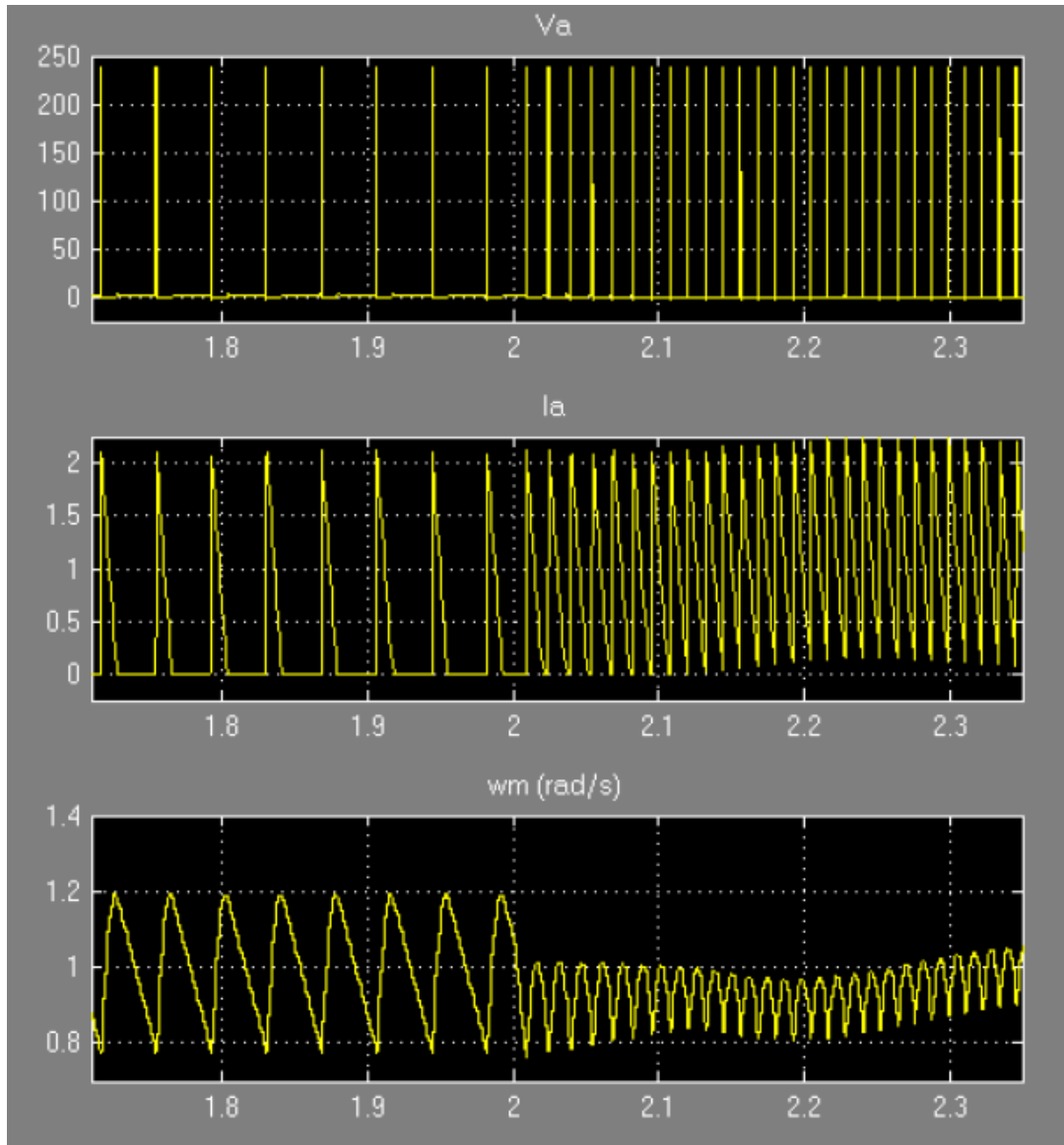


Figure 4.59: Armature voltage, armature current and rotor speed of DC motor with frequency load condition

#### 4.12 Conclusion

This chapter discusses model of DC motor. This model has been taken for developing simulink model of DC motor control using type-1 and type-2 fuzzy logic controller. Type-2 fuzzy logic controllers has not shown promising results as compared to type-1 in terms of settling time. However as shown in the graphs the response plots for type-2 fuzzy controller closely follow the changes made in armature current of the motor. Here type-2 is superior over type-1.

---

# CHAPTER 5

## RESULTS AND DISCUSSIONS

---

### 5.1 Control evaluation

This thesis describes the fuzzy type-1, fuzzy type-2 and neuro fuzzy control of synchronous generator and DC motor. The fuzzy speed control strategies have been evaluated with the help of different control parameters like integral absolute error (IAE) and integral time square absolute error (ITAE). This chapter summarizes all the aspects of the synchronous generator and DC motor.

A performance index is a quantitative measure of the performance of a system and is chosen so that emphasis is given to the important system specifications. The performance index is a number that should either be positive or zero. The best system is defined as the system that minimizes these indices. There are four performance indices available in classical control literature. However the two best that is IAE and ITAE have only been considered. The desirable feature of performance indices is selectivity and its power to distinguish between optimum and non-optimum system. These indices are easier to implement and also mathematically quite convenient both for analysis as well as computation.

The ITAE is most popular measure of performance since it does not discriminate against the large initial error in the response following a step demand, but does penalize smaller errors at a later time. Moreover it results in conservative settings and it is simpler and more timesaving than others especially integral square error (ISE).

In this thesis we have developed fuzzy based speed control techniques, neuro-fuzzy based speed control techniques for synchronous generator and DC motor. In fuzzy control we have investigated type1 and type-2 membership function. For each of the case studies different control performance is evaluated. This thesis emphasizes on speed control of synchronous generator and DC motor with varying load.

This section provides a comparative study of fuzzy control (both type-1 and type-2) strategies in varying load condition. The following load conditions have been considered for synchronous generator and DC motor.

1. No load condition
2. Pure resistive load
3. Inductance reactive load added 50VAR
4. frequency load added at 200Hz
5. Active power load added at 200W

#### 5.1.1 Control evaluation: Synchronous generator

In synchronous generator we have simulated and analyzed the characteristics of voltage, stator current, power, torque and  $V_f$ . In DC motor  $V_a$ ,  $I_a$  and  $w_m$  for varying load conditions have been analyzed. When no load is applied the change in voltage and current is shown in Figure 5.1. The voltage graph shows the frequency at 55 Hz and magnitude of 700V peak to peak. The current graph shows the different color phases having a phase difference of 60 degrees. Figure 5.1 shows the torque and electrical power at constant magnitude. The  $V_f$  graph shows a constant period train of pulses.

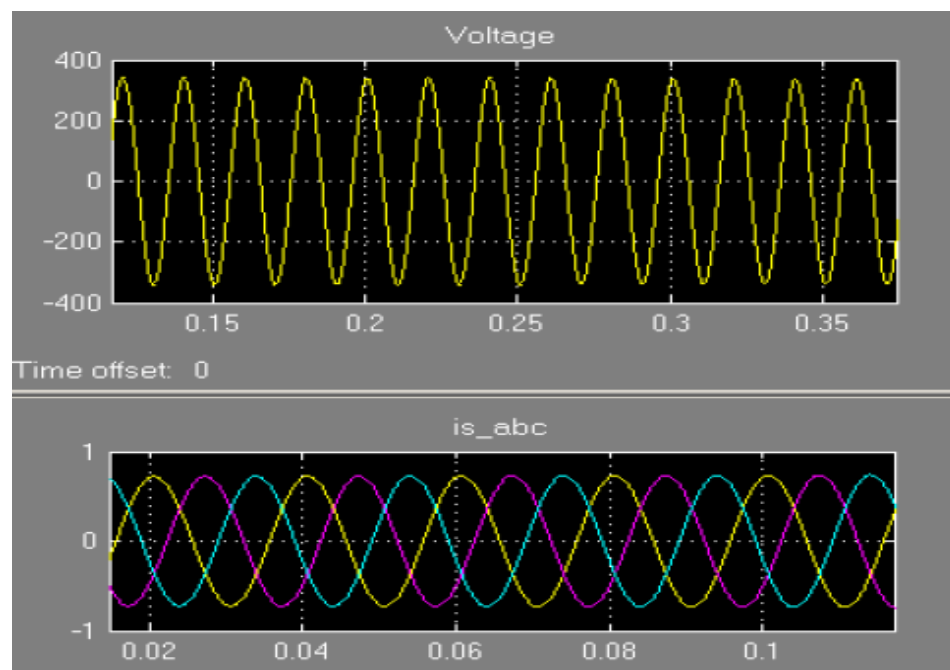


Figure 5.1: Variation in voltage and current of synchronous generator at no load condition

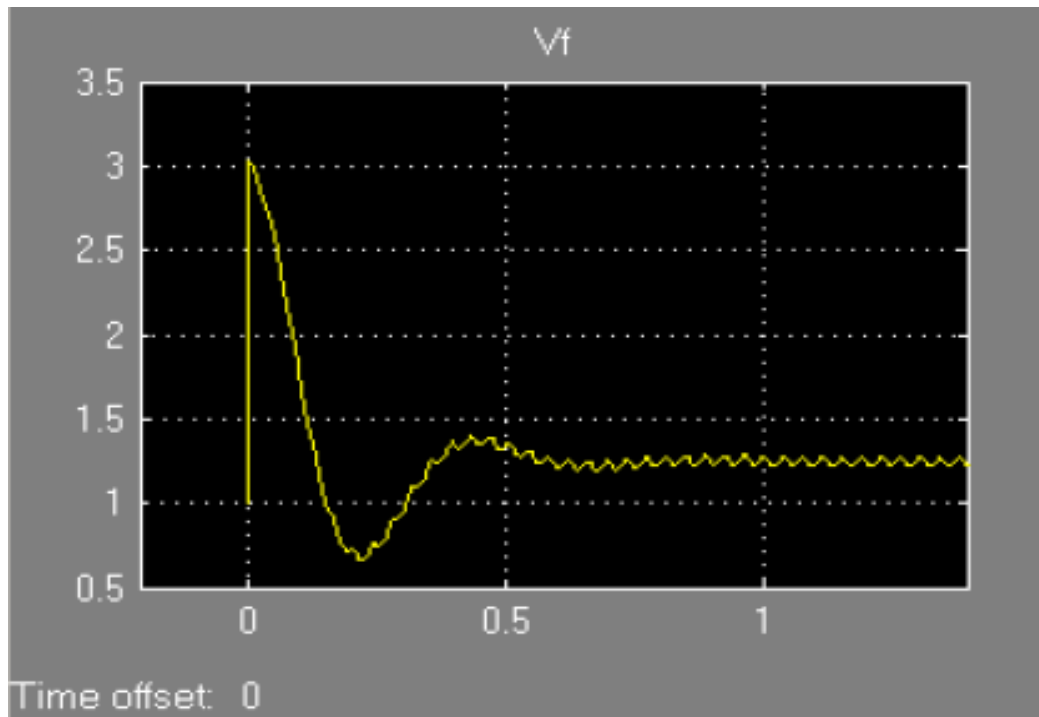
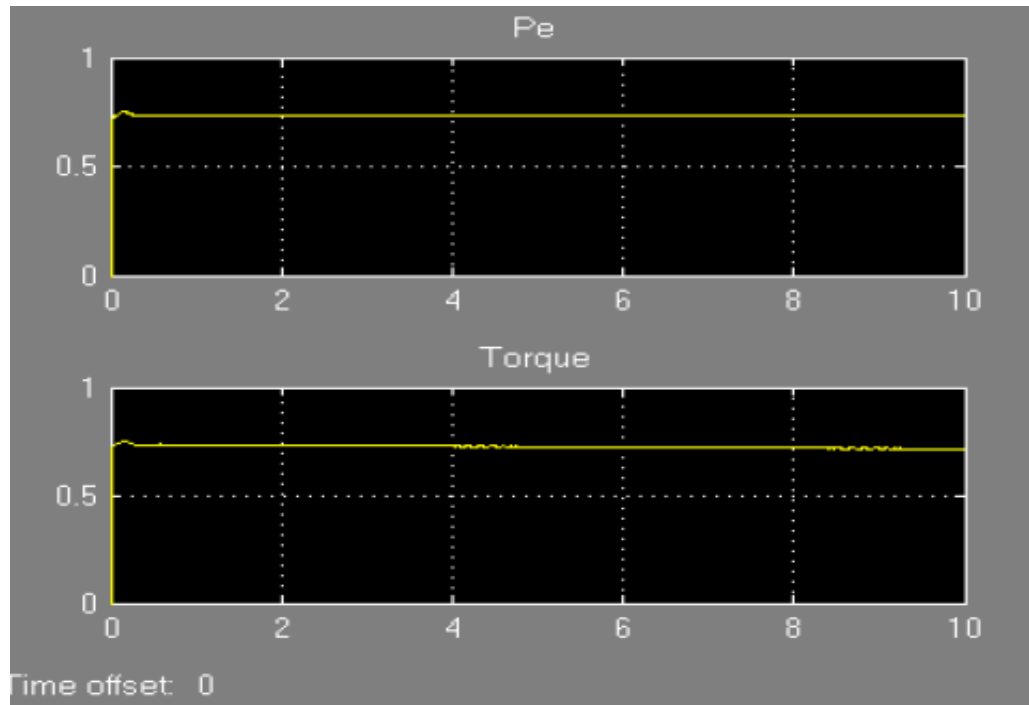


Figure 5.2: Variation in power, torque and  $V_f$  of synchronous generator at no load Condition

When a pure resistive load is added to the generator system the voltage, current, power, torque and  $V_f$  is shown in subsequent Figure 5.3.

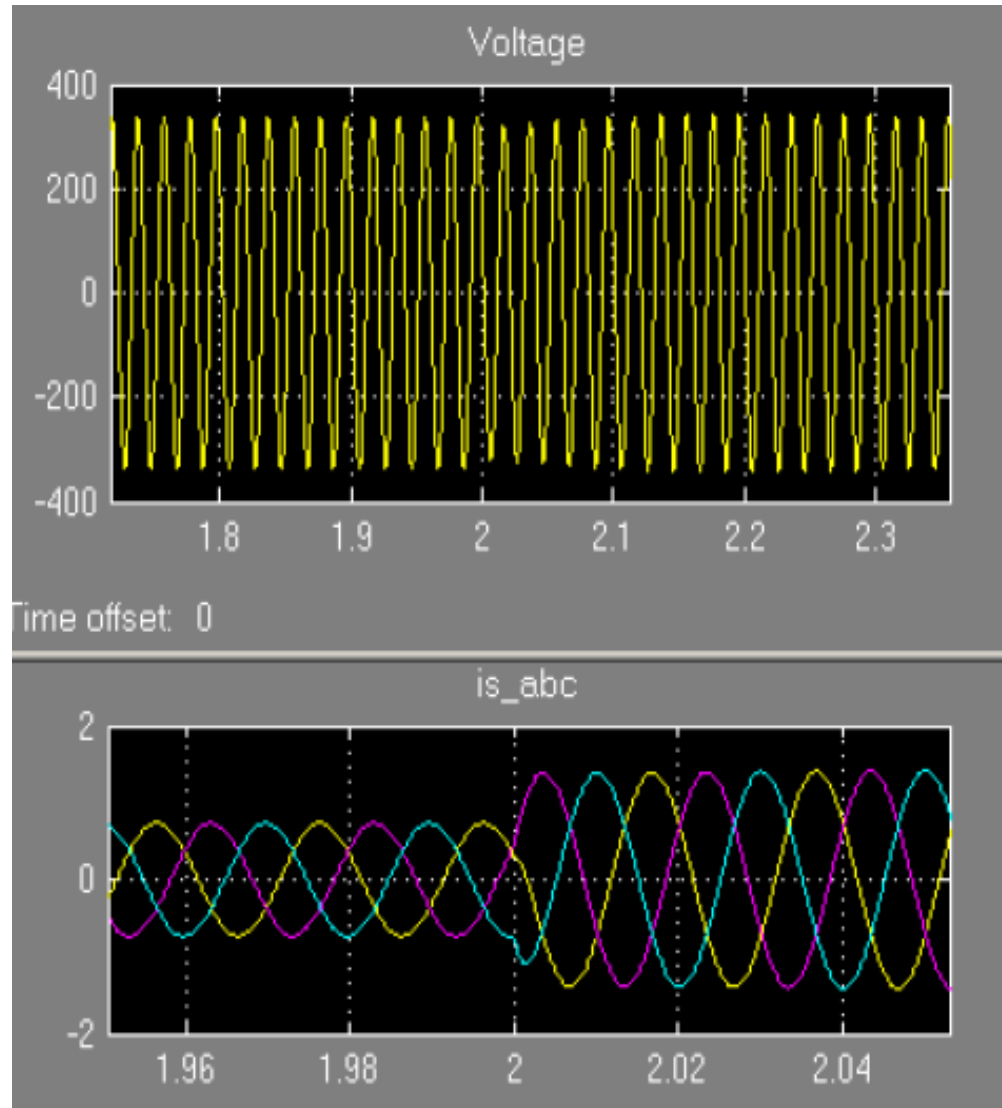


Figure 5.3: Variation in voltage and current of synchronous generator at resistive load

Figure 5.4 shows the power waveform for synchronous generator up to 2 time units with magnitude of both power and torque is less than 1 but increase suddenly to a level of 1.5 units approximately with some initial overshoot. The torque and power waveform is similar because torque and power are proportional to each other.

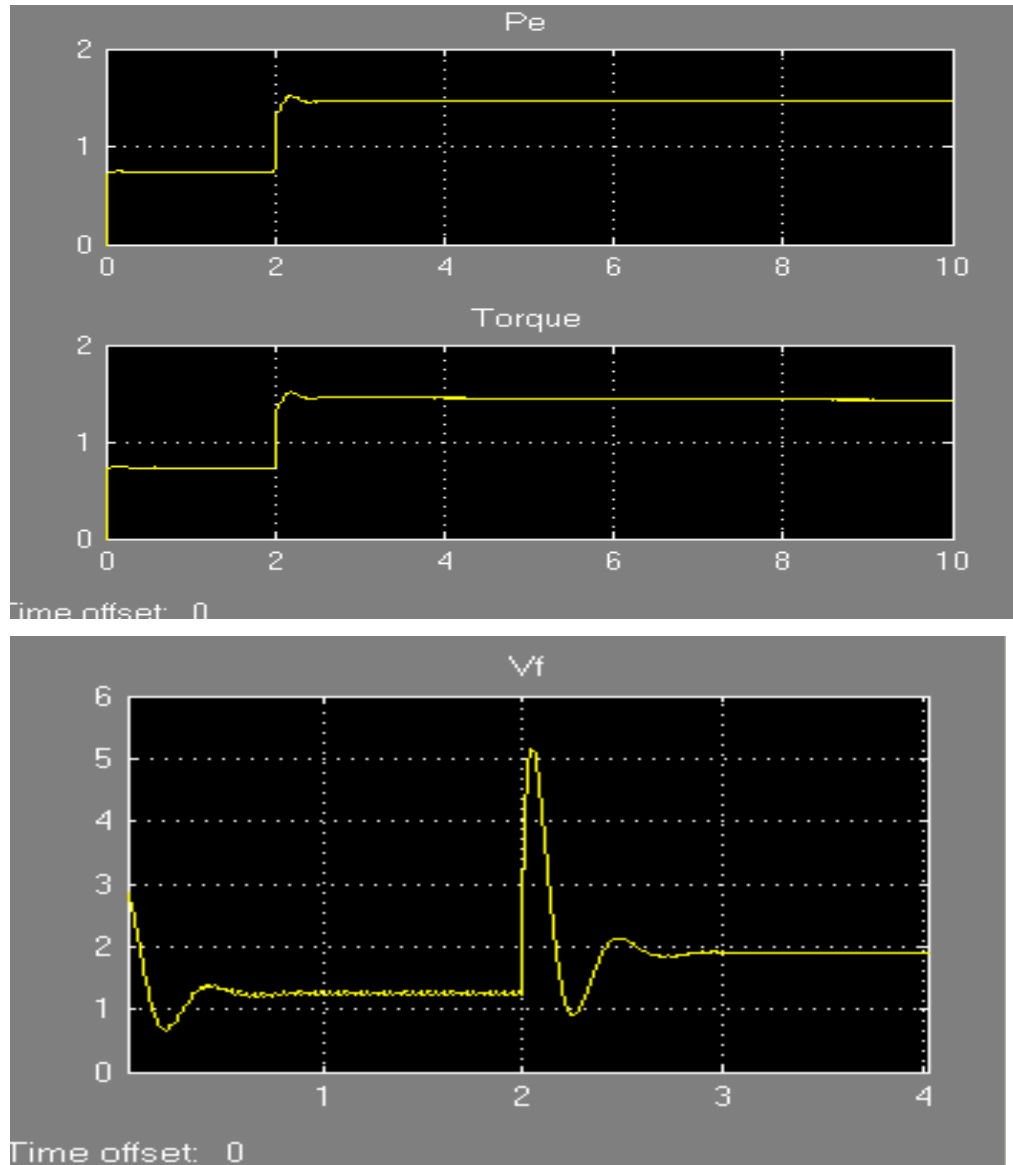


Figure 5.4: Variation in torque,  $V_f$  and power of synchronous generator at resistive load

The graph in Figure 5.4 shows the torque and electrical power of synchronous generator. Both graphs are similar except for the state after  $t=2$ . For the torque, after  $t=2$ , it decreases gently after a step in magnitude. For the electrical power, the magnitude remains constant after the step. The graph shows the response of  $V_f$  for the generator. After  $t=2$ , the magnitude of  $V_f$  increases by 50%. The overshoot of the response at  $t=2$  is 10%.

The load now has a reactance of 50 VAR of inductance. At  $t=2$ , the three phase stator current,  $I_s$  has a shift in the magnitude equally with respect to the first phase. For the voltage, the magnitude fluctuates after  $t=2$ , but slowly goes to steady state as time increases. The frequency remains the same.

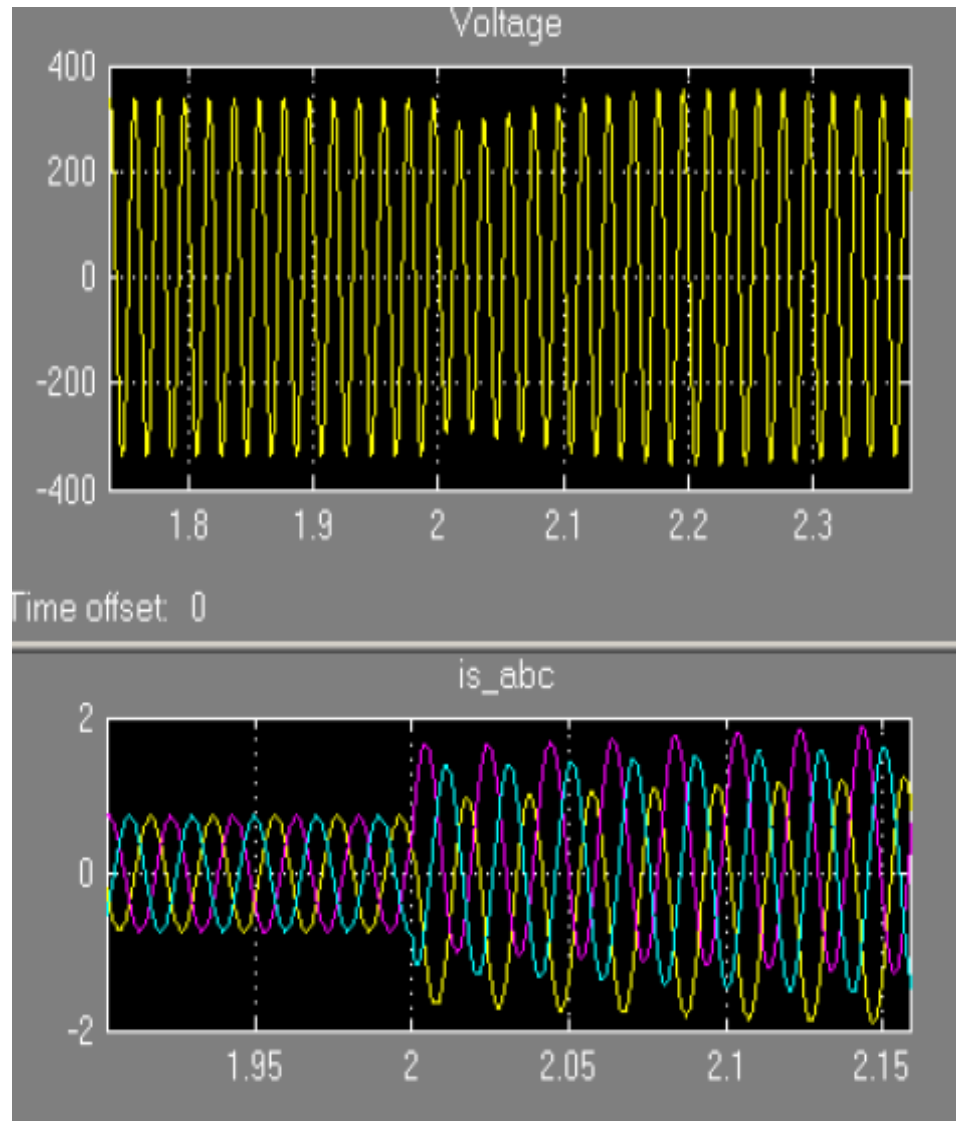


Figure 5.5: Variation in voltage and current of synchronous generator for inductive load

As shown in Figure 5.5 the voltage is continuously varying approximately 50Hz. The stator current magnitude up to 2 time units is 2V P-P. After 2 time units it is trying to stabilize at 4 V P-P.

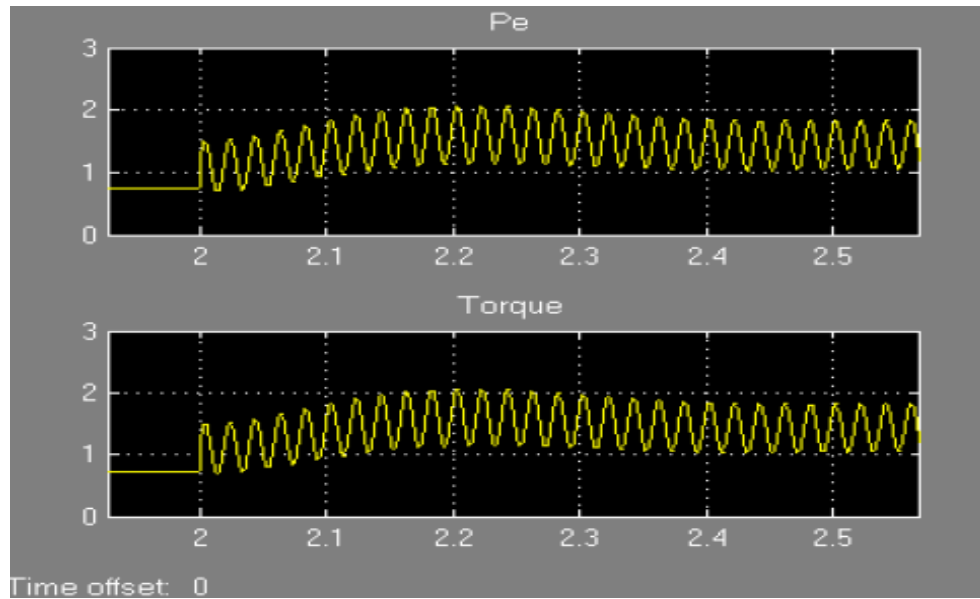


Figure 5.6: Variation in torque,  $V_f$  and power of synchronous generator at load added at 50 var

Now the frequency has been changed from 50 Hz to 200Hz. The frequency of the output voltage is 50 Hz. At  $t=2$ , again the magnitude of the stator current increases to twice. But the magnitude of the output voltage remains constant even after  $t=2$  as in Figure 5.7

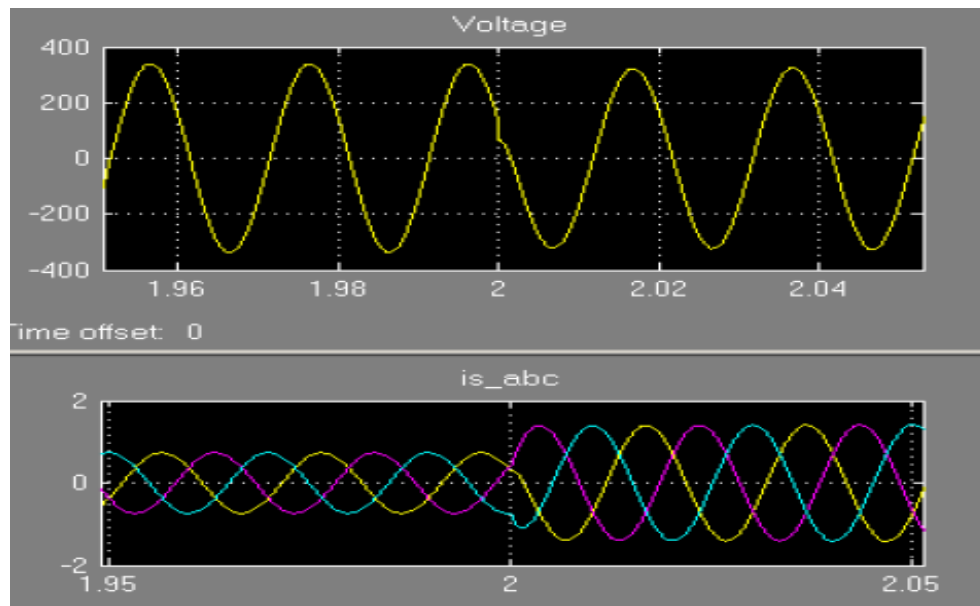


Figure 5.7: Variation in voltage, current of synchronous generator at frequency load added at 200 Hz

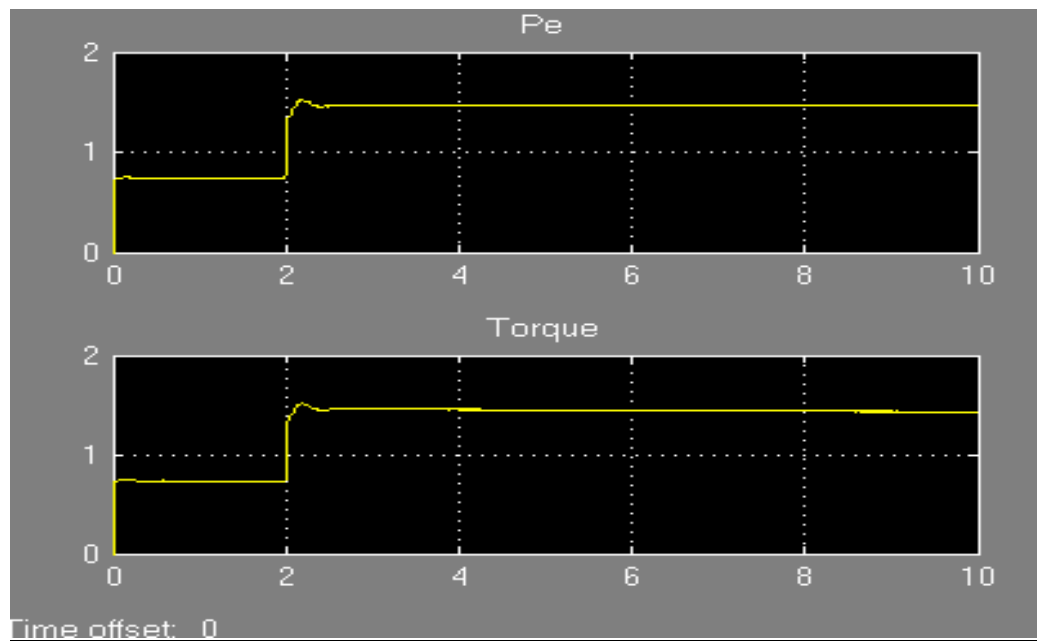
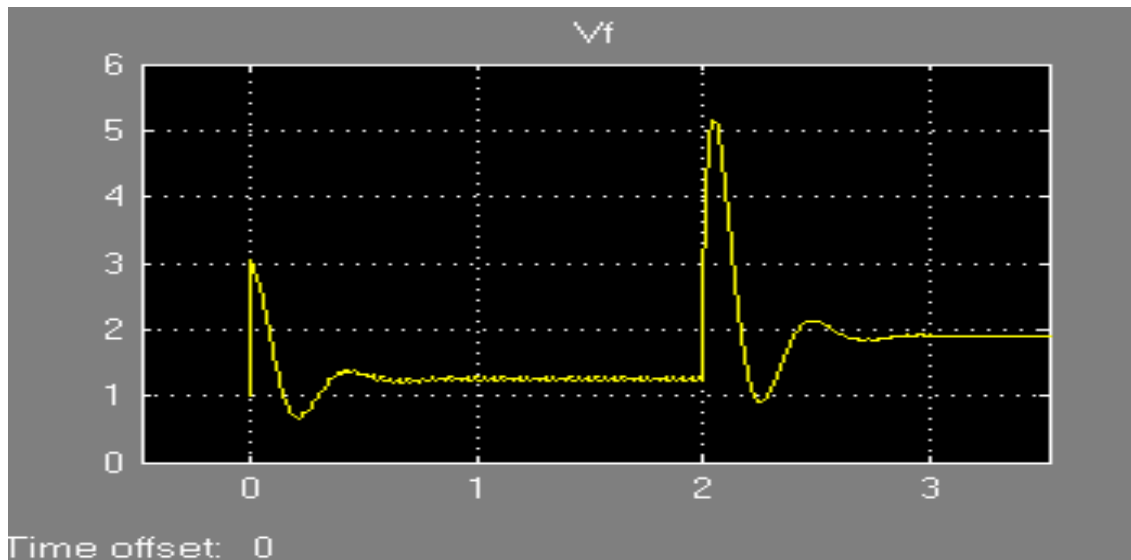


Figure 5.8: Variation in torque,  $V_f$  and power at 200Hz load

Active power of the added load has been now changed from 80W to 200W. The increase in the magnitude of the stator current is 1.8 times after  $t=2$ . The magnitude of the output voltage remains constant with increasing time. The graph shows the  $V_f$  increase in

magnitude of 1 to 3 when  $t=2$ . The torque and power both are similar as both increase steadily after  $t=2$  as in Figure 5.8

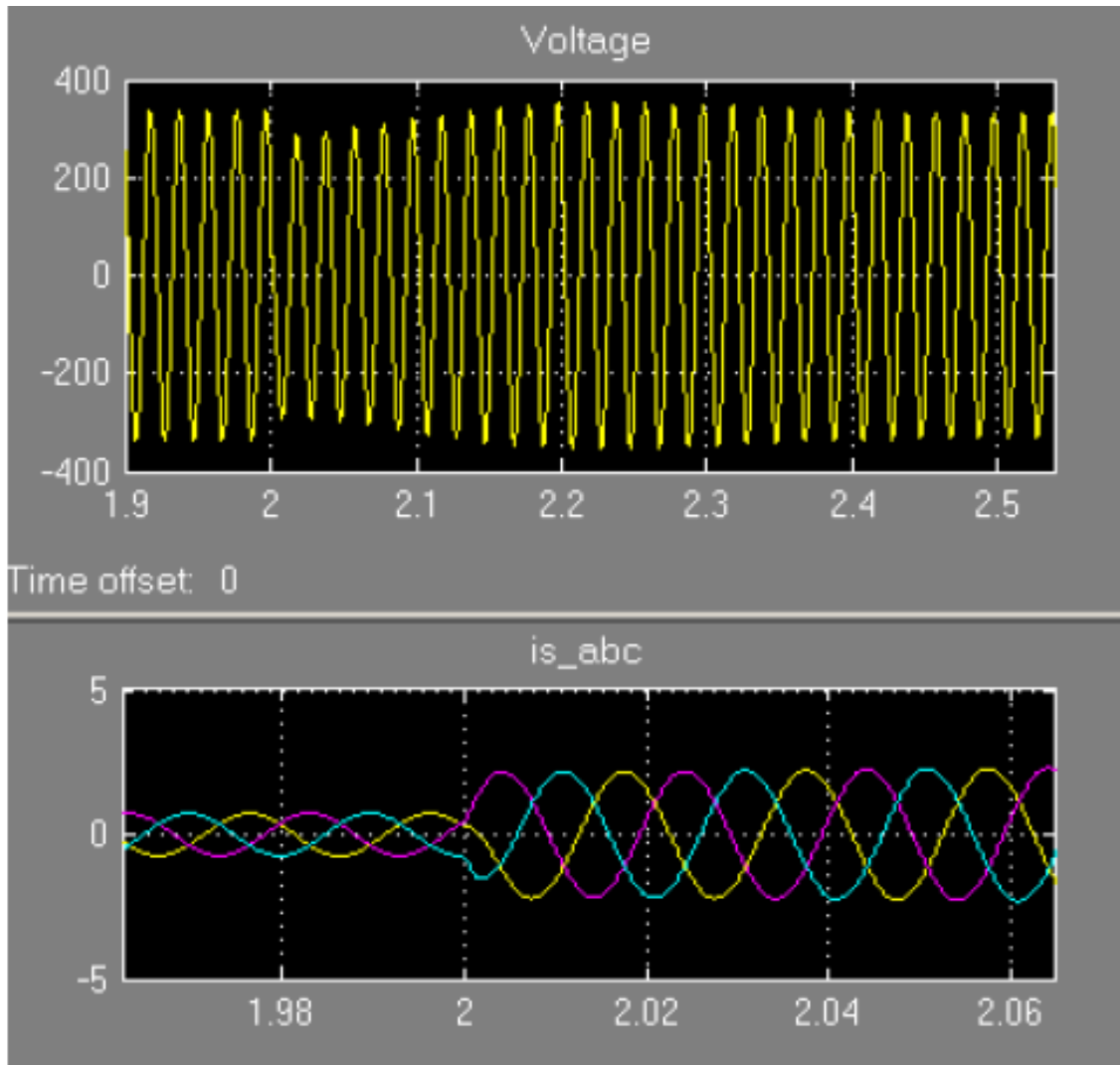


Figure 5.9: Variation in voltage and current when active power load added at 200W

Variation in voltage and current when active power load added at 200W are shown in Figure 5.9 which shows change in stator current at  $t=2$  and stabilizing at value 2.9 then after. Figure 5.10 shows the variations in torque,  $V_f$  and power at 200W load conditions. Power and torque stabilize after  $t=2$  and  $V_f$  stabilize after  $t=2.9$ .

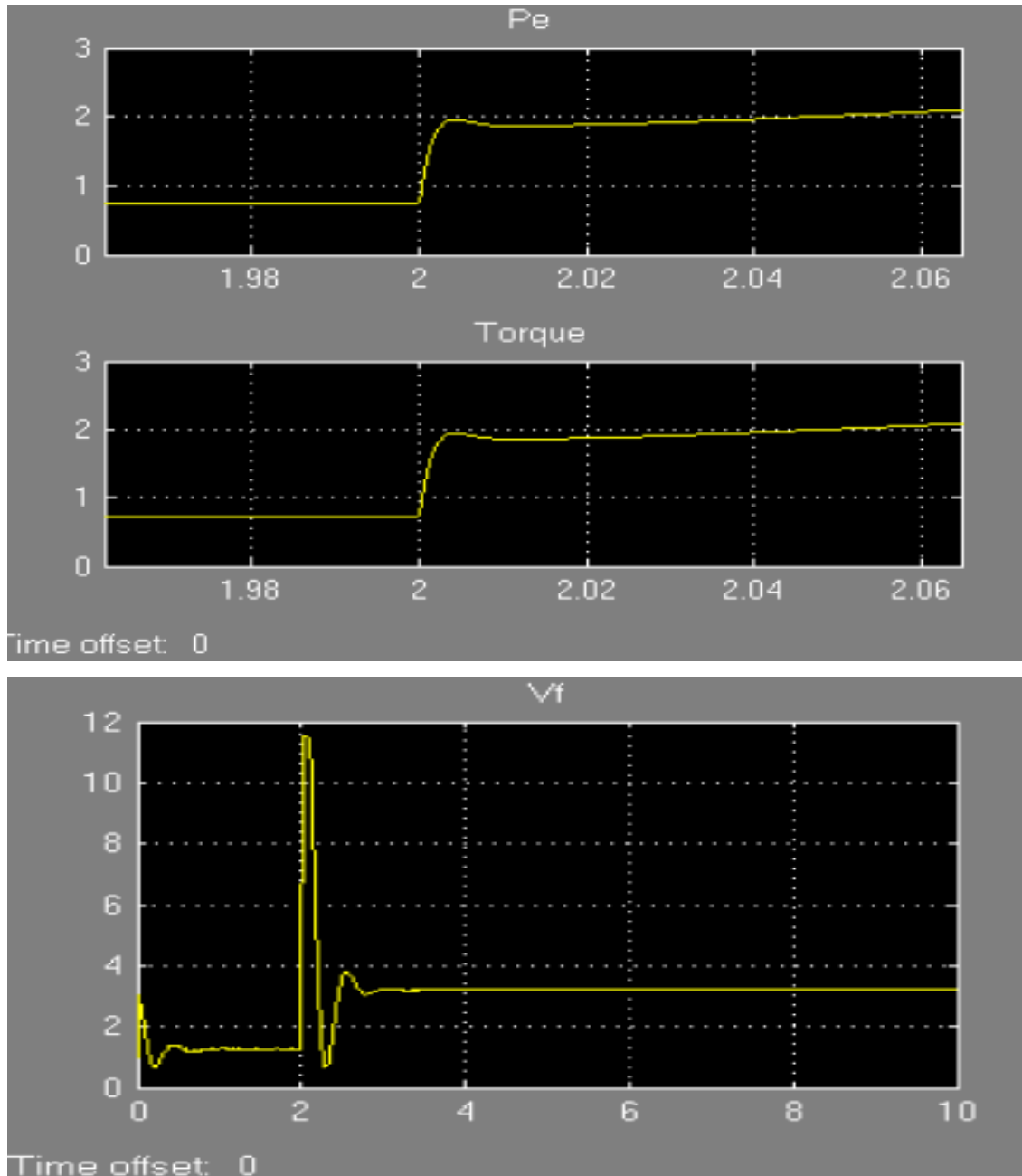


Figure 5.10: Variation in torque,  $V_f$  and power at 200W load condition

### 5.1.2 Control evaluation: DC motor

In DC motor with no load the response of motor shows periodic pulses. There are no changes in frequency. Changes are there in steady state as indicated in Figure 5.11.

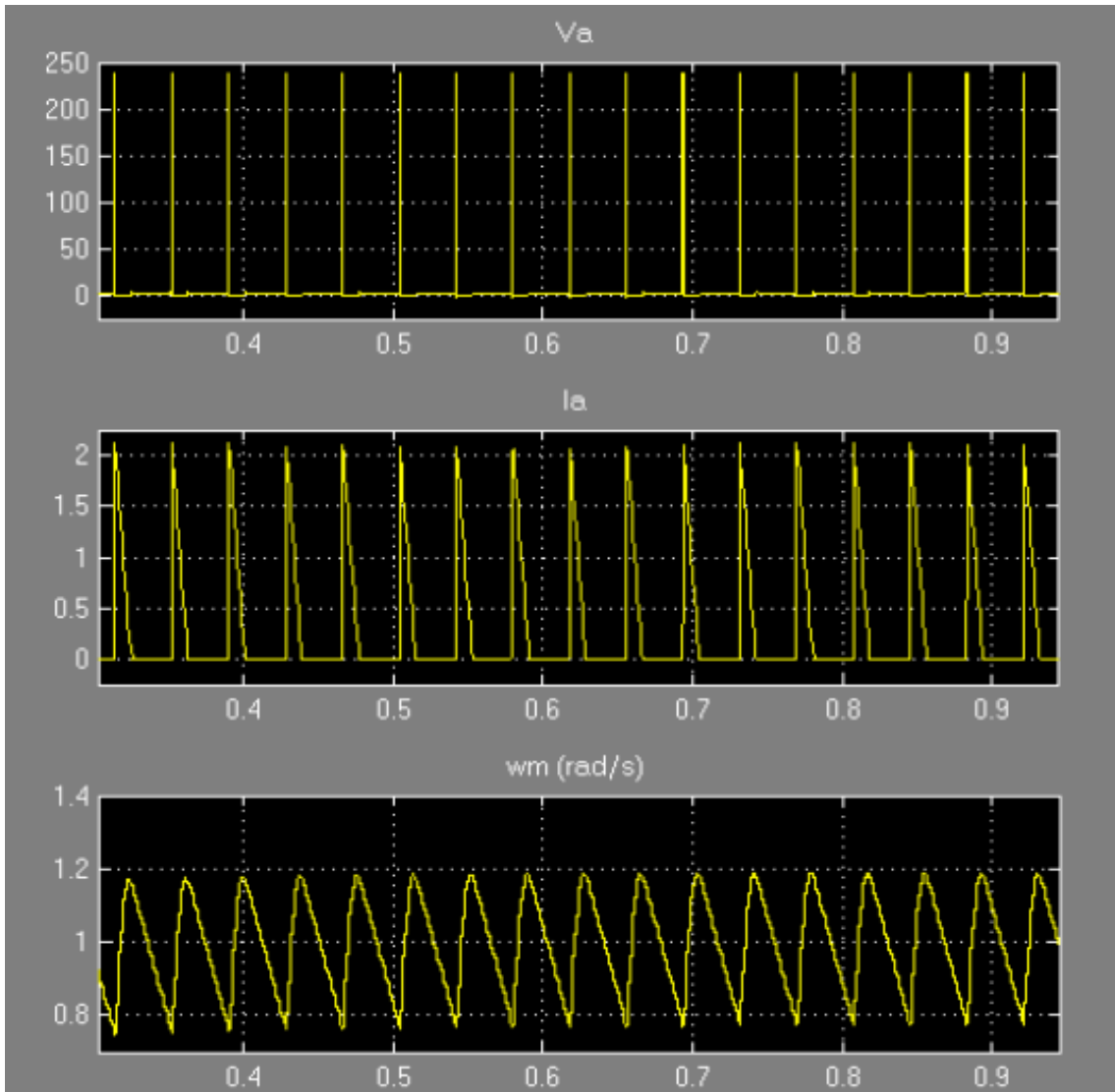


Figure 5.11:  $V_a$ ,  $I_a$  and  $\omega_m$  of DC motor with no load condition

The three graphs shown in Figure 5.11 are the responses of the DC motor. The topmost graph shows the voltage being supplied to the armature circuit of the motor. The magnitude is 240V. But at  $t=2$  onwards, the frequency is doubled. The middle graph shows the armature current. The waveform is similar armature voltage waveform. Since  $V$  is proportional to  $I$ . The bottom graph shows the speed of the motor. At every armature current peak, the speed will be at its peak and decreased gradually till the next  $I_a$  peak occurs.

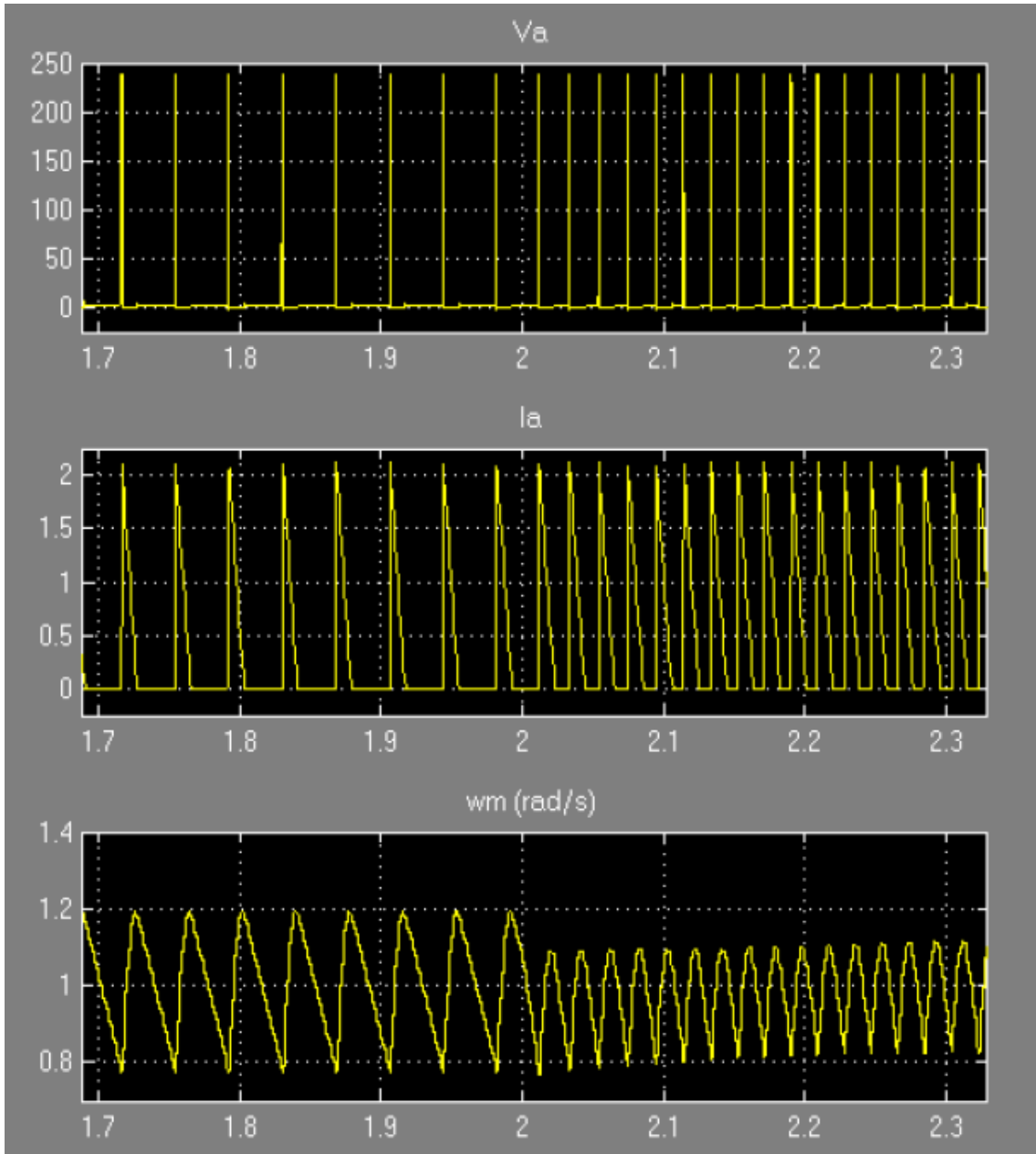


Figure 5.12:  $V_a$ ,  $I_a$  and  $\omega_m$  of DC motor with pure resistive load condition

The Figure 5.12 shows  $V_a$ ,  $I_a$  and  $\omega_m$  of DC motor with pure resistive load condition. The frequency of  $V_a$  and  $I_a$

The only changes in the graphs of Figure 5.13 above are the frequencies after  $t=2$  have been increased at reactive load of 50 VAR. And as for the speed graph, the magnitude after  $t=2$  tends to fluctuates a bit before it goes to a constant value.

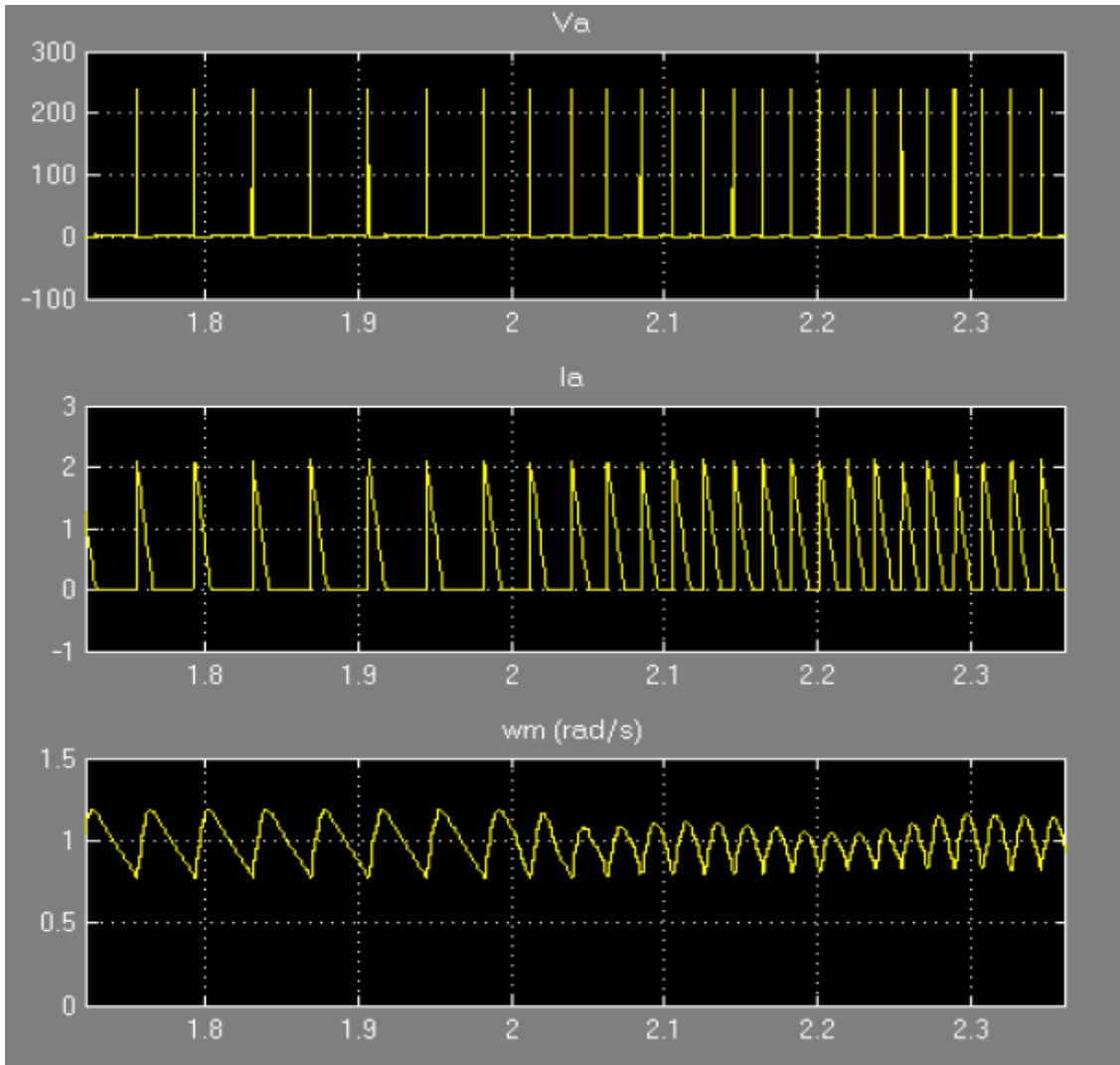


Figure 5.13:  $V_a$ ,  $I_a$  and  $\omega_m$  of DC motor with reactive load condition at 50 var

There is no change for the DC motor parameters when a frequency load of 200Hz is added. Except for the frequency after  $t=2$  and the magnitude for the speed graph after  $t=2$  as shown in Figure 5.14

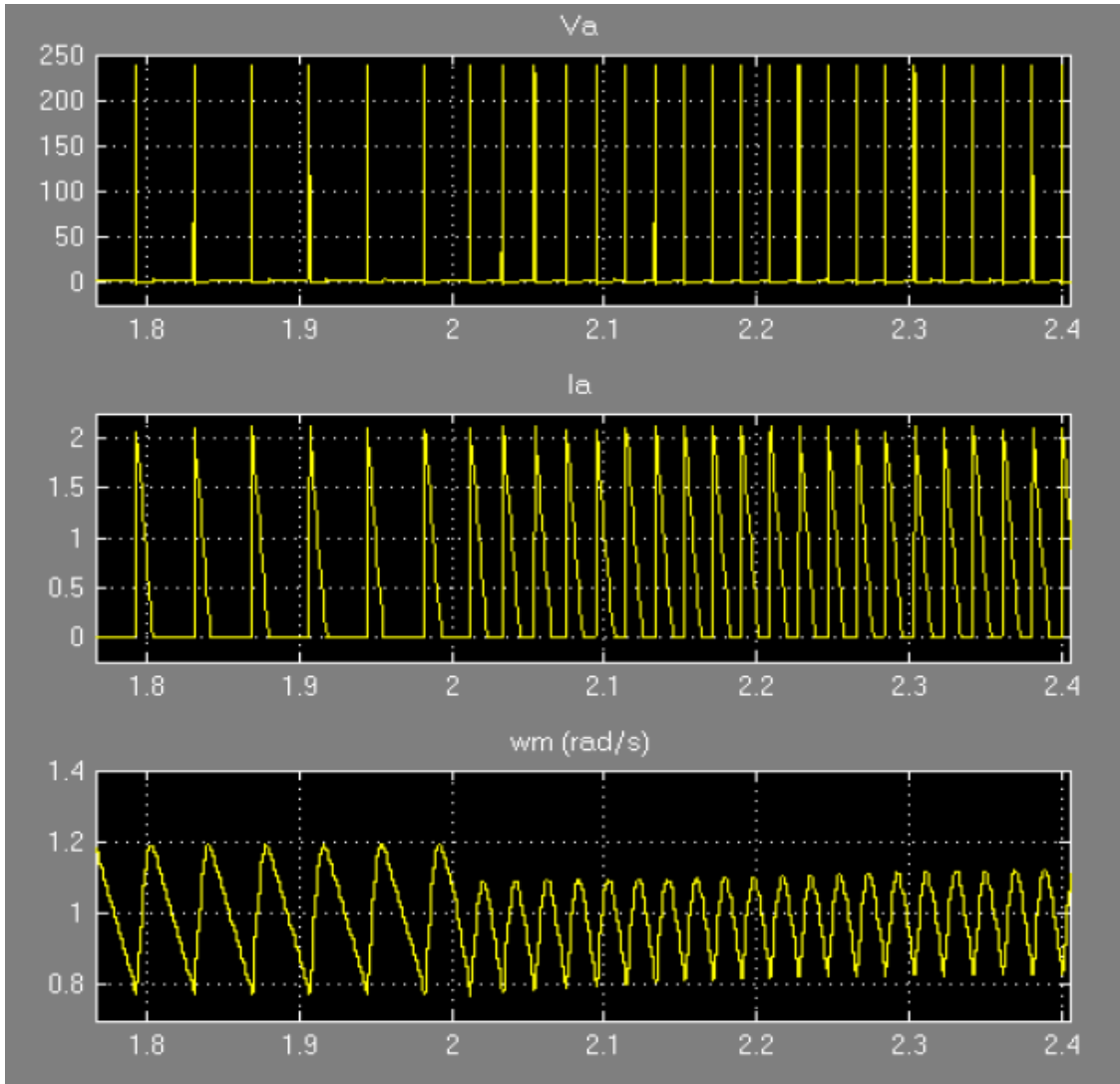


Figure 5.14:  $V_a$ ,  $I_a$  and  $\omega_m$  of DC motor with frequency load condition added 200hz

## 5.2 Control parameters

The following table depicts and compares the different control parameters of fuzzy and fuzzy neuro speed control of synchronous generator and dc motor. The control criterion of IAE, ISE, ITAE, ITSE has been successfully analyzed for both the cases of synchronous and dc motor keeping the fuzzy contemporary models in view. The control criterion helps the user to implement the specific fuzzy controlled contemporary model for best results. These intelligent control strategies are proving their worth by providing better control in any of the system.

### 5.2.1 Synchronous Generator

In the case study of synchronous generator the comparative analyses for different control parameters as well as different contemporary intelligent control strategy has been shown in tabular form in table 5.1 and table 5.2.

Table 5.1 Different control parameters for controllers in synchronous generator

S.No	Parameters	Type-1	Type-2	Neuro-Fuzzy
1	Overshoot	38.38%	30.04%	5.94%
2	Settling time	115.2 sec	91.34 sec	30 sec
3	Peak Time	45.95 sec	44.63 sec	41 sec

Table 5.2 Different control criterion for controllers in synchronous generator

S.No	Controller	IAE	ISE	ITAE	ITSE
1	Type-1	4.755	0.366	192.6	6.333
2	Type-2	4.428	0.31	186.8	5.539
3	Neuro-fuzzy	7.243	0.603	490.2	12.9

### 5.2.2 DC Motor

In the case study of DC motor the comparative analyses for different control parameters as well as different contemporary intelligent control strategy has been shown in tabular form in table 5.3 and table 5.4.

Table 5.3 Different control parameters for controllers in DC motor

S.No	Parameters	Type-1	Type-2	Neuro-Fuzzy
1	Overshoot	27.8%	16.7%	5.94%
2	Settling time	105 sec	79 sec	30 sec
3	Peak Time	39 sec	31 sec	25 sec

Table 5.4 Different control parameters for controllers in synchronous generator

S.No	Controller	IAE	ISE	ITAE	ITSE
1	Type-1	8.7	0.159	200.9	8.55
2	Type-2	8.45	0.27	187.8	7.59
3	Neuro-fuzzy	8.26	0.45	345.9	11.1

### **5.3 Conclusion**

This chapter provides discussion on results obtain from both the case studies of synchronous generator and DC motor. In the case study of synchronous generator the comparisons table for type-1, type-2 and neuro-fuzzy are shown. Also, in case study of DC motor similar analyses have been carried out for IAE and ITAE. Table 5.1, Table 5.2, Table 5.3 and Table 5.4 summarize the analysis.

---

## CONCLUSION AND FUTURE SCOPE

---

This research work emphasizes on intelligent control aspects of the synchronous generator and DC motor. Synchronous generator and DC motor have wide variety of industrial applications. Speed control is needed in different processes and applications. Though conventional speed control techniques using PI controller, PID controller, lead-lag controller are available but the need of intelligent controller can't be ignored. Intelligent controller gives an intelligent way to control the speed and adapt itself according to the change in environmental conditions. Fuzzy logic is used for modeling of imprecise data. Artificial neural network (ANN) is used for training the model with input data.

Design and analysis of a system consisting of a variable-speed synchronous generator that supplies an active DC load (inverter) through a three-phase diode rectifier requires adequate modeling in both time and frequency domain. In particular, the system's control-loops, responsible for stability and proper impedance matching between generator and load, are quite difficult to design without an accurate small-signal model. A particularity of the described system is strong non-ideal operation of the diode rectifier, a consequence of the large value of generator's synchronous impedance. This non-ideal behavior influences both steady state and transient performance.

In two case studies type-2 is better with regard to control and error over type-1. It is concluded that reliability of the data is the key for selection of either type-1 fuzzy logic model or type-2 fuzzy logic model. Only in those cases where data reproducibility and repeatability is not high type-2 fuzzy logic model is a definitely better control proposition.

As per the simulation results of this thesis type-1 fuzzy logic control exhibits faster settling of the response however the steady state error is less in type -2. It is due to the reason that type-2 fuzzy sets are complex as compared to type-1. As a result the transition dynamics of type-1 is better and steady state dynamics of type-2 is better.

As a future scope hardware implementation of fuzzy logic control can be done using various kinds of microprocessors and microcontrollers. Digital fuzzy speed control can be achieved using digital signal processor and discrete VHDL controller. The developed controller can be fabricated in an ASIC. Genetic algorithm, particle swarm optimization based optimization can be performed for better results in both type-1 and type-2 membership functions.

---

## REFERENCES

---

- 1 Soliman F Hussein, Sharaf A M, Mansour M M “A Fuzzy Logic Tunable Speed Controller For A Rectifier Fed PMDC Motor Drives,” IEEE Transactions 1994, pp. 22-26.
- 2 Yu Yiming, “Rule Based Fuzzy Logic Inferencing”, IEEE Transactions 1994, pp. 465-570.
- 3 M. Cipolla, J. M. Moreno-Eguilaz, J. Peracaula, "Fuzzy control of an induction motor with compensation of system dead-time," IEEE Power Electronics Specialist Conference, vol. 1, PESC'96, pp.677-681.
- 4 S. Bologna I, M. Zigliotto, "Fuzzy logic control of a switched reluctance motor drive", IEEE Transaction On Industrial Application, vol. 32 No. 5, 1996, pp.1063-1068.
- 5 P Tiitinen, "The next generation motor control method, DTC direct torque control", Proceedings of the IEEE International Conference on Power Electronics, Drives, and Energy Systems for Industrial growth, 1996, pp. 37-43.
- 6 Minh Ta-Cao, J.L. Silva Neto, Hoang Le-Huy.” Fuzzy logic based controller for induction motor drives”, IEEE IECON Record 1996, pp.631-634.
- 7 P. Guillermin, “Fuzzy Logic Applied to Motor Control”, IEEE Transaction on Industrial Applications, vol. 32, no. 1, 1996, pp. 51-56.
- 8 Jaime Fonseca, Joo L. Afonso, Jilio S. Martins, Carlos Couto, “Evaluation of Neural Networks and Fuzzy Logic Techniques Applied to the Control of Electrical Machines”, in Proceedings of the 5th UK Mechatronics Forum International Conference, vol. 2, 1996, pp. 15-20.
- 9 I. Kioskeridis, N. Margaris, "Loss minimization in scalar controlled induction motor drives with search controllers," IEEE Transactions on Power Electronics, vol. 11, no. 2, 1996, pp. 213-220.
- 10 E. Chiricozzi, F. Parasiliti, M. Tursini, D. Q. Zhang, “Fuzzy Self-tuning PI Control of PM Synchronous Motor Drives,” International Journal of Electronics,

- 1996,pp. 211-221.
- 11 F. Parasiliti, M. Tursini, D.Q. Zhang, "Adaptive Fuzzy Logic Control for High Performance PM Synchronous Drives, Proceedings of Melecon '96, 1996, pp. 323-327.
  - 12 N. Matsui, "Sensorless PM brushless DC motor drives," IEEE Transaction of Industrial Electronics, vol. 43, Apr. 1996, pp. 300-308.
  - 13 H.-X. Li, H.B. Gatland, "Conventional fuzzy control and its enhancement", IEEE Transactions on System Man and Cybernetics, vol. 26, no. 5, 1996, pp. 791-797.
  - 14 L. Zhen, L. Xu, A ComDarison, "Study of three fuzzy schemes for indirect vector control of induction machine drives", Proceedings of IEEE IAS Annual Meeting, 1996, pp. 1725-1731.
  - 15 J.L. Silva, Le Huy, "A fuzzy logic control blockset for simulink", Proceedings of ELETRIMACS'96, vol. 2, 1996, pp. 587-592.
  - 16 Ashrafzadeh F, Nowicki E P, Boozarjomehrytan R, Salmon J C, "Optimal synthesis of fuzzy sliding mode controllers", IEEE Transactions 1996, pp. 1741-1745.
  - 17 P. Mehrotra, J. E. Quaiocoe, R. Venkatesan, "Development of an artificial neural network based induction motor speed estimator," PESC '96 IEEE Power Electronics Specialists, Vol. 1, 1996, pp. 682-688.
  - 18 F.Filippetti, G. Franceschini, C. Tassoni, P. Vas., "AI techniques in induction machines diagnosis including the speed ripple effect", ZEEE-IAS Annual meeting conference, 1996, pp. 655-662.
  - 19 M. F. Lai, M. Nakano, G. -C. Hsieh, "Application of fuzzy logic in phase-locked loop speed control of induction motor drive," IEEE Transaction on industrial Electronics, vol. 43, no. 6, December 1996, pp. 630-639.
  - 20 R. J. Hammell, T. Sudkamp, "An adaptive hierarchical fuzzy model," Expert Systems with Applications, vol. 1 , no. 2, 1996, pp. 125-136.
  - 21 M.G. Simoes, B.K. Bose, "Neural network based estimation of feedback signals for a vector controlled induction motor drive", IEEE Transaction on Industrial Application, vol. 31, 1997, pp. 620-629.

- 22 B. K. Bose, N. Patel, "A sensorless stator flux oriented vector controlled induction motor drive with neuro fuzzy based performance enhancement", IEEE IAS Conference Recording, vol 1,1997, pp.393-400.
- 23 S.Guo, L.Peters, H.Surman, "Design and application of analog fuzzy logic controller", Proceedings of IEEE International Conference on Fuzzy System, vol. 4 , 1997, pp.429-438.
- 24 Ye Limeng, Jiang Jianguo, Su Pengsheng, "Failure diagnosis of induction motor with fuzzy logic", New Technique of Electrician And Electric Energy, vol.1, 1997, pp. 30-38.
- 25 G. Lightbody, G. W. Irwin, "Nonlinear control structures based on embedded neural system models", IEEE Transactions on Neural Networks, vol. 8(3), 1997, pp. 553-567.
- 26 D. Leggate, R. J. Kerkman, "Pulse-based dead-time compensator for pwm voltage inverters," IEEE Transaction on Industrial Electronics, vol. 44, no. 2, 1997, pp.191-197.
- 27 Chang-Eob Kim, Yong-Bae Jung, Sang-Baeck Yoon, Dal- Ho Im. "The fault diagnosis of rotor bars in squirrel cage induction motors by time stepping finite element method", IEEE Transactions on magnetics, vol.33, 1997, pp.2131-2134.
- 28 A. M. A. Amin, "Neural network-based tracking control system for slip-energy recovery drive," in Proceedings of the 1997 IEEE International Symposium on Industrial Electronics, 1997, pp.1247-1252.
- 29 E. Cermto, A. Consoli, A. Raciti, A. Testa, "Fuzzy adaptive vector control of induction motor drives," IEEE Transaction on power electronics, vol. 12, No.6, 1997, pp.1028-1040.
- 30 S. Wade, M. W. Dunnigan, B. W. Williams, "Modeling and simulation of induction machine vector control with rotor resistance identification," IEEE Transactions on Power Electronics, vol. 12, no. 3, 1997, pp. 495 -506.
- 31 J. M. Moreno-Eguilaz, M. Cipolla, P. Branco, J. Peracaula, "Fuzzy logic based improvements in efficiency optimization of induction motor drives," IEEE International Conference on Fuzzy Systems 1997, pp.219-224.
- 32 L.A. Cabrera, M.L. Elbuluk, I. Husain, "Tuning the stator resistance of induction

- motors using artificial neural network,” IEEE Transaction on Power Electronics, vol.12, No.5, 1997, pp.779-787.
- 33 T. Nouguchi, S. Kondo, I. Takahashi, “Field-oriented control of an induction motor with robust on-line tuning of its parameters,” IEEE Transaction on Industrial Application, vol.33, 1997, pp.35-42.
- 34 B. Heber, Longa Xu, Y. Tang, “Fuzzy logic enhance speed control of an indirect field-oriented induction motor drive,” IEEE Transaction on Power Electronics, vol. 12, No. 5 , 1997, pp.772-778.
- 35 B.K. Bose, N.R. Patel, K. Rajashekara, “A neuro-fuzzy-based on line efficiency optimization control of a stator flux-oriented direct vector-controlled induction motor drive” IEEE Transaction on Industrial Electronics, 1997, pp.70-75.
- 36 G. Buja, “Direct torque control of induction motor drives”, ISE Conference proceedings, 1997, pp. TU2-TU8.
- 37 W.G. dasilva, P.P. Acarnley, "Fuzzy logic controlled dc motor drive in the presence of load disturbance". European Power Electronics Conference,1997,pp.2.424-2.430.
- 38 P. Mattavelli, L. Rossetto, G. Spiazzi, Paolo Tenti, “General-purpose fuzzy controller for dc–dc converters”, IEEE Transaction on Power Electronics, vol. 12, 1997, pp. 79-86.
- 39 B. Robyns, F. Labrique, H. Buyse, “ Reduction of the flux control sensitivity to electrical parameter uncertainties in induction machine field oriented control by using fuzzy logic”, European Power Electronics Conference, 1997, pp.2.403-2.208.
- 40 E. Cerruto, A. Consali, A. Raciti, A. Testa, “Fuzzy adaptive vector control of induction motor drives”, IEEE Transaction on Power Electronics, vol.12, No. 6, 1997, pp. 1028-1039.
- 41 Moreno-Eguilaz, J.,“Induction motor optimum flux search algorithms with transient state loss minimization using a fuzzy logic based supervisor”, vol. 2, IEEE, 1997, pp.1302-1308.
- 42 Scott Wade, Matthew W. Dunnigan, Barry W. Williams, “Modeling and simulation of induction machine”, IEEE Transaction on Power Electronics, vol.

- 12, no. 3, 1997, pp. 495-506.
- 43 Alfio Consoli, Angelo Raciti, Antonio Testa., "Fuzzy adaptive vector control of induction motor", IEEE Transaction on Power Electronics, vol. 12, no. 6, 1997, pp. 1028-1040.
- 44 S. Chun et al., "A fuzzy expert system for vibration cause identification in rotating machines," Proceedings of the 1997 IEEE International Conference on Fuzzy Systems, vol. 1, pp. 555-560.
- 45 G. C. Mouzouris, J. M. Mendel, "Dynamic non-singleton fuzzy logic systems for nonlinear modelling", IEEE Transactions on Fuzzy Systems, vol. 5, no. 2, 1997, pp. 199-208.
- 46 K. Erenay, I. Ciprut, L. Tezduyar, Y. E.Cerruto, A. Consoli, A. Recite, A. Testa, "Fuzzy adaptive vector control of induction motor drives", IEEE Transactions on Power Electronics, Vol 12 No. 62, 1997, pp. 1028-1039.
- 47 L.A. Cabrera, M.L. Elbuluk, I. Husain, "Tuning the stator resistance of induction motors using artificial neural network," IEEE Transactions on Power Electronics, vol.12, No.5, 1997, pp.779-787.
- 48 Scott Wade, Matthew W. Dunnigan, Barry W. Williams., "Modeling and simulation of induction machine", IEEE Transaction on Power Electronics, vol. 12, No. 3, 1997, pp. 1890-1895.
- 49 Lai Mao Fu, Chang Chen, "Fuzzy logic in the phase-locked loop dc motor speed control system", IEEE Transactions 1997, pp. 1222-1227.
- 50 C. B. Jacobina, M. B. R. Correa, E. R. C da Silva, A. M. N. Lima, "Induction motor drive system for low power applications," IEEE Conference on Industry Applications Society (IAS) Annual Meeting, 1997, pp. 605-612.
- 51 M. G. Rodrigues, W. I. Suemitsu, P. Branco, J. A. Dente, L. G. B. Rolim, "Fuzzy logic control of a switched reluctance motor," Proceedings of ISIE'97, vol. 2, 1997, pp. 527-531.
- 52 L. Baghi, H. Razik, A. Rezzouq, "Comparison between fuzzy and classical speed control within field oriented method for induction motors," 7<sup>th</sup> European Conference Power Electronics & Applications, 1997, pp. 2.444-2.448.
- 53 S.Altug "Comparative analysis of fuzzy inference systems implemented on

- neural structures,” International Conference on Neural Networks, vol.1, 1997, pp. 426-431.
- 54 J. Boyce, “Pump motor vibration analysis and fault detection using artificial neural/fuzzy system,” International Conference on Neuro-fuzzy systems, vol. 2, 1997, pp. 60.01–60.15.
- 55 S. Caldara, “A fuzzy diagnostic system: application to linear induction motor drives,” IEEE Instrumentation Measurement Technology Conference, vol.1, 1997, pp. 257–262.
- 56 P. Van den Broek, “Fuzzy reasoning with continuous piecewise linear membership functions,” North American Fuzzy Information Processing Society 1997, pp.371–376.
- 57 B. Burton, R. G. Harley, G. Diana, J. L. Rodgerson, “Implementation of a neural network to adaptively identify and control VSI-Fed induction motor stator currents,” IEEE Transactions in Industrial Application, vol. 34, No. 3, 1998, pp. 580–588.
- 58 H. Chen, G. Xie, "Open-loop speed control for switched reluctance motor drive." in Proceedings of the 3rd Asia-Pacific Conference on Control & Measurement, 1998, pp. 287-290.
- 59 M.Y. Chow, “Set theoretic based neural-fuzzy motor fault detector,” Proceedings of International Conference of the IEEE Industrial Electronics Society, vol. 4, 1998 ,pp. 1908-1913.
- 60 G. Goddu, “Motor bearing fault diagnosis by a fundamental frequency amplitude based fuzzy decision system,” Proceedings of International Conference of the IEEE Industrial Electronics Society, vol. 4, 1998, pp. 1961-1965.
- 61 N. Ertugrul, A. D. Cheok, “Indirect angle estimation in switched reluctance motor drives using fuzzy logic based predictor/corrector,” in Proceedings of IEEE Power Electronics, 1998, pp. 845–851.
- 62 P. J. Costa Branco, J. A. Dente, “An experiment in automatic modeling an electrical drive system using fuzzy logic,” IEEE Transaction on System, Man, Cybernetics, vol. 28, 1998, pp. 254–262.
- 63 J. van den Berg, D. Ettes, “Representation and learning capabilities of additive

- fuzzy systems,” Proceedings of IEEE International Conference on IES, 1998, pp. 121–126.
- 64 Smith F S, Shen Q, “Selecting inference and defuzzification techniques for fuzzy logic control”, UKACC International Conference on Control ‘98, Conference Publication No. 455, 1998, pp.54-59.
- 65 M. A. Rahman, M. A. Hoque, “On-line adaptive artificial neural network based vector control of permanent magnet synchronous motors”, IEEE Transaction on Energy Conversion, vol. 13, No. 4, 1998, pp. 311-318.
- 66 M. R. Emami, I. B. Turksen, A. A. Goldenburg, “Development of a systematic methodology of fuzzy logic modeling,” IEEE Transaction on Fuzzy Systems, vol. 6, 1998, pp. 346–361.
- 67 B. Singh, V. K. Sharma, S. S. Murthy, “Performance analysis of adaptive fuzzy logic controller for switched reluctance motor drive system,” in Conference Recording IEEE-IAS Annual Meeting, 1998, pp. 571–579.
- 68 K. Erenay, I. Ciprut, L. Tezduyar, Y. Istefanopulos, “Application of fuzzy algorithms to the speed control of washing machines with brushless DC motors,” in Proceedings of International Conference in Electric Machines, 1998, pp. 1231–1236.
- 69 M. F. Rahman, L. Zhong, K. W. Lim, “A direct torque-controlled interior permanent magnet synchronous motor drive incorporating field weakening,” IEEE Transaction on Industrial Application, vol. 34, 1998, pp. 1246–1253.
- 70 Z. Ibrahim, E. Levi, D. Williams, “A self-tuning method for fuzzy logic speed controller in high performance ac drives,” in Proceedings of UPEC’98, vol. 2, 1998, pp. 819-822.
- 71 Chatterjee J K, Kumar Sanjiv, Singh Bhim, “Hybrid speed controller for vector controlled cage induction motor drive” IEEE Transactions 1998, pp. 147-152.
- 72 J.L Silva, H. Le-Huy, "An improved fuzzy learning algorithm motion control application," Industrial Electronics Society. IECON Annual Conference of the IEEE, vol.1, 1998, pp.1 -5.
- 73 G.Betta, C.Liguori. An advanced neural-network-based instrument fault detection and isolation scheme. IEEE Transactions on Instrumentation and

- Measurement, vol. 47, 1998, pp. 507-512.
- 74 M. Tsuji, S. Chen, K. Izumi, E. Yamad, "Stability improvement of speed sensorless induction motor vector control system using q-axis flux with stator resistance identification, " IEEE, Power Electronics Specialists Conference, 1998, pp. 1587 -1592.
- 75 N. Derbel, M. Chtourou, A. Masmoudi, "Reduced order model based neural network control of a squirrel cage induction motor drive", International Journal of Systems Science, vol. 29, No.9, 1998, pp.981-987.
- 76 Keller A, Klawonn F, "Context sensitive fuzzy clustering", Fuzzy Information Processing Society, NAFIPS. 18th International Conference of the North American,1999, pp.347-351.
- 77 N.R. Garrigan, W.L. Soong, C.M. Stephens, A. Storace, and T.A. Lipo, "Radial force characteristics of a switched reluctance machine," Proceedings of IEEE/IAS Annual Meeting, vol.4, 1999, pp.2250-2258.
- 78 R. Nolan, P. Pillay, T. Haque: "Application of genetic algorithms to motor parameter determination for transient torque calculation", IEEE Transaction on Industrial Applications, vol. 33,No. 5, 1997, pp. 1273-1282.
- 79 J. O. P. Pinto, B. K. Bose, L. E. Borges, M. P. Kazmierkowski, "A neural network based space vector PWM controller for voltage-fed inverter induction motor drive," in Proceedings of IEEE-IAS Annual Meet, 1999, pp. 2614-2622.
- 80 Ramo Sendelz, Vladan Devedzic, " Representational hirerchy of fuzzy logic concept in OBOA model," Multiple approaches to intelligent systems: 12<sup>th</sup> International Conference on Industrial and Engineering Applications of Artificial Intelligence and Expert Systems, Springer, 1999, pp. 54-63.
- 81 A. Fanni, M. Marchesi, A. Serri, M. Usai, "Performance improvement of a hybrid algorithm for electromagnetic devices design," IEEE Transaction on Magnetics, vol. 35, no. 3, 1999, pp. 1698–1701.
- 82 Nandi S, Toliyat H A, "Condition monitoring and fault diagnosis of electrical machines - A review," IEEE-IAS Annual meeting, 1999, pp. 197-204.
- 83 W.T. Thomson, D. Rankin, D.G. Dorrell, "On-line current monitoring to diagnose airgap eccentricity in large three-phase induction motors- Industrial

- case histories,” Verify The Predictions, vol. 14, No. 4, 1999, pp. 1372-1378.
- 84 A. E. Eiben, R. Hinterding, Z. Michalewicz, "Parameter control in evolutionary algorithms," IEEE Transactions on Evolutionary Computation, vol. 3, No. 2, 1999, pp. 434-440
- 85 N. Phadern, P. Pragasen, C. Susan E., "Evolutionary Algorithms for Induction Motor Parameter Determination", IEEE Transaction on Energy Conversion, vol. 14, No. 3, 1999, pp. 447-453,.
- 86 W. J. Wang, J. Y. Chen, "A new sliding mode position controller with adaptive load torque estimation for an induction motor," IEEE Transaction on Energy Conversion, vol. 14, 1999, pp. 413-418.
- 87 Cheong E, Lai R, "Designing a hierarchical fuzzy logic controller using differential evolution", IEEE International Fuzzy Systems Conference Proceedings, 1999, pp. 277-282.
- 88 Palani. S, Sundareswaran K, "Fuzzy logic approach for energy efficient voltage controlled induction motor drive", IEEE 1999 International Conference on Power Electronics and Drive Systems, PEDS'99, 1999, pp. 552-554.
- 89 C. Y. Huang, T. C. Chen, C. L. Huang, "Robust control of induction motor with a neural-network load torque estimator and neural-network identification", IEEE Transactions on Industrial Electronics, vol. 46, No. 5, 1999, pp. 990-997.
- 90 T. T. Sheu, T. C. Chen, "Self-tuning control of induction motor drive using neural network identifier", IEEE Transactions on Energy Conversion, vol. 14, No. 4, 1999, pp. 881-886.
- 91 S. Moreau, J.C. Trigeassou, G. Champenois, J.P. Gaubert, "Diagnosis of Induction machines: A procedure for electrical fault detection and localisation," IEEE Int. Symposium. on Diagnostics for Electrical Machines, Power Electronics and Drives, 1999, pp. 225-230.
- 92 C. Huang, T. Chen "Robust control of induction motor with a neural network load torque estimator and a neural network identification, ", IEEE Trans. Id, Electron., vol. 46, No. 5, 1999, pp. 990-998.
- 93 M. A. Brdys, G. Kulawski "Dynamic neural controllers for induction motor", IEEE Transaction Neural Network, vol. 10, No. 2, 1999, pp. 340-355.

- 94 T.Sheu, T.Chen "Self- tuning control of induction motor drive using neural network identifier", IEEE Transaction on Energy Conversion, vol.14. No.4, 1999, pp.881-886.
- 95 Lee Jong Bae, Im Tae Bin, Sung Ha Kyong, "A low cost speed control system of brushless dc motor using fuzzy logic" IEEE Transactions, 1999, pp. 433-437.
- 96 L. E. B. daSilva, B. K. Bose, J. O. P. Pinto, "Recurrent neural network based implementation of a programmable cascaded low pass filter used in stator flux synthesis of vector controlled induction motor drive," IEEE Transaction on Industrial Electronics, vol. 46, No. 3, 1999, pp. 662–665.
- 97 A. Dumitrescu, D. Fodor, T. Jokinen, M. Rosu, S. Bucurencio, "Modeling and simulation of electric drive systems using Matlab/Simulink environments," International Conference on Electric Machines and Drives (IEMD), 1999, pp. 451-453.
- 98 V. Sadegh "An on-line loss minimization controller for the Interior Magnet motor drives", IEEE Transactions on Energy Conversion, vol. 14, No. 4, 1999, pp.1435-1440
- 99 S. Mir, M. E. Elbuluk, I. Hossain, "Torque ripple minimization in switched reluctance motors using adaptive fuzzy control", IEEE Transaction on Industrial Application, vol. 35, No.2, 1999, pp. 461-468.
- 100 A. Altug, M.-Y. Chow, "Fuzzy inference systems implemented on neural architectures for motor fault detection and diagnosis," IEEE Transaction on Industrial Electronics, vol. 46, No. 6, 1999, pp. 1069–1078.
- 101 M. E. H. Benbouzid, "Bibliography on induction motors faults detection and diagnosis," IEEE Transaction on Energy Conversion, vol. 14, 1999, pp.1065–1074.
- 102 T. Orłowska-Kowalska, K. Jaszczak, K. Szabat, "Robustness of fuzzy-logic control with simple parameter adaptation for DC motor drive," in Proceedings of PEMC'00, vol. 6, 2000, pp. 6.82–6.86.
- 103 M. Morimoto, "Application specific permanent magnet motors and reluctance motors," Proceedings of International Power Electronics Conference IPEC, vol.1, 2000, pp. 241-246.

- 104 Fiorenzo Filippetti, Vas P., "Recent developments of induction motor drive fault diagnosis using AI techniques", vol. 4, Industrial Electronics Society, 2000, pp.1966-1973.
- 105 Yiping Liu, Yi Shen, Zhiyan Liu, "An approach to fault diagnosis for non-linear system based on fuzzy cluster analysis," Proceedings of the 17th IEEE Instrumentation and Measurement Technology Conference, vol. 3, 2000, pp. 1469-1473.
- 106 M. Morimoto, "Application specific permanent magnet motors and reluctance motors," Proceedings of International Power Electronics Conference IPEC, vol.1, 2000, pp.241-246.
- 107 Jun Oh jang, Pyeong Gi Lee, "Neuro-fuzzy control for dc motor friction compensation", Proceedings of the 39th IEEE Conference on decision and control, 2000, pp. 3550-3555.
- 108 R.M.Tallam, T.G.Habetler, R.G.Harley, "Transient model for induction machines with stator winding turn faults," in Proceedings of IEEE-IAS Annual meeting, vol. 1, 2000, pp. 304-309.
- 109 Kraft D.H., Chen, J. Mikulcic, "A combining fuzzy clustering and fuzzy inferencing in information retrieval", Fuzzy Systems IEEE International Conference, vol. 1, 2000, pp. 375-380.
- 110 Steven Schockaert, Martine De Cock, Etienne E. Kerre, "Automatic acquisition of fuzzy footprints", IEEE International Conference on fuzzy system, vol. 1, 2000, pp. 176-180.
- 111 Ching-Hung Lee, Ching-Cheng Teng, "Identification and control of dynamic systems using Recurrent Fuzzy neural network", IEEE Transactions on Fuzzy Systems, vol. 8 No.4, 2000.
- 112 A. Arias, J. L. Romeral, E. Aldabas, M. G. Jayne, "Fuzzy logic direct torque control," Proceedings of IEEE International Symposium in Industrial Electronics, 2000, pp. 253-258.
- 113 Y. S. Lai, J. H. Chen, and C. H. Liu, "A universal vector controller for induction motor drives fed by voltage-controlled voltage source inverter," Proceedings of IEEE PES Summer Meeting, 2000, pp. 2493-2498.

- 114 K.Sundareswaran, Merugu Vasu,"Genetic tuning of PI controller for speed control of DC motor drive", Proceedings of IEEE Conference, 2000, pp.521-525.
- 115 P. Grabowski, M. P. Kaunierkowski, B. K. Bose, F.Blaabjerg, "Simple direct torque neuro-fuzzy control of induction motor drives", IEEE Transaction on Industrial Electronics, vol. 47, 2000, pp. 234-243.
- 116 Chowdhuri Sumana, Mukherjee Abhik, "An evolutionary approach to optimize speed controller of dc machines" IEEE Transactions 2000, pp. 682-687.
- 117 D. Fuessel, R. Isermann, "Hierarchical motor diagnosis utilizing structural knowledge and a self-learning neuro-fuzzy scheme", IEEE Transactions on Industrial Electronics, vol. 47, No. 5, 2000, pp. 1070-1077.
- 118 F.F.Bernal, A.G.Cerrada, R.Faure, "Model-based loss minimization for dc and ac vector-controlled motors including core saturation", IEEE Transaction on Industrial Applications, vol. 36, No. 3, 2000, pp. 755-763.
- 119 A. Rubaai, R. Kotaru, M. David Kankam, "A continually online trained neural network controller for brushless DC motor drives," IEEE Transaction on Industrial Applications, vol. 36, 2000, pp. 475-483.
- 120 Kolla S, Varatharasa L, "Identifying three-phase induction motor faults using artificial neural networks," ISA Transactions, vol. 39, 2000, pp. 433-439.
- 121 Rubaai Ahmed, Kotaru Raj "Online identification and control of a dc motor using learning adaptation of neural networks," IEEE transactions on industry applications, vol. 36, No. 3, 2000, pp. 935-942.
- 122 C. M. Kwan,F. L. Lewis, "Robust backstepping control of induction motors using neural networks," IEEE Transactions on Neural Networks, vol.11, No. 5, 2000, pp. 1178-1187.
- 123 B. Robyns, F. Berthereau, JP. Hautier, H. Buyse, "A fuzzy-logic based multimodal field orientation in an indirect FOC of an induction motor" IEEE Transactions on Industrial Electronics, vol. 47,No. 2,2000,pp. 380-388.
- 124 H. A. F. Mohamed, W. P. Hew, "A fuzzy logic vector control of induction motor," Proceedings of TECON 2000, vol. 3,2000, pp. 324-328.

- 125 Uddin M N, "Performances of novel fuzzy logic based indirect vector control for induction motor drive", IEEE Transactions 2000, pp.1225-1231.
- 126 I. Rivals, L. Personnaz, "Nonlinear internal model control using neural networks: Application to processes with delay and design issues", IEEE Transaction on Neural Networks, vol. 11(1), 2000, pp. 80-90.
- 127 R.S.Toqeer, N.S.Bayindir, "Neurocontroller for induction motors", Proceedings of 12th International Conference on Microelectronics, 2000, pp. 227-230.
- 128 F. Montagna, "An algebraic approach to propositional fuzzy logic," Journal of Logic Language Information, vol. 9, 2000, pp. 91–124.
- 129 H. T. Nguyen, A. Kandel, and V. Kreinovich, "Complex fuzzy sets: toward new foundations," in Proc. 2000 IEEE International Conference on Fuzzy Systems, 2000, pp.1045–1048.
- 130 J. O. Jang, G. J. Jeon, "A parallel neuro-controller for dc motors containing nonlinear friction," Journal of Neuro computing, vol. 30, No.1–4, 2000, pp. 233–248.
- 131 C.S.Chang, D.Y.Xu, " Differential evolution based tuning of fuzzy automatic train operation for mass rapid transit system," IEE Proceedings Electrical Power Applications, vol. 147, No.3, 2000, pp.207-212.
- 132 Y. S. Lai, J. H. Chen, "A new approach to direct torque control of induction motor drives for constant inverter switching frequency and torque ripple reduction," IEEE Transaction on Energy Conversion, vol. 16, 2001, pp.220–227.
- 133 Rubaai, A., Kankam, D., "On line training of parallel neural network estimators for control of induction motors," IEEE Transaction on Industrial Application, vol. 37, No. 5, 2001, pp.1512-1520.
- 134 Jang Jun Oh, "A dead zone compensator of a DC motor system using fuzzy logic control", IEEE Transactions On Systems, Man and Cybernetics—part c: applications and reviews, vol. 31, No. 1, 2001, pp. 234-243.
- 135 Cao-Minh Ta, Yoichi Hori, "Convergence improvement of efficiency optimization control of induction motor drives", IEEE Transaction on Industrial Applications., vol.37, No. 6, 2001, pp. 1746-1753.

- 136 P. P. Cruz, J. J. R. Rivas, "A small neural network structure application in speed estimation of an induction motor using direct torque control" IEEE 32nd Annual Power Electronics Specialists Conference, vol. 2, pp. 2001, 823-827.
- 137 S. H. Kim, T. S. Park, J. Y. Yoo, G. T. Park, "Speed-sensorless vector control of an induction motor using neural network speed estimation" IEEE Transactions on Industrial Electronics, vol. 48, 2001, pp. 609-614.
- 138 Q. Song, L. Yin, "Robust adaptive fault accommodation for a robot system using a radial basis function neural network", International Journal of system science, vol. 32, No. 2, 2001, pp.195-204.
- 139 Sankaran R, Nair P.S Chandramohanan "Adaptive neuro-fuzzy controller for improved performance of a permanent magnet brushless dc motor" IEEE International Fuzzy System Conference, 2001, pp. 493-496.
- 140 J. R. Heredia, F.Perez Hidalgo, J. L. Duran Paz "Sensorless control of induction motor by artificial neural networks", IEEE Transaction on Industrial Electronics, Vol.48, No.5, 2001, pp. 1038 -1040.
- 141 R. M. Tallam, T. G. Habetler, R. G. Harley, "Continual on-line training of neural networks with applications to electric machine fault diagnostics," IEEE 32<sup>nd</sup> Annual in Power Electronics Specialists Conference PESC 2001, vol. 4, pp.2224–2228.
- 142 G. J. Wang, C. T. Fong, K. J. Chang, "Neural network based self tuning PI controller for precise motion control of PMAC motors," IEEE Transaction on Industrial Electronics, vol. 48, no. 2, 2001, pp. 408–415.
- 143 R. J. Wai, "Total sliding mode controller for PM synchronous servomotor drive using recurrent fuzzy neural network," IEEE Transactions on Industrial Electronics, vol. 48, no. 5, 2001, pp. 926–944.
- 144 H.Le-Huy, "Modeling and simulation of electrical drives using Matlab/Simulink and Power System Blockset," The 27th Annual Conference of the IEEE Industrial Electronics Society, 2001, pp.1603-1611.
- 145 B. Karanayil, M.F. Rahman, C. Grantham, "Rotor resistance identification using artificial neural networks for an indirect vector controlled induction motor drive", Proceedings of the 27 the Annual Conference of Industrial Electronics

- Society, vol. 2, 2001, pp. 1315-1320.
- 146 G. J. Wang, C. T. Fong, K. J. Chang, "Neural-network-based self tuning PI controller for precise motion control of PMAC motors," IEEE Transaction on Industrial Electronics, vol. 48, 2001, pp. 408–415.
- 147 Y. Yi, D. M. Vilathgamuwa, M. A. Rahman, "A new artificial neural network controller for interior permanent magnet motor drive," in Conference Recording IEEE Industry Applications Society (IAS) Annual Meeting, 2001, pp. 945–952.
- 148 Oyama J, Ogawa K, Higuchi T, Rashad E, Mamo M, Sawamura M, "Sensorless vector-control of ipm motors over whole speed range" 4th IEEE International Conference Proceedings on Power Electronics and Drive Systems, vol. 2, 2001, pp. 448 – 451.
- 149 I. Guney, Y. Oguz, F. Serteller, "Dynamic behaviour model of permanent magnet synchronous motor fed by pwm inverter and fuzzy logic controller for stator phase current, flux and torque control of pmsm," in IEEE Proceedings 2001, pp. 479-485.
- 150 Hoang Le-Huy "Modeling and simulation of electrical drives using matlab/simulink and power system blockset" IECON'01: The 27th Annual Conference of the IEEE Industrial Electronics Society, vol. 3, 2001, pp. 1603-1611.
- 151 A. M. Trynadlowski, "Comparative investigation of diagnostic media for induction motors: a case of rotor cage faults," IEEE Transactions of Industrial Electronics, vol. 47, 2001, pp. 1092–1099.
- 152 N. Karnik, J. Mendel, "Operations on type-2 fuzzy sets," Fuzzy Sets and Systems, vol. 122, 2001, pp. 327-348.
- 153 A. Hassan, "Improving the power efficiency of a rotor flux-oriented induction motor drive", Electric Power Components and Systems, vol. 30, 2002, pp. 431-442.
- 154 T. C. Chen, T. T. Sheu, "Model reference neural network controller for induction motor speed control", IEEE Transactions on Energy Conversion, vol. 17, No. 2, 2002, pp. 157-163.

- 155 F. J. Lin, R. J. Way, "Adaptive fuzzy-neural network control for induction spindle motor drive", IEEE Transactions on Energy Conversion, vol. 17, No. 2, 2002, pp. 507-513.
- 156 S. K. Mondal, J. O. P. Pinto, B. K. Bose, "A neural network based space-vector PWM controller for a three voltage-fed inverter induction motor drive", IEEE Transaction on Industrial Application, vol. 38, No. 3, 2002, pp. 660-669.
- 157 A. Rubaai, D. Rickattes, M. D. Kankam, "Development and implementation of an adaptive fuzzy-neural network controller for brushless drives," IEEE Transaction on Industrial Applications, vol. 38, No. 2, 2002, pp. 441-447.
- 158 A. Rubaai, D. Rickattes, M. D. Kankam, "Development and implementation of an adaptive fuzzy-neural network controller for brushless drives," IEEE Transaction on Industrial Applications, vol. 38, No. 2, 2002, pp. 441-447.
- 159 F. J. Lin, R. J. Wai, W. D. Chou, S. P. Hsu, "Adaptive backstepping control using recurrent neural network for linear induction motor drive," IEEE Transaction on Industrial Electronics, vol. 49, No. 1, 2002, pp. 134-146,.
- 160 Jeon-Tae Park, Cheol-Gyun Lee, Min-Kyu K, Hyun-Kyo Jung, "Application of fuzzy decision to optimization of induction motor design", IEEE Transactions on magnetics, vol. 33, No. 2, 2002, pp. 225-232.
- 161 M. N. Uddin, T S. Radwan ,M. A. Rahman, "Performance of fuzzy logic- based indirect vector control for induction motor drive", IEEE Transaction on Industrial Applications, vol. 38, No. 5, 2002, pp.1219-1225.
- 162 Z. Ibrahim, E. Levi. "A comparative analysis of fuzzy logic and pi speed control in high performance ac drives using experimental approach", IEEE Transaction on Industrial Applications, vol. 38, No. 5, 2002, pp. 1210-1218.
- 163 S. Bel Hadj Ali, A. El Abed-Abdelkrim, M. Benrejeb, "An internal model control strategy using artificial neural networks for a class of nonlinear systems", IEEE International Conference on Systems, Man and Cybernetics, vol. 5, 2002, pp. 4-7.
- 164 D. Ramot, R. Milo, M. Friedman, A. Kandel, "Complex fuzzy sets," IEEE Transactions on Fuzzy Systems, vol. 10, 2002, pp. 171-186.

- 165 Ramot Daniel, Friedman Menahem, Langholz Gideon, Kandel Abraham, "Complex Fuzzy Logic", IEEE transactions on fuzzy systems, vol. 11, No. 4, 2003, pp. 450-461.
- 166 L. Wenzhe, A. Keyhani, A. Fardoun, "Neural network based modeling and parameter identification of switched reluctance motors," IEEE Transaction on Energy Conversion, vol. 18, No. 2, 2003, pp. 284–290.
- 167 C. Wang, B. K. Bose, V. Oleschuk, S. Mondal, J. O. P. Pinto, "Neural network based SVM of a three-level inverter covering overmodulation region and performance evaluation on induction motor drives," in Proceedings of Conference Recording IEEE IECON, 2003, pp. 1–6.
- 168 H. J. Guo, S. Sagawa, T. Watanabe, O. Ichinokura, "Sensorless driving method of permanent-magnet synchronous motors based on neural networks," IEEE Transactions on Magnetics, vol. 39, No. 5, 2003, pp. 3247–3249.
- 169 Grantham Colin, Karanayil Baburaj, Rahman Fazlur Muhammed, "Stator and rotor resistance observers for induction motor drive using fuzzy logic and artificial neural networks", IEEE Transactions 2003, pp. 124-131.
- 170 Lai Yen-Shin, "New hybrid fuzzy controller for direct torque control induction motor drives", IEEE Transactions on Power Electronics, vol. 18, No. 5, 2003, pp. 1211-1219.
- 171 Rahman Khwaja M, Hiti Silva, "Identification of machine parameters of a synchronous motor", IEEE Transactions 2003, pp. 409-415.
- 172 T. D. Batzel, K. Y. Lee, "An approach to sensorless operation of the permanent-Magnet synchronous motor using diagonally recurrent neural networks," IEEE Transactions on Energy Conversion, vol. 18, 2003, pp. 100–106.
- 173 Y. Yang, D. M. Vilathgamuwa, M. A. Rahman, "Implementation of an artificial-neural-network-based real-time adaptive controller for an interior permanent-magnet motor drive," IEEE Transaction on Industrial Application, vol. 39, No. 1, 2003, pp. 96–104.
- 174 T. Pajchrowski, K. Urbanski, K. Zawirski, "Robust speed control of PMSM servo drive based on ANN application," in Proceedings of 10th European Conference on Power Electronics Application, 2003, pp. 833-836.

- 175 C. Butt, M. A. Hoque, M. A. Rahman, "Simplified fuzzy logic based mtpa speed control of ipmsm drive." IAS Annual Meeting Conference Record. vol.1, 2003, pp. 499–506.
- 176 Ciftcioglu Ozer, "Design enhancement by fuzzy logic in architecture", IEEE International Conference on Fuzzy Systems 2003, pp. 79-84.
- 177 Siddique, A., Yadava, G.S. and Singh,B. "Applications of artificial intelligence techniques for induction machines stator fault diagnostics: review," IEEE International Symposium SDEMPED'03,2003, pp. 29-34.
- 178 B.Karanayil, M. F. Rahman, C. Grantham, "Implementation of an on-line resistance estimation using artificial neural networks for vector controlled induction motor drive", IECON '03 29th Annual Conference of the IEEE Industrial Electronics Society, vol. 2, 2003, pp. 1703-1708.
- 179 S. Wu, T. W. S. Chao, "Induction machine fault detection using SOM-based RBF neural networks," IEEE Transactions on Industrial Electronics, vol.51, No. 1, 2004, pp. 183–194.
- 180 M. N. Uddin, M. A. Abido, M. A. Rahman, "Development and implementation of a hybrid intelligent controller for interior permanent magnet synchronous motor drive," IEEE Transaction on Industrial Application, vol. 40, 2004, pp. 68–76.
- 181 W. Qian, S. K. Panda, J. X. Xu, "Torque ripple minimization in pm synchronous motors using iterative learning control", IEEE Transaction on Power Electronics, vol. 19, No.2, 2004, pp. 272-279.
- 182 Ichikawa Shinji, Tomita Mutuwo, Doki Shinji, "Sensorless control for all types of synchronous motors using an on-line parameter identification", The 30th Annual Conference of the IEEE Industrial Electronics Society, 2004, pp. 975-980.
- 183 Elenita Victor H.,Edgar N. Sanchez "Neural block control for a synchronous electric generator." IEEE Transactions, 2004, pp. 2919-2924.
- 184 F. Doctor, H. Hagrass, V. Callaghan, "A type-2 fuzzy embedded agent for ubiquitous computing environments," in Proceedings of FUZZ-IEEE, 2004, pp. 1105–1110.

- 185 Gabriel Gallegos-Lopez, Kani S. Gunawan, James E. Walters, "Optimum torque control of permanent-magnet AC machines in the field-weakened region," *IEEE Transactions on Industrial Application*, vol. 41, 2005, pp.1020-1028.
- 186 Song Yujie, Ponc Ferdinanda "A novel brushless dc motor speed estimator based on space-frequency localized wavelet neural networks," *IEEE Transactions*, 2005, pp. 927-932.
- 187 Lotfi A. Zadeh, Masoud Nikraves, Mo Jamshidi , "The legacy of accomplishment, excellence and people who contribute to the advancement of science and technology to better serve global community," *Berkeley Initiative in Soft Computing, FORGING NEW FRONTIERS 40th of Fuzzy Pioneers*,2005, pp.25-28.
- 188 Dick Scott, "Toward complex fuzzy logic", *IEEE Transactions on fuzzy systems*, vol. 13, No. 3, 2005, pp. 405-414.
- 189 Park Jung-Wook, Venayagamoorthy Ganesh Kumar "Mlp/rbf neural-networks-based online global model identification of synchronous generator" *IEEE Transactions on Industrial Electronics*, vol. 52, No. 6, 2005, pp. 1685-1695.
- 190 Yang jia-qiang, Huang jin, "Direct torque control system for induction motors with fuzzy speed pi regulator", *Proceedings of the Fourth International Conference on Machine Learning and Cybernetics*, 2005, pp. 778-783.
- 191 S. Greenfield, R. John, S. Coupland, "A novel sampling method for Type-2 defuzzification," in *Proceedings of UKCI* , 2005, pp. 120–127.
- 192 H. P. Wang, Y. T. Liu, "Integrated design of speed-sensorless and adaptive speed controller for a brushless DC motor," *IEEE Transactions on Power Electronics*, vol. 21, 2006, pp. 518-523.
- 193 Kar C Narayan, M. El-Serafi Ahmed, "Effect of voltage sag on the transient performance of saturated synchronous motors", *IEEE Transactions* 2006, pp. 1246-1251.
- 194 Pajchrowski T., Urbanski K., Zawirski K, "Artificial neural network based robust speed control of permanent magnet synchronous motors," *COMPEL*, vol. 25, No. 1, 2006, pp. 220-234.

- 195 Dick, S. Sadia A., "Fuzzy clustering of open-source software quality data: a case study of mozilla", International Joint Conference on Neural Network, 2006, pp. 4089- 4096.
- 196 H. A. F. Mohamed, S. Yaacob, "Direct inverse speed control of induction motor using artificial neural networks", MS2006 Proceedings of International Conference on Modeling and Simulation, 2006, pp. 125-130.
- 197 Jerry M. Mendel, Feilong Liu, "Super-Exponential Convergence of the Karnik–Mendel Algorithms for Computing the Centroid of an Interval Type-2 Fuzzy Set", IEEE Transactions on Fuzzy Systems, vol. 15, No. 2, 2007, pp.309-320.
- 198 LeiWu, LeiPeng, "A Dynamic immune algorithm with immune network for data clustering". IEEE Conference on Communications, Circuits and Systems, vol 1, 2007, pp. 919–923.
- 199 Hansen Brink Hans, Bendtsen Dimon Jan, "A hybrid model of brushless dc motor" 16th IEEE International Conference on Control Applications Part of IEEE Multi-conference on Systems and Control, 2007, pp. 1-3.
- 200 G. Aissaoui, M. Abid, H. Abid, A. Tahour, A. K. Zebalah, "A FuzzyLogic Controller for Synchronous Machine," Journal of Electrical Engineering, vol. 58, 2007, pp. 285-290.
- 201 Tipsuwan Yodyium, Srisabye Jirat "An experimental study of network-based dc motor speed control using Sanfis" The 33rd Annual Conference of the IEEE Industrial Electronics Society (IECON), 2007, pp. 426-432.
- 202 Kang Yuan, Chu Ming-Hui "The self-tuning neural speed regulator applied to dc servo motor" Third International Conference on Natural Computation, 2007, pp. 1-6.
- 203 Najafi Shahram, Kar C Narayan, "Effect of short-circuit voltage profile on the transient performance of saturated permanent magnet synchronous motors", IEEE Transactions 2007, pp. 1-6.
- 204 T. Pham-Dinh, T. Nguyen-Thanh, "Fuzzy speed controller for rotor flux oriented control of permanent magnet synchronous machine," in Proceedings of ISEE , 2007, pp. 72-78.

- 205 M. N. Uddin, M. A. Rahman, "High speed control of ipmsm drives using improved fuzzy logic algorithms", IEEE Transactions on Industrial Electronics, vol. 54, No. 1, 2007, pp. 190-199.
- 206 Barazane L, Khwaldeh A, Jumah M , Ouiguini , "Linguistic fuzzy modelling of an asynchronous motor", IEEE Transactions 2007, pp. 1-7.
- 207 Pajchrowski T., Zawirski K., "Application of artificial neural network to robust speed control of servodrive," IEEE Transaction on Industrial Electronics, vol.54, No.1, 2007, pp. 200-207.
- 208 Cortajarena J A, Marcos J. De , "Indirect vector controlled induction motor with four hybrid P+Fuzzy PI controllers", IEEE Transactions, 2007, pp. 197-202.
- 209 S. Coupland and R. John, "Geometric type-1 and type-2 fuzzy logic systems," IEEE Transactions on Fuzzy Systems, vol. 15, No.1, 2007, pp. 3-15.
- 210 J. Mendel, "Type-2 fuzzy sets and systems: an overview," IEEE Computational Intelligence Magazine, vol. 2, 2007, pp. 20-29.
- 211 A. Karakaya, E. Karakas, "Performance analysis of pm synchronous motors using fuzzy logic and self tuning fuzzy PI speed controls," The Arabian Journal for Science and Engineering, vol. 33, 2008, pp. 153-177.
- 212 Sumina Damir, Bulic Neven "Simulation model of neural network based synchronous generator excitation control," 13th International Power Electronics and Motion Control Conference , IEEE Transactions,2008, pp. 556-560.
- 213 Guo Hong, Wang Wei, Xing Wei, Li Yanming, "Design and research on electrical/ mechanical hybrid four-redundancy brushless dc motor system", IEEE Vehicle Power and Propulsion Conference (VPPC), 2008.pp. 332-339
- 214 Gadoue Shady M., Giaouris Damian, Finch J. W., "Neural network based stator current mras observer for speed sensorless induction motor drives," IEEE Transactions, 2008, pp. 650-655.
- 215 Christian Wagner, "zSlices – Towards bridging the gap between interval and general type-2 fuzzy logic", IEEE International Conference on Fuzzy Systems, 2008, pp. 489-497.
- 216 Xia Changliang, Li Zhiqiang, "Current threshold on-line identification control themen based on intelligent controller for four-switch three phase brushless dc

- motor” Proceedings of IEEE International Conference on Mechatronics and Automation, 2008, pp. 954-958.
- 217 Kamalasan Sukumar, Swann Gerald. “An intelligent hybrid controller for speed control and stabilization of synchronous generator” Proceedings of International Joint Conference on Neural Networks, 2009, pp. 1481-1488.
- 218 Liu Xingqiao, Zhang Xiangmei “Three-motor synchronous decoupling control based on bp neural network” 2009 chinese control and decision conference”, IEEE Transactions 2009, pp. 5365-5368.
- 219 Rahimpour M., Talebi M. A. “On line synchronous generator parameters estimation based on applying small disturbance on excitation system using ANN” IEEE Transactions, 2009, pp. 445-449.
- 220 Fang Hongwei, Xia Changliang “A fuzzy neural network based fault detection scheme for synchronous generator with internal fault,” Sixth International Conference on Fuzzy Systems and Knowledge Discovery. IEEE Transactions 2009, pp. 433-437.
- 221 Cheng Zhiqiang, Hou Chongsheng “Global sliding mode control for brushless dc motors by neural networks” International Conference on Artificial Intelligence and Computational Intelligence, 2009, pp. 3-6.
- 222 Hsu Chia-Yu, Hsu Chun-Fei, “Adaptive position tracking control of a bldc motor using a recurrent wavelet neural network” Proceedings of the IEEE International Conference on Networking, Sensing and Control, 2009, pp. 25-30.
- 223 Jongman Hong, Hyun Doosoo, Yoo Jiyeon, “Automated monitoring of magnet quality for permanent magnet synchronous motors at standstill”, IEEE Transactions, 2009, pp. 2326-2333.
- 224 Imam Robandi, Bedi Kharisma, “ Design of Interval type-2 fuzzy logic based power system stabilizer” , International Journal of Electrical and Electronics Engineering 3 , 2009, pp. 593-600.
- 225 Andersen Peter Scavenius, Dorrell David G, “Synchronous torques in split-phase induction motors”, vol. 46, No. 1, IEEE Transactions on Industry Applications, 2010, pp. 222-231.

- 226 Hong-jun Wang , Hui Zhao, “Design of fuzzy-neuro controller applicated to a synchronous generator excitation control system”, 2010 International Conference on Measuring Technology and Mechatronics Automation. IEEE Transactions 2010, pp. 997-999.
- 227 Richard F Vancil, M.Gopal, “Control System Principle and Design”,1963, Tata McGraw-Hill Education.
- 228 Ion Boldea, “The Electric Generators Handbook Synchronous Generators”, 2006, Taylor and Francis CRC Press.
- 229 P.S.Bhimbra, “Generalized Theory of Electrical Machines”, 1995, Khanna Publishers.
- 230 I.J. Nagrath, M. Gopal, “Control Systems Engineering”,1982, Wiley Eastern Publisher.
- 231 Timothy J.Ross, “ Fuzzy Logic With Engineering Applications”, 1995, John Wiley & Sons Limited U.K.
- 232 S. N. Sivanandam, S.Sumathi, S.N.Deepa, “Introduction To Neural Networks Using MATLAB 6.0”, 2006, Tata McGraw-Hill Education.